SYMPOSIUM ON RESEARCH RESULTS FROM THE 2005 SUMMER
INSTITUTE ON ATMOSPHERIC AND HYDROSPHERIC SCIENCES
Friday, August 12, 2005
Building 33, Conference Room A128

9:00a Opening remarks -- Per Gloersen
9:15a Testing holographic optical elements and instrument programming (2)
-- Ian C. Brown, University of Colorado (Geary Schwemmer/613.1, mentor)
9:30a Observations of moisture and temperature variability in a non-convective dryline (14)
-- Teresa Inman, Lyndon State College. (Belay Demoz/613.1, mentor)
9:45a Visualization and analysis of fire radiative energy measurements from MODIS (32)
-- Luke T. Ellison, Bethel University. (Charles Ichoku/613.2/SSAI, mentor)
10:00a Assessing the transport of aerosols around the world (48)
-- Kristen M. Mihalka, University of Missouri. (Yoram Kaufman/613.2, mentor)
10:15a Comparisons of tropospheric aerosol optical thickness using GOCART, MODIS, TOMS, and AERONET data (63)
-- Andrea May, Millersville University (Yogesh Sud/613.2, mentor)
10:30a Characterization of dust events in Patagonia using 15 years of surface observations (82)
-- Edward Liske, Northland College (Santiago Gassó, mentor)
10:45a BREAK
11:00a Correlations of MODIS and particulate matter (2.5) measurements in the mid Atlantic region (95)
-- Edward Nowottnick, University of Maryland. (Robert Levy/613.2/SSAI, mentor)
11:15a A graphical analysis of tropical cyclones globally using satellite observations (113)
-- Ahmed Tawfik, North Carolina State University. (Yaping Zhou/613.2/UMBC, mentor)
11:30a Uncovering the Milankovitch cycle in the Vostok ice core using the Hilbert Huang Transform (126)
-- Kevin Leavor, Washington & Jefferson College. (Norden Huang/614.2 & Per Gloersen/614.1, mentors)
11:45a The melting layer: Modeling the microphysical and single scattering properties (154)
-- Erik Swenson, St. Cloud State University. (Gail Jackson & Ben Johnson/614.6, mentors)
12:00 LUNCH BREAK
01:00p Improving the EPA BASINS-HSPF Nonpoint Source Pollution Model (176)
-- Anna Nowack, Northland College. (David Toll/614.3, mentor)
01:15p The search for global teleconnections: A hydroclimatic analysis of 25 years of modeled water cycle data (204)
-- Mathew D. Stepp, Millersville University. (Matt Rodell/614.3, mentor)
01:30p Tracking icebergs in the Ross Sea (221)
-- Tamara McDunn, Valparaiso University. (Thorsten Markus/614.6, mentor)
01:45p MAC UAV: Prototype and mission profile (241)
-- Brian P. Smith, University of Maryland. (Marko Bulmar/698/UMBC, mentor)
02:00p ADJOURN

Testing Holographic Optical Elements and Instrument Control

Summer Institute

By Ian Brown

Introduction

- About LIDAR
- The purpose of HARLIE
- Testing infrared holographic gratings
- Testing ultraviolet holographic optical elements (HOEs)
- Using LabVIEW to make virtual controls for HARLIE instrument

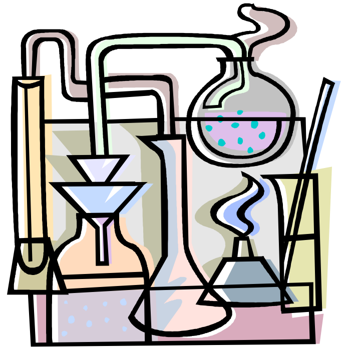

LIDAR and NASA

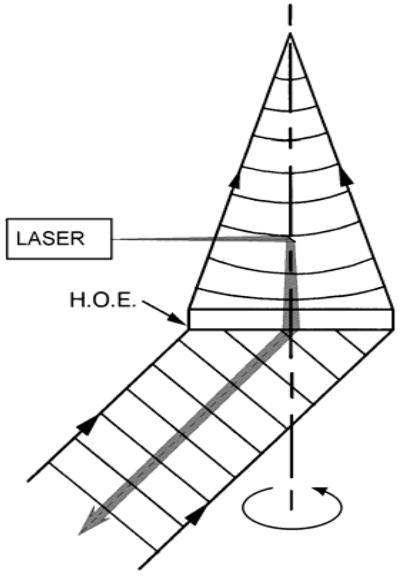

- Light detection and ranging (LIDAR)
- Similar to RADAR, using lasers
- Goal: to have a space based scanning LIDAR for atmospheric wind profiles

- Holographic airborne LIDAR instrument experiment (HARLIE) is the first step towards goal
- Scanning telescope with holographic optical element (HOE)
- Lighter, smaller, and cheaper to put into space

Testing Properties of Holographic Gratings with an IR laser

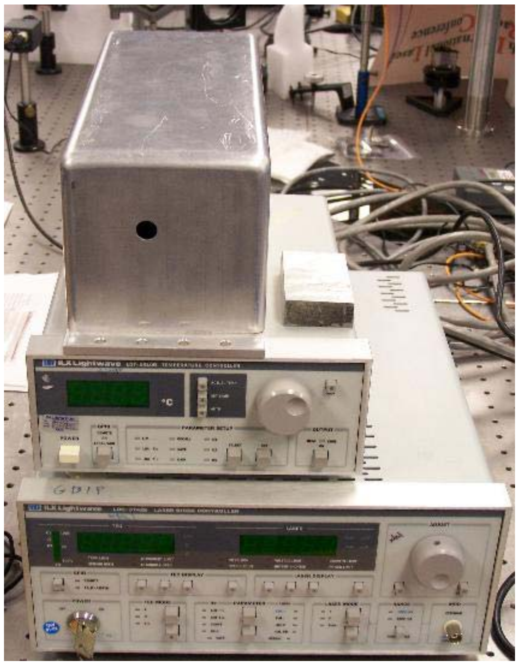

- Using 2050nm light
- Very difficult to see
- Fringe patterns split beam into orders
- Only responds to one wavelength of light

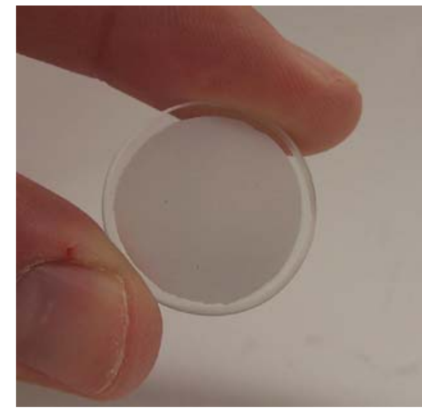

- Angle of hologram to optical axis is critical.

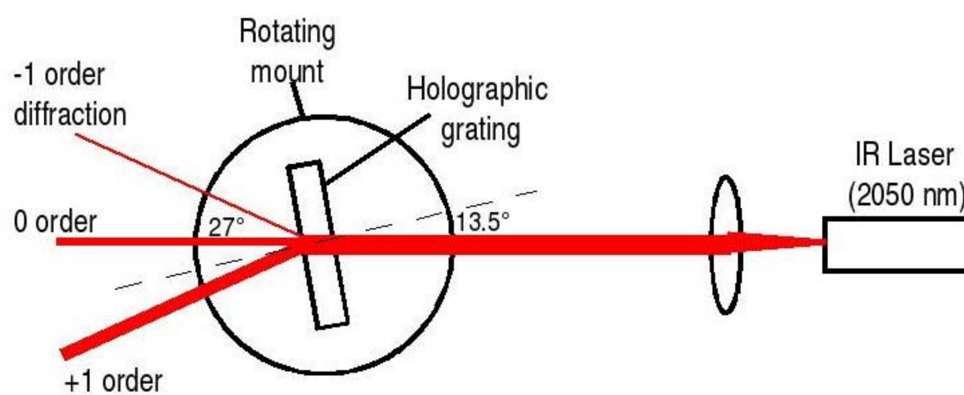

Holographic Grating Data

Testing SHADOEs with UV Lasers

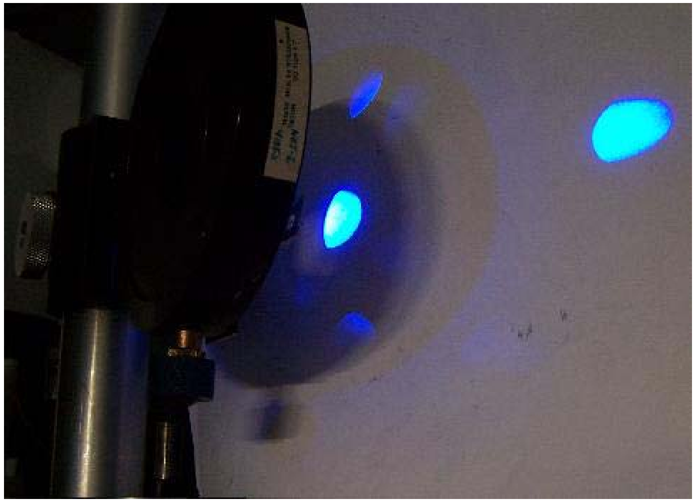

- Shared aperture diffractive optical element (SHADOE)
- Made of five HOEs at equally-spaced angles
- React only to UV light incident at 45^{o}
- Other light passes through
- Diffracts only into 0 and +1 orders

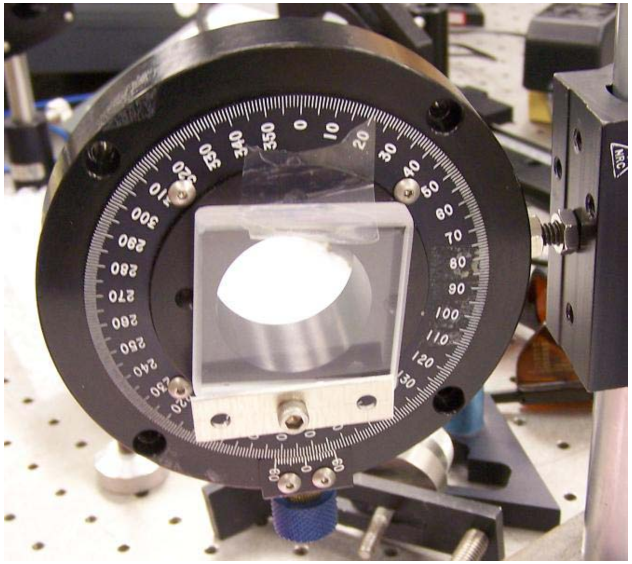

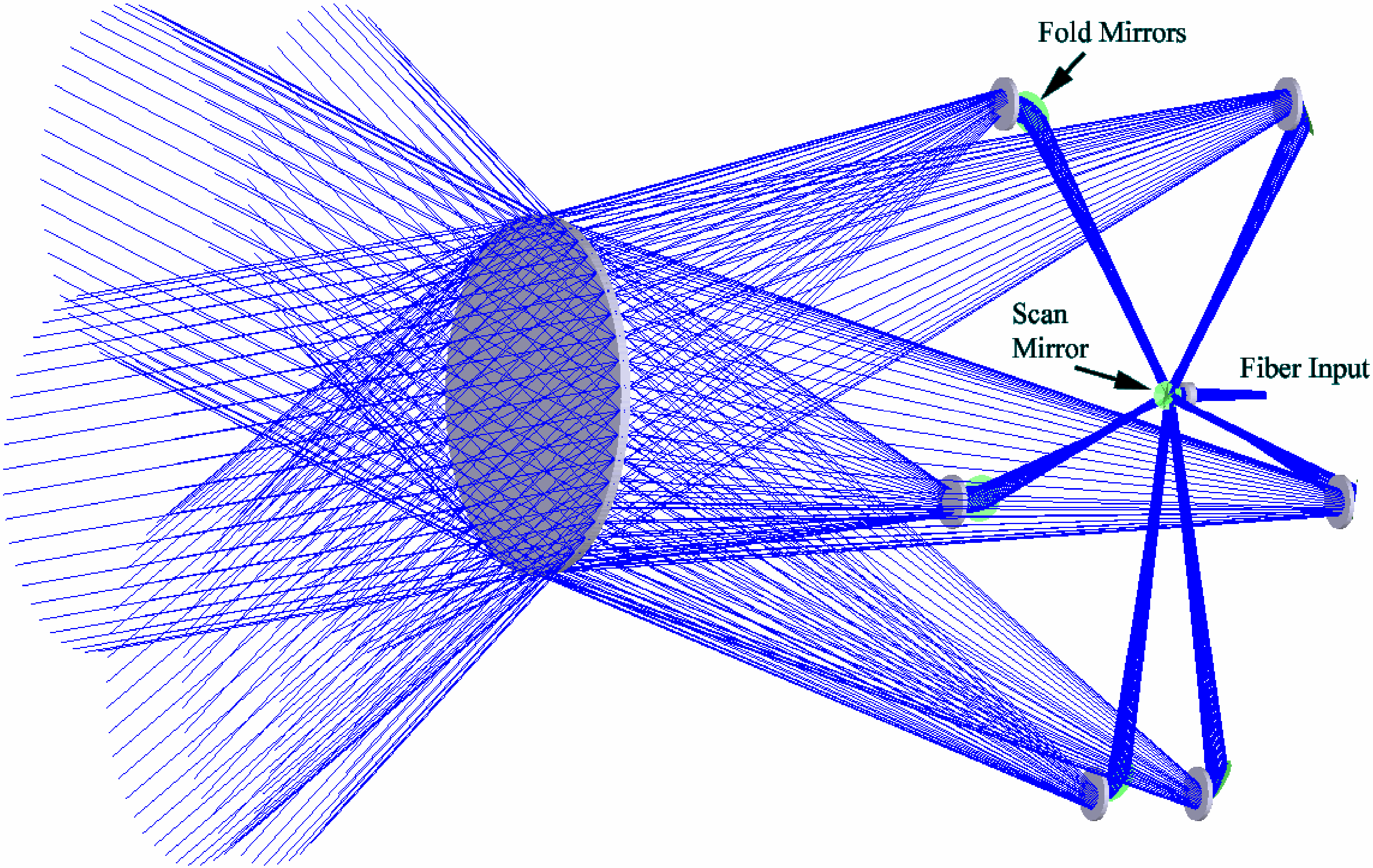
Fold Mirrors
Scan
Mirror
Fiber Input

Testing SHADOEs with UV Lasers

- Shared aperture diffractive optical element (SHADOE)
- Made of five HOEs at equally-spaced angles
- React only to UV light incident at 45^{o}
- Other light passes through
- Diffracts only into 0 and +1 orders

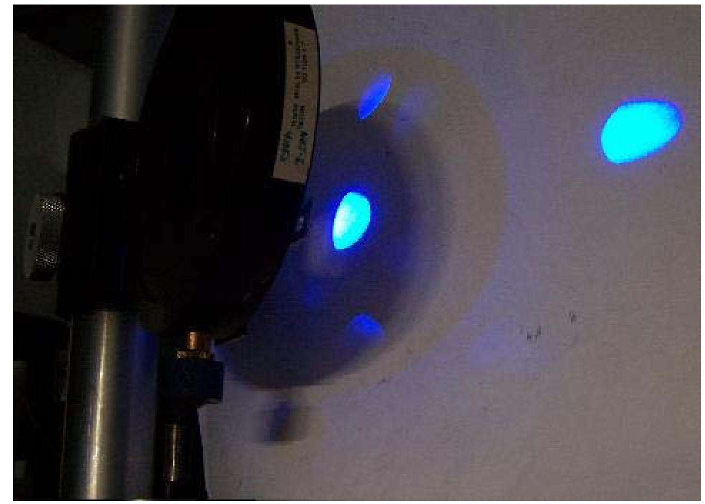

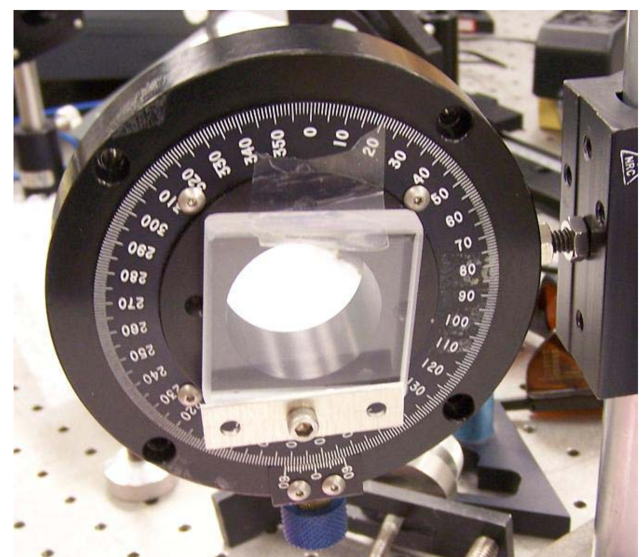

LabVIEW to Make Virtual Controls

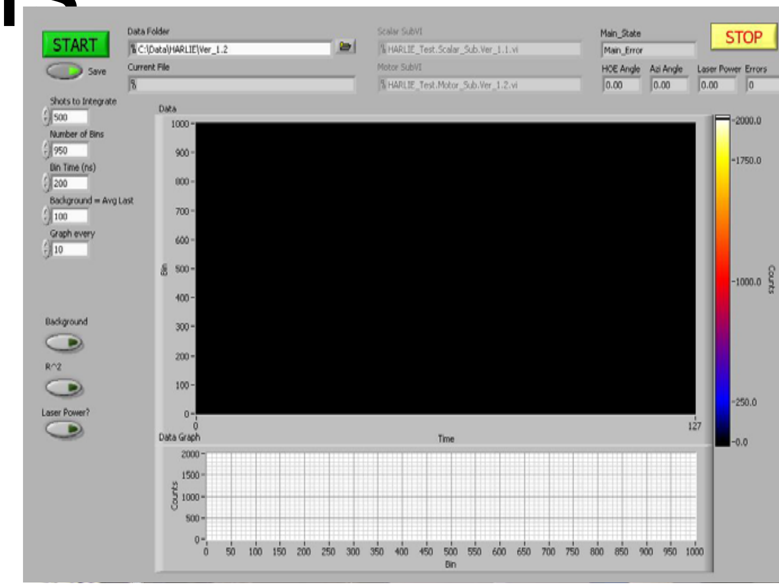

- Added on to existing LabVIEW program.
- Before controlled only rotation of HOE and data gathering
- Now control of the azimuth base
- Allows for full volumetric scan of a hemisphere

LabVIEW to Make Virtual Controls

- Added on to existing LabVIEW program.
- Before controlled only rotation of HOE and data gathering
- Now control of the azimuth base
- Allows for full volumetric scan of a hemisphere

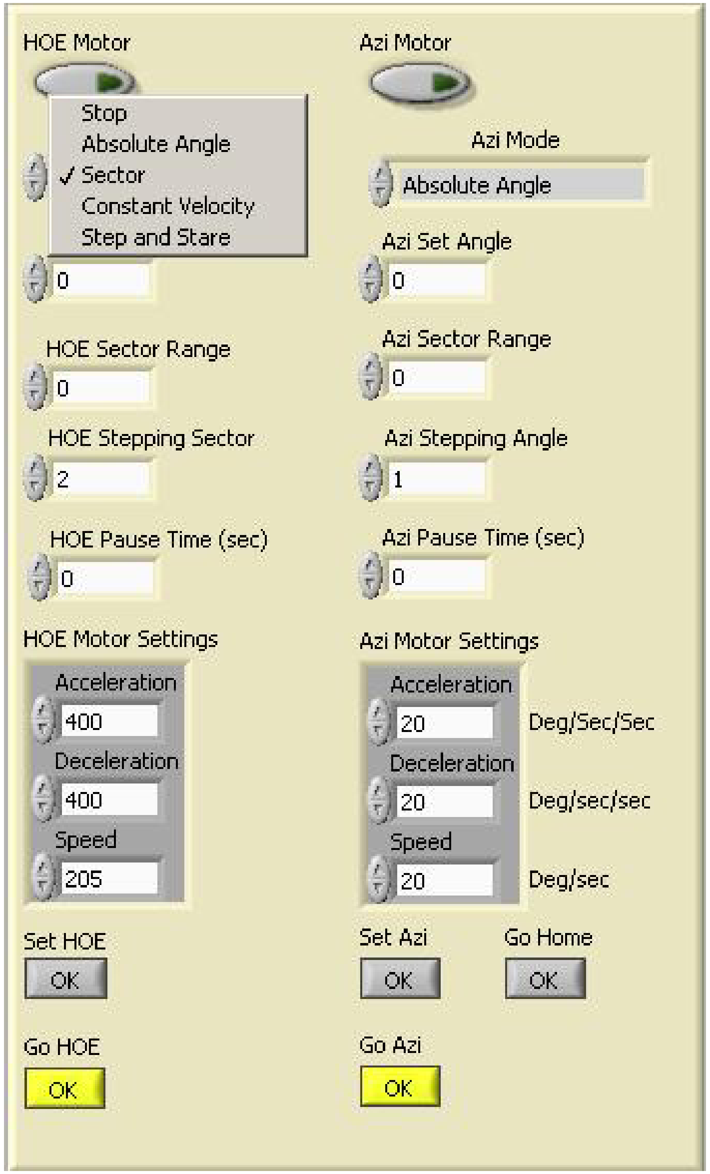

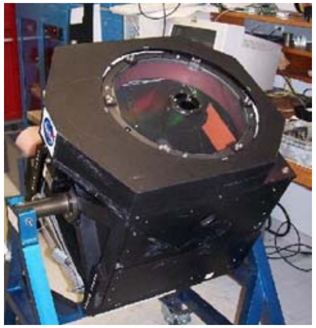

Results

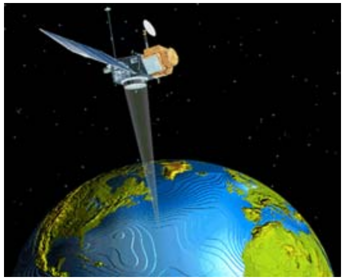

- Worked with state of the art holographic technology
- Tested developmental holographic elements and found areas for improvement
- Learned how to program in LabVIEW
- Upgraded HARLIE instrument with additional axis control

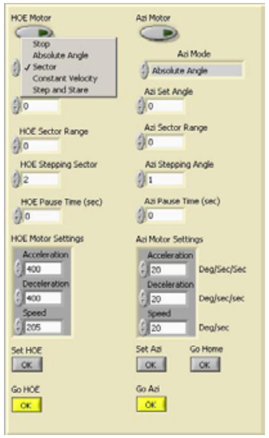

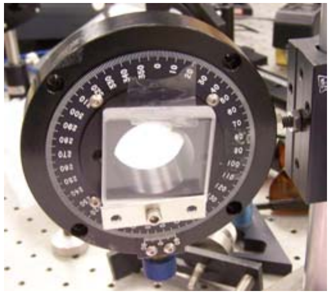

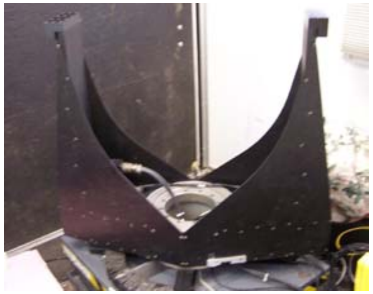

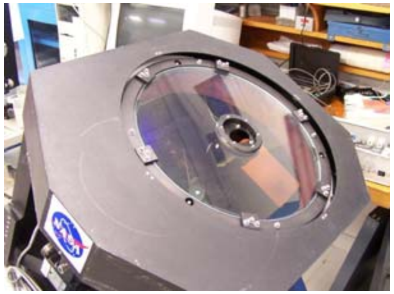

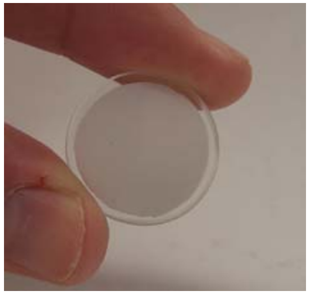

Thank you

- Geary Schwemmer for the enjoyable project and great advising
- David Miller for his computer expertise
- Per Gloersen for setting up the program
- Tammy Paolino for arranging the details
- All the students, who made this summer most enjoyable

Observations of Moisture and Temperature Variability in a Non-convective Dryline

NASA Summer Institute 2005

Teresa Inman
Lyndon State College
Mentor: Belay Demoz

Outline

- What is IHOP
- Why is it important to study drylines?
- Current Hypothesis
- AERI and King Aircraft
- Current Research
- Future Research Possibilities

The International H_2O Project (IHOP)

<u>IHOP2002_tidbits</u>

- The largest land-based experiment in the Continental US
- 22 May – 23 June 2002
- CI and H_2O Variability
- Profiling site:
  - Oklahoma panhandle, site called “*Homestead*”
  - Multi-lidar and multi-aircraft data collection

<u>Case Study:</u>

- Double dryline event on 22 May 2002 studied

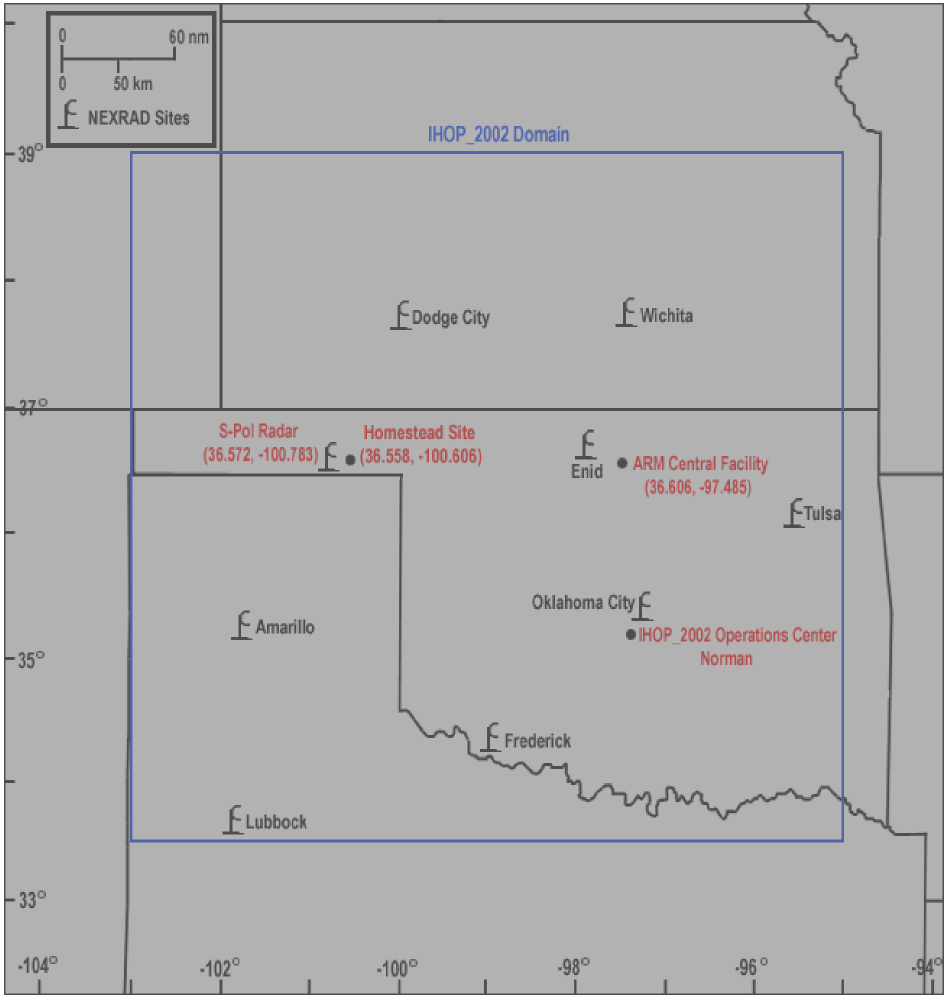

Why Study Drylines?

- Drylines are regions where frequent severe storms form
- Little is known about how moisture is being mixed in a dryline and how drylines affect convective initiation (CI)

Why study 22 May 2002

- Severe weather was forecasted to form but didn't
  - ➔ Null case

- It was found that there was enough lift/convection for clouds to reach the Lifting Condensation Level (LCL) but they did not reach the Level of Free Convection (LFC), which is required to form severe storms.

Current Hypothesis

- More than a lifting mechanism is required for CI, such as:
  - Deep and sustained moisture profile
  - Sustained convergence

Current Research - Tasks

Understand the mixing processes on 22 May 2002

1) Understand temperature and moisture as derived by the Atmospheric Emitted Radiance Inferometer (AERI) data

2) Understand the moisture/temperature data measured by the University of Wyoming King Aircraft data

3) Understand the mixing mechanism at work:
   - Plot *Moisture* versus *Potential Temperature* for each instrument platform and combine the data to see similarity/difference between the two instruments.
   - *Explain the mixing mechanisms on that day.*

1) AERI: *Atmospheric Emitted Radiation Instrument*

- Measure the absolute infrared spectral radiance

- From these measurements vertical profiles can be created of temperature and pressure

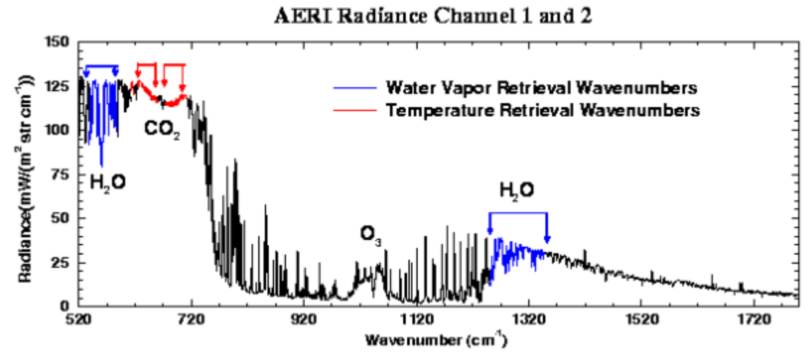

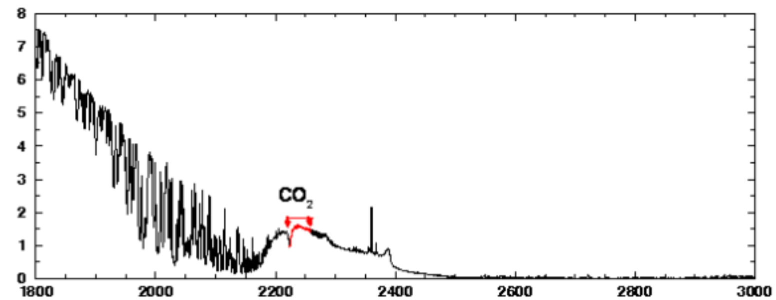

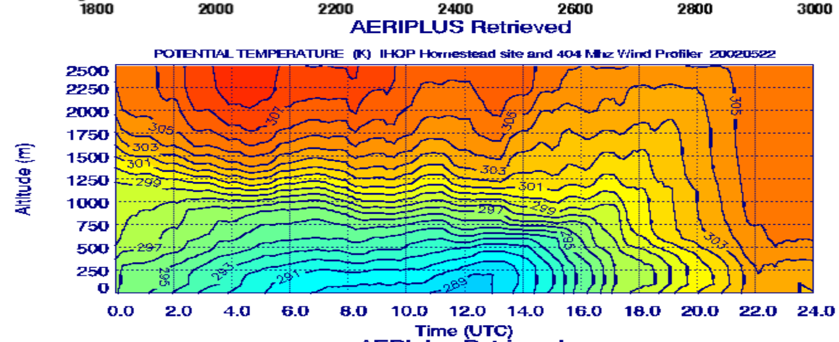

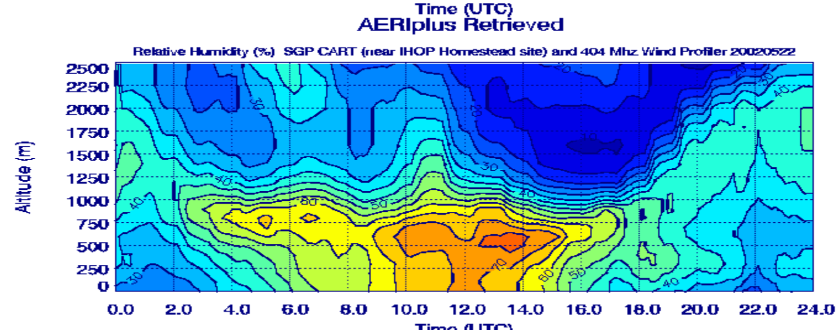

2) University of Wyoming King Aircraft

- Collects “point” measurements of the state parameters (T, P, moisture) much of the same data as the AERI in addition to radar profiles
- Makes several passes over the Homestead area, where the AERI remains in a fixed position
- Datasets that transect the dryline from east to west and are close to Homestead were used

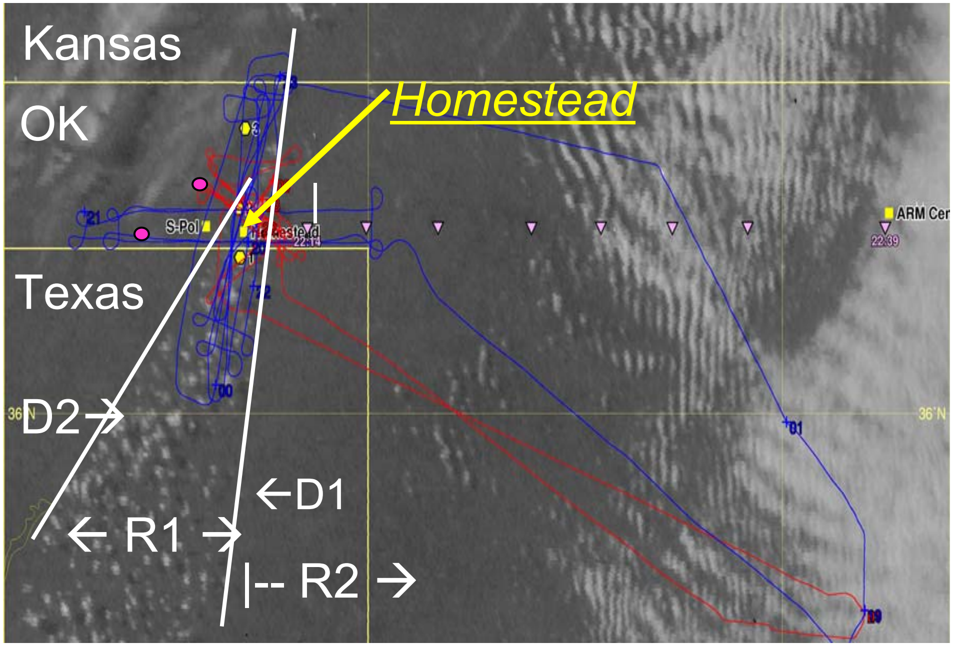

3) Understand the moisture mixing mechanism at work on 22 May 2002

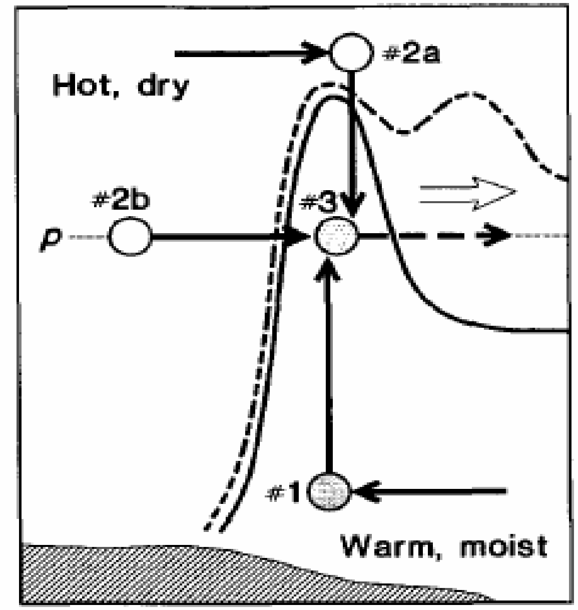

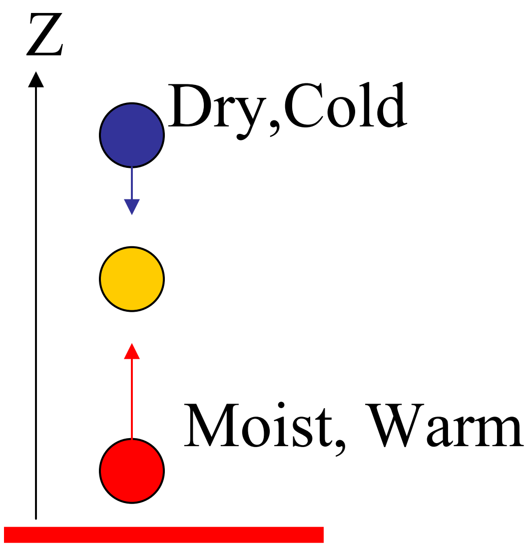

Convective "parcel" Mixing

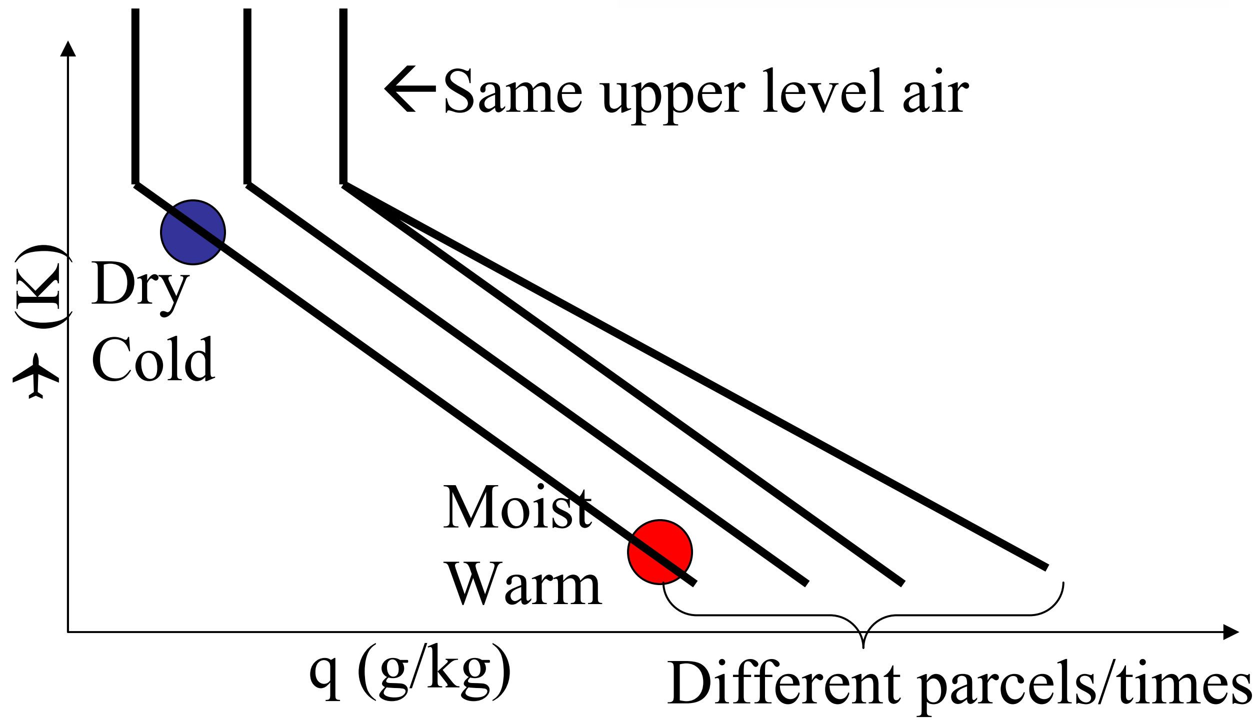

3) 22 May 2005: *Mixing Mechanism at Work*

1) Potential temperature versus moisture plots:
    1) Linear trends reveal the action of convective mixing in the CBL
    2) As Z varied from 0.5km to 3.0 km, for the time series, the variability decreased ➔ Hint of convergence to a point.
    3) Convergence to a "point" ➔ upper trop is the same airmass!

2) We need to see temporal variation of the mixing line.

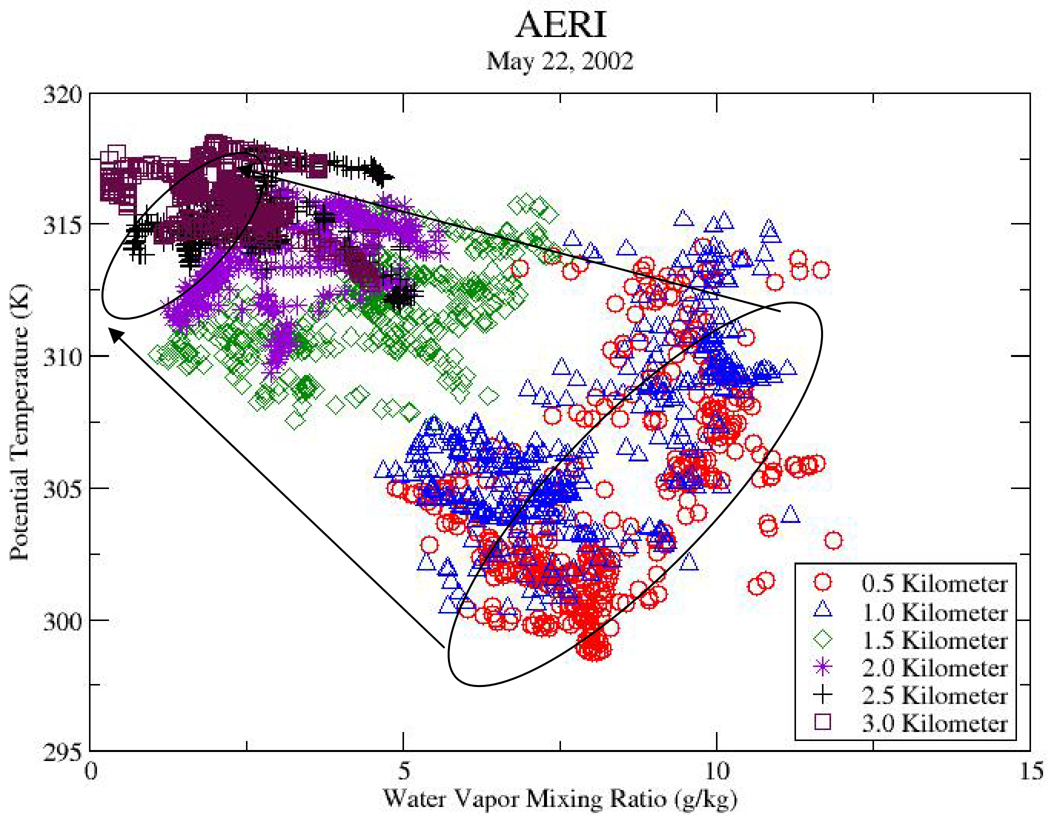

3) 22 May 2005: *Mixing Mechanism at Work*

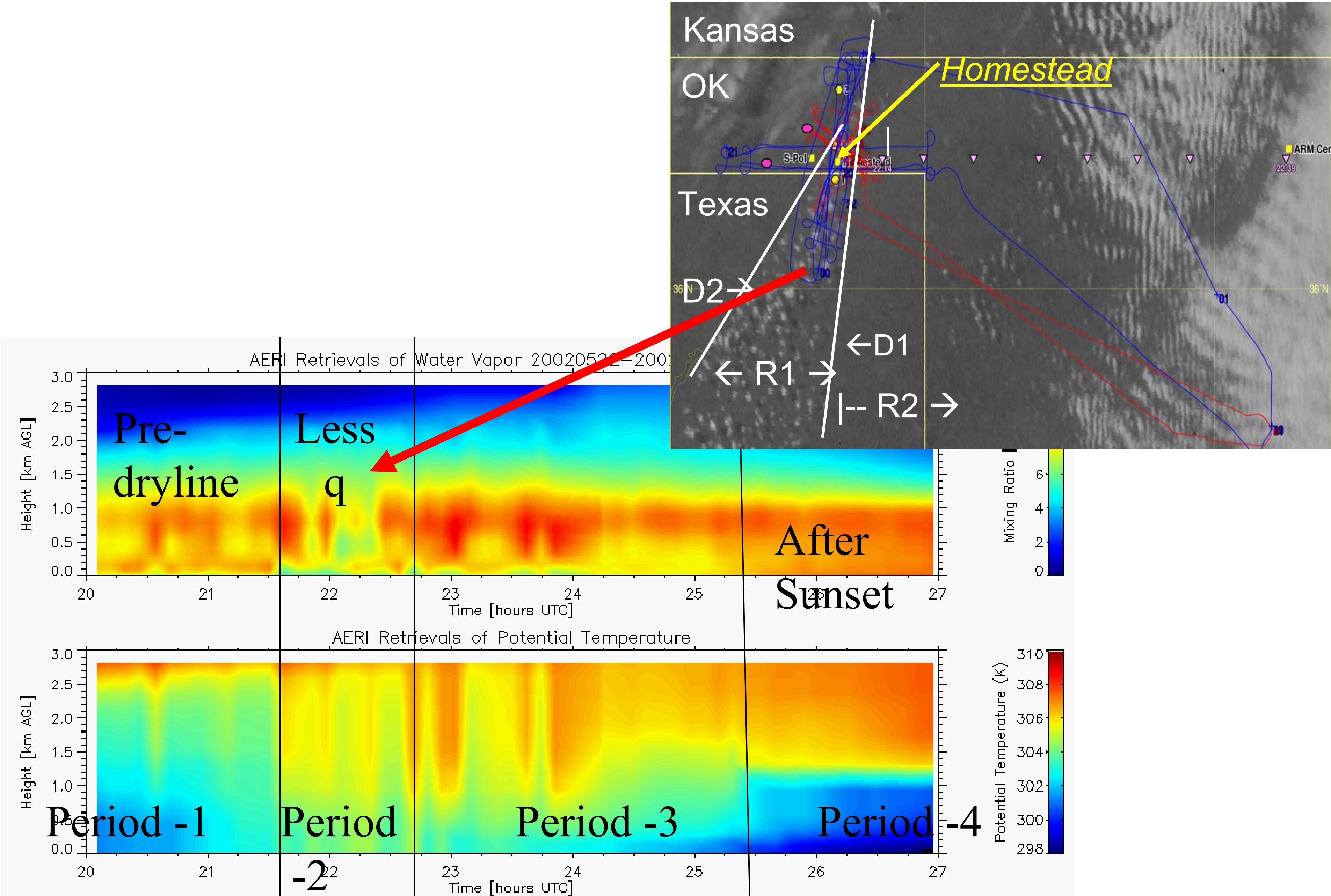

3) 22 May 2005: *Mixing Mechanism at Work*

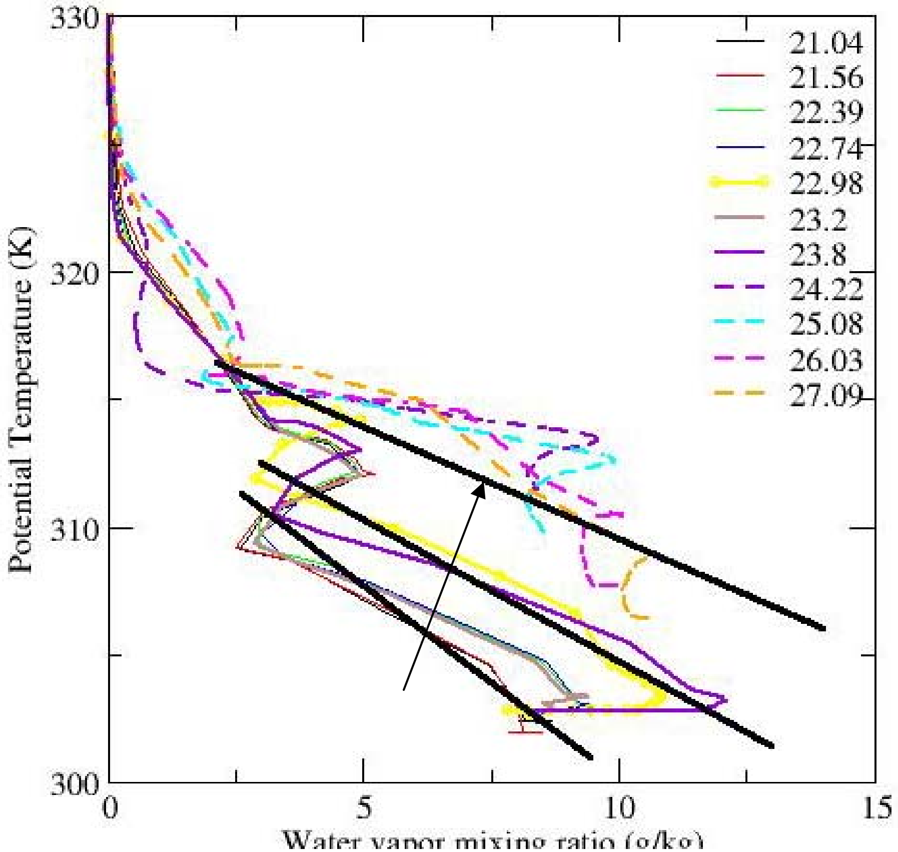

- Earlier in the day the moisture profile “jumps” as mixing is occurring from another airmass
- As time increases the amount the moisture profile jumps decreases
- This is due to mixing throughout the layer

3) 22 May 2005: *Mixing Mechanism at Work*

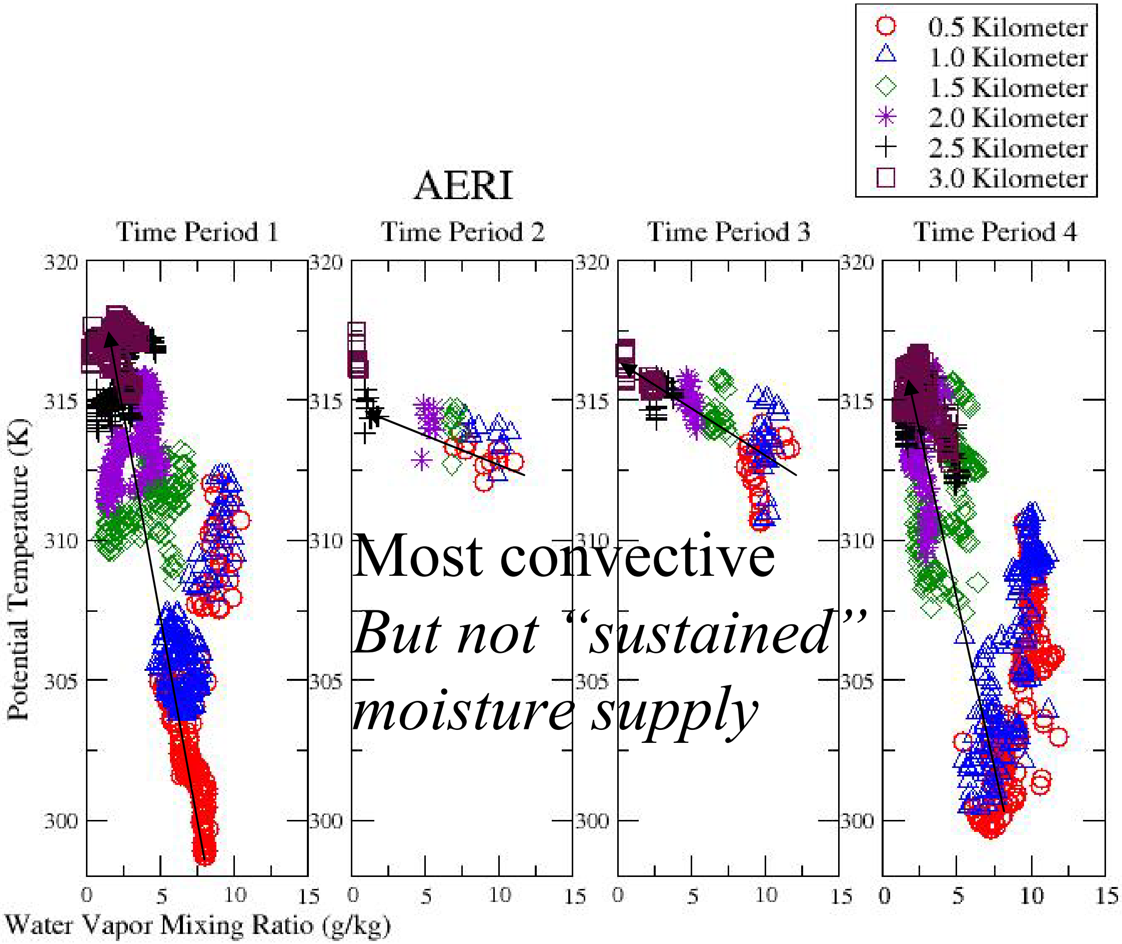

The change in the slope indicates differences in CBL (how convective the region was) and the location of the airmass – west or east side of the dryline.

King Aircraft Data

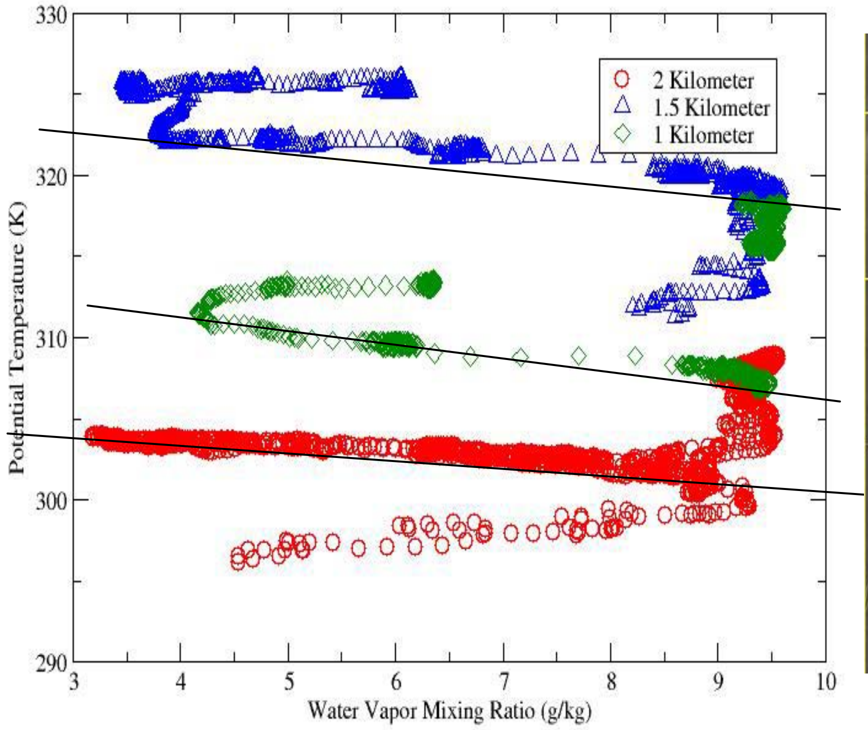

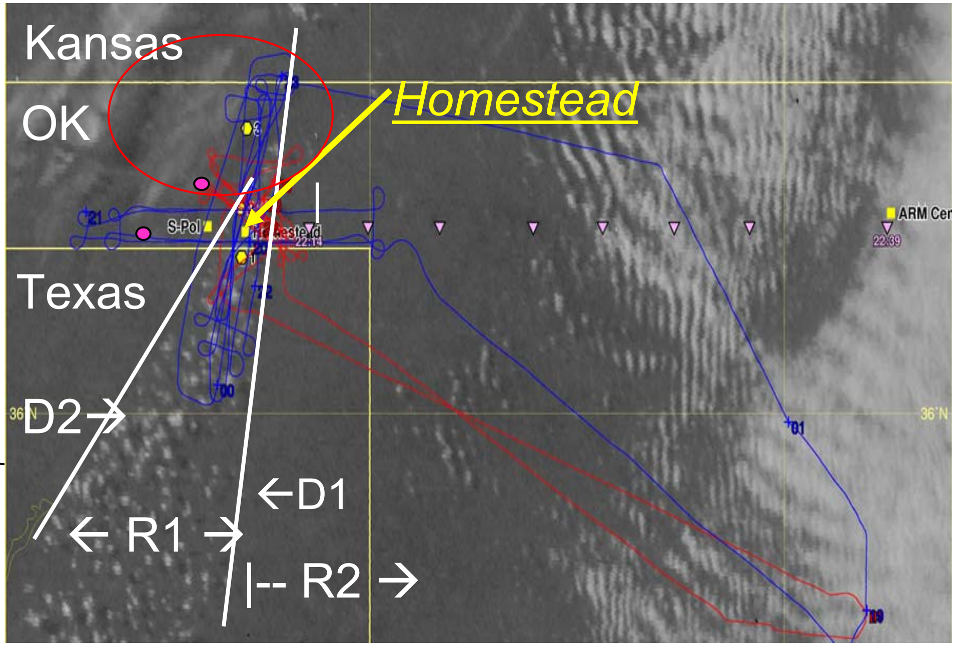

This does not seem to converge to a point. Possible reasons could be that

1) Advection of air is more prominent (in particular at 2km)
2) The hypothesis may not work when considering large distances (King air legs could be ~60km (10min*60sec/min*100m/sec)

More work is needed!

Future Research

- Explain the King Air data.
- Do the same graphs and research for the Scanning Raman Lidar (SRL) and also compare results to wind data.
- Compare data from different instruments.
- Perform same studies on more dryline cases!

Questions?

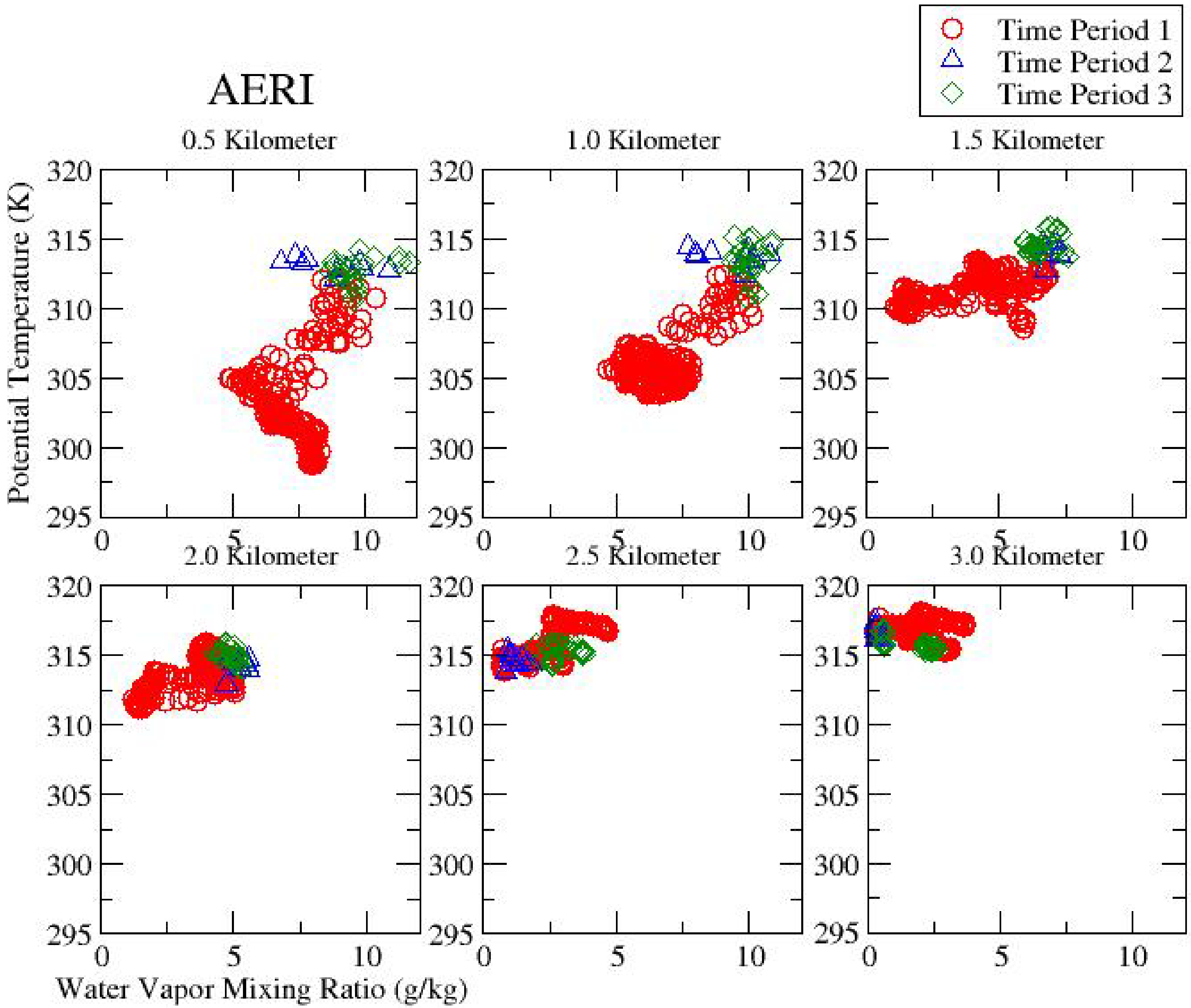
AERI
Time Period 1
Time Period 2
Time Period 3
0.5 Kilometer
1.0 Kilometer
1.5 Kilometer
2.0 Kilometer
2.5 Kilometer
3.0 Kilometer
Potential Temperature (K)
Water Vapor Mixing Ratio (g/kg)
320
315
310
305
300
295
0
5
10

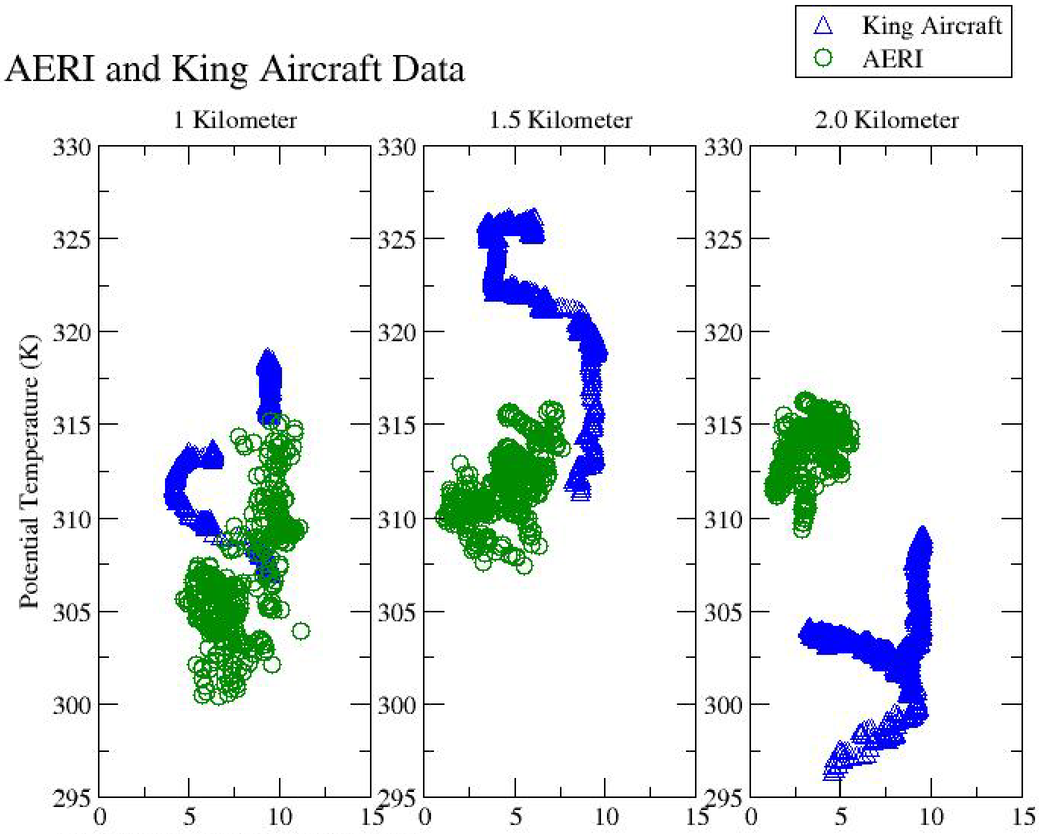

AERI and King Aircraft Data
King Aircraft
AERI
1 Kilometer
1.5 Kilometer
2.0 Kilometer
Potential Temperature (K)
330
325
320
315
310
305
300
295
0
5
10
15

Visualization and Analysis of Fire Radiative Energy measurements from MODIS

Luke Ellison
Charles Ichoku, mentor

August 12, 2005

Goal

FRP=fire radiative power

MODIS' scanning characteristics

Large volume of data is difficult to analyze without visual aid

Solution: Develop visualization tool

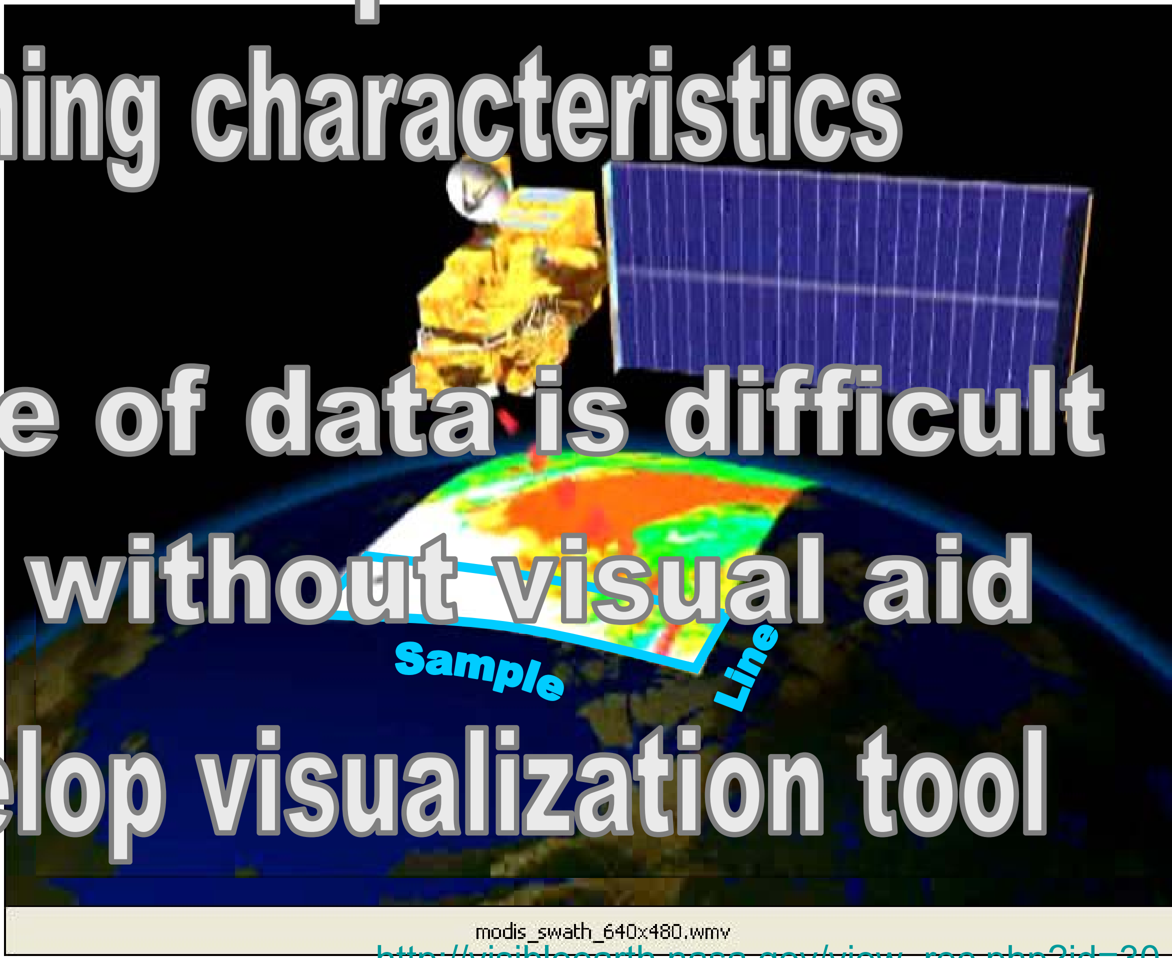

http://visibleearth.nasa.gov/view_rec.php?id=30

Visualization

Previously:

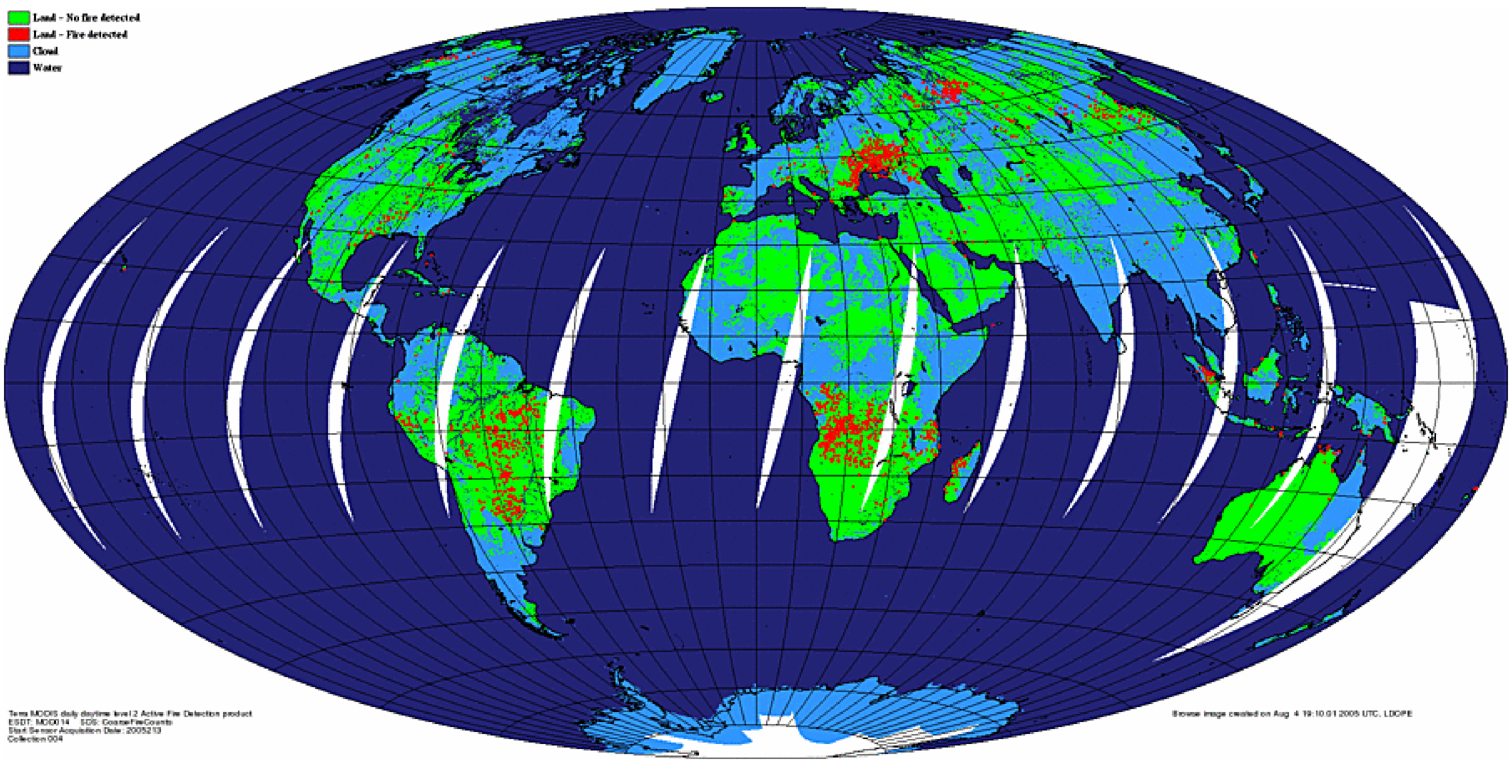

Visualization

- appearance of fire pixels
- fires are color-coded
- picture background for comparison
- save methods for easy access to data

Analysis EXPECTED

Example 1

Alaska, July 11, 2004

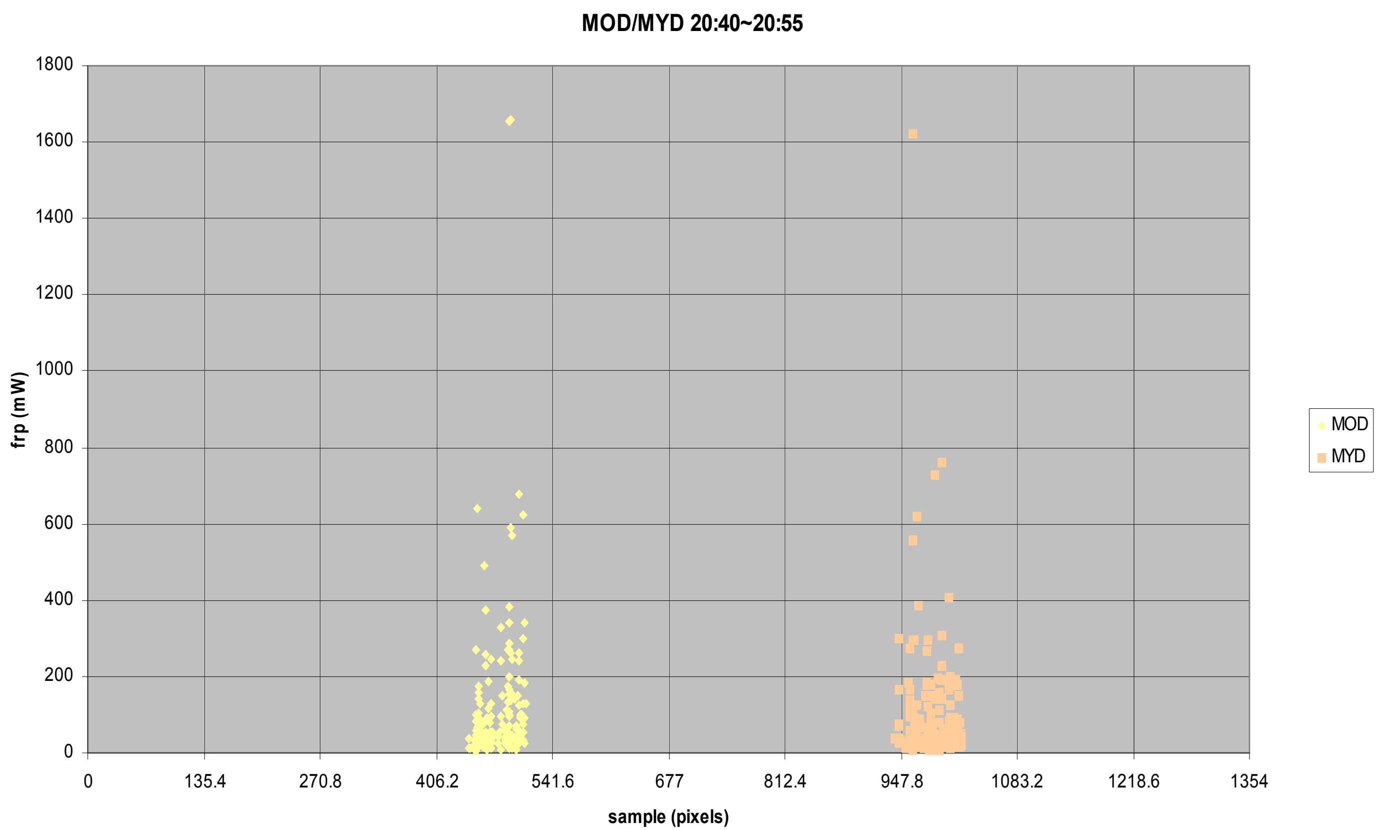

# fires=	354
ave sample=	478.0508
total frp=	45317.01
# fires=	348
ave sample=	984.569
total frp=	35590.01

difference	% difference
-6	-1.7094017
506.5181	69.2617608

Analysis EXPECTED

Example 2

**Alaska,
July 13, 2004**

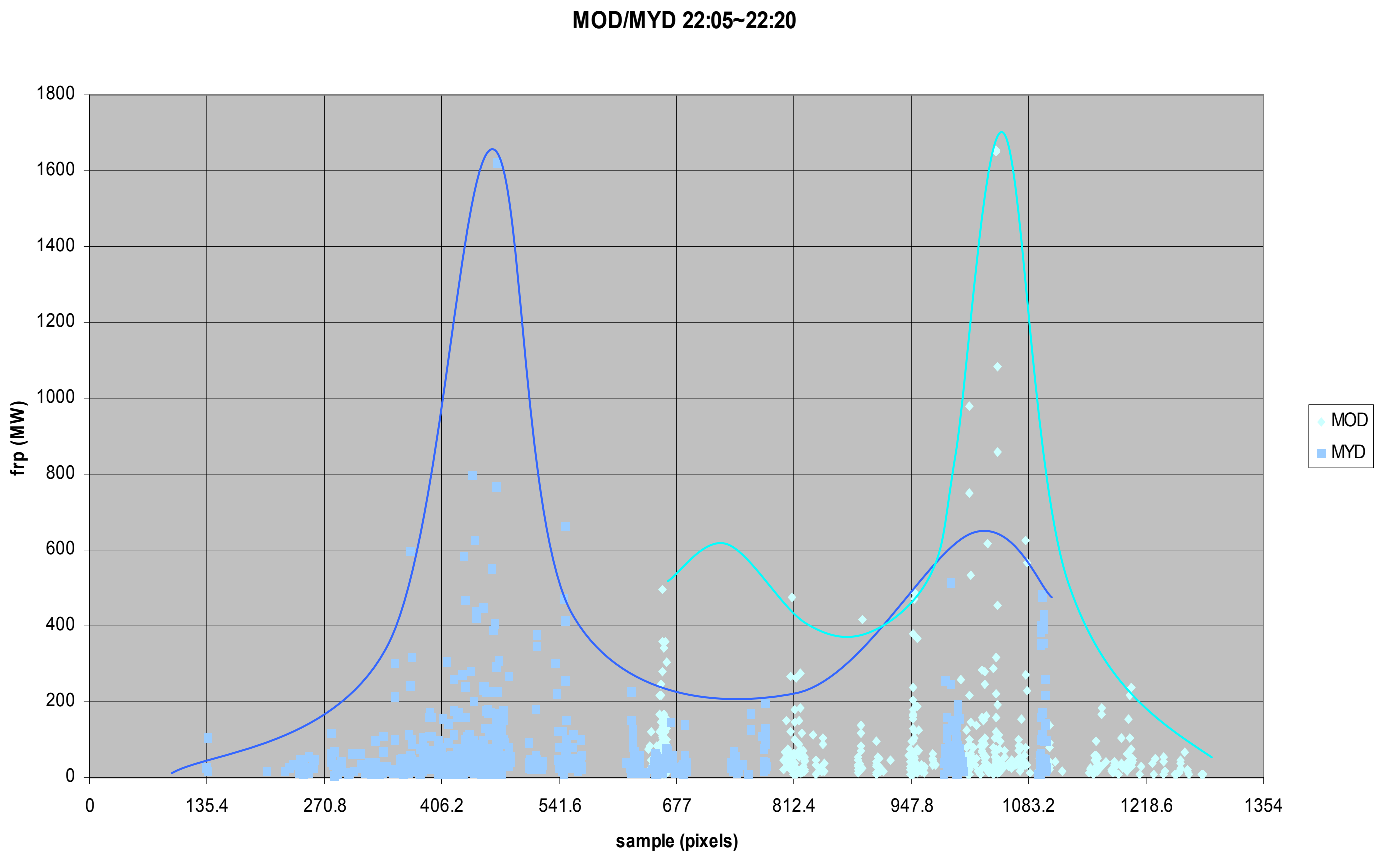

# files=	1040
ave sample=	957.2846
total frp=	92951.46
# files=	722
ave sample=	557.6828
total frp=	54778.7

difference	% difference
-318	-36.0953462
-399.602	-52.75384528

Analysis EXPECTED

Example 3

**Russia,
July 15, 2003**

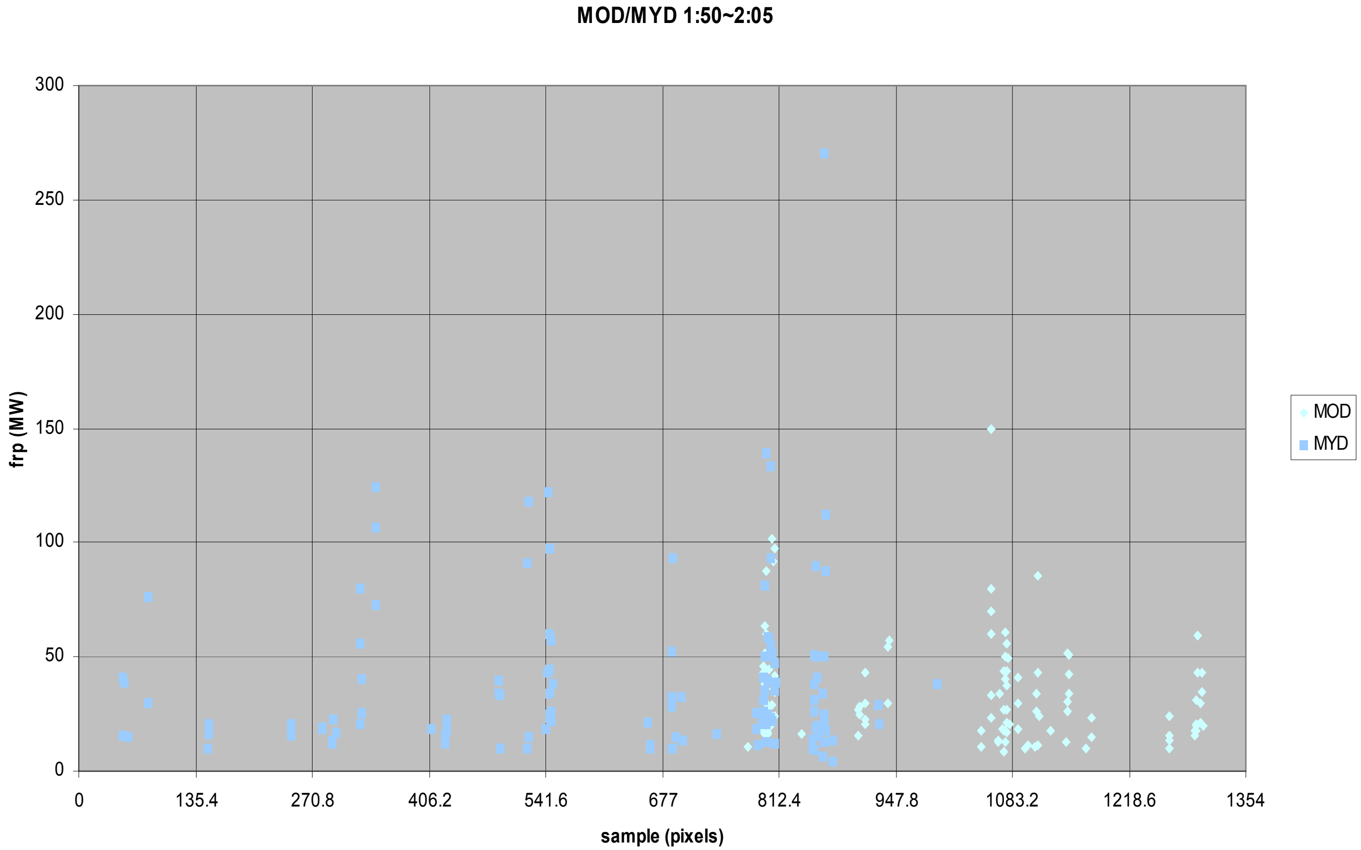

# fires=	464
ave sample=	1018.112
total frp=	15822.78

# fires=	391
ave sample=	629.3785
total frp=	15081.12

difference	% difference
-73	-17.07602339
-388.734	-47.19098922

Analysis ERRORS

Example 4: March 9~13, 2005

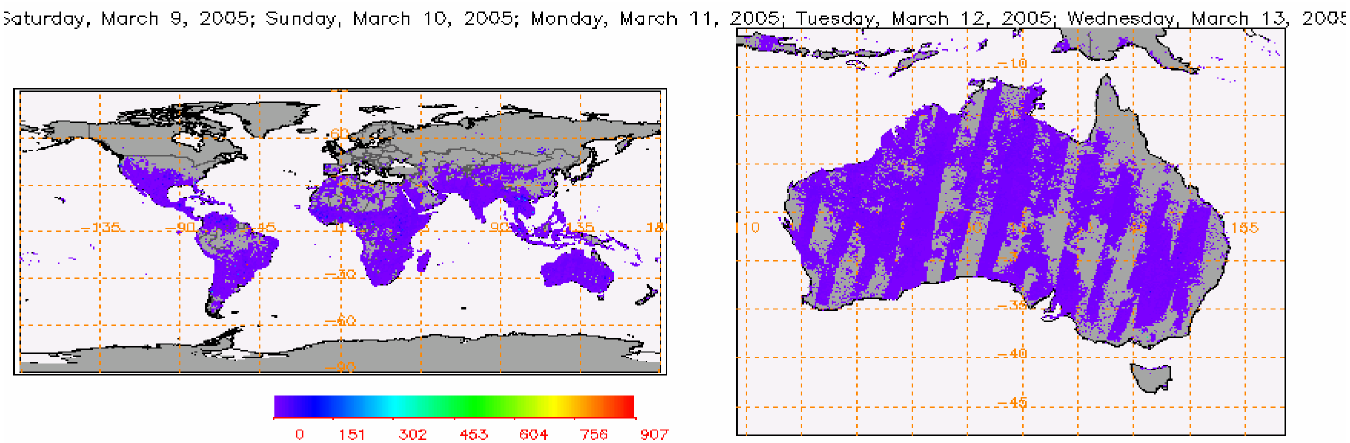

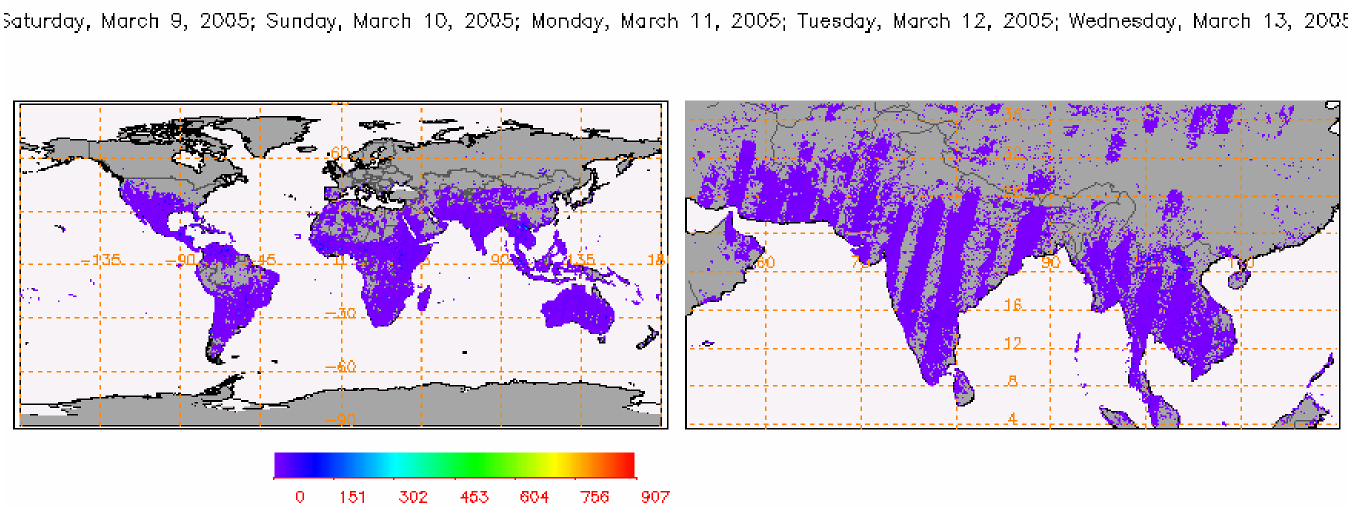

Analysis ERRORS

3/7/05

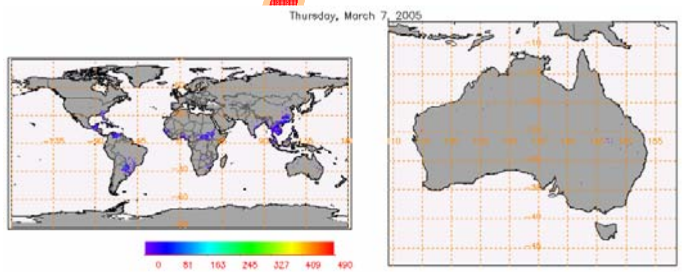

3/8/05

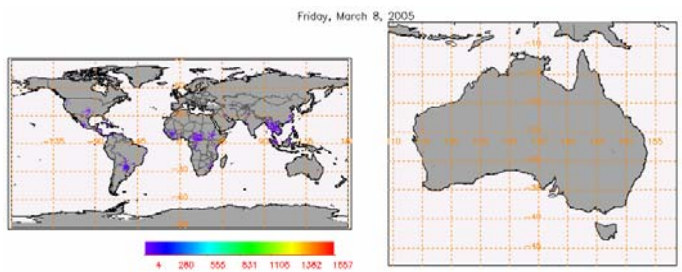

3/9/05

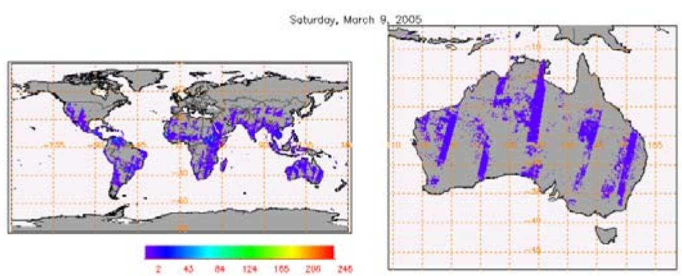

3/10/05

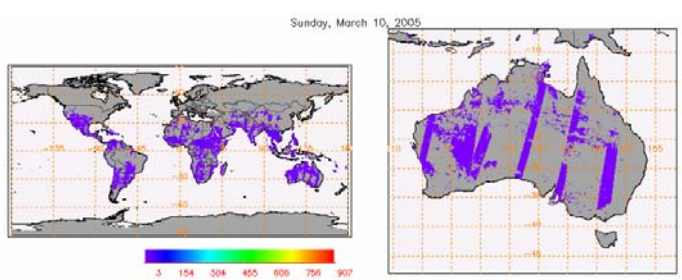

3/11/05

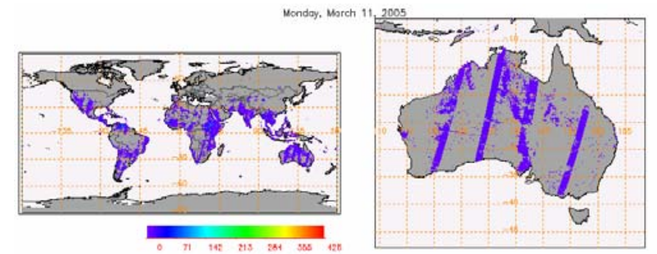

3/12/05

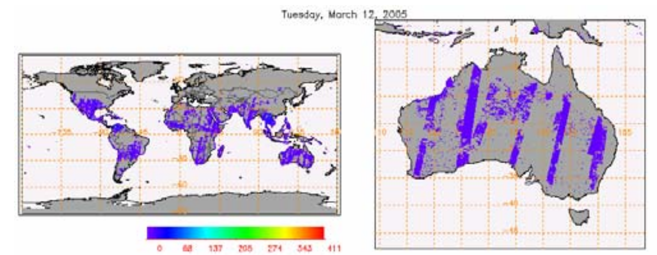

3/13/05

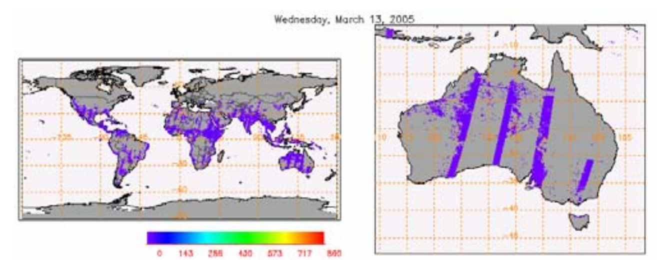

3/14/05

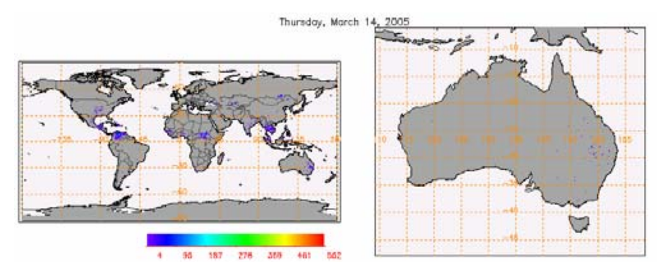

Analysis INCONGRUENCIES

Example 5: July 1, 2004

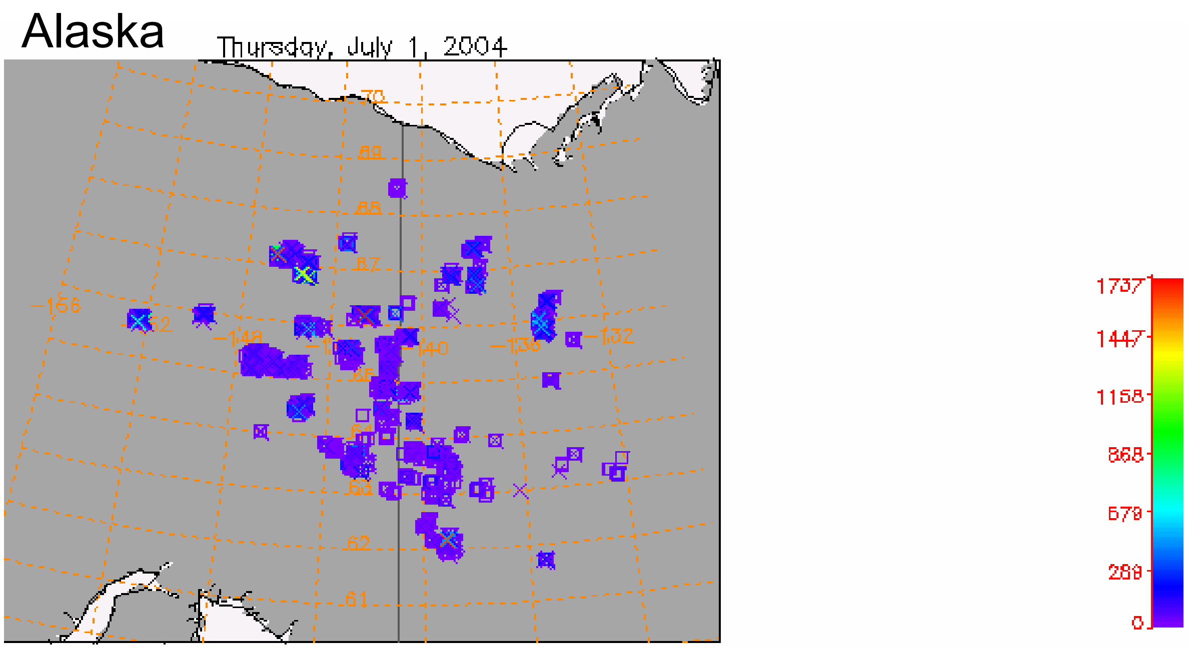

Analysis INCONGRUENCIES

Example 5: July 1, 2004

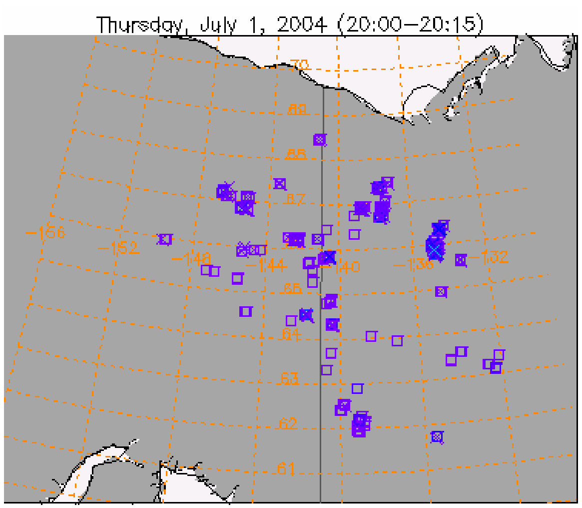

MOD/MYD 20:00~20:15

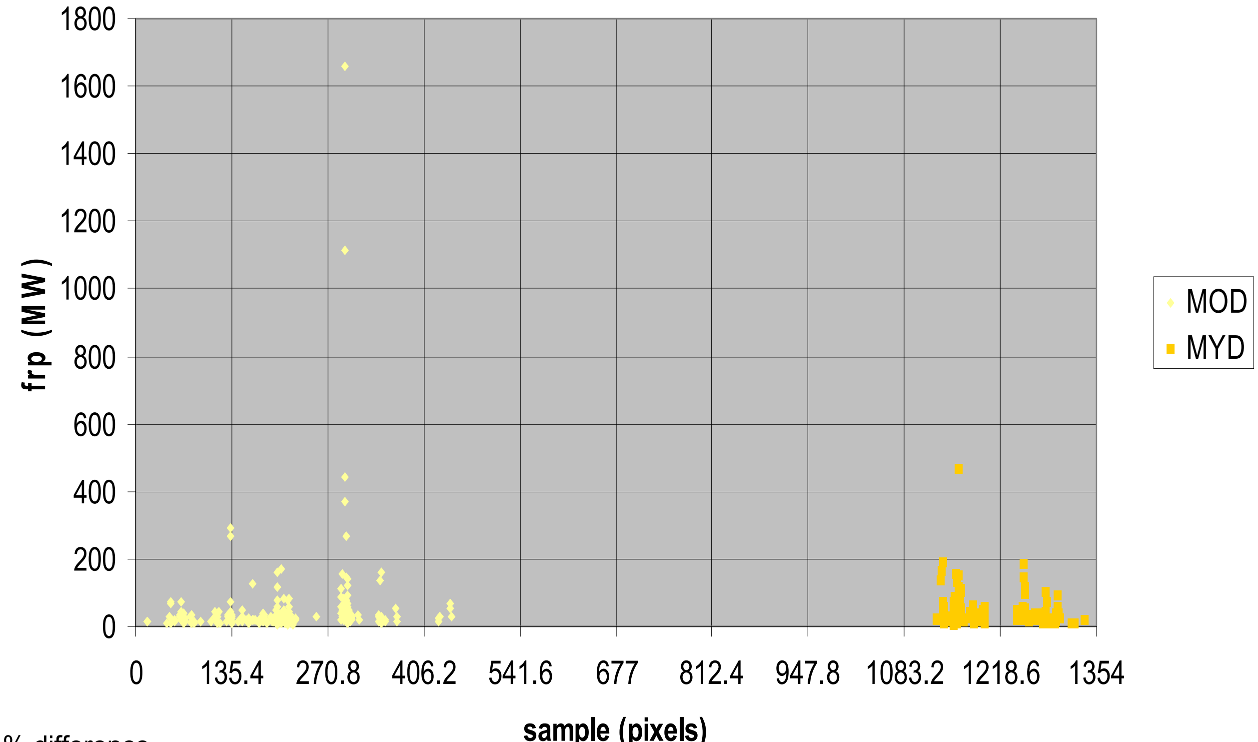

# fires=	241
ave sample=	206.7054
total frp=	12511.4

# fires=	166
ave sample=	1210.602
total frp=	7377.392

difference	% difference
-75	-36.85503686
1003.897	141.6625256

Analysis INCONGRUENCIES

Example 5: July 1, 2004

MOD/MYD 23:15~23:30

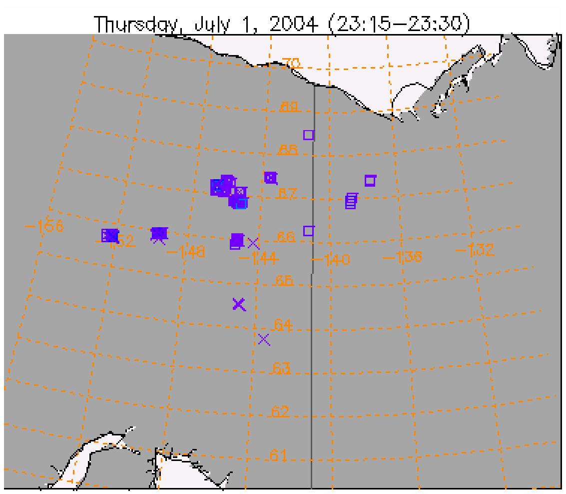

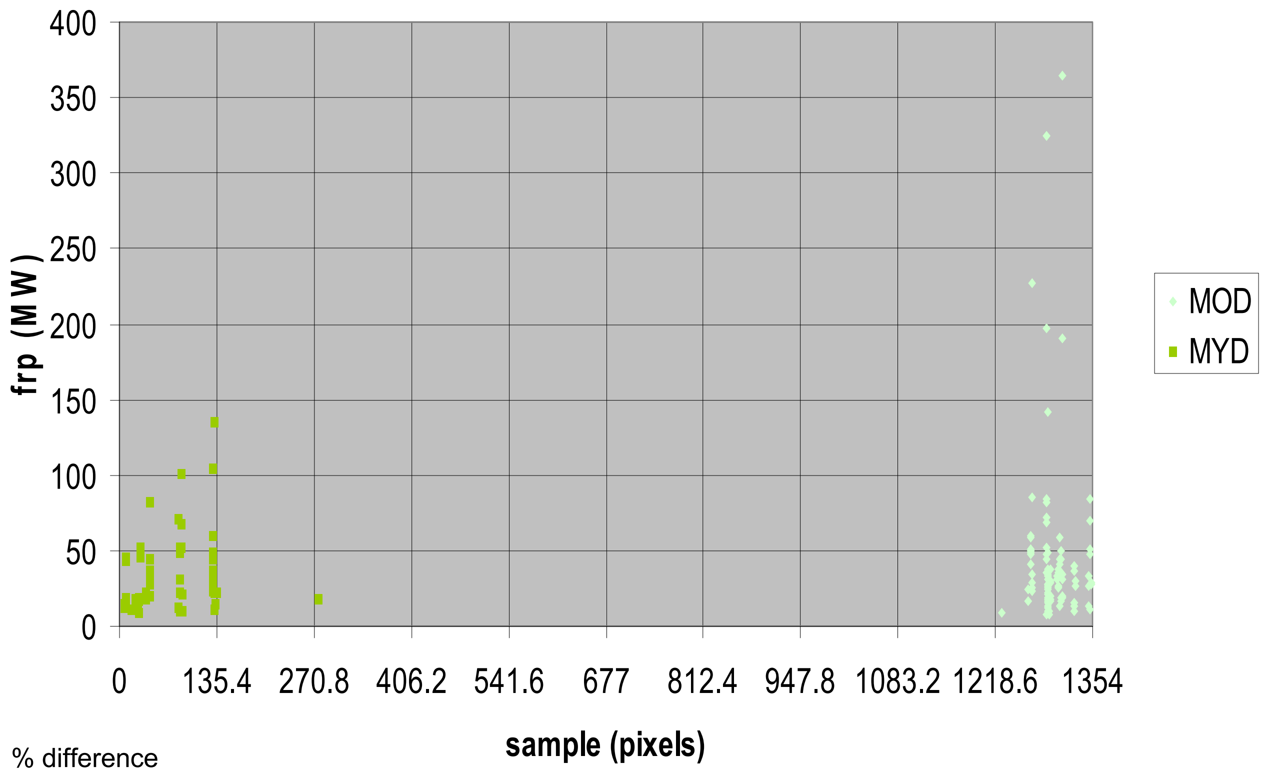

# fires=	100
ave sample=	1300.29
total frp=	4561.497
# fires=	54
ave sample=	74.42593
total frp=	1825.622

difference	% difference
-46	-59.74025974
-1225.86	-178.3443475

Analysis INCONGRUENCIES

Example 5: July 1, 2004

MOD/MYD 21:40~21:55

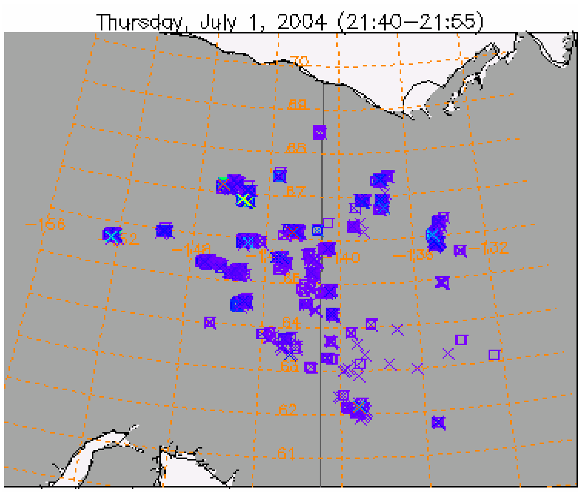

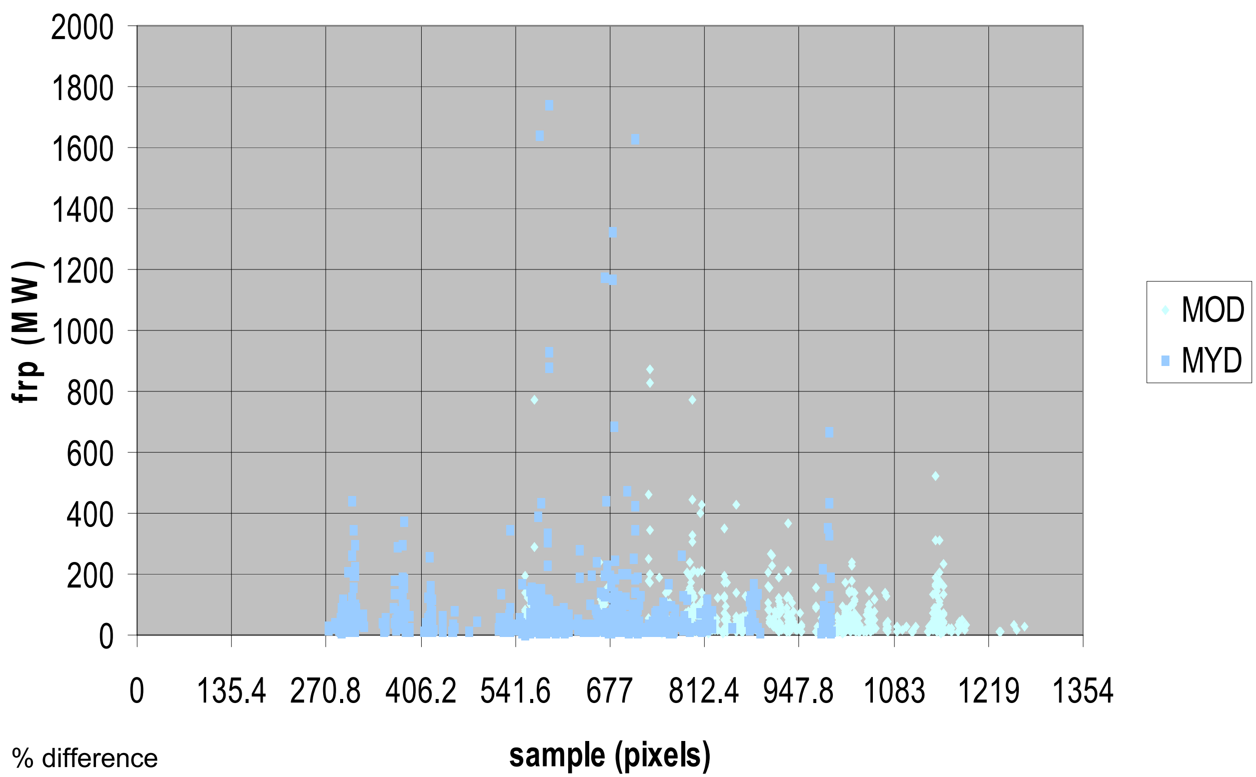

# fires=	666
ave sample=	908.8994
total frp=	42625.46

# fires=	869
ave sample=	607.5512
total frp=	59575.63

difference	% difference
203	26.4495114
-301.348	-39.74388478
16950.17	33.17023917

Analysis INCONGRUENCIES

Example 6

Russia, August 1, 2005

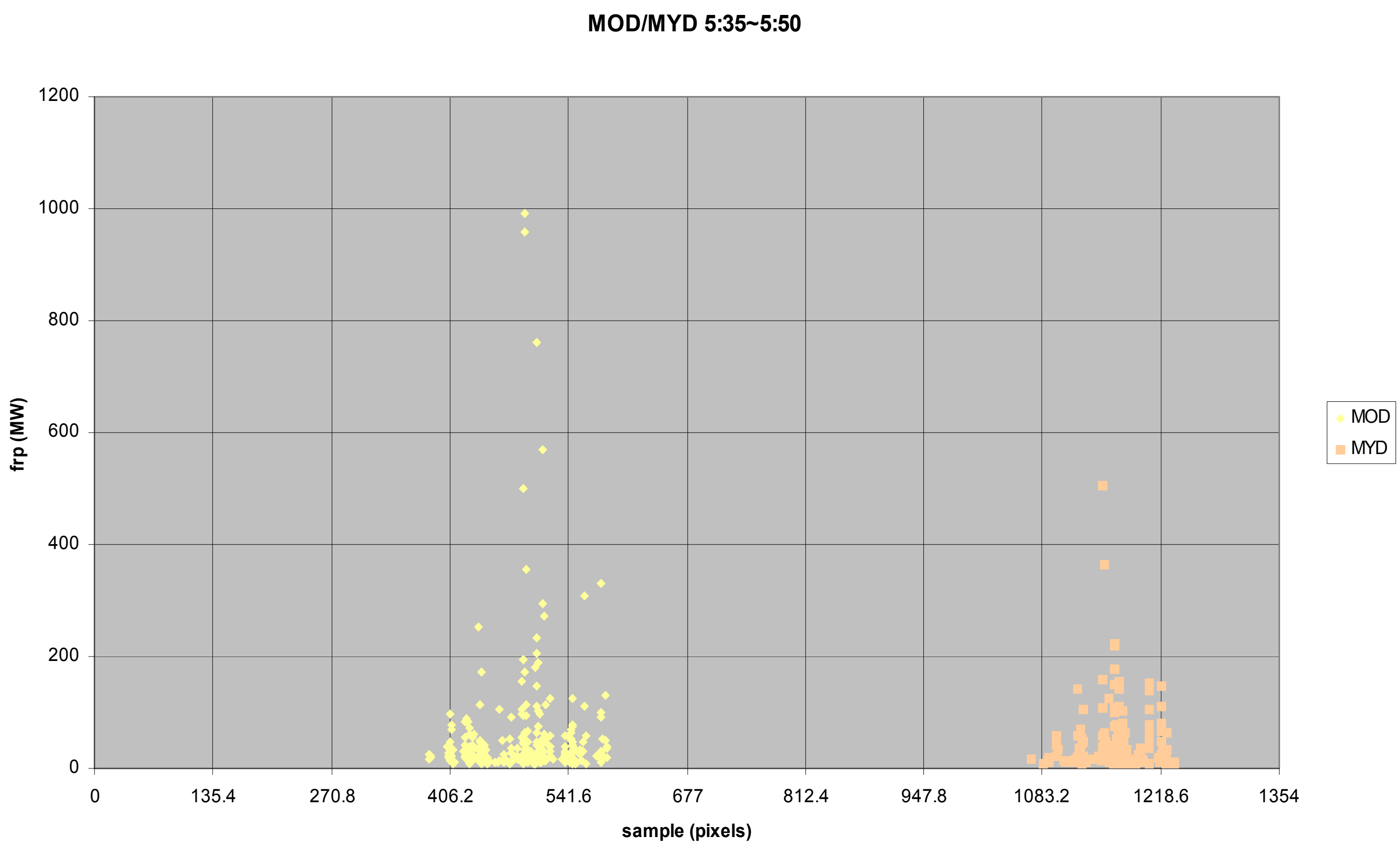

# fires=	292
ave sample=	486.7226
total frp=	16953.81
# fires=	169
ave sample=	1166.509
total frp=	7817.13

difference	% difference
-123	-53.362256
679.7863	82.2372767

Future

continue analyzing data to find problems

fix algorithms to correct problems if needed

find relations b/w fire data and other parameters

fix MappingFRP program

Resources

PEOPLE:

• Charles Ichoku (mentor): Was my mentor and therefore gave me a job for the summer. He helped me understand my tasks quickly and reasonably.

• Jeff Guerber (via Stephen Fiegles via Per Gloersen): He gave me much assistance in the IDL language when I was stuck.

• any others who helped me here and there including those who took time to encourage me. Thank you.

BOOKS:

•Fanning, David W., Ph. D. IDL Programming Techniques. Fort Collins, CO: Fanning Software Consulting, 1999.

•IDL Reference Books Version 5.1. Research Systems, Inc, 1998.

WEBSITES:

• Alphabetical List of IDL Routines. http://idlastro.gsfc.nasa.gov/idl_html_help/idl_alph.html.

Assessing the Transport of Aerosols Around The World

Kristen Mihalka

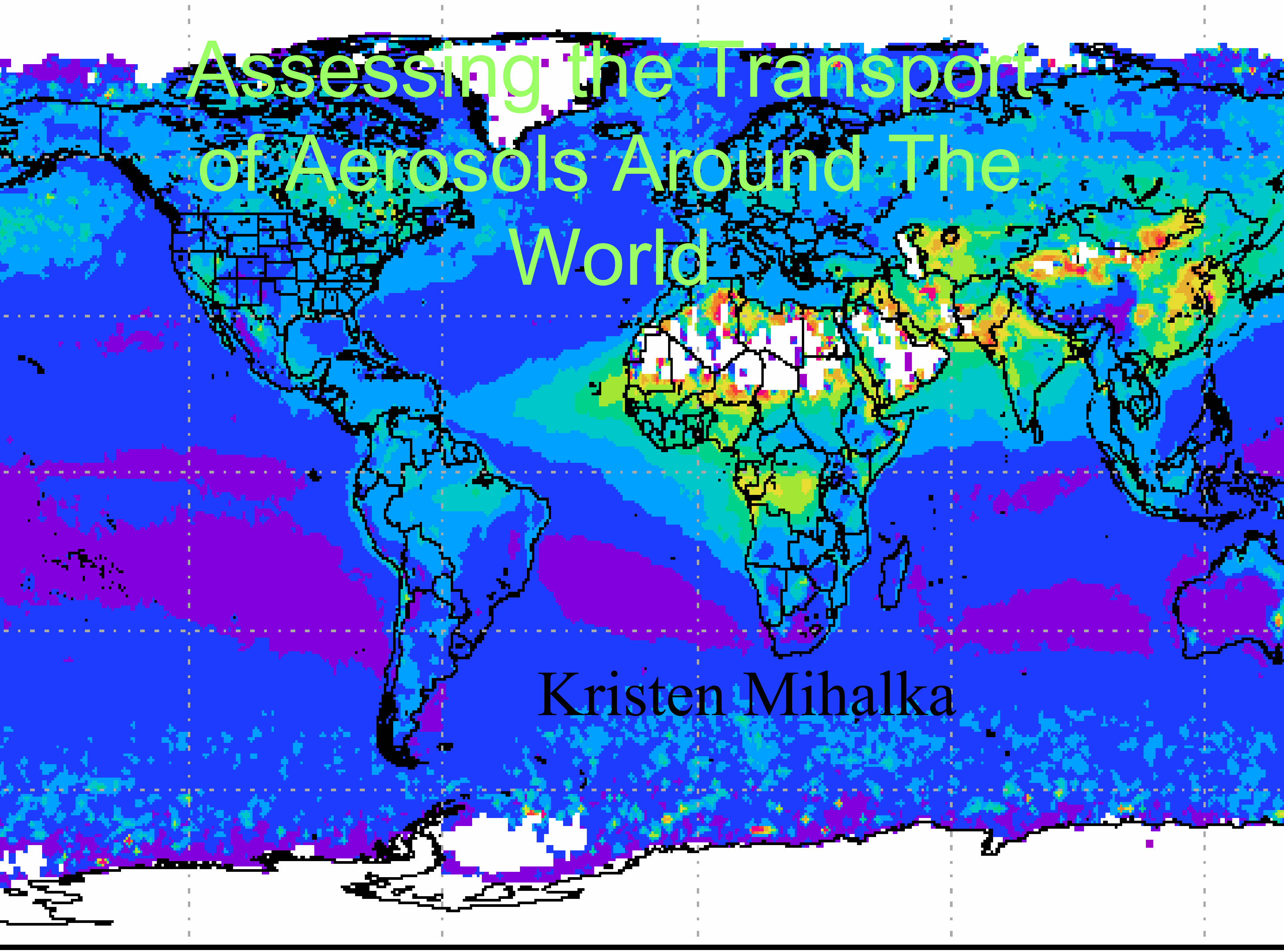

Aerosols

- Affects Earth’s albedo, surface temperature and atmosphere temperature
- Impacts cloud amount and precipitation
- Coarse and Fine
- Maritime, Smoke and Dust
- AOT-opacity of media
- Fine Fraction-helps in splitting up different types of aerosols

Satellite

July 19, 2005 Dust storm off the coast of West Africa 1420utc

- Multiple Channels needed
- POLDER first satellite design to detect Aerosols
- Aqua and Terra
- MODIS
- Nine channels

Objective

- Find the flux of Smoke and Dust
- Convert AOT to volume
- Get rid of Maritime's influence on the data
- Find the equations for Smoke and Dust based on volume
- Convert mass to volume
- Find the height in the atmosphere that the particles are located

Program

- National Center for Environment Prediction
- MODIS data for AOT
- 4 location
- Different box sizes

MOVAS

- Allows you to look examine aerosols monthly since 2000
- AOT
- White areas-clouds or too reflective
- Purple Maritime

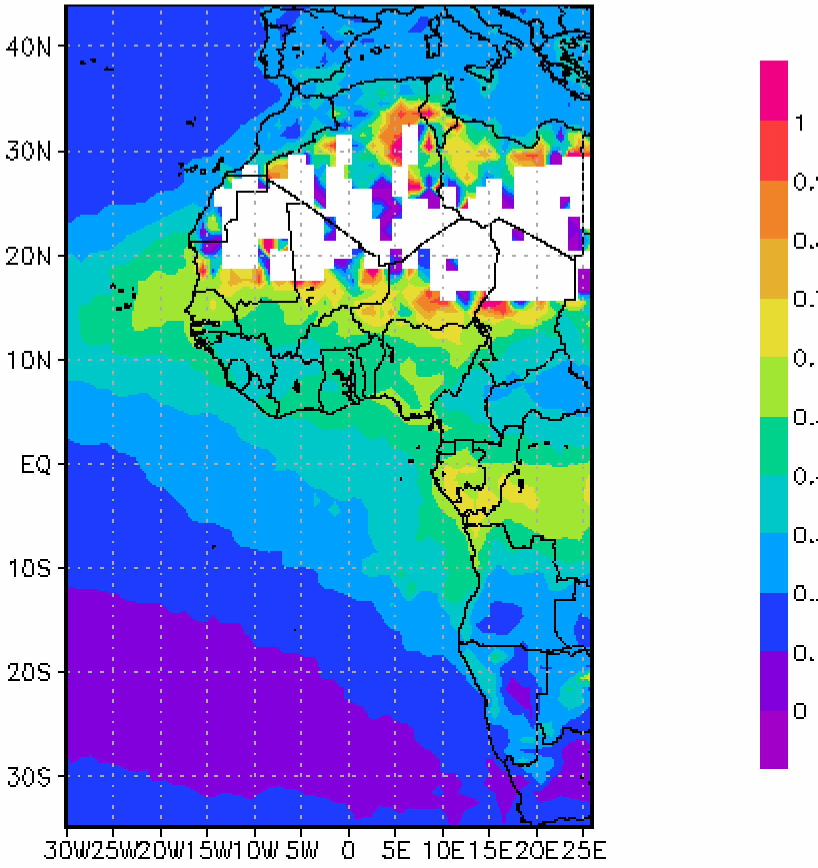

•http://g0dup05u.ecs.nasa.gov/Giovanni/

Maritime

Season	Coarse	Fine
Winter	=.0064*W	=.0005*W+.0001
Spring	=.008915*W	=.0003*W+.0067
Summer	=.0081*W	=.000133*W+.0049
Fall	=.008715*W	=.000133*W+.0056

Maritime aerosol is mostly Sea salt

1000mb winds

20S to 30s

Pure Maritime aerosols

Seasonal equations

Graph volume of fine vs magnitude of wind

Coarse mode find slope

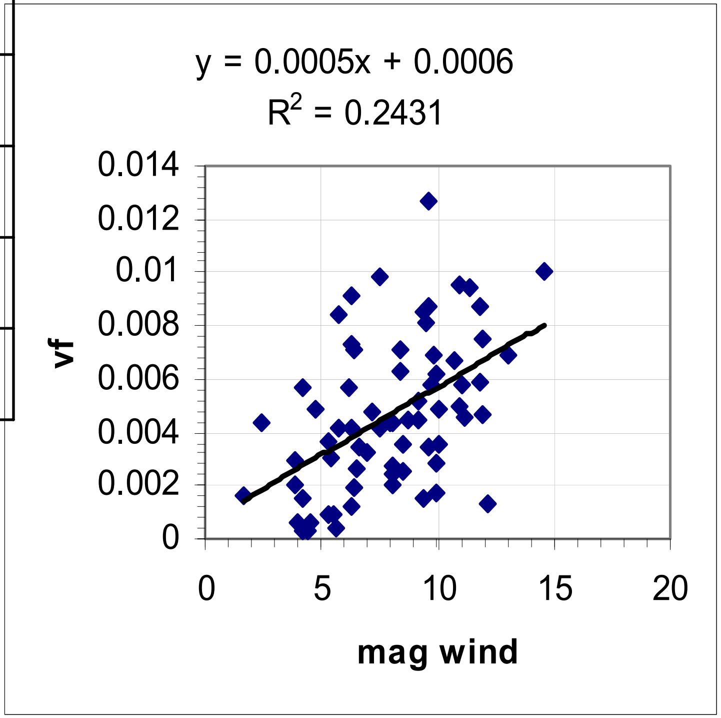

Spring Fine Mode Correlation

Smoke and Dust

- Depends on Fine and Coarse Modes
- Case studies
- Percent of total volume that is fine and coarse

$$VS = \frac{(73*Vf-17*Vc)}{60}$$

$$VD = \frac{(77*Vc-23*Vf)}{60}$$

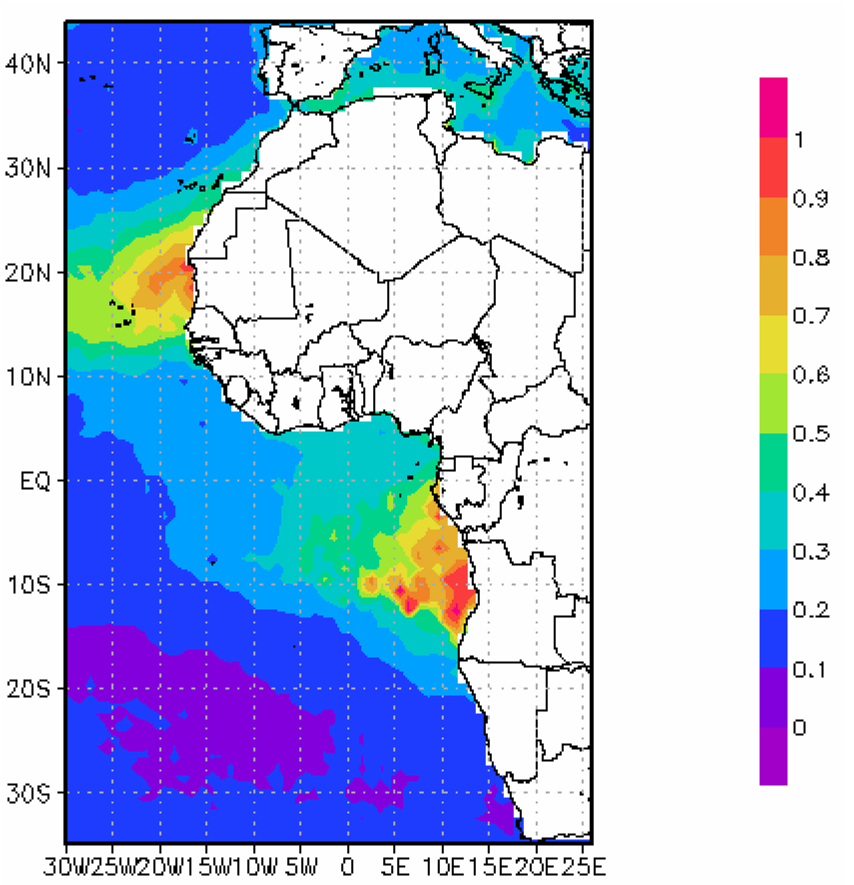

•http://g0dup05u.ecs.nasa.gov/Giovanni/

Height Correlation

- Find the location of dust and smoke in the atmosphere
- Correlation between height and mass of smoke and dust

	SS correl	SS height	FW correl	FW height
Smoke	.25	1000 mb	.22	750 mb
Dust	.28	1000 mb	.35	750 mb

Flux

- Flux=mass*wind speed
- Land to Ocean is postive
- Ocean to Land is negative
- Use winds that is perpendicular to the shore

	Smoke	Dust	Total
Area 1	15.1	6.6	21.7
Area2	10.5	-72	-62
Area 3	.18	164	164

*Results inTg/month/°4

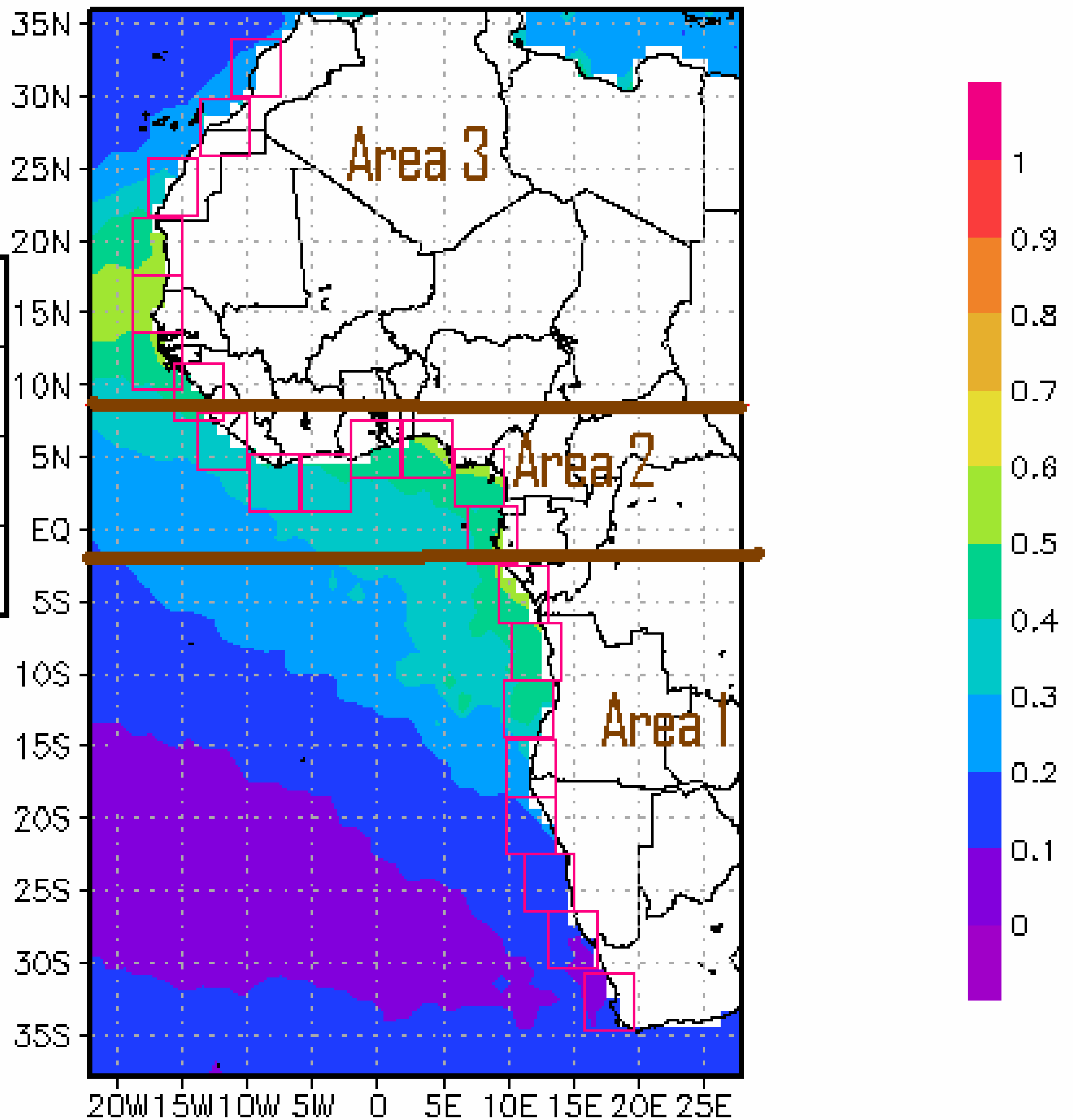

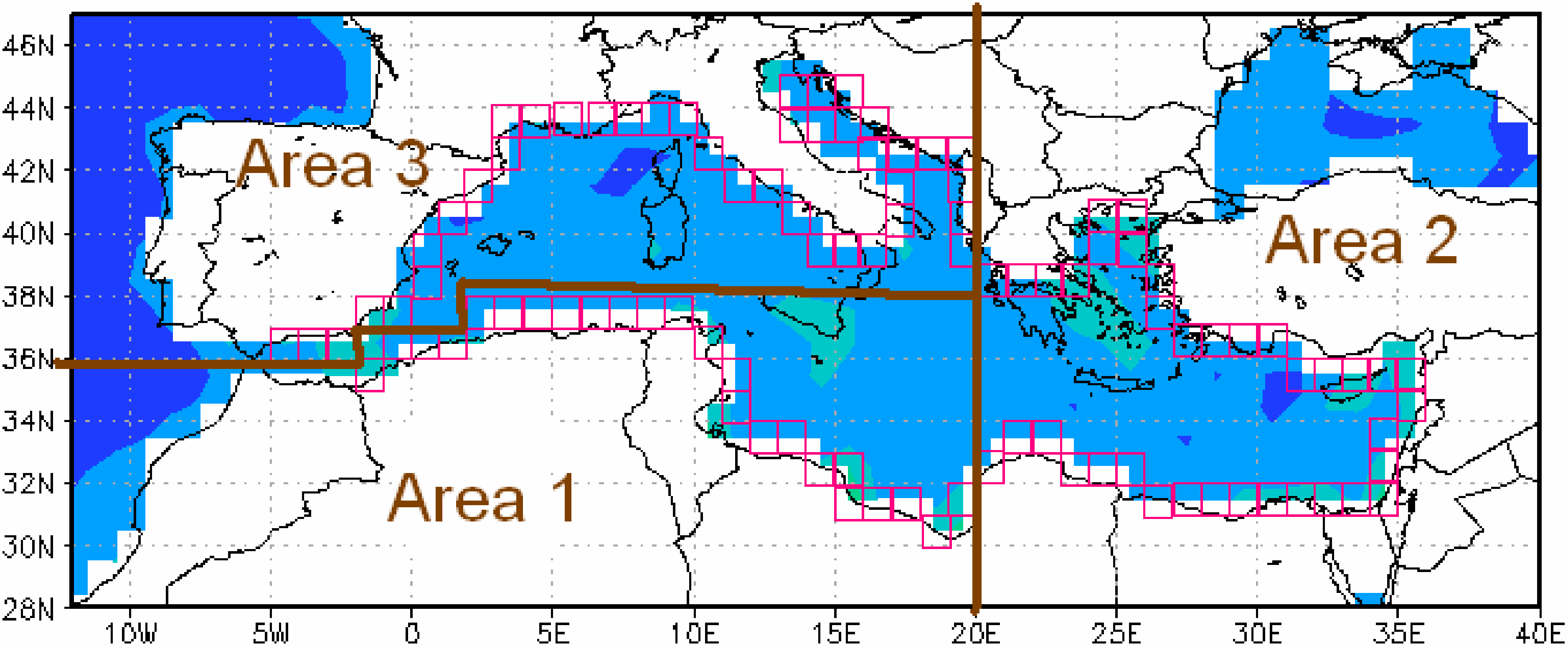

	Smoke	Dust	Total
Area 1	-3.3	22.8	19
Area 2	-3	18.6	15.5
Area 3	-.5	5.47	5

*Results in Tg/month/%

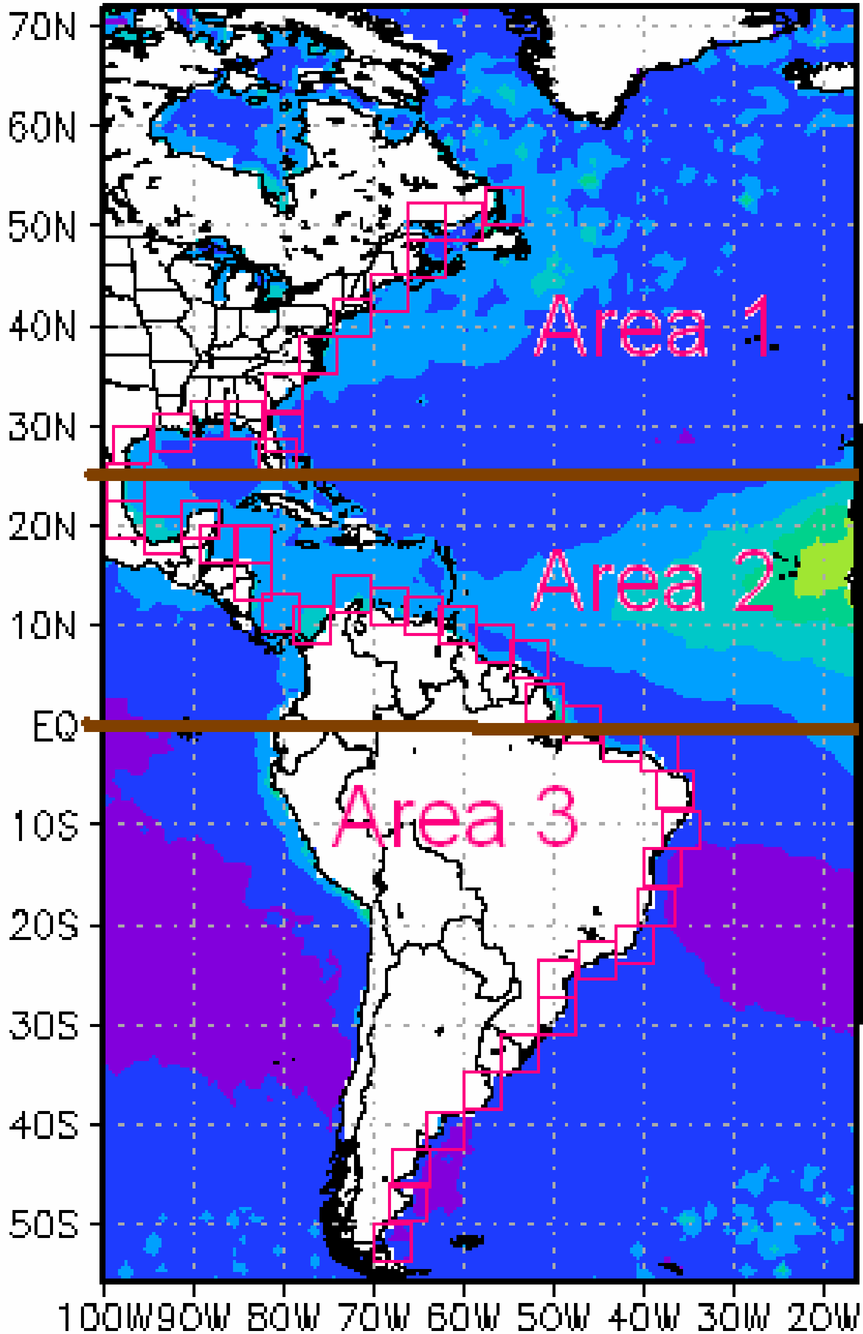

	Smoke	Dust	Total
Area 1	-34.5	-54	-89
Area 2	55.1	174	229
Area 3	19.0	.59	19.6

*Results inTg/month/°4

	Smoke	Dust	Total
Area 1	1.6	-35	-34
Area 2	7.8	7.7	15.4

*Results in Tg/month/°4

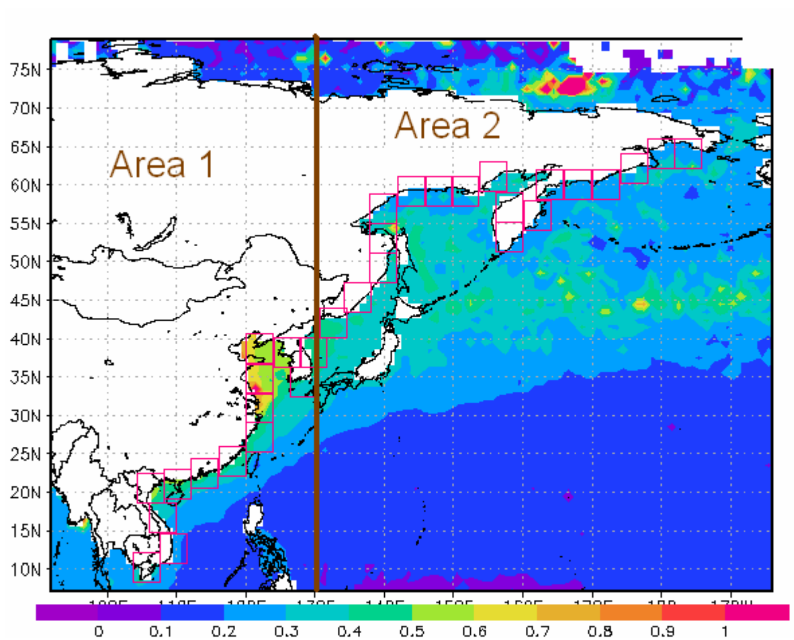

Acknowledgments and References

Acknowledgments to Kevin Leavor, Shanna Mattoo, Yorman Kaufman, and Per Gloersen.

Kaufman, D. Tanre, and O. Boucher, 2002: A satellite view of aerosols in the climate System. *Nature,* **419**, 215-223

Remer L. A., Y. J. Kaufman, D. Tanre, S. Mattoo, d. a. Chu, J. V. Martins, R.-R. Li, C. Ichoku, R. C. Levy, R. G Kleidman, T. F. Eck, E. Vermote, and B. N. Holben, 2005: The MODIS Aerosol Algorithm, Products, and Validation. *J. Atmos. Sci.,* **62**, 947-973

Koren, I., and Y. J. Kaufman, 2004: Direct wind measurements of Saharan dust events From Terra and Aqua satellites. *J. Geophys. Res.,* **31**, 1-4

Kaufman, Y. J., I. Koren, L. A. Remer, D. Tanre, P. Ginoux, and S. Fan, 2005: Dust Transport and deposition observed from the Terra-Moderate Resolution Imaging Spectroradiometer (MODIS) spacecraft over the Atlantic Ocean. *J. Geophys. Res.,* **110**, 1-16

Smirnov, A., B. N. Holben, T.F. ECK, O. Dubovik, and Slutsker, 2003: Effect of wind Speed on columnar aerosol optical properties at Midway Islands. *J. Geophys. Res.,* **108**, 1-8

http://g0dup05u.ecs.nasa.gov/Giovanni

Intercomparison of Satellite Observations and GOCART Model Aerosol Data with the Aim of Preparing a Realistic Aerosol Dataset for Use in Climate Models

Andrea May

August 12, 2005

Mentor: Yogesh Sud

Outline

- Objectives and Purpose
- Explanation of the model and data used
- Intercomparisions of MODIS and GOCART
- Intercomparision of MODIS and GOCART to AERONET
- Conclusions

Objectives & Purpose

- To find if the GOCART model or MODIS data is better suited for use in the Global Climate model.
- Use AERONET data to compare both the MODIS satellite data and GOCART model.
- Determine how the model can be improved for future use

GOCART Model

- Climatology data for the years 2000 and 2001
- Grid spacing of 2.5 x 2
- Used 55 vertical sigma layers
- Model includes prediction of five major aerosols:dust, organic carbon, black carbon, sulfates and sea salt
- GOCART calculates the aerosol optical thickness by $\tau = B\ M$ where b refers to the specific or mass coefficient and M simply refers to the aerosol dry mass

MODIS Satellite Data

- MODIS data is used from a climatology of 2000 – 2004
- MODIS satellite data is plotted using a 1 x 1 degree resolution
- To keep the model and data uniform the MODIS data was re-grided to a 2.5 x 2 degree grid for easy comparison.
- Satellite data from version 4, level 2 was used.
- MODIS aerosol retrieval uses separate algorithms for both land and ocean in order to obtain aerosol optical properties in cloud free areas and also includes total aerosol optical thickness and fine mode aerosol fractions (Tanre´ et al., 1997).

AERONET Data

- AERONET data is the most accurate data for representing τ, however this data is only available for the latitude and longitude of the remote sensing instrument.
- For this research I used only the direct measurements taken at 500 nm
- A two year climatology data set was used for the years 2000 - 2001
- Between 98 and 127 sites were used depending on the availability of the site for the years we were interested in.
- The type of AERONET data used was the level 2.0 climatology which is cloud-screened and quality-assured..

Seasonal MODIS Data

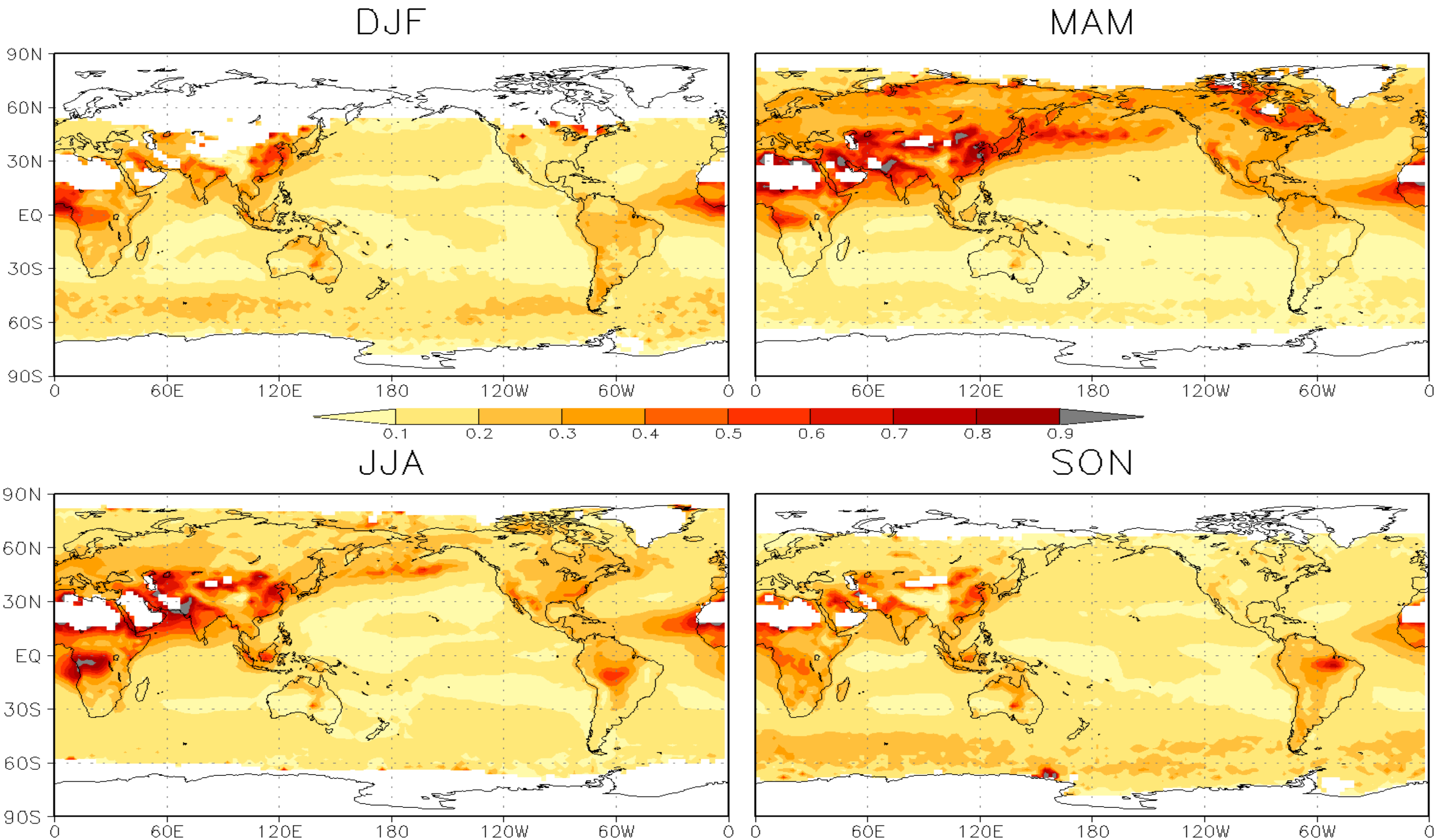

Aerosols in the MODIS Satellite Data

- Major areas of aerosol concentrations in MODIS are found in Africa, the Middle East, and along the coast of eastern Asia.
- These areas have high concentrations of τ due to dust, and biomass burning.
- Higher values of τ in North Africa and the Middle East are seen in the spring and summer.
- Higher values of τ in South Africa and South American are seen during the fall months.

Seasonal GOCART Model

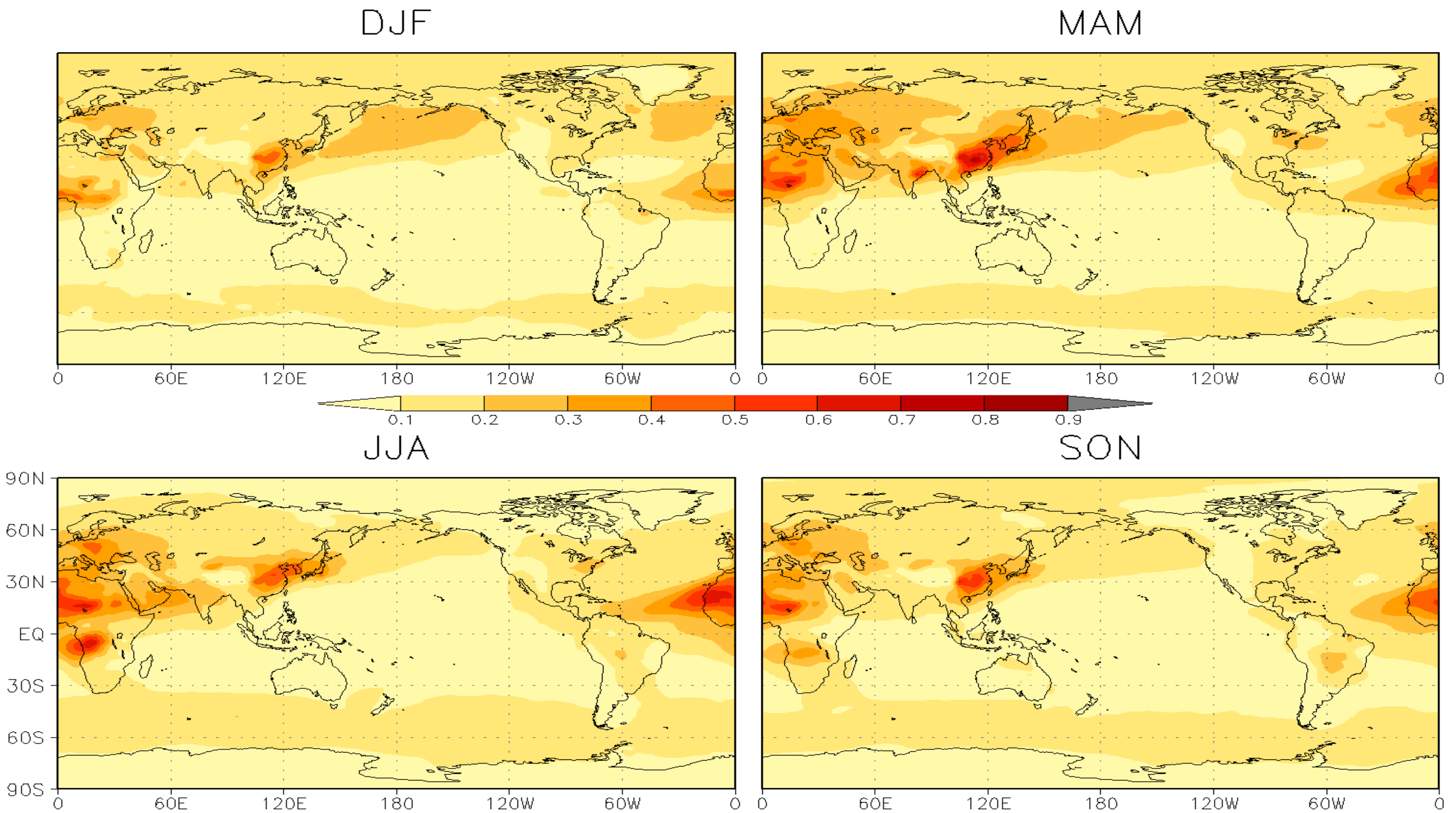

Aerosols in the GOCART Model

- There are large amounts of aerosols being modeled along the east coast of Asia.
- During the spring and summer months there are large amount of aerosols in Africa with values of 0.3 –0.6
- Values of the total optical thickness in North and South American have low values during all modeled seasons.
- Increase in aerosols in Europe during the spring months

MODIS - GOCART

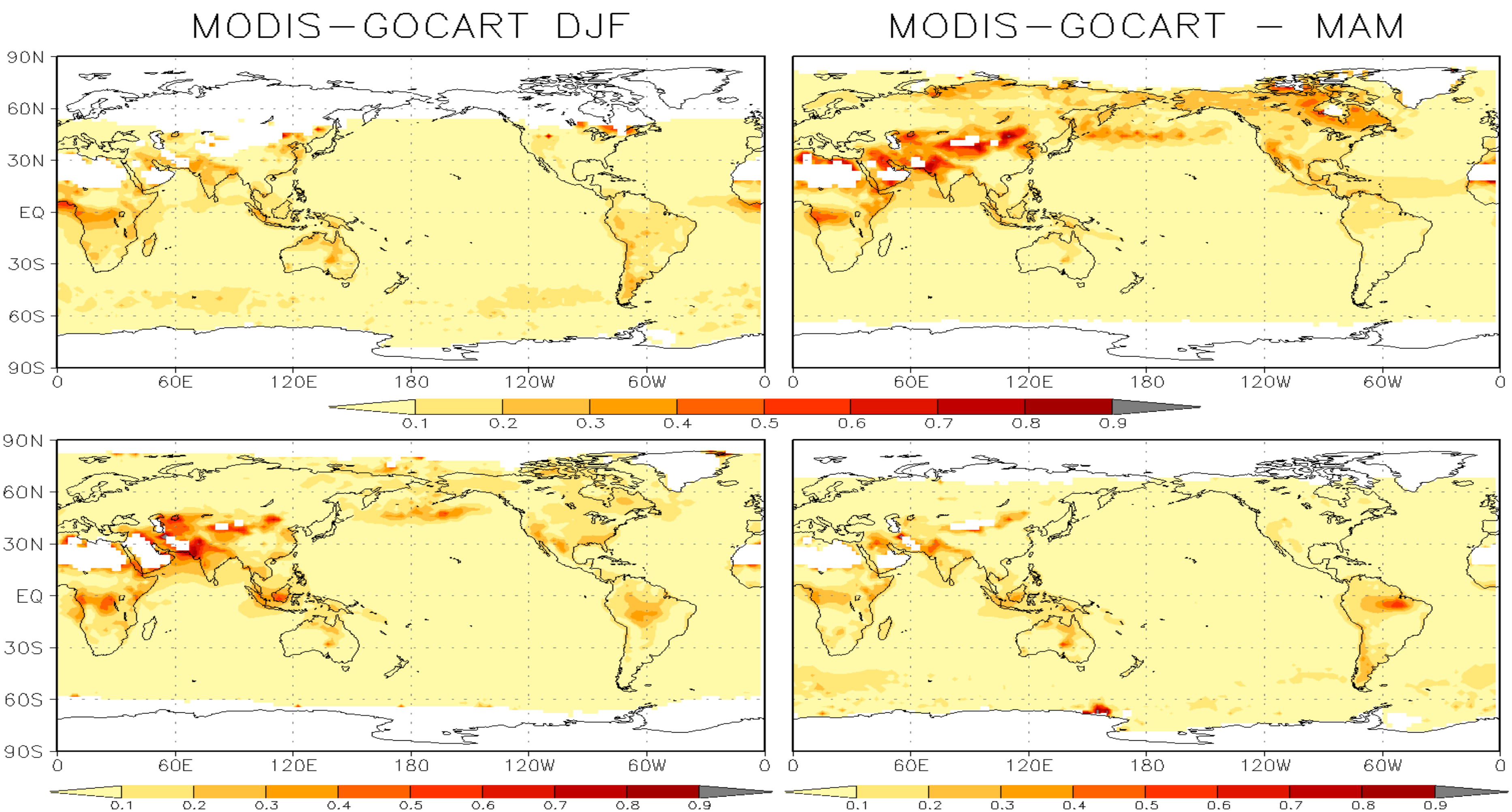

JJA — Summer (bottom left) and SON — Fall (bottom right)

Comparisons with AERONET

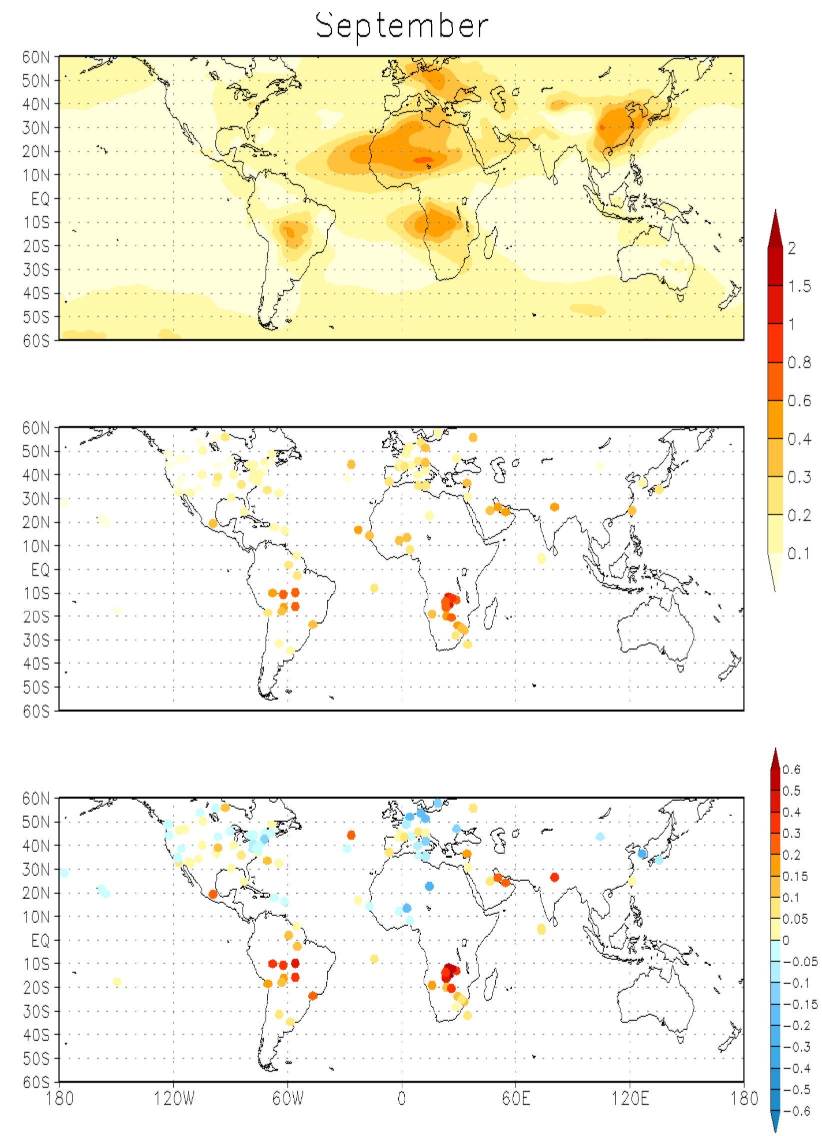

September AOT: GOCART (top), AERONET (middle); AERONET minus GOCART (bottom)

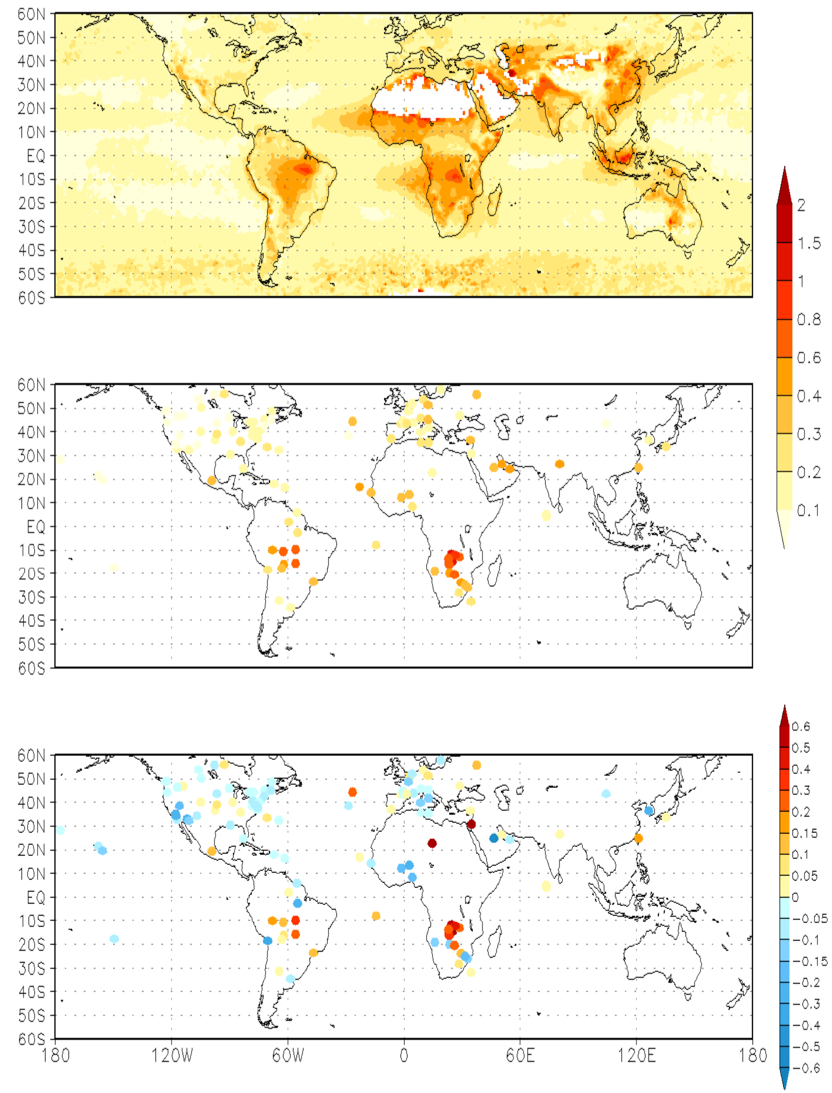

September AOT: MODIS (top), AERONET (middle); AERONET minus MODIS(bottom)

AERONET Values for September

- Both the model and satellite data are underestimating the aerosol values in South Africa
- GOCART is underestimating aerosols in South America. MODIS seems to be slightly better in representing the aerosols due to biomass burning.
- The model and satellite data is underestimating the aerosols in the Middle East
- Both the model and satellite data seem to be estimating the values of aerosol optical thickness in Europe well with values ranging from 0.5 to - 0.1

Differences in AERONET and GOCART for September

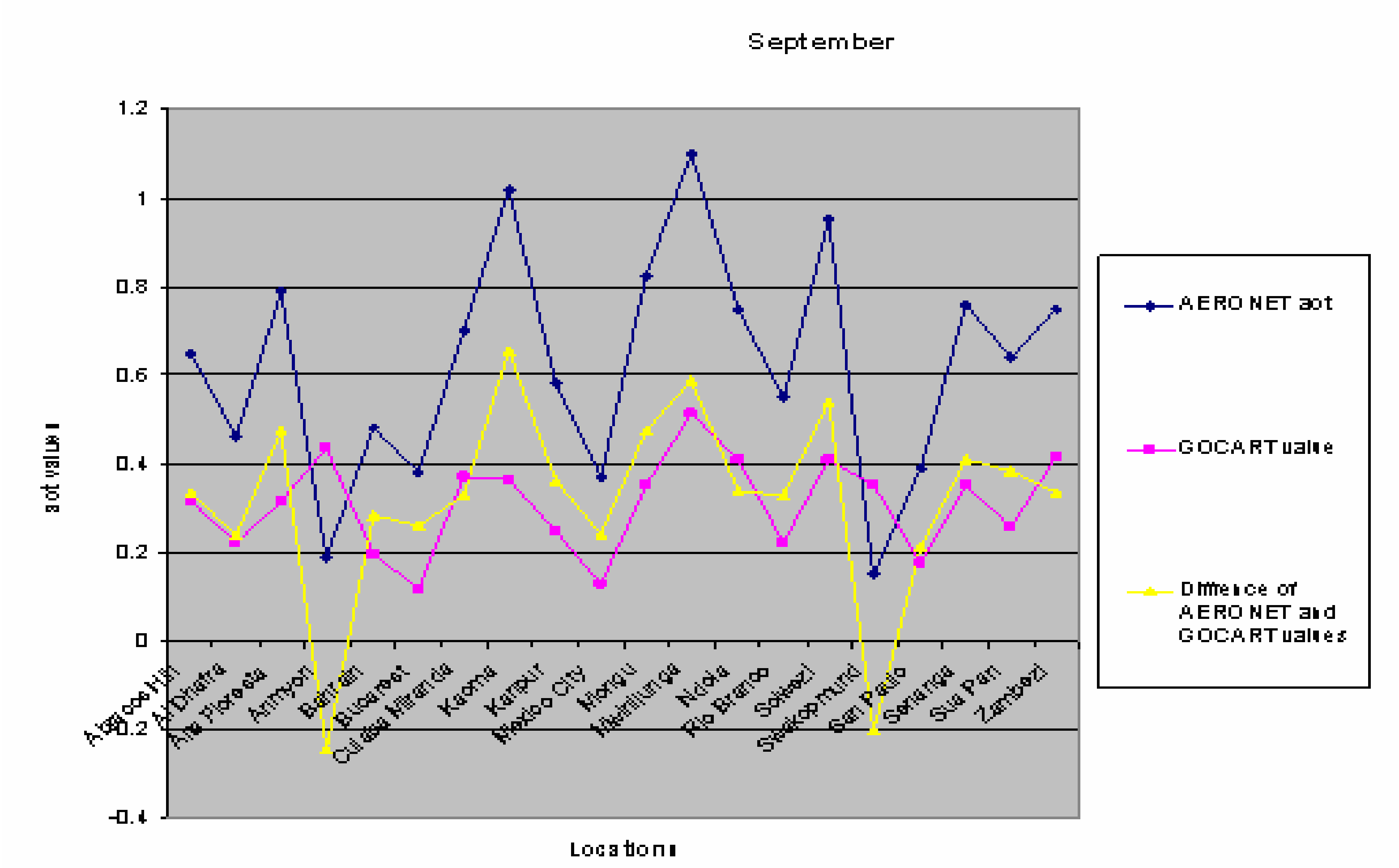

Comparisons with AERONET

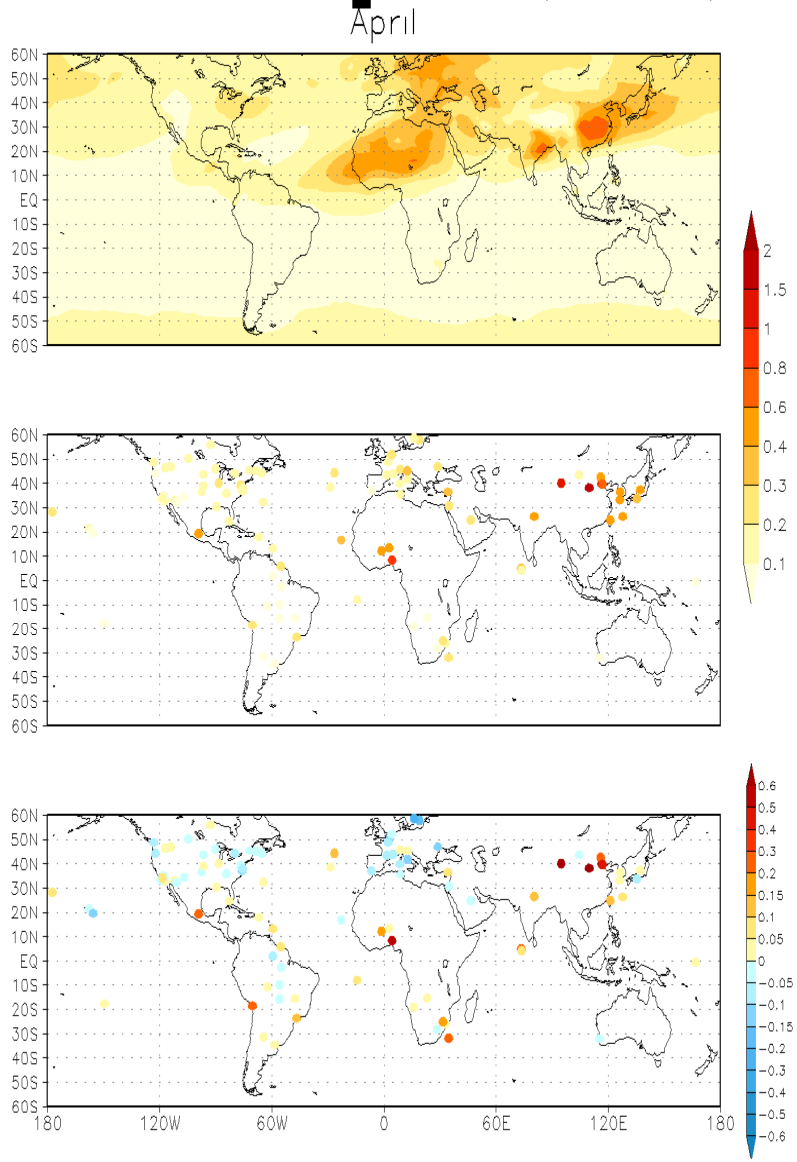

April AOT: GOCART (top), AERONET (middle); AERONET minus GOCART (bottom)

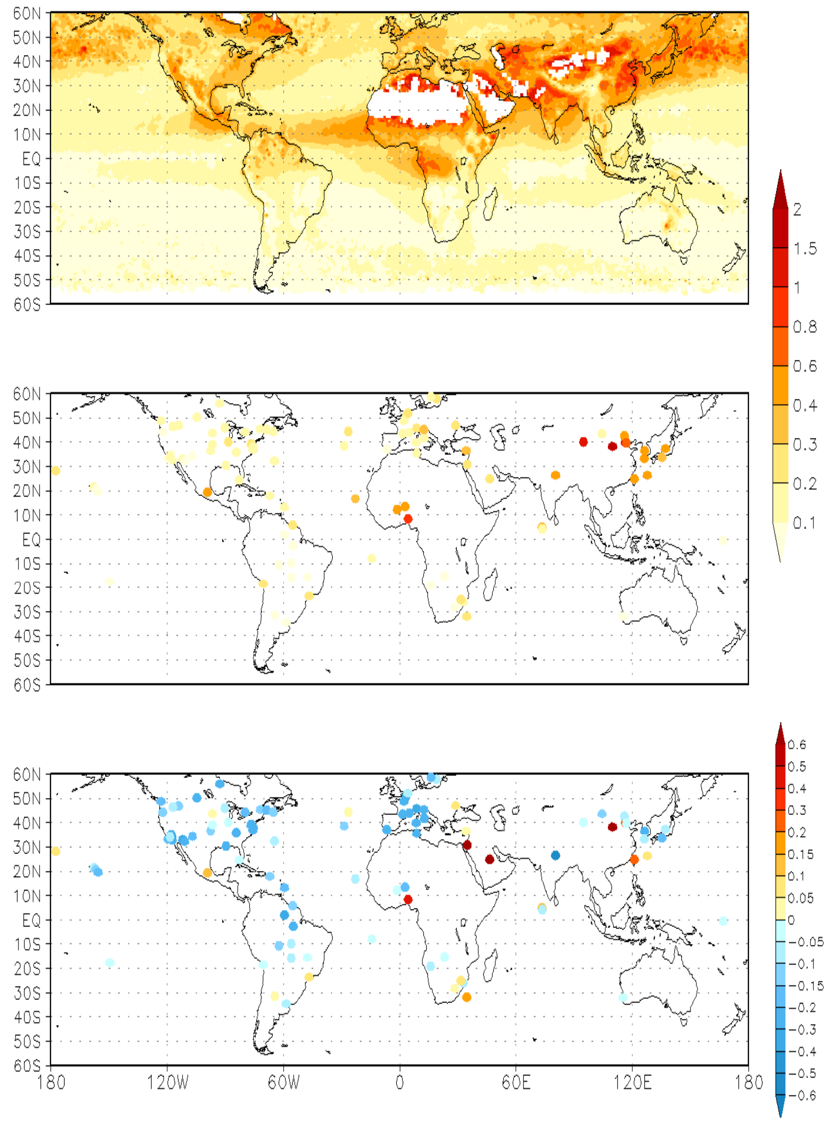

April AOT: MODIS (top), AERONET (middle); AERONET minus MODIS(bottom)

AERONET Values for April

- GOCART is modeling the aerosols in North America and Europe very well. The difference between the model and data is only 0 - 0.5.
- MODIS seems to be overestimating these areas with values of 0.3 greater then the AERONET values
- As seen the month of September GOCART is doing a better job of estimating the aerosol values in the Middle East (ME).
- GOCART values for the ME 0.05 to –0.05
- MODIS values for ME 0.05 – 0.6

Conclusions

- GOCART is modeling the total aerosol optical thickness than the MODIS satellite data.
- There are still problem areas in GOCART that are underestimating or overestimating τ values.
- The MODIS data tends to be extremely large in the Middle East and in parts of North America where GOCART tends to have lesser τ values.
- The major problem with GOCART and MODIS is the ability to estimate the amount of organic and black carbon which helps to estimate the amount of biomass burning in the world.
- MODIS tends to overestimate the aerosol optical thickness which is most likely due to cloud contamination.

Future Studies

- Continue to improve the GOCART model by obtaining new estimations of burned biomass from long-tem satellite observations of global fire.
- Further studies should be conducted on verifying the total optical thickness of aerosols over ocean. Since I treat the AERONET data as the 'truth', it is only limited to land based measurements.

? Questions ?

- I would like to thank my mentor, Yogesh Sud for his guidance throughout this project, Greg Walker for assisting me with the programing aspect, and Lorraine Remier for her assistance.

Characterization of Dust Events in Patagonia Using 15 Years of Weather Observations

Edward Liske
Mentor: Santiago Gasso

Summer Institute 2005
NASA Goddard Space Flight Center

The Data

- 22 weather stations scattered over all of Patagonia.
- Data range is from January 1, 1990 through May 1, 2005. (frequency depends on station.)
- Variables used include: wind direction and speed, cloud cover, temperature and dew point, and current weather observations.

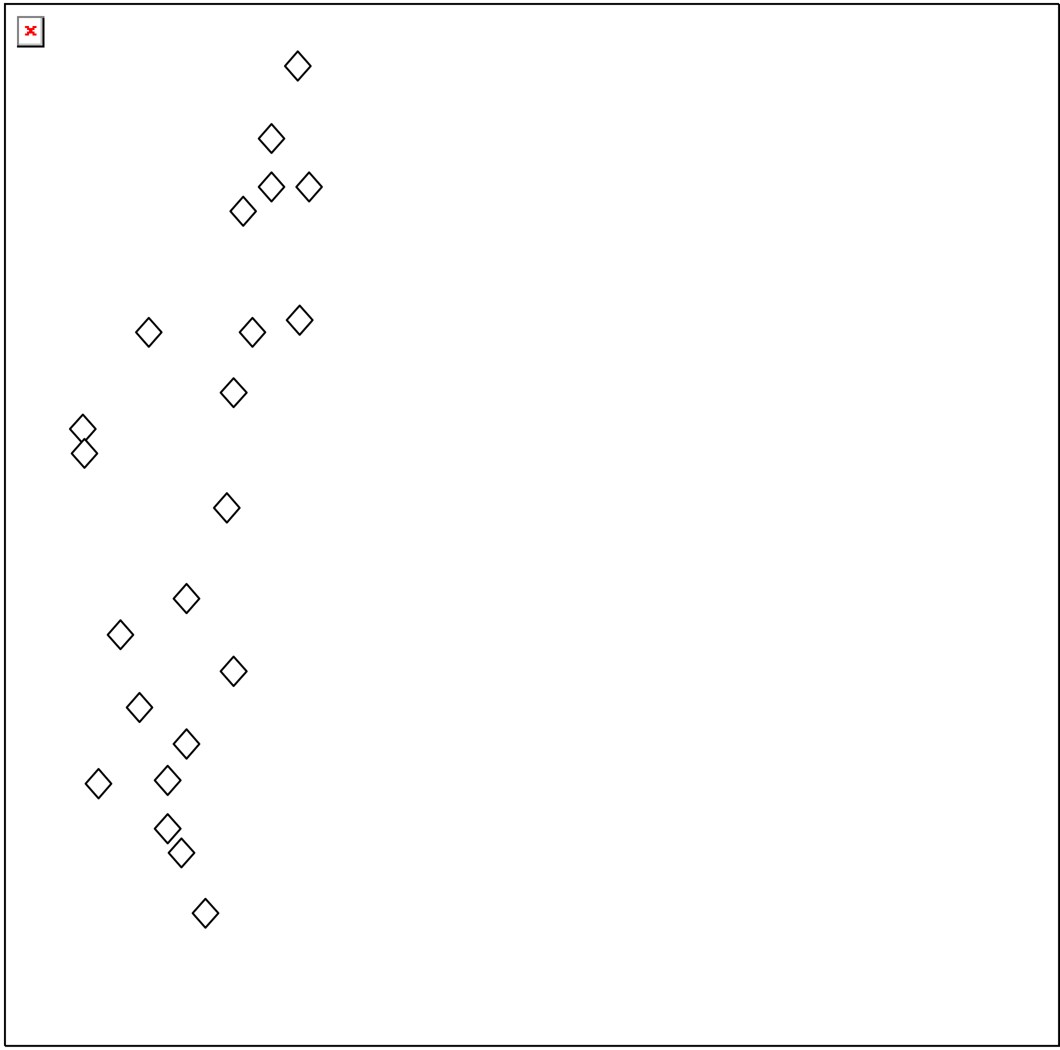

Data Manipulation and Surface VS. Satellite

- Main purpose of project is to see what the satellites are missing due to clouds or other problems.
- Most of project dealt with manipulating and interpreting data in excel.
- Separate files were made to answer certain questions.

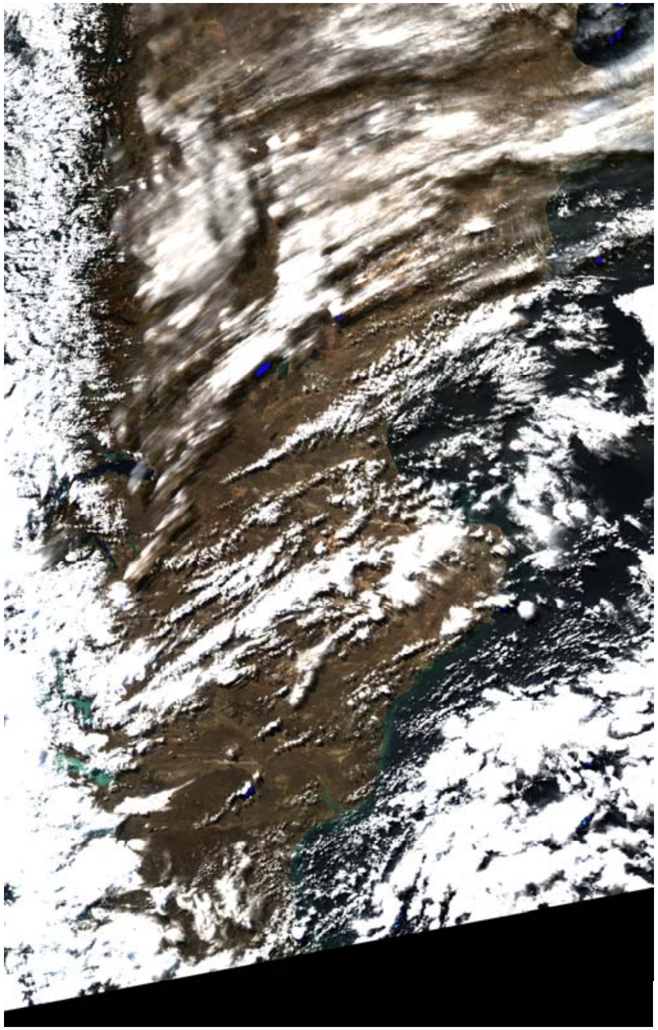

Dust events

- Any number of dust observations at a station that are all within 24 hours of each other.
- Can last for a few hours or a few days and affect many stations all at once.

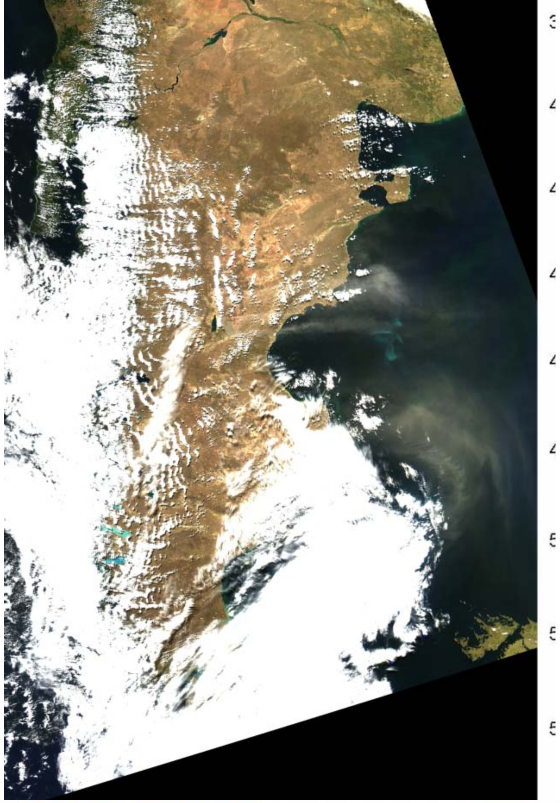

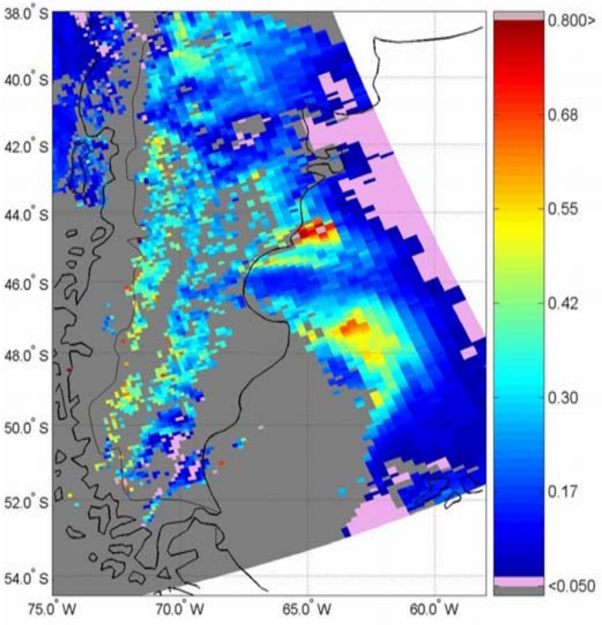

What are we looking for?

- What is the frequency of dust events in Patagonia?
- Is there a trend in the number of dust events?
- How large are these events?
- Is the sky clear or are there clouds when these events are occurring?
- Is there a threshold wind speed above which these dust events start, and if so what is it?

Dust event frequency

- Southern Patagonia: 6 events/year
- Central & northern Patagonia: 10 events/year
- North of Patagonia: 20 events/year.
- At most stations the occurrence of duststorms was at most one or two a year.

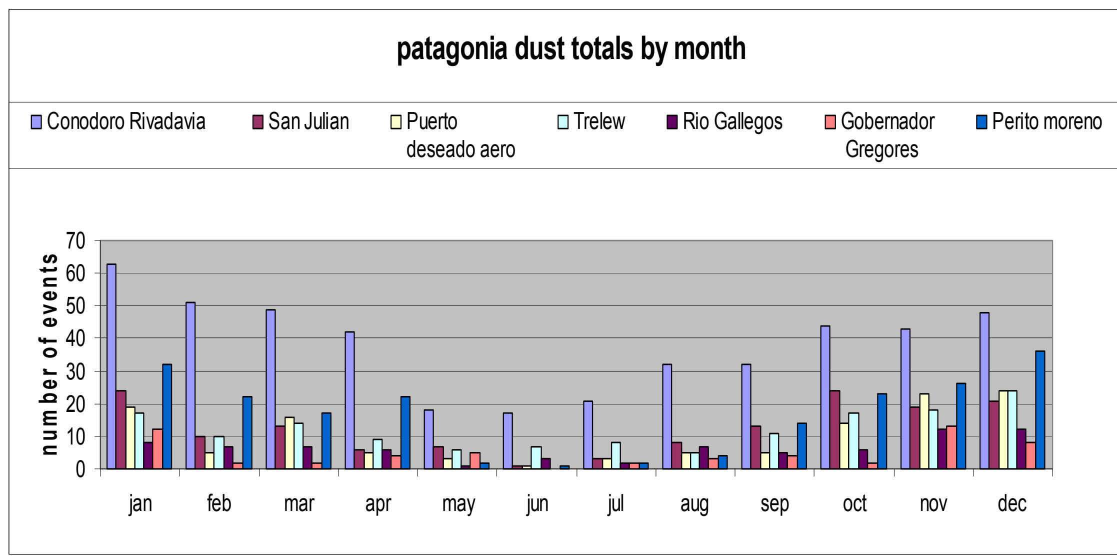

Size and length

- 70% of these dust events are local short duration events.
- The major events (affecting three or more stations) only occur 14 % of the time and can last for many days.

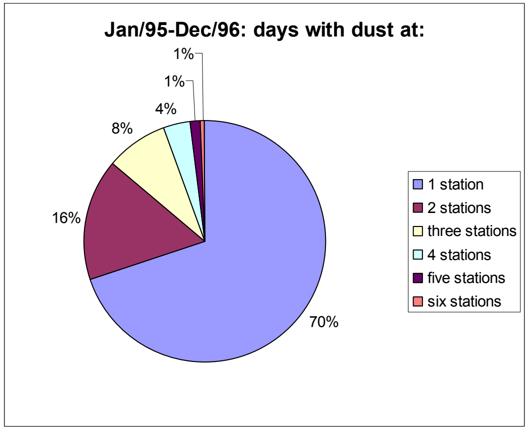

Cloud cover

- The presence of clouds make it difficult to detect dust events from space.
- At least half of the dust events occur during cloudy conditions.
- Satellites need a better cloud detection scheme

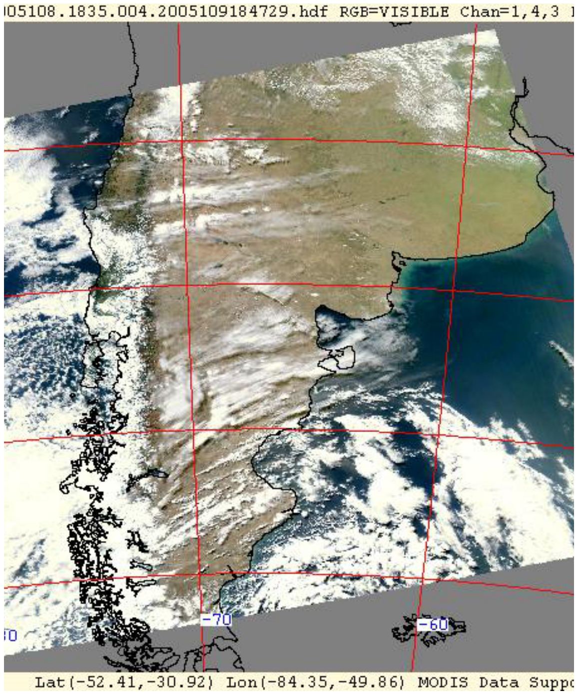

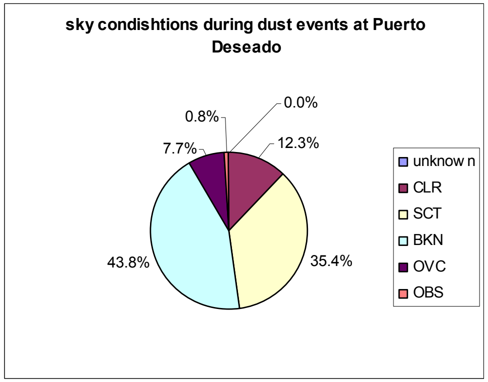

Wind and moisture

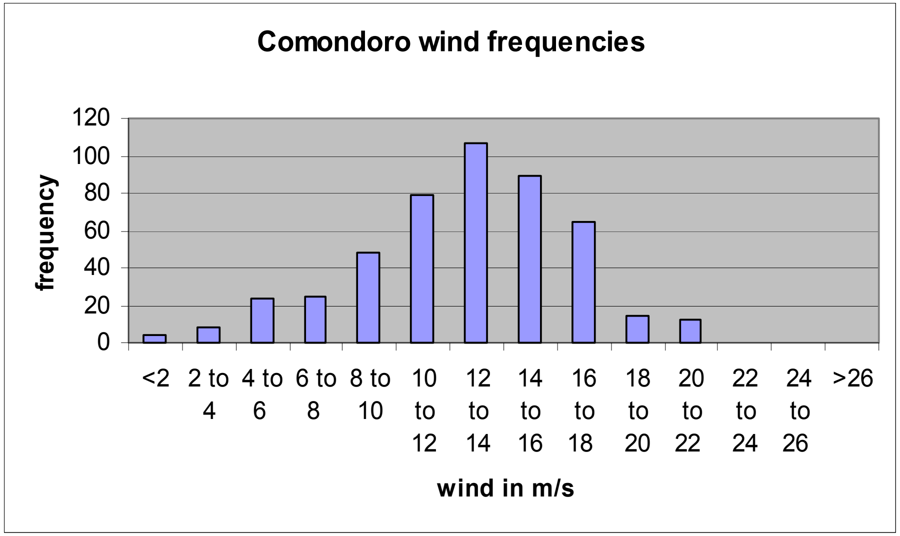

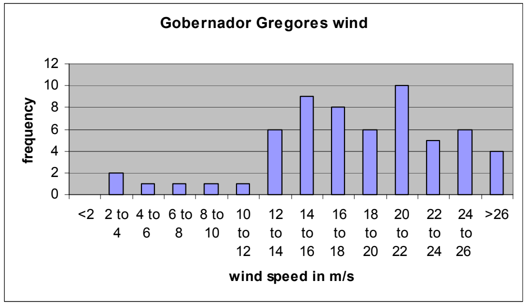

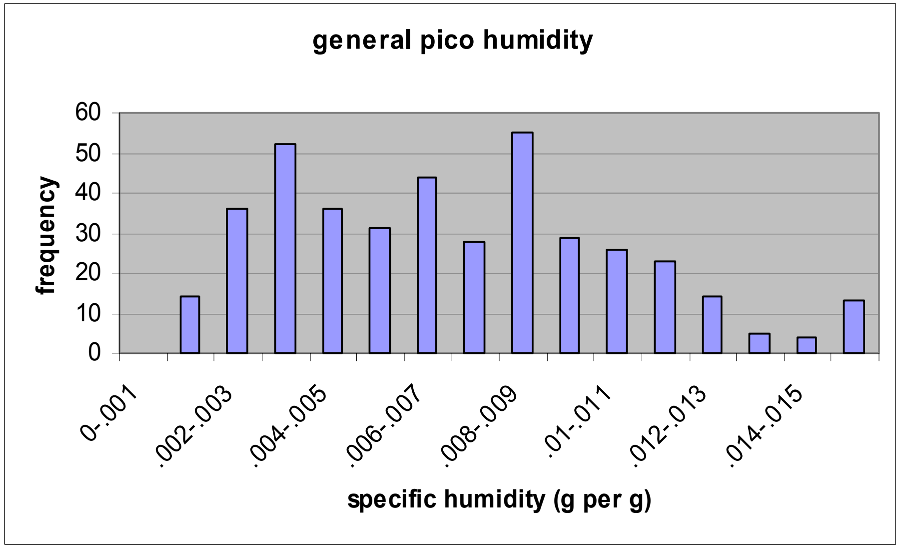

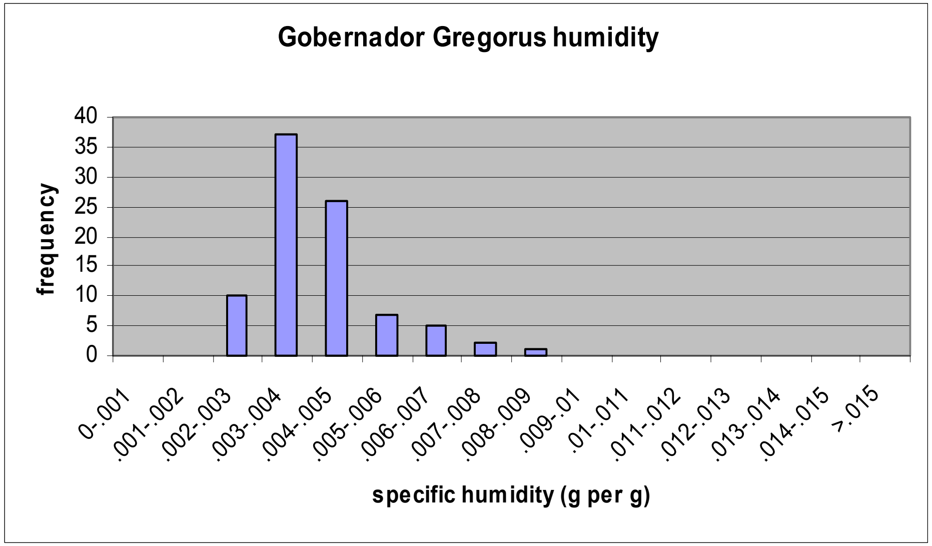

Dust event trends and comparisons.

- Precipitation remained steady through the 90s but increased in 2002-2004.
- As a result the number of dust events has decreased from what they were in the early 90s over most of the region.
- Comparison with Prospero

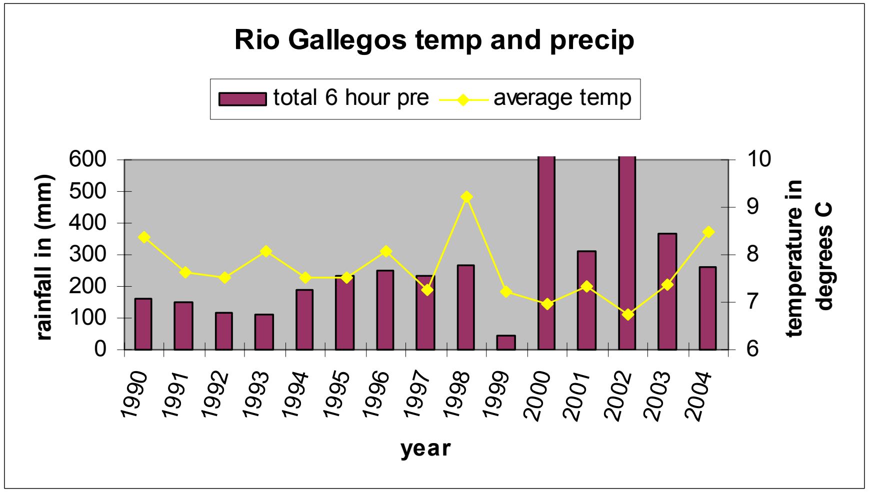

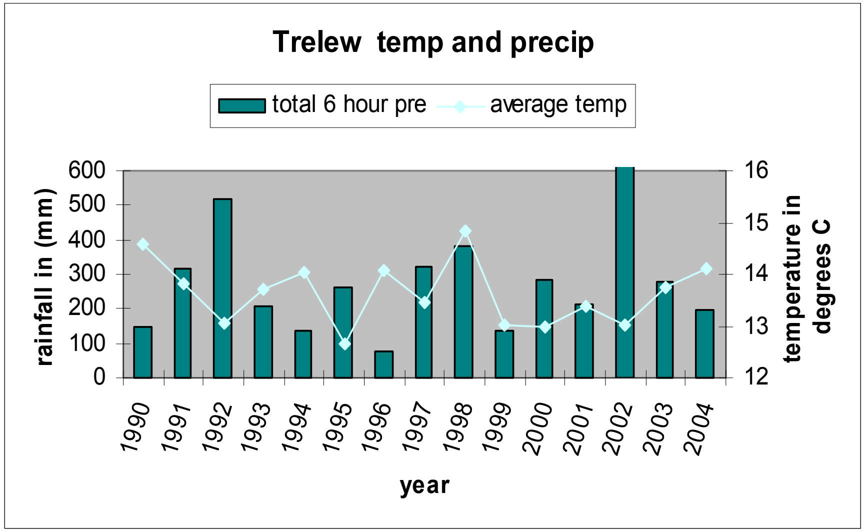

Summary

- In Patagonia dust events occur an average about 6 to 10 times per year in the South end and about xx to xx in the Norht.
- Compare with Prospero, …. What you put in the paper
- Most are localized short duration events.
- At least half of the events occur when the sky is cloudy
  - Satellites need a better way of distinguishing clouds from dust in this area
- Threshold winds… *this important for global aerosol modelers*.


• QUESTIONS?

- THANKS TO ALL WHO MADE THIS SUMMER INSTITUTE POSSIBLE AND FOR SELECTING ME TO HAVE THE OPPERTUNITY TO PARTICIPATE IN IT. THE EXPERIENCE AND CHALLENGES PRESENTED WILL HAVE A LASTING IMPACT ON ME.

Correlations of MODIS and PM 2.5 Measurements in the Mid-Atlantic Region

Ed Nowottnick

Rob Levy - Mentor

8/12/2005

MODIS Basics

- MODIS Terra started taking measurements in February 2000
- Polar Orbiting Satellite
- Measures Aerosol Optical Depth (AOD)
- Takes measurements at 36 spectral bands
- 1 km resolution

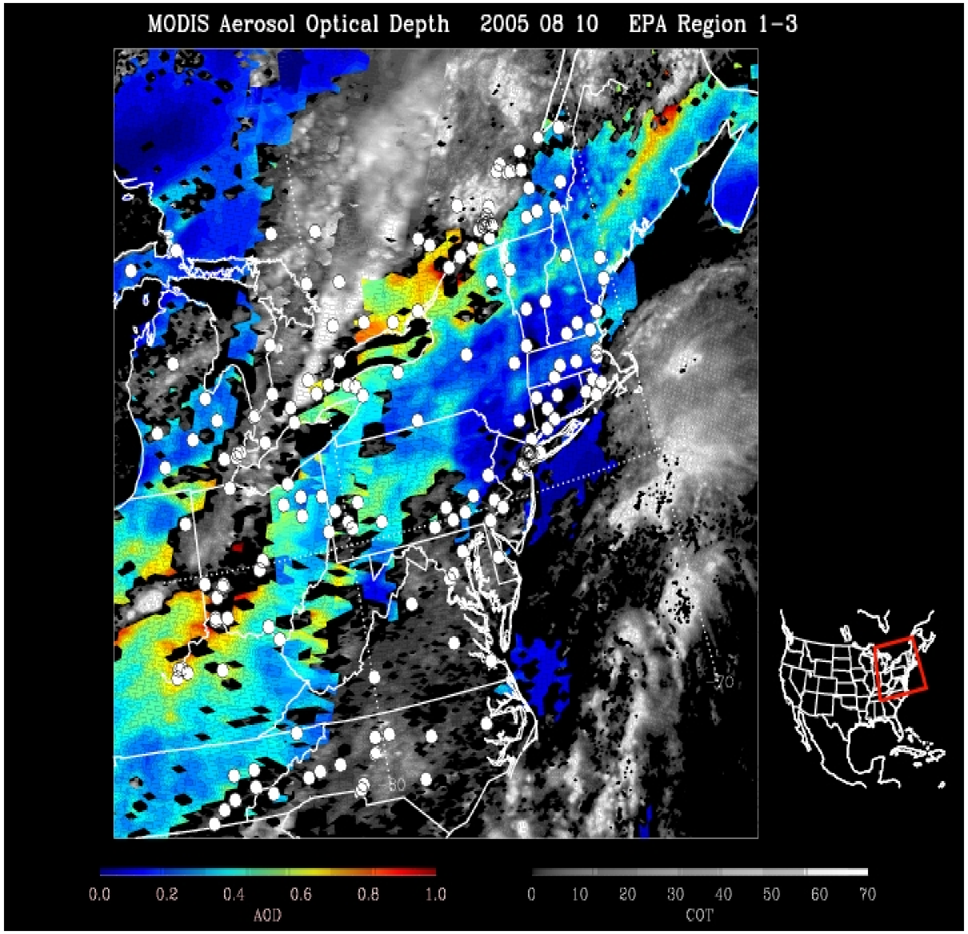

MODIS Terra Path

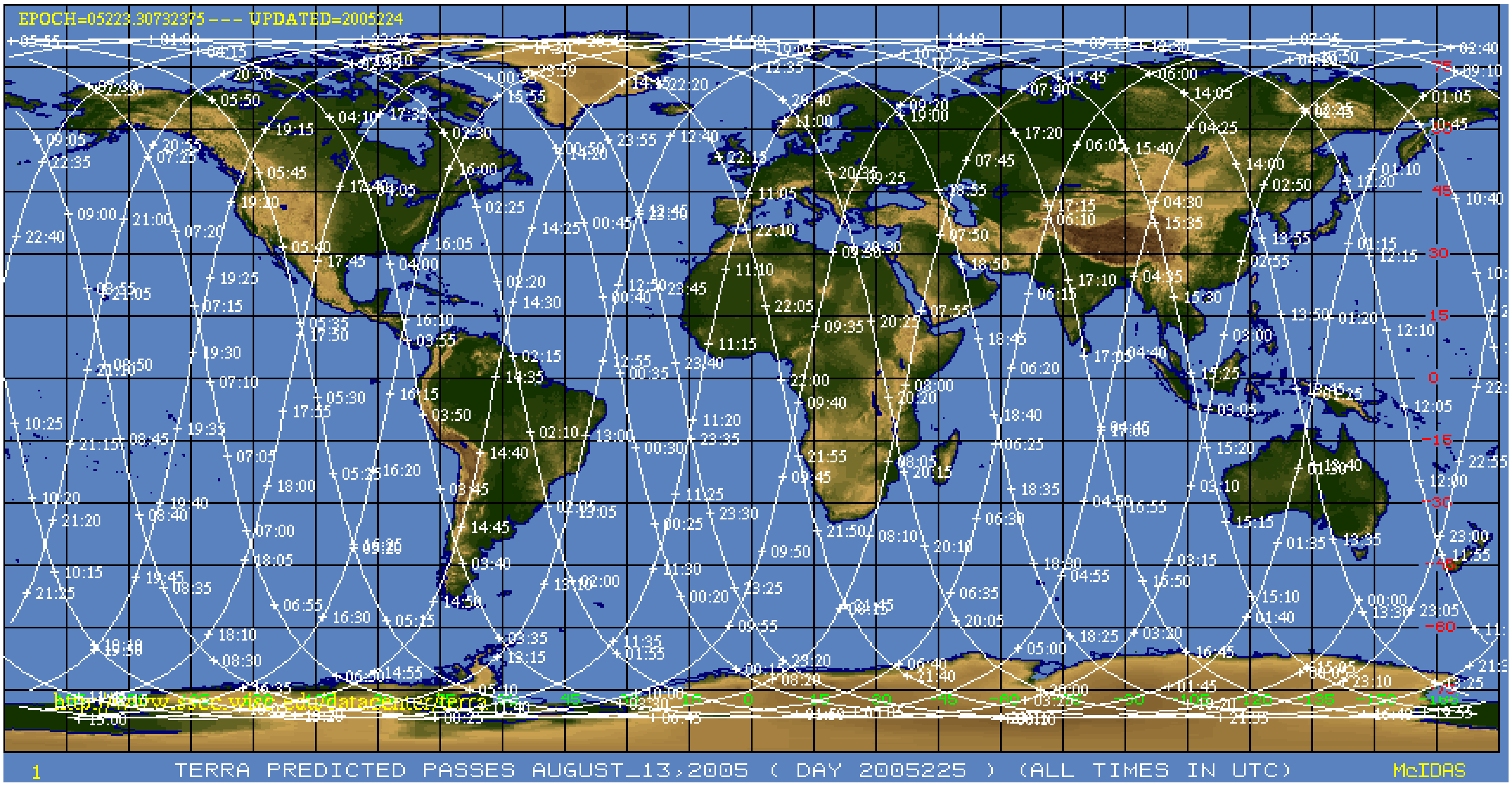

Particulate Matter 2.5 Basics

- Aerosols less than 2.5 microns in diameter
- Consist of dust, dirt, soot, smoke, and liquid droplets
- Measured in ug/m^3
- Particles from the surface can be suspended into the upper boundary layer for weeks
- Reduces visibility
- Serious health effects especially for those with asthma and other respiratory and

Particulate Matter Basics Continued

- Ground level monitors make hourly measurements and are assigned an AQI (Air Quality Index)
- The breakpoint concentrations for PM2.5 are 0-15, 15-40, 40-65, 65-150, and 150+ ug/cm^3

Air Quality Index (AQI): Particle Pollution

Index Values	Levels of Health Concern	Cautionary Statements
0 - 50	Good	None
51 - 100*	Moderate	Unusually sensitive people should consider reducing prolonged or heavy exertion.
101 - 150	Unhealthy for Sensitive Groups	People with heart or lung disease, older adults, and children should reduce prolonged or heavy exertion.
151 - 200	Unhealthy	People with heart or lung disease, older adults, and children should avoid prolonged or heavy exertion. Everyone else should reduce prolonged or heavy exertion.
201 - 300	Very Unhealthy	People with heart or lung disease, older adults, and children should avoid all physical activity outdoors. Everyone else should avoid prolonged or heavy exertion.
301 - 500	Hazardous	People with heart or lung disease, older adults, and children should remain indoors and keep activity levels low. Everyone else should avoid all physical activity outdoors.

Is there a correlation between AOD and PM2.5?

- Under the right conditions, can MODIS be used to help forecast air pollution?
- Do certain regions have better correlations that others?
- Under what conditions do AOD levels and PM levels agree?
- Under what conditions do they disagree?
- When aerosols are near the surface, AOD and PM should be correlated
- What if the aerosols are aloft? Is there

Ground level PM measurements with MODIS overlay

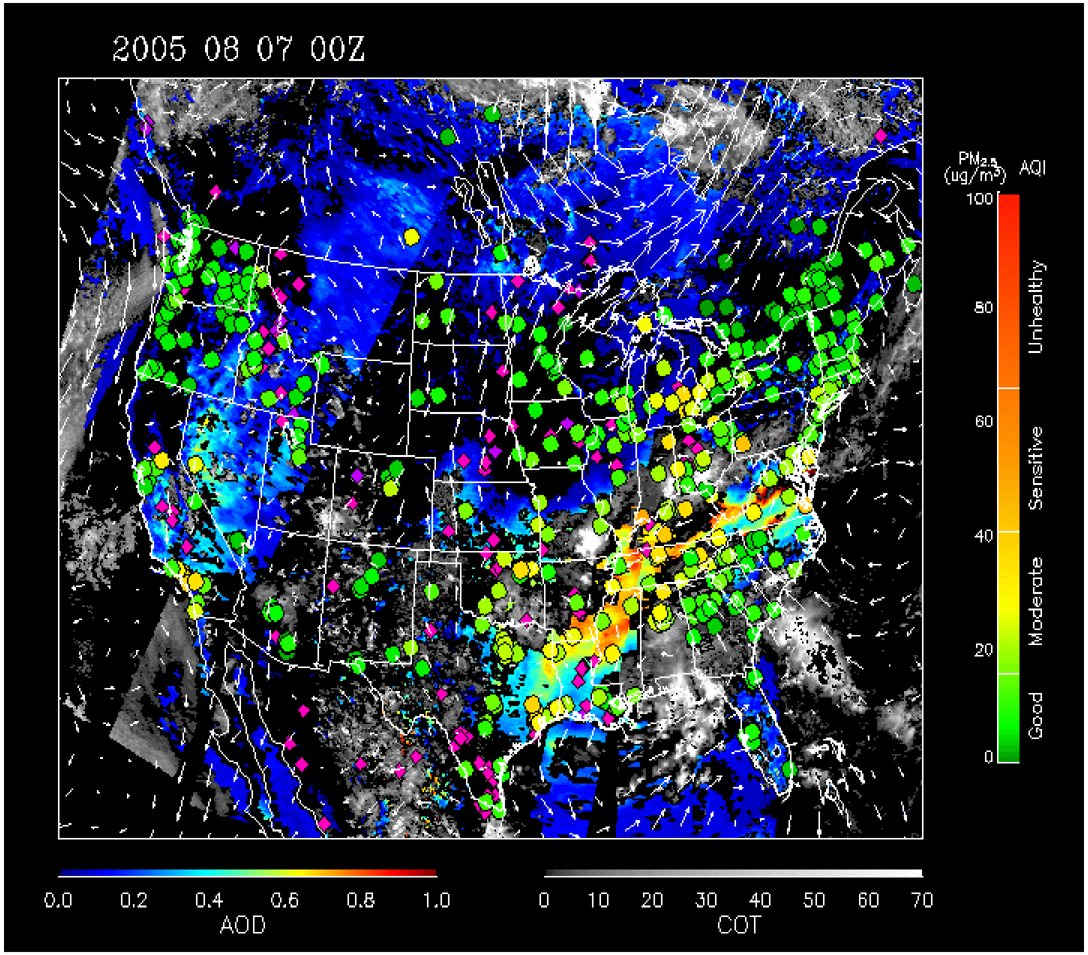

Mid-Atlantic Region

- PA, NJ, DE, MD, WV, VA, and NC
- 47 hourly monitors in region
- Wrote a script that found when MODIS passed over the monitor locations and averaged the PM concentrations for +/- 2 hours of MODIS passing

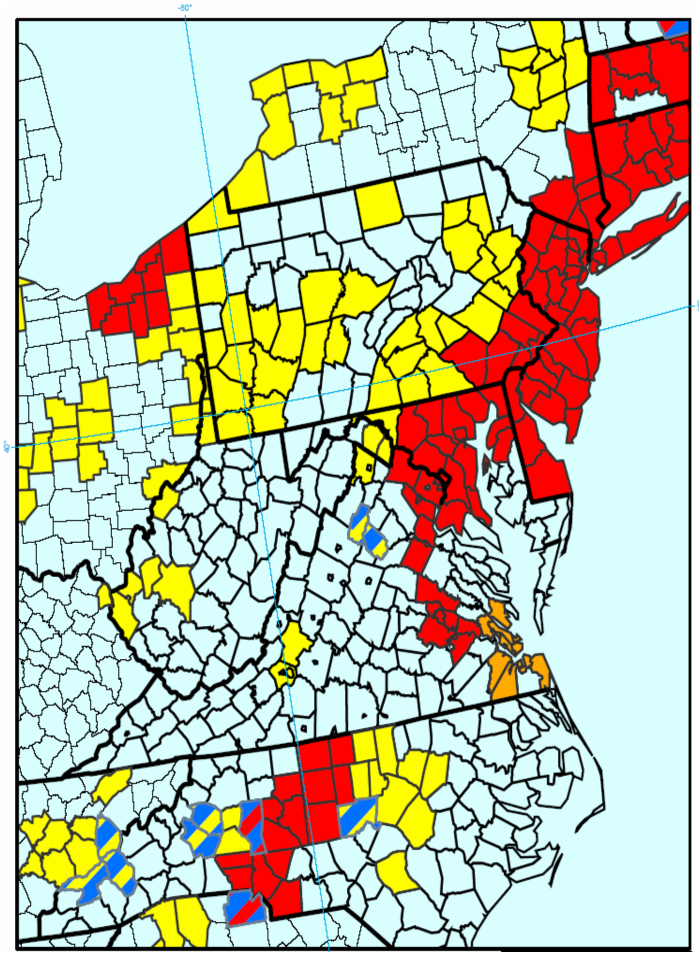

Time Series for AOD vs. PM2.5

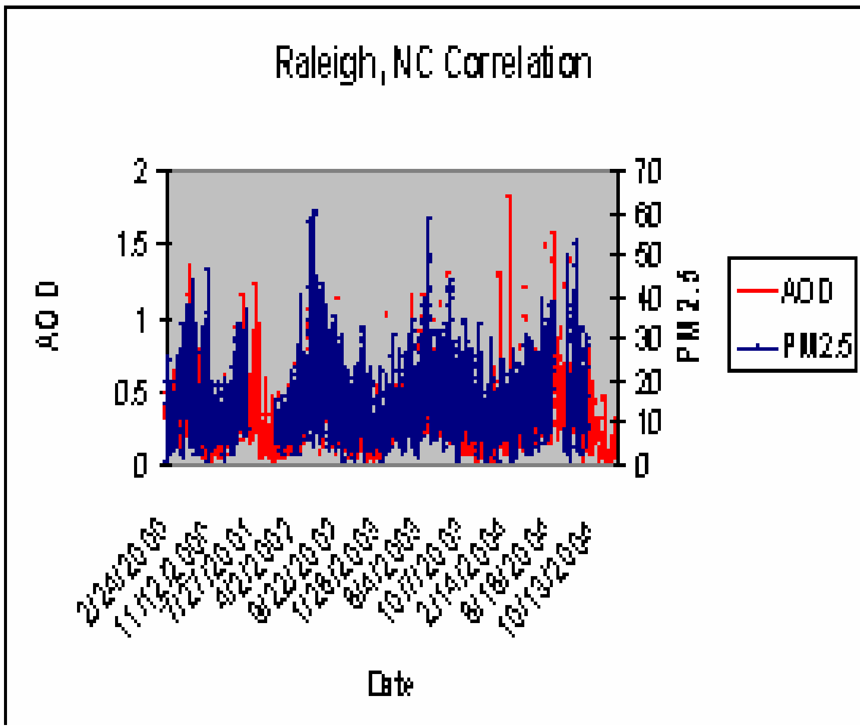

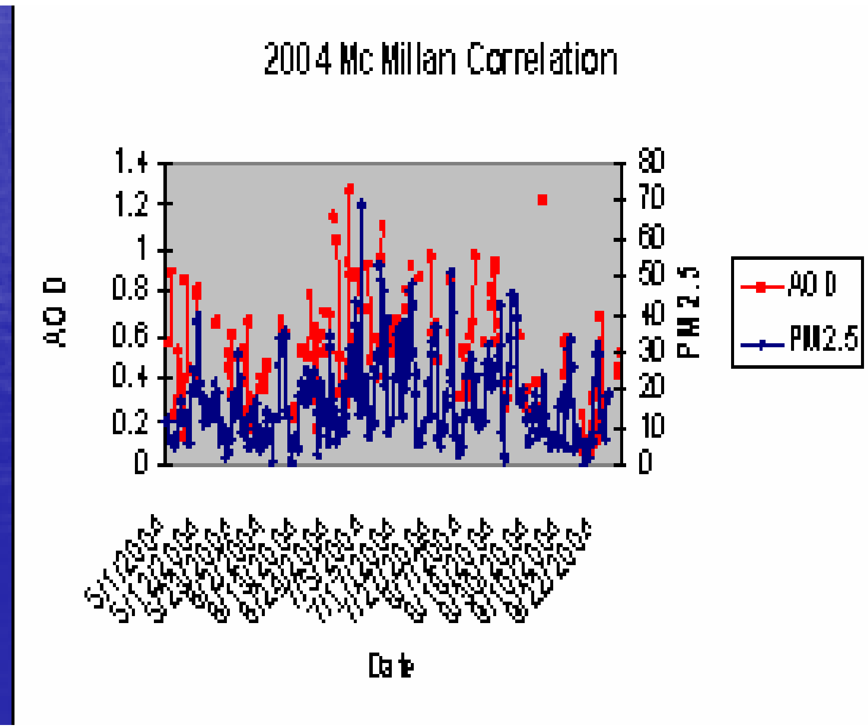

Annual Correlation Plots

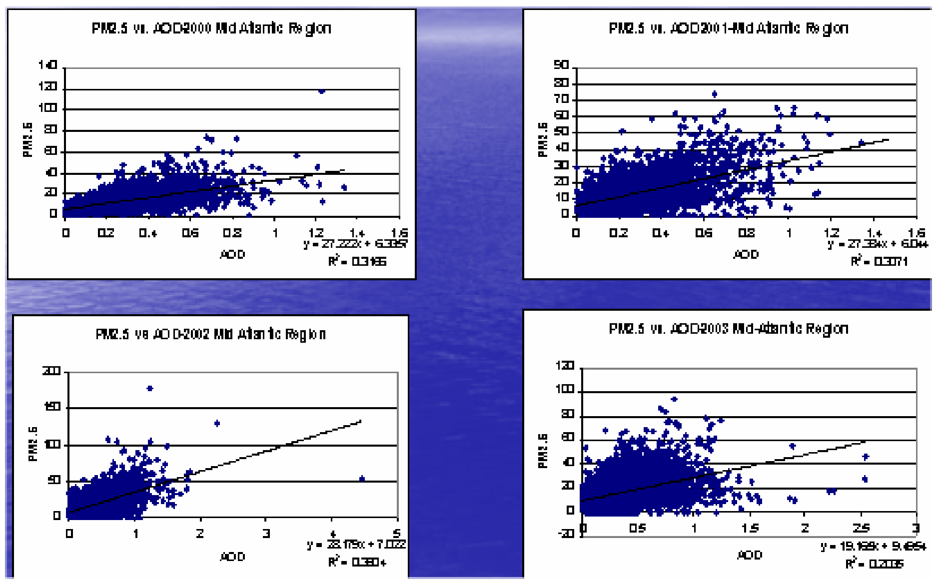

Annual Correlation Plots Continued

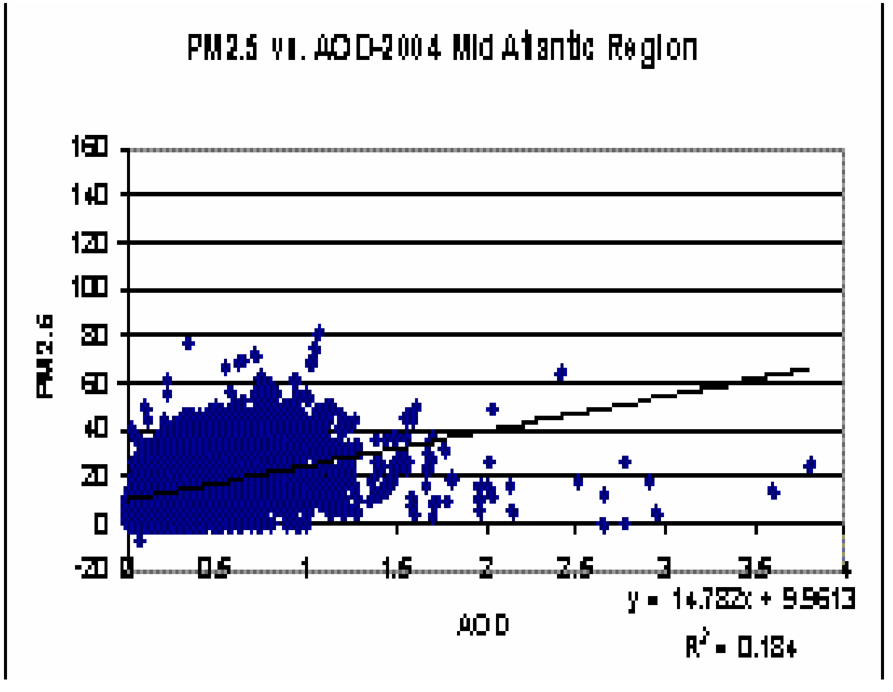

- Most years show r^2 values of 0.20-0.30
- Slope of trendlines also show moderate agreement as well

MODIS and PM Matches

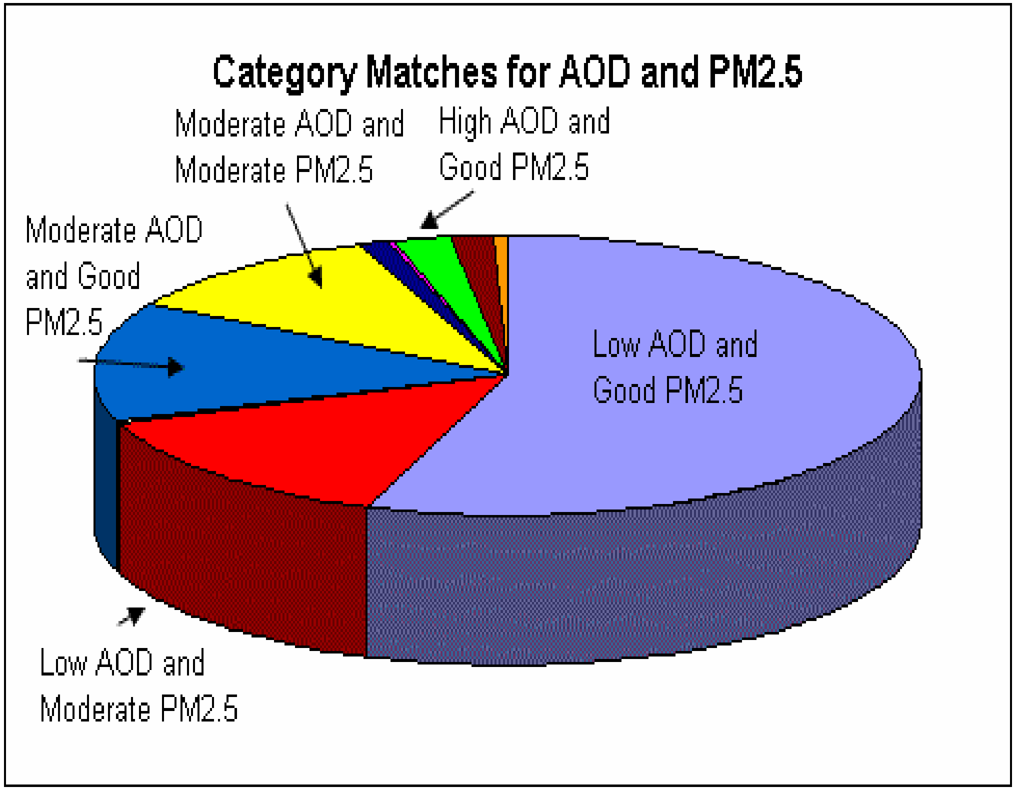

- Divided AOD into three levels: Low (0.0-0.4), Moderate (0.4-0.8), and High (0.8+)
- Used the EPA ranges for PM data
- There are many times where AOD was high and PM2.5 was low at the surface
- What were the conditions?
- Case Study: Yukon

Case Study: Yukon Smoke Plume

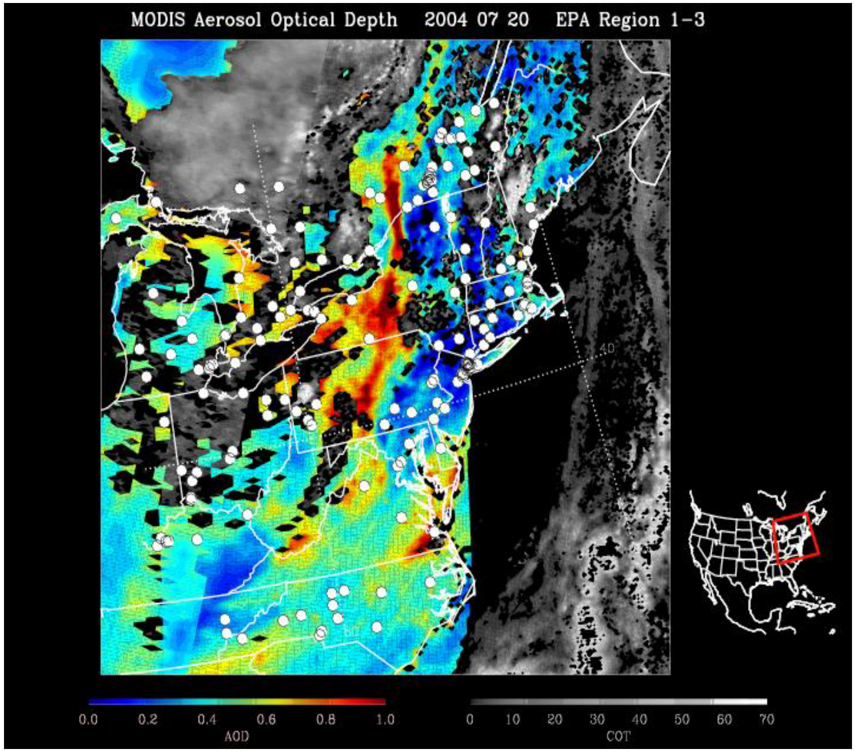

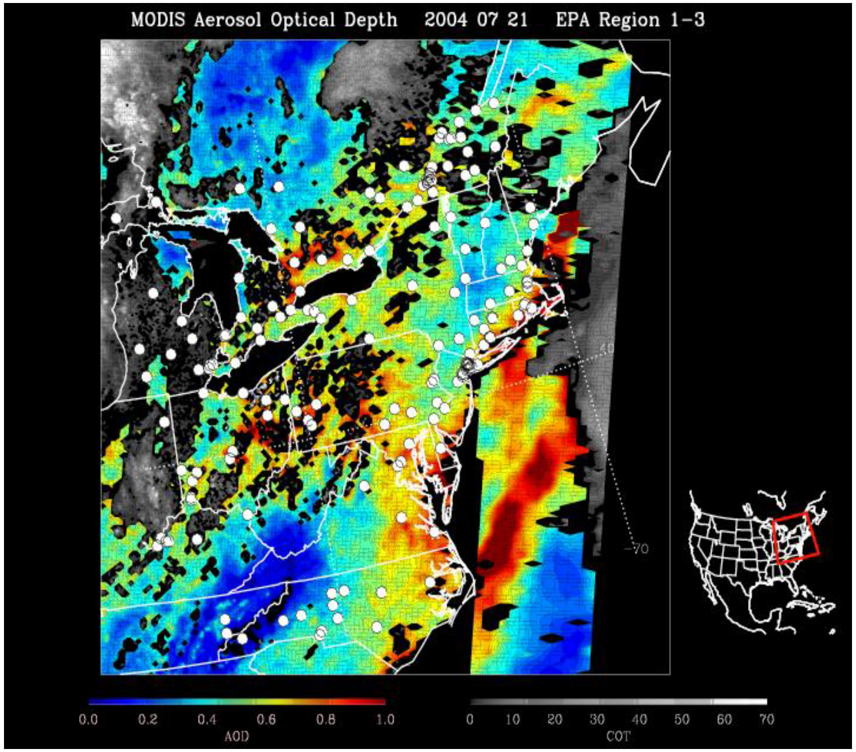

Case Study: Yukon Smoke Plume

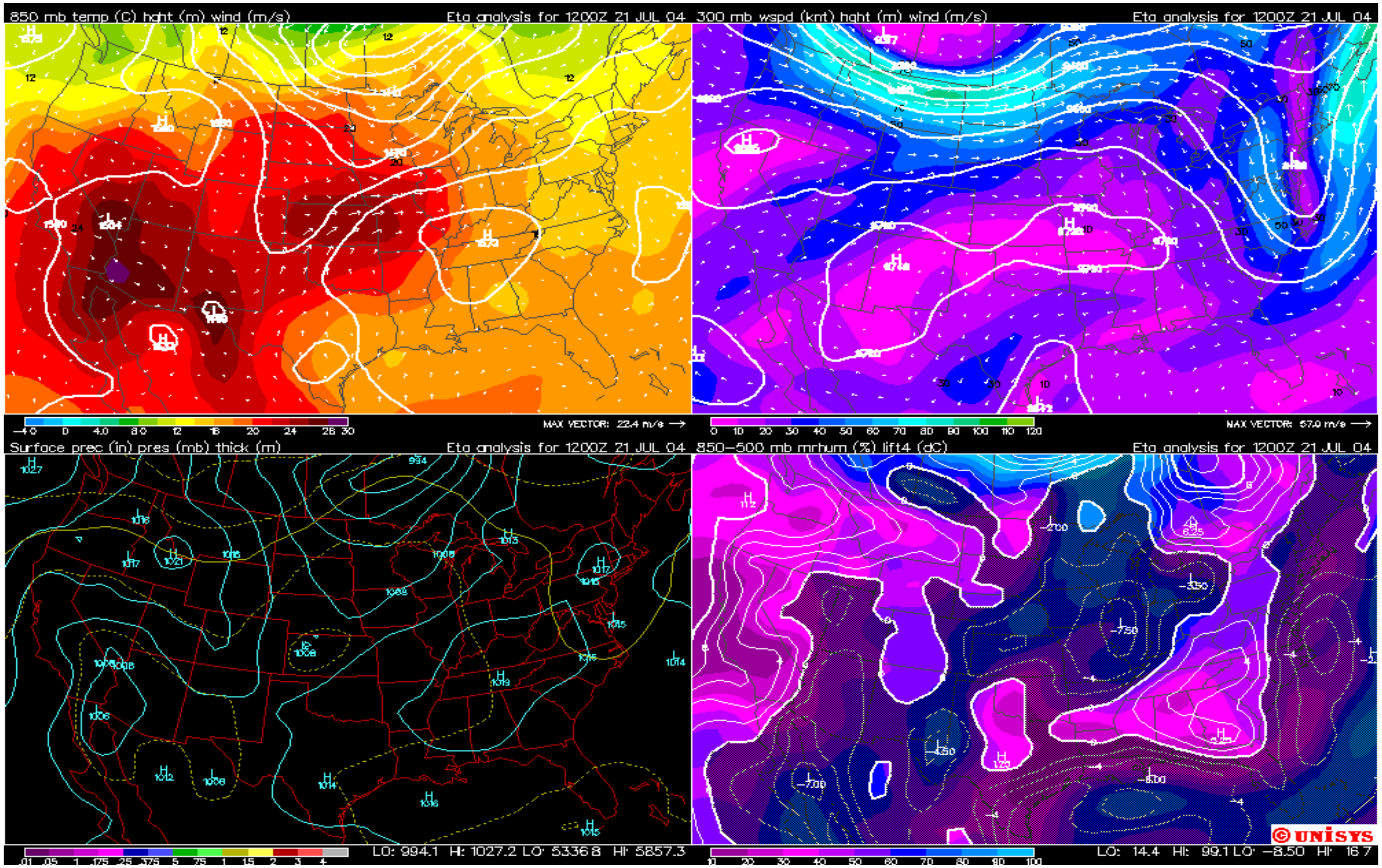

Case Study: Yukon Smoke Plume

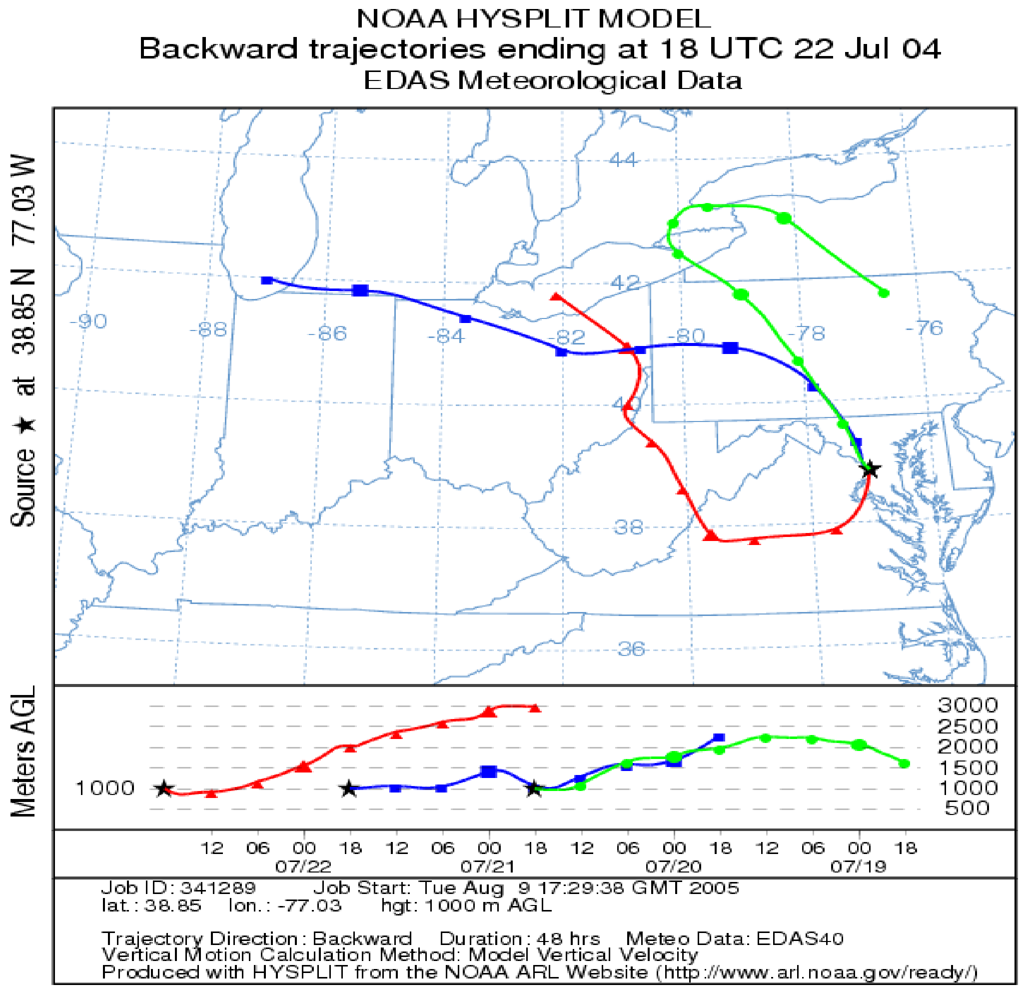

LIDAR and AERONET Measurements

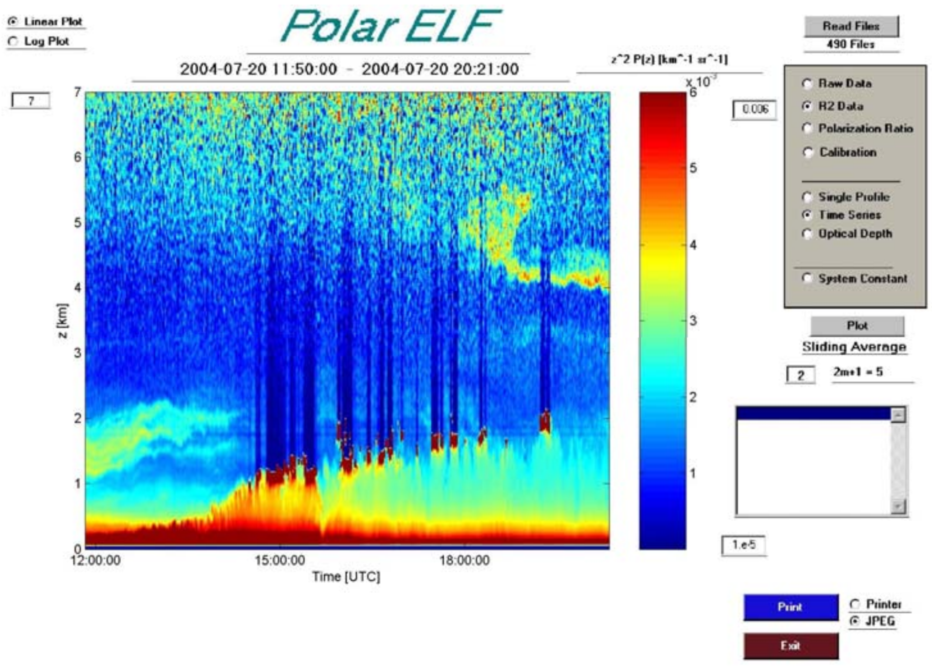

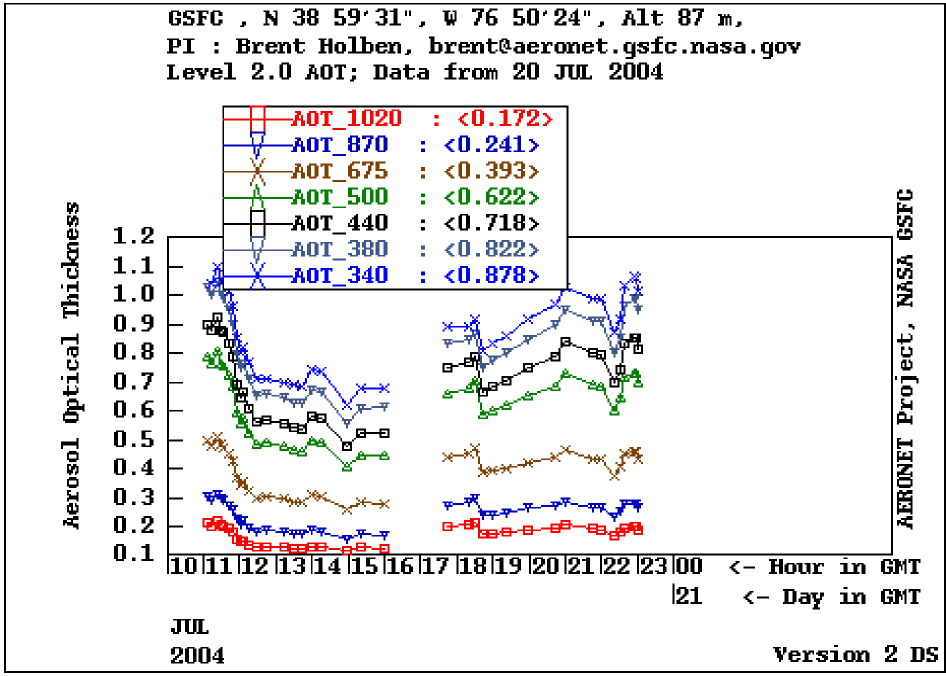

Conclusions

- MODIS is can be a valuable forecaster under the right conditions
- Look for low PM values and high AOD for possible dust events
- The use of other tools such as LIDAR and AERONET can also be useful
- Needs to be more analysis of wind direction and other meteorological conditions to better understand when MODIS is useful for air pollution

Questions?

An Analysis of Tropical Cyclone Precipitation Using Satellite Observations

By: Ahmed Tawfik
North Carolina State University

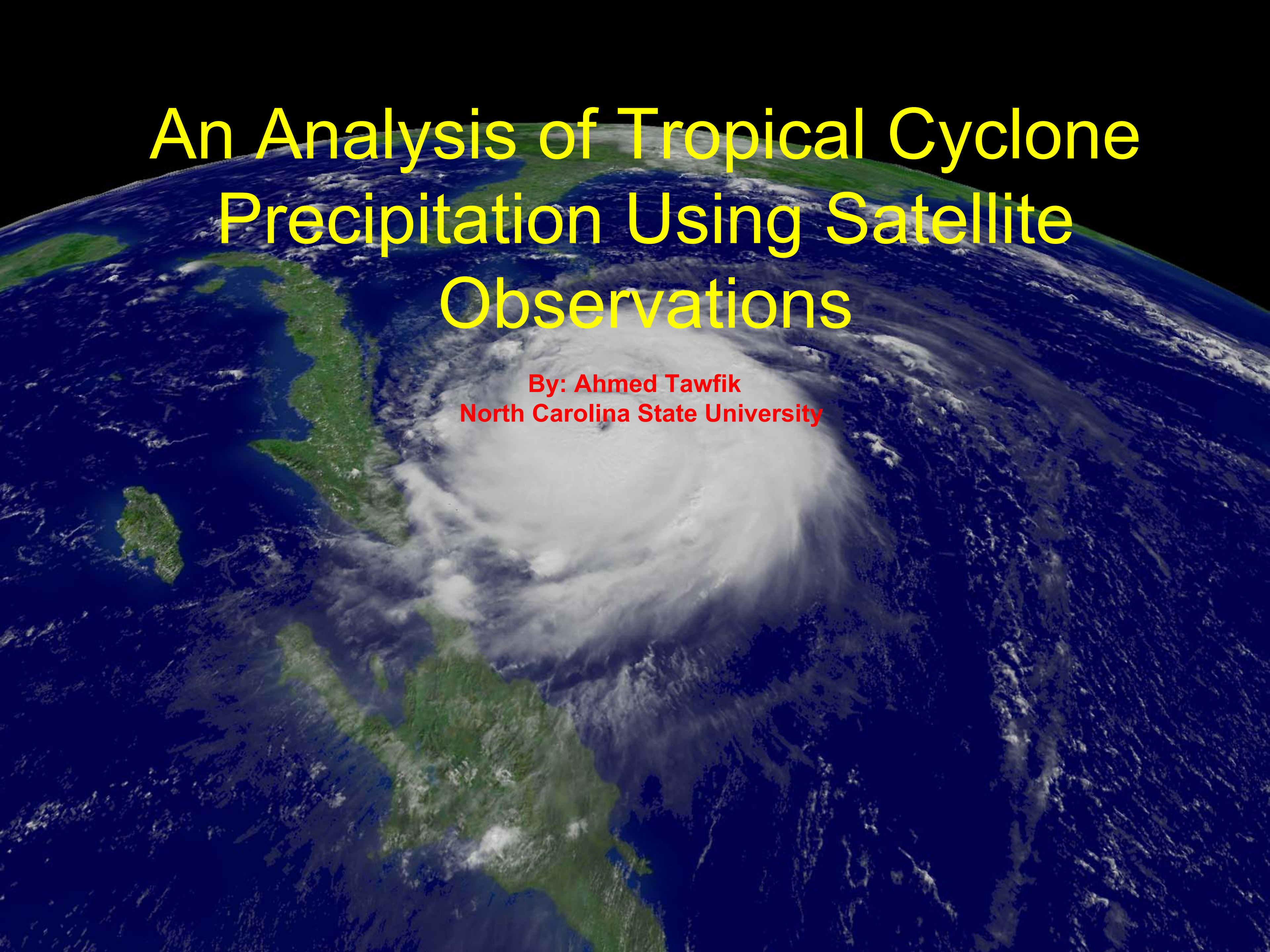

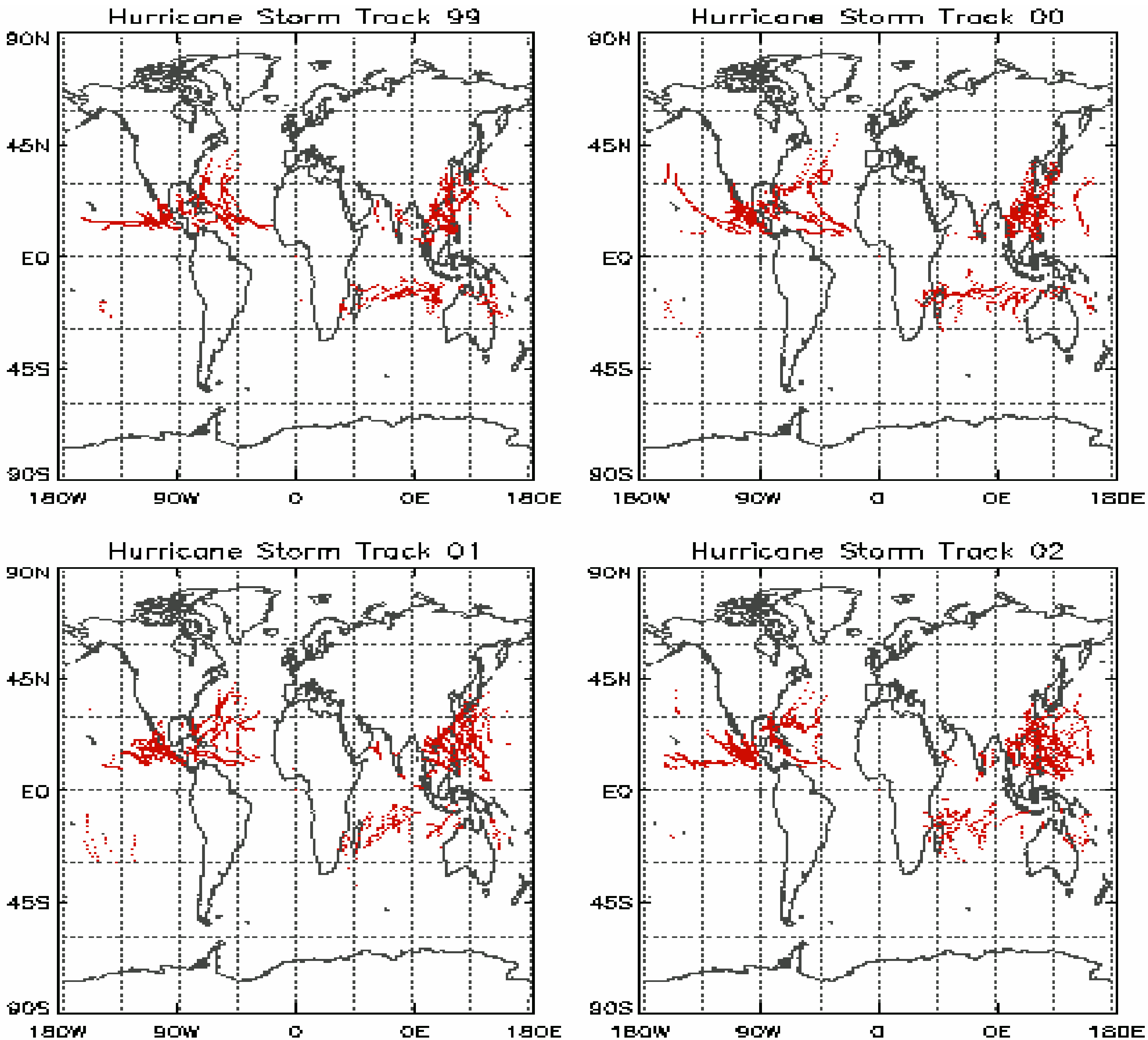

Hurricane Storm Track 99
Hurricane Storm Track 00
Hurricane Storm Track 01
Hurricane Storm Track 02
90N
45N
EQ
45S
90S
180W
90W
0
180E

Average Strike Frequency

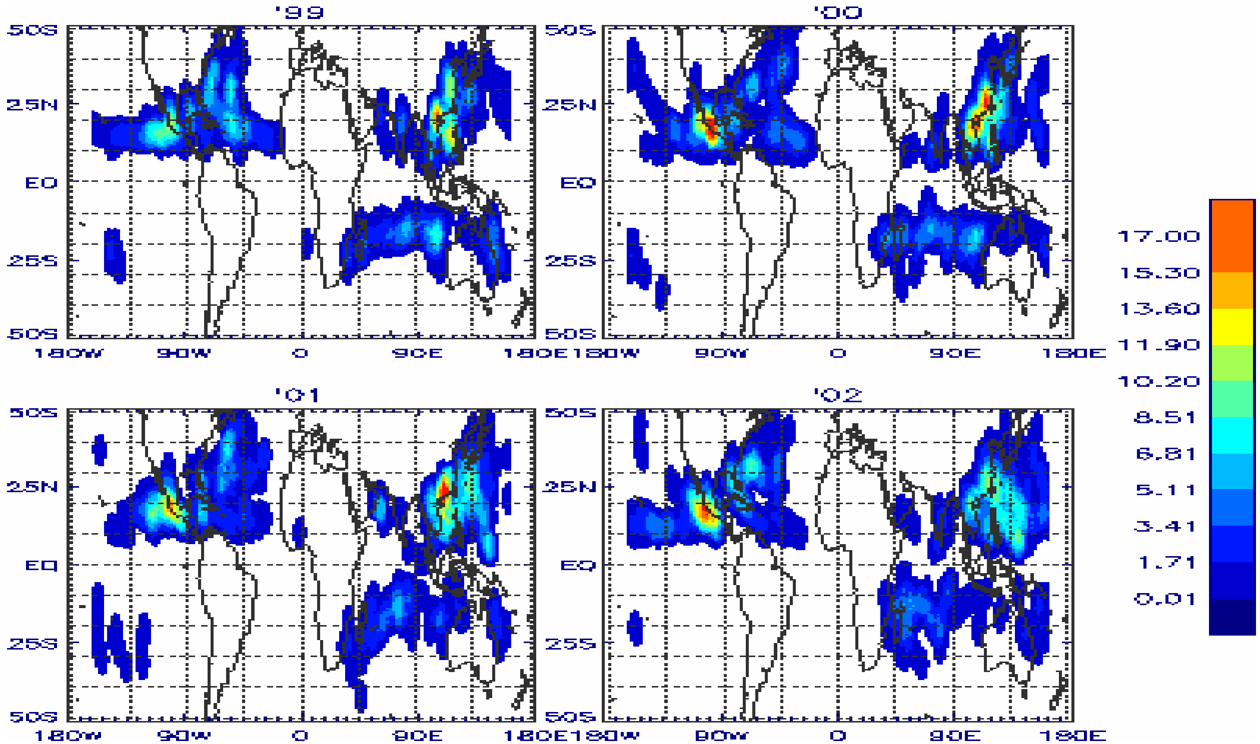

– Lower average strike occurrence in the East Pacific during '99 cold episode relative to '02 warm episode

Year	DJF	JFM	FMA	MAM	AMJ	MJJ	JJA	JAS	ASO	SON	OND	NDJ
1999	**-1.6**	**-1.2**	**-0.9**	**-0.7**	**-0.8**	**-0.8**	**-0.9**	**-0.9**	**-1.0**	**-1.2**	**-1.4**	**-1.6**
2000	**-1.6**	**-1.5**	**-1.1**	**-0.9**	**-0.7**	**-0.6**	-0.4	-0.3	-0.4	**-0.5**	**-0.7**	**-0.7**
2001	**-0.7**	**-0.5**	-0.4	-0.2	-0.1	0.1	0.2	0.1	0.0	-0.1	-0.2	-0.2
2002	-0.1	0.1	0.3	0.4	**0.7**	**0.8**	**0.9**	**0.9**	**1.1**	**1.3**	**1.5**	**1.3**

Total Monthly Average Precipitation

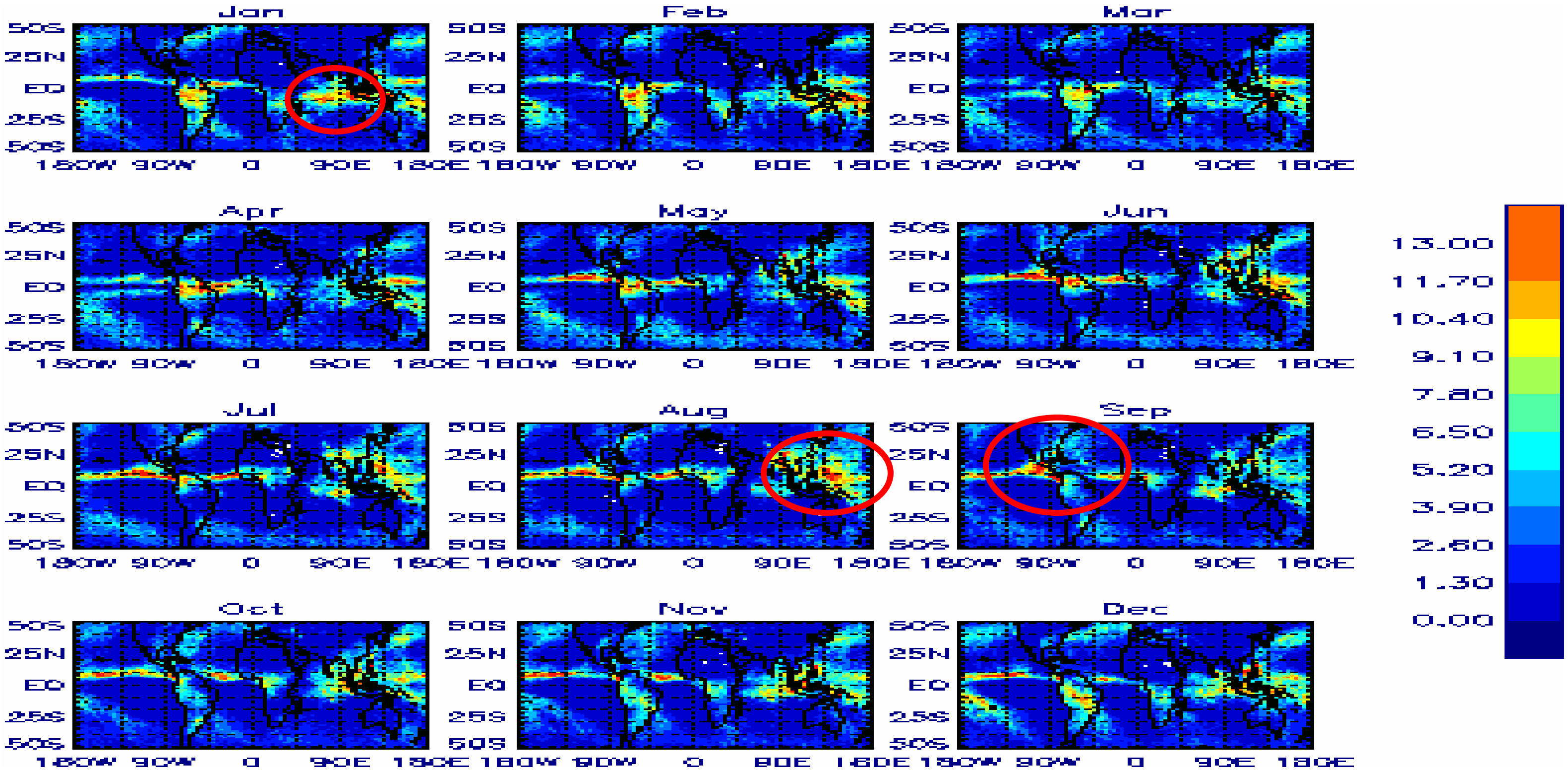

***Averaged monthly for 1999 through 2002 measured in mm / day

- Total precipitation noticeably increases during regional hurricane seasons

Average Monthly Hurricane Precipitation

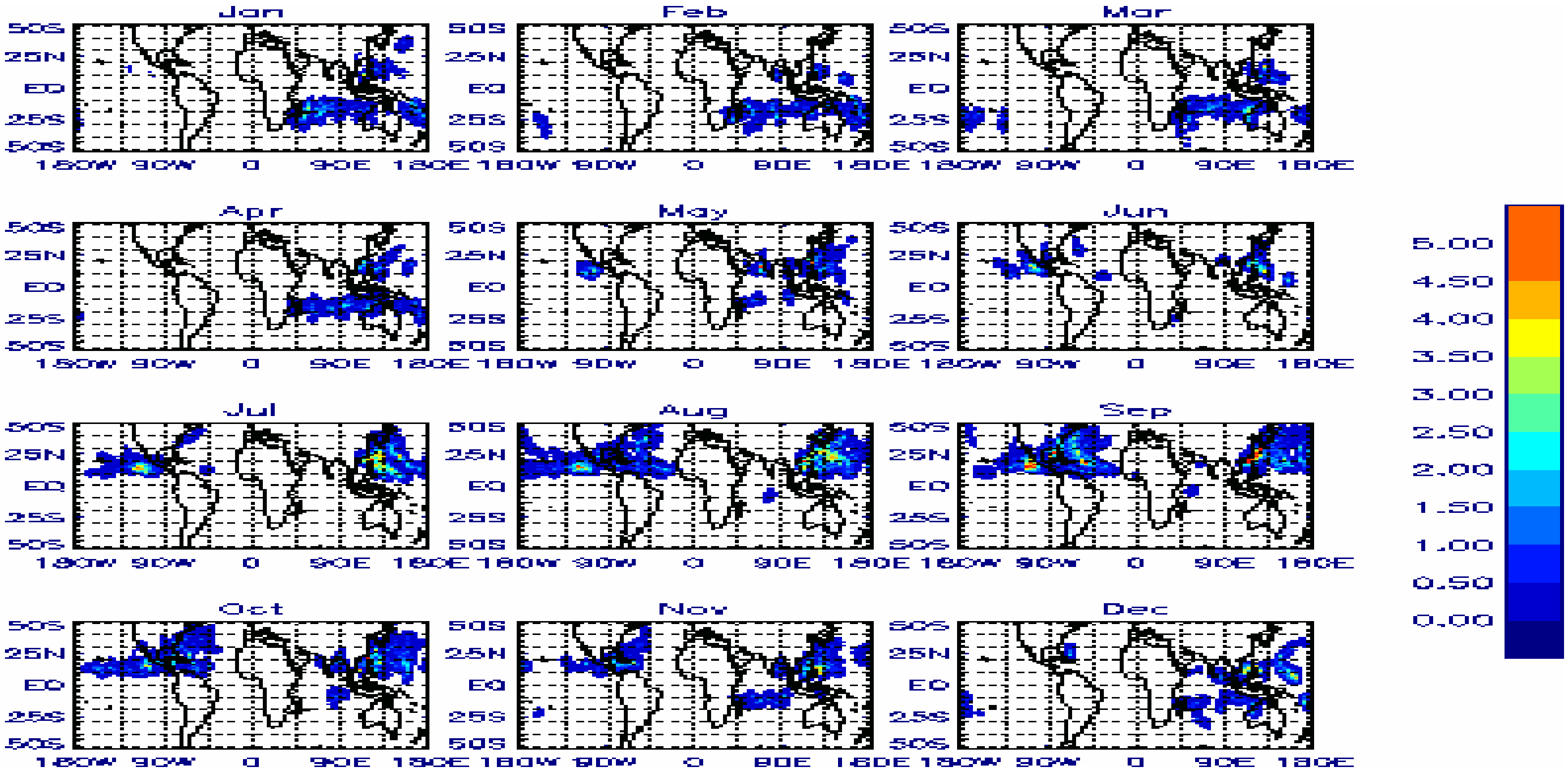

***Averaged monthly for 1999 through 2002 measured in mm / day

Average Monthly Hurricane % Precipitation

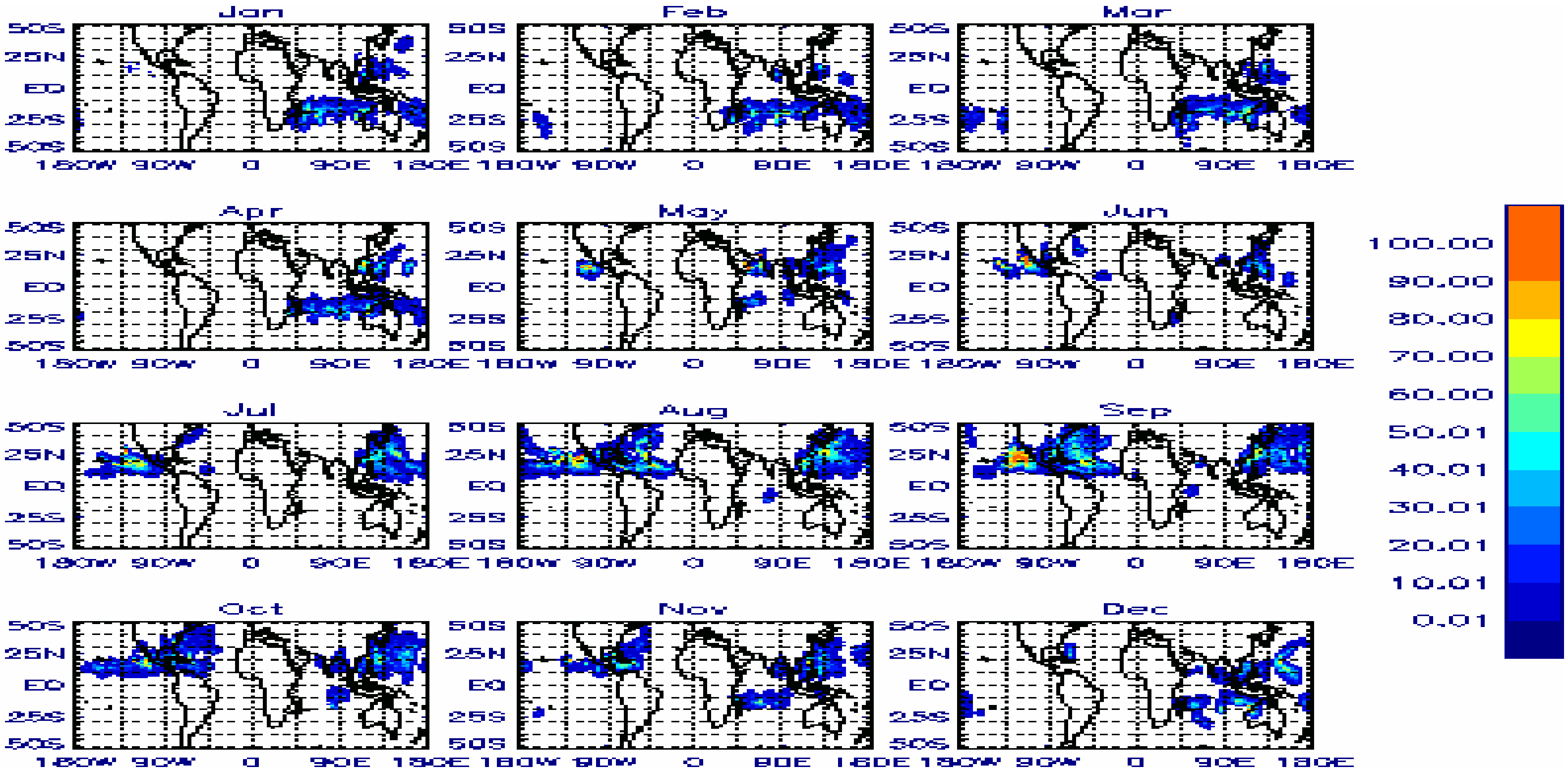

***Averaged monthly for 1999 through 2002 measured as a percentage

Max Average Monthly Hurricane % Precipitation

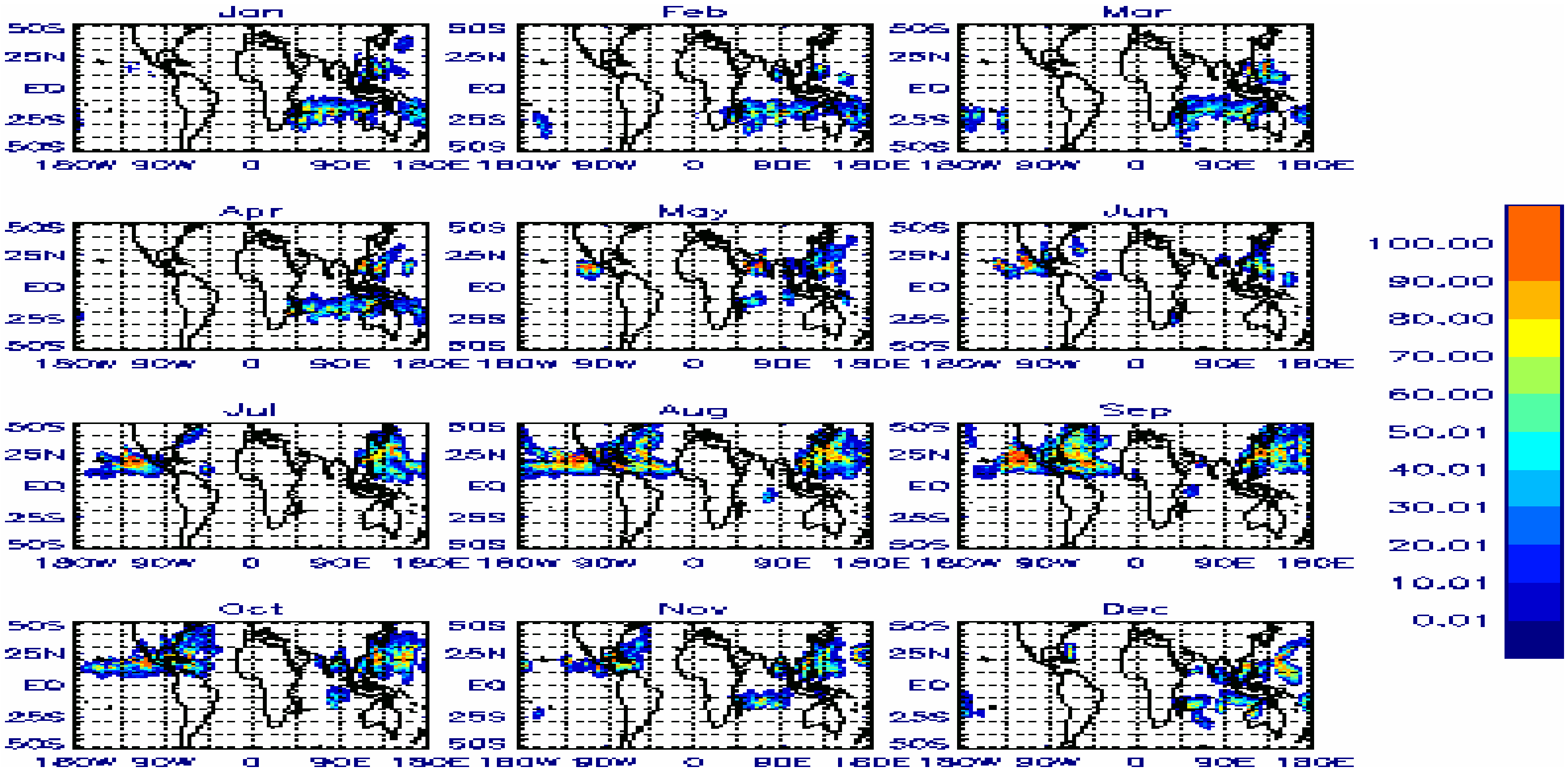

***Averaged monthly for 1999 through 2002 measured as a percentage

Atlantic Ocean Hurricane Season

El Nino ('02)

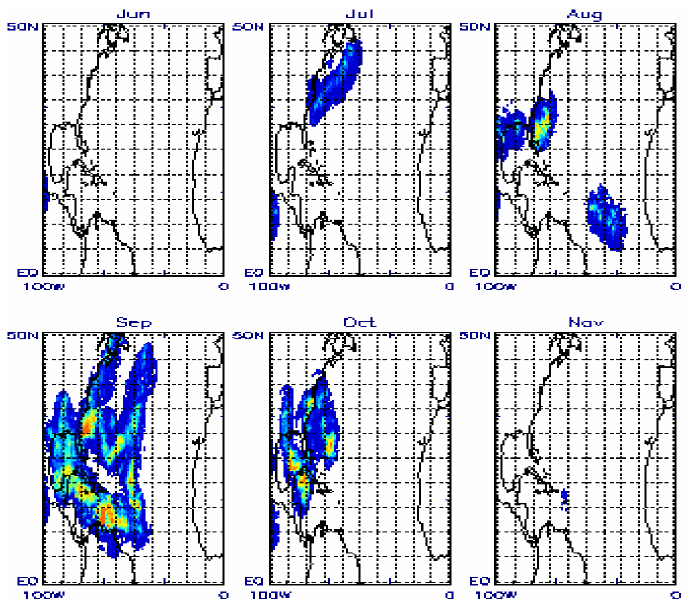

Anti-El Nino ('99)

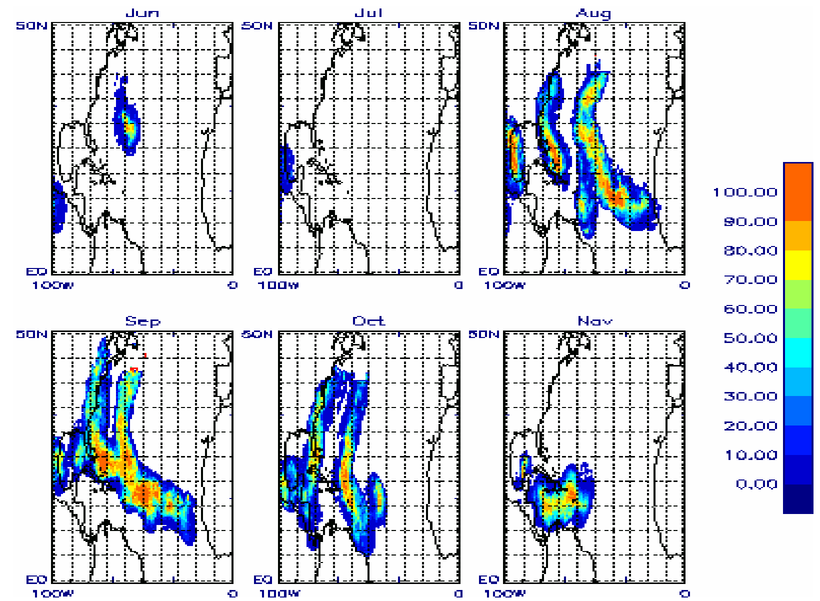

- Considerably less TC precipitation contribution to total during El Nino

- Migration to West Atlantic with less TC formation near Africa during El Nino

- Appears to be shorter hurricane Season during El Nino event

- Results seem to coincide with Gray et al. (1992) and Rodgers (2001)

Northwest Pacific Ocean Hurricane Season

El Nino ('02)

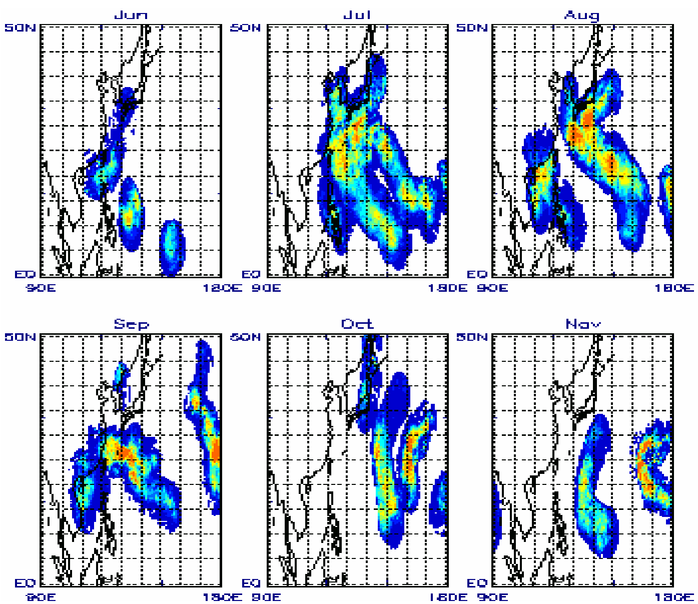

Anti-El Nino ('99)

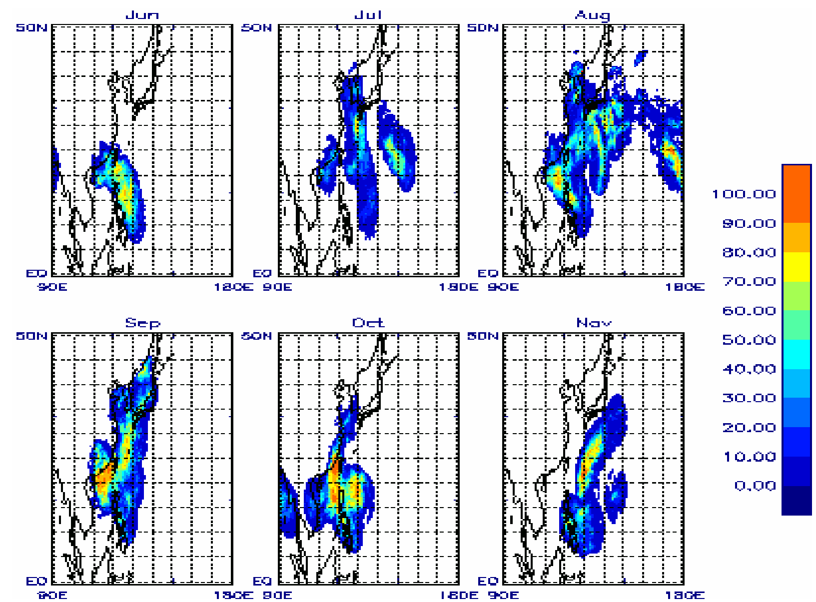

- Greater TC precipitation Contribution to the region During El Nino
- High concentration of TC strikes around southern China and lower Latitudes during Anti-El Nino events
- TCs appear to originate in the Northwest Pacific region rather than Migrate from the Central and East Pacific during Anti-El Nino event

TC Precipitation Percent Contribution to Region

	Adler Findings	Using Adler Region	Using Specific Region
West Pacific	12	10.5986	8.53364
Central Pacific	3	2.4853	1.96101
East Pacific	4	8.77703	6.60095
Entire Pacific	7	7.28698	5.69853
West Atlantic	4	7.13341	6.67391
East Atlantic	3	2.16558	2.67803
Entire Atlantic	4	4.64949	4.67597
West Indian	*****	*****	0.608608
East Indian	*****	*****	0.420142
Entire Indian	*****	*****	0.514375

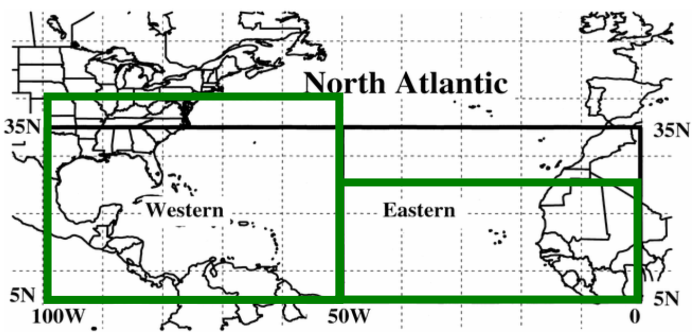

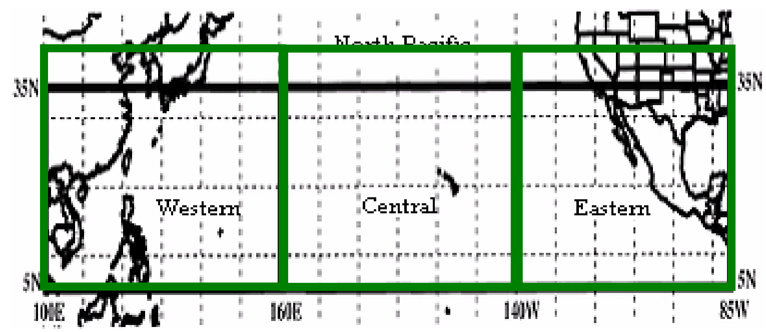

*** Black region is Adler; Green is Specific (Rodgers et al. 2001)

Regional Latent Heat Averaged Monthly

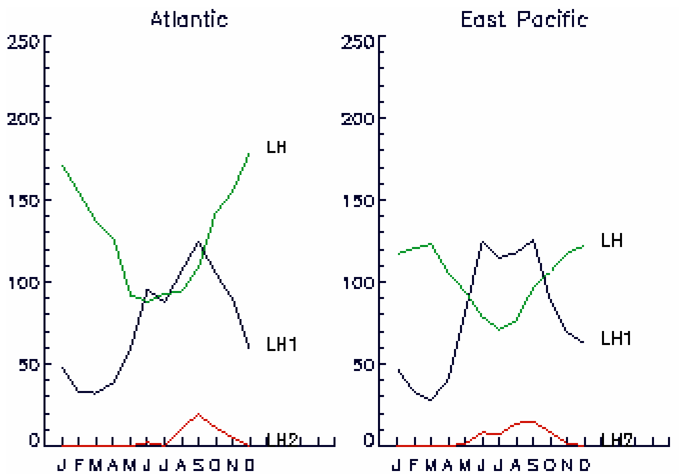

- Latent heat from total precipitation (LH1) Appears to exceed the sea surface Latent heat (LH) during each region's TC months

- Indian Ocean seems to be the exception

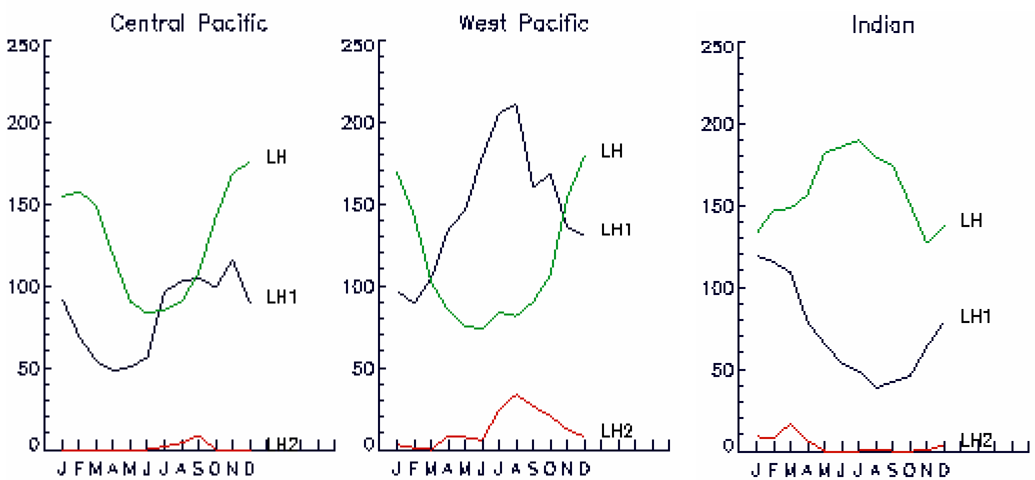

*** **LH: Sea surface latent heat release**

LH1: Total precipitation Latent heat release

LH2: TC precipitation Latent heat release

Latent heat measured in W/m^2

Seasonal Latent Heat Averages

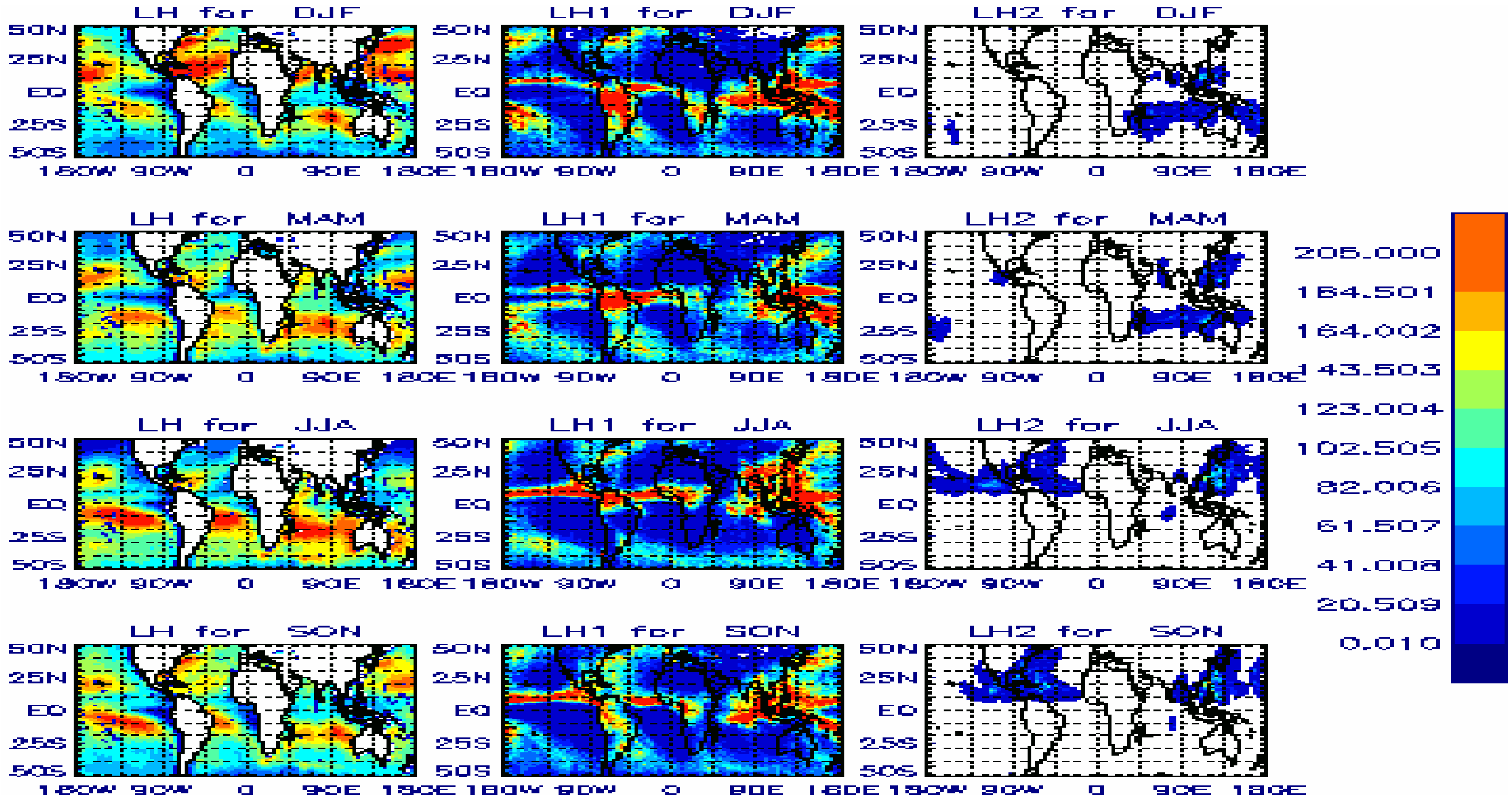

*** LH is the Sea Surface Latent heat release ; LH1 is latent heat release of total precipitation
LH2 is the latent heat release from tropical cyclones (all plots are in W/m^2)

References

Rodgers, E. B., R. F. Adler, and H. F. Pierce, 2001: Contribution of Tropical Cyclones to the North Atlantic Climatological Rainfall as Observed from Satellite. *J. Appl. Meteor.,* ***40****, 1785-1800.*

Rodgers, E. B., R. F. Adler, and H. F. Pierce, 1999: Contribution of Tropical Cyclones to the North Pacific Climatological Rainfall as Observed from Satellite. *J. Appl. Meteor.,* ***39****, 1658-1678.*

Elsner, J. B., A. B. Kara, and M. A. Owens, 1999: Fluctuations in North Atlantic Hurricane Frequency. *J. Climate.,* ***12****, 427-437.*

Lonfat, M., F. D. Marks Jr, and S. S. Chen, 2004: Precipitation Distribution in Tropical Rainfall Measuring Mission (TRMM) Microwave Imager: A Global Perspective. *Monthly Weather Rev.,* ***1****645 -1660.*

Elsner, J. B., A. B. Kara, and M. A. Owens, 1999: Fluctuations in North Atlantic Hurricane Frequency. *J. Climate.,* ***12****, 427-437.*

Pielke Jr, R. A., and C. N. Landsea, 1999: La Nina, El Nino, and Atlantic Hurricane Damages in the United States. *AMS Bulletin.,* ***80****, 2027-2033.*

http://www.bom.gov.au/bmrc/pubs/tcguide/globa_guide_intro.htm

Acknowledgements

I appreciate and am thankful for the research opportunity here at Goddard Space Flight Center. I would also like to thank my mentor, Yaping Zhou, and Per Gloerson. Special thanks to Kevin Leavor as well.

Uncovering the Milankovitch Cycle in the Vostok Ice Core Using the Hilbert-Huang Transform

Kevin Leavor
Washington and Jefferson College
August 12, 2005

Modus Operandi

- Why Ice Core Data?
- What is the Hilbert-Huang Transform (HHT)?
- What Are We Looking For?
- Procedure
- Findings
- Conclusion
- References

Why Ice Core Data?

- Vostok Ice Core
  - Taken from Antarctica
  - Extends back 422,766 years
    - Allows for the analysis of long term cycle
    - Important for understanding long term climate change
- Reliability
  - Gases trapped in the ice allow for dating
- Similar Studies Exist
  - Ocean Floor
  - Coral Reefs

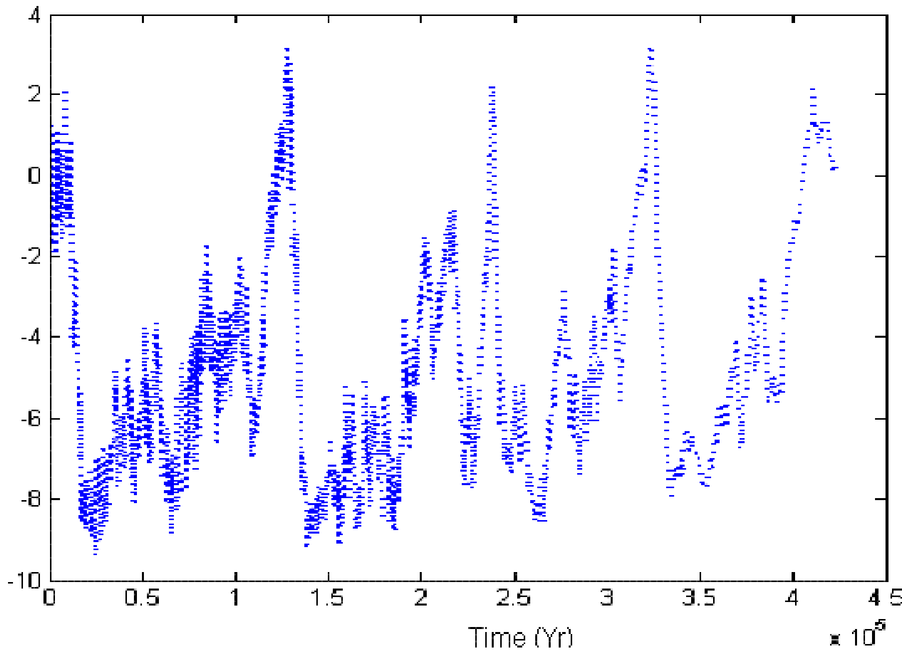

What is the HHT?

- Data Analysis technique
  - Incorporates the Hilbert Transform
  - Nonlinear and Non-stationary data
- Empirical Mode Decomposition
  - Intrinsic Mode Functions (IMFs)
    - Derived from the data
    - Adaptability
  - Reconstruction
    - Summation of IMFs yields the original function

What are We Looking For?

- 3 Cycles (Earth's Orbital Dynamics)
  - Precession (~19 000 - ~23 000 years)
  - Obliquity (~41 000 years)
  - Eccentricity (~100 000 years)
- Eccentricity is difficult to pinpoint
  - Some believe "the 100 ka period in paleoclimate data is unrelated to Milankovitch orbital forcing" (Bradley 23)

Procedure

- HHT
  - HHT-DPS
    - Intermittency
      - Removes “insignificant” short-term oscillations
    - Isolate IMFs
  - MATLAB
    - Perform Hilbert Transform
    - Perform Marginal Spectrum Analysis

- Fourier
  - MATLAB
    - Use Welch Power Spectrum Analysis
    - Compare to HHT marginal

Procedure - 2

Necessary Processing Steps

- Data Condensation
  - Data points become too sparse in later portions of the data
    - Taken to 1 point for every 20 years
- Intermittency
- MATLAB Procedures
  - [n,t,f]=nnsp(cy(:,18:22),0,422.766,800,2114,0,0.2,0,422.766, ‘hilbert','spline',3);
  - q = fspecial(‘ga’, 5, . 5’);
  - ns = filter2(q,n);
  - ns = filter2(q,ns);
  - ns = filter2(q,ns);
  - ms = mspc(ns,f);
  - [p,w]=pwelch(y, hanning(21138),0,21138,50);

Findings

All IMFs After Intermittency

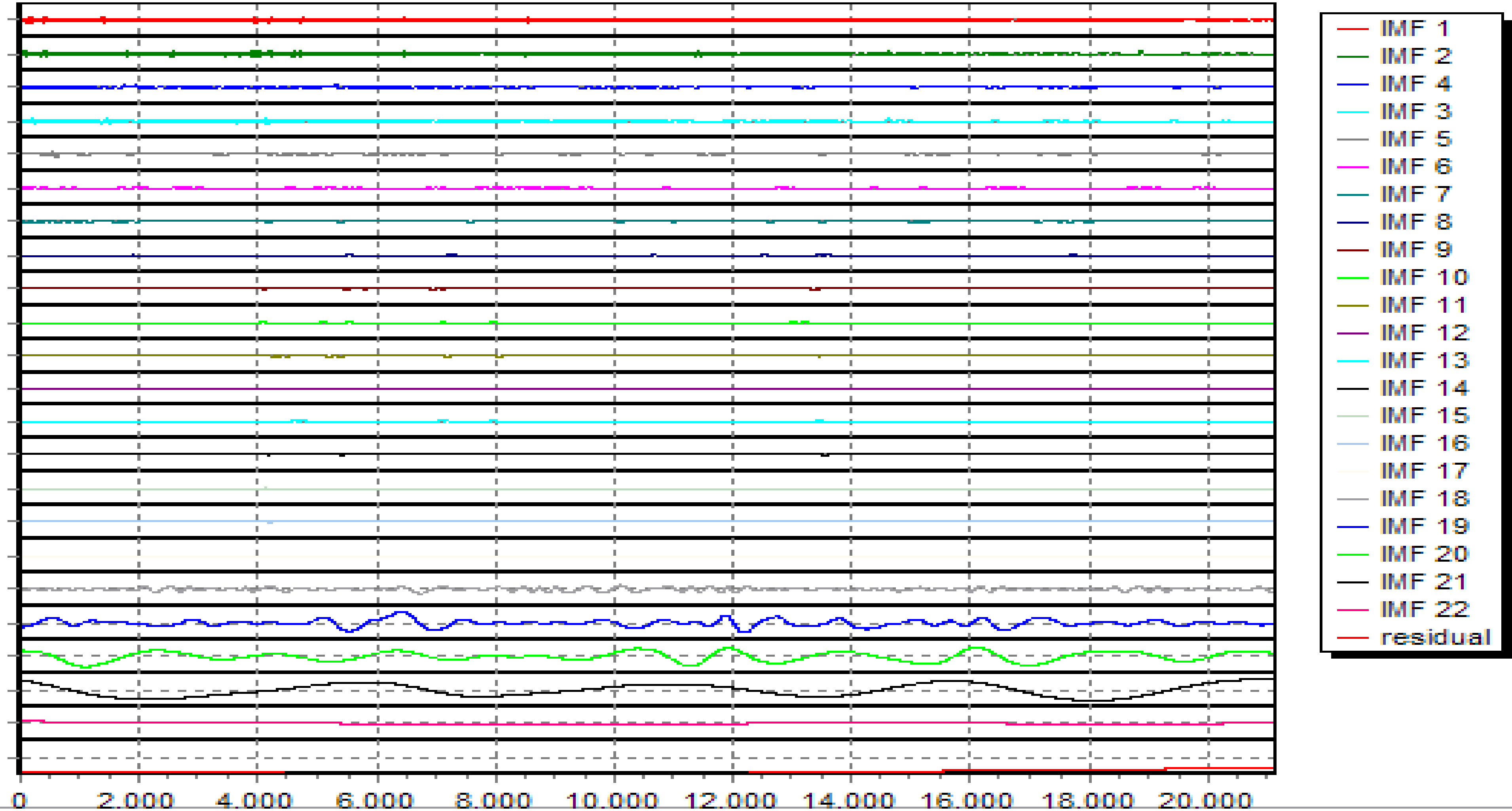

Findings

Overlay of All IMFs

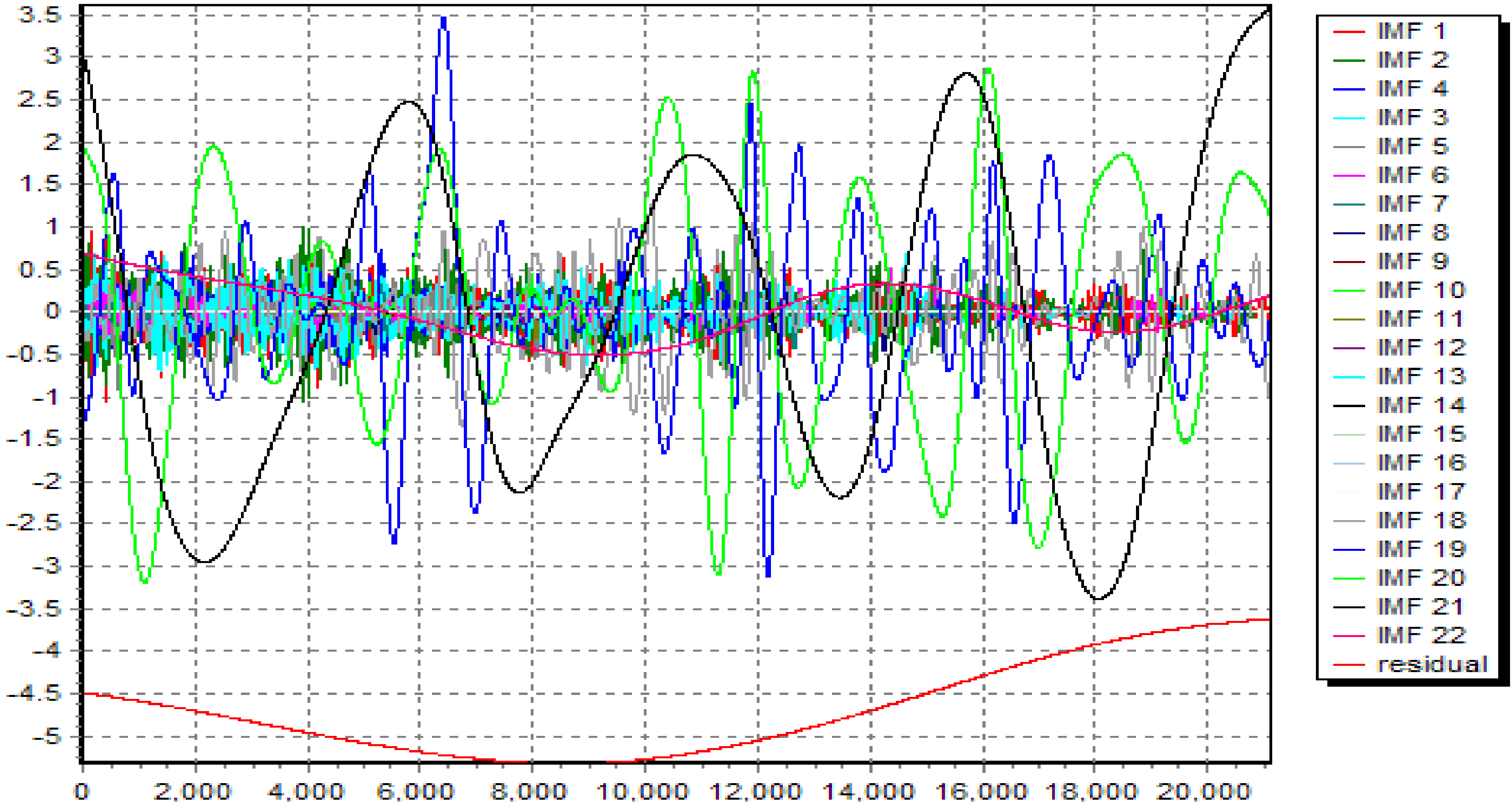

Findings
5 Lowest Components (No Residual)

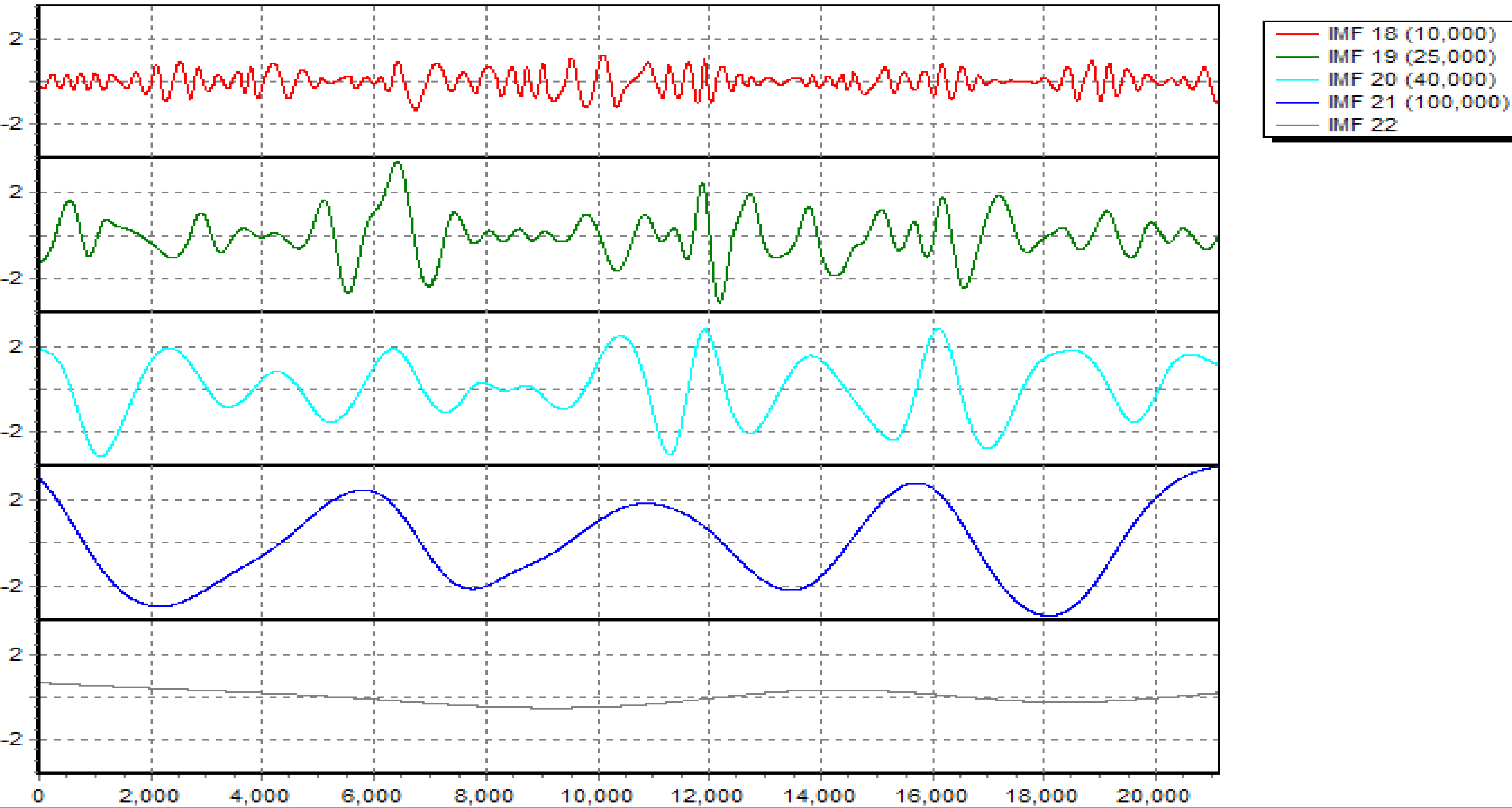

Findings

Overlay of 5 Lowest Components

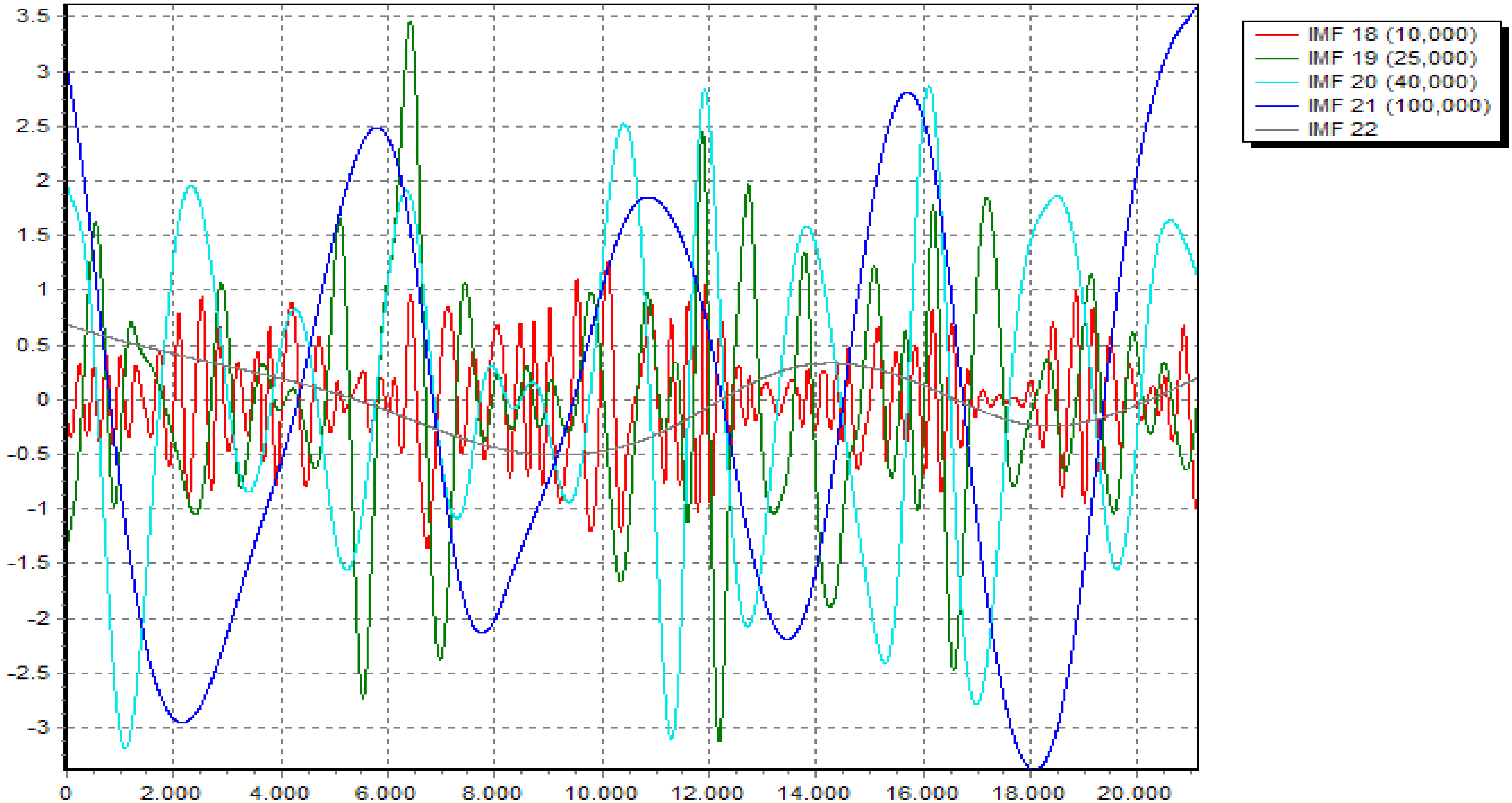

Findings

Hilbert Spectrum of the Components

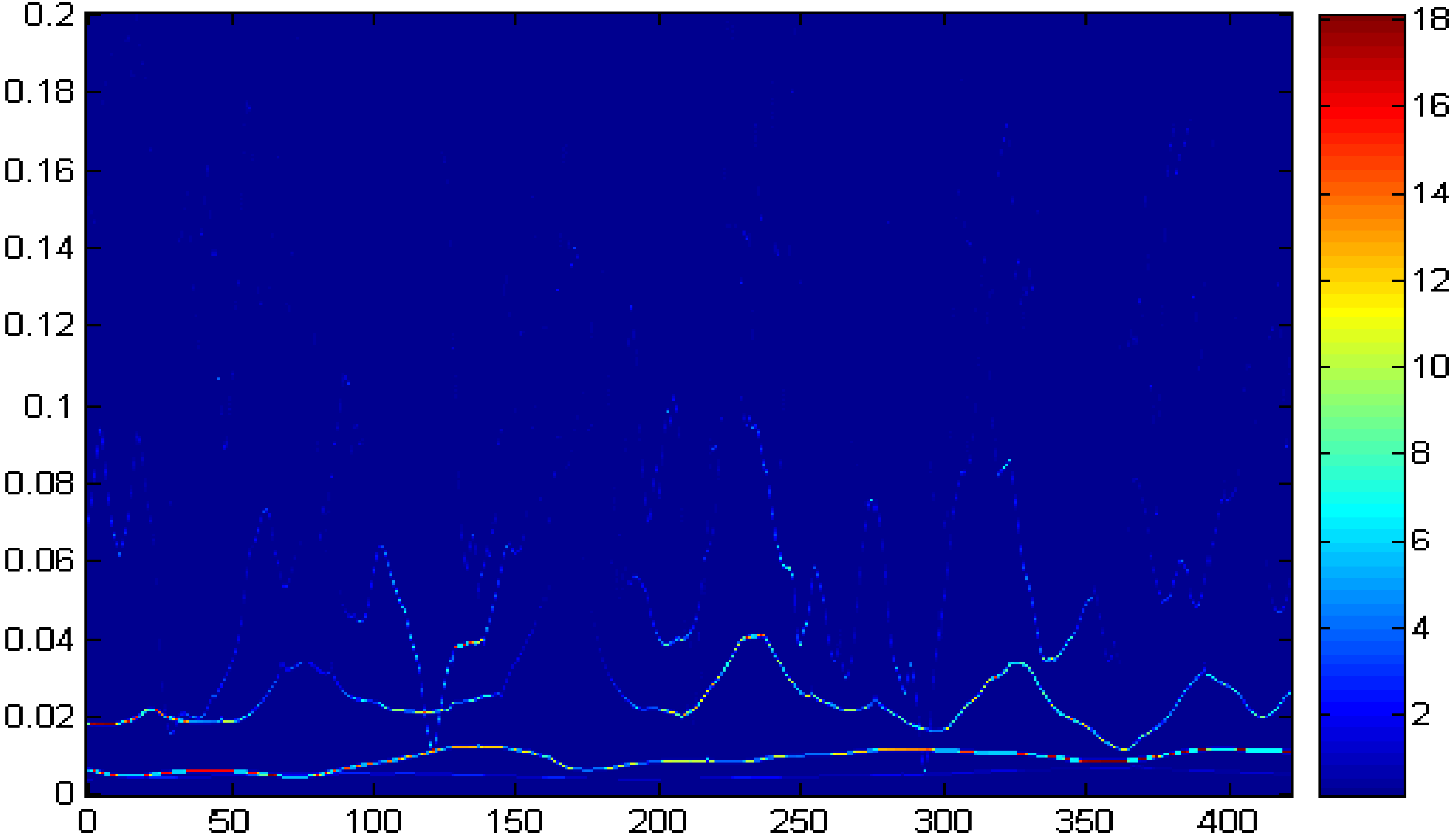

Findings

Hilbert Spectrum with Increased Resolution

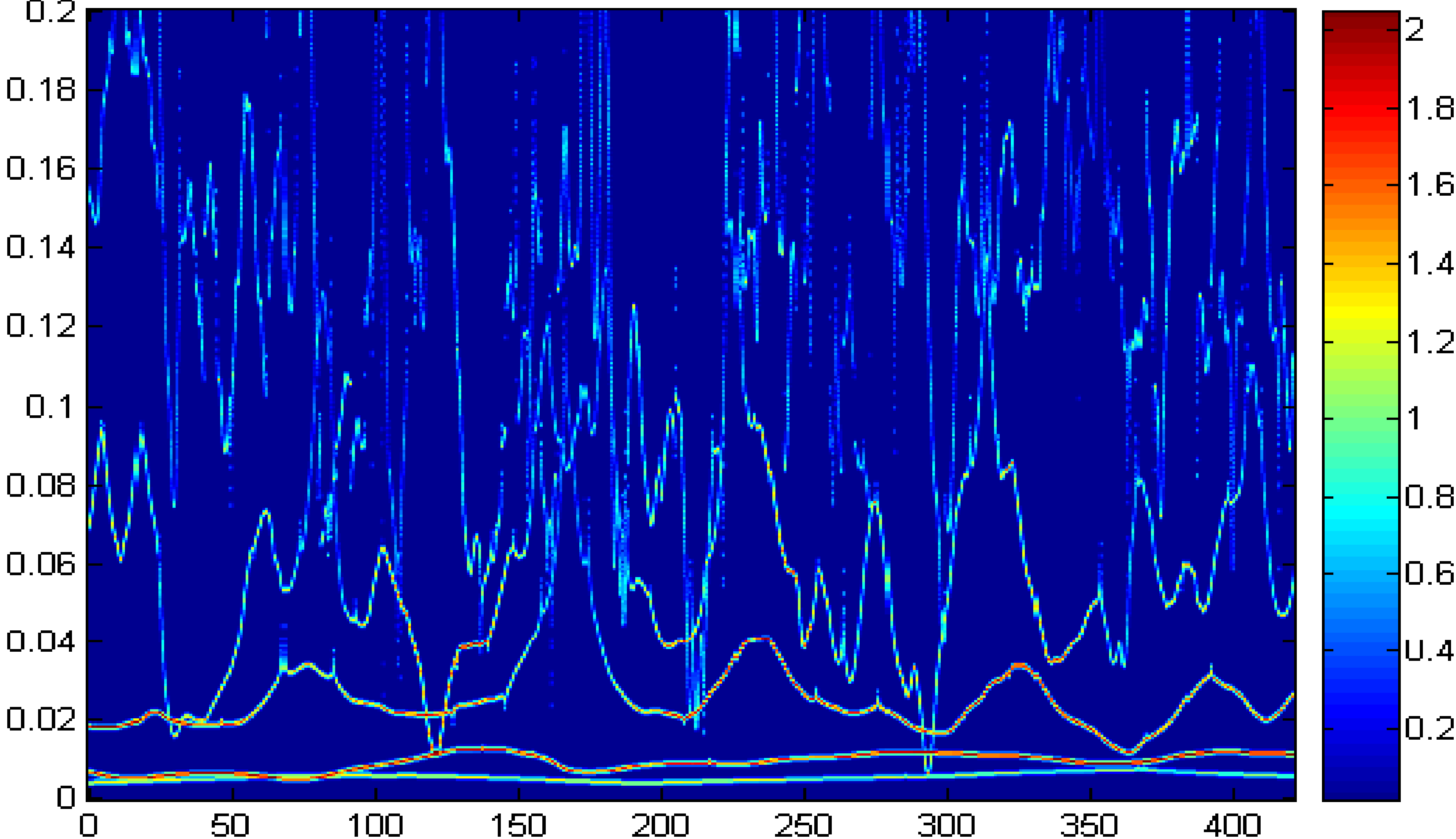

Findings

Marginal Spectrum

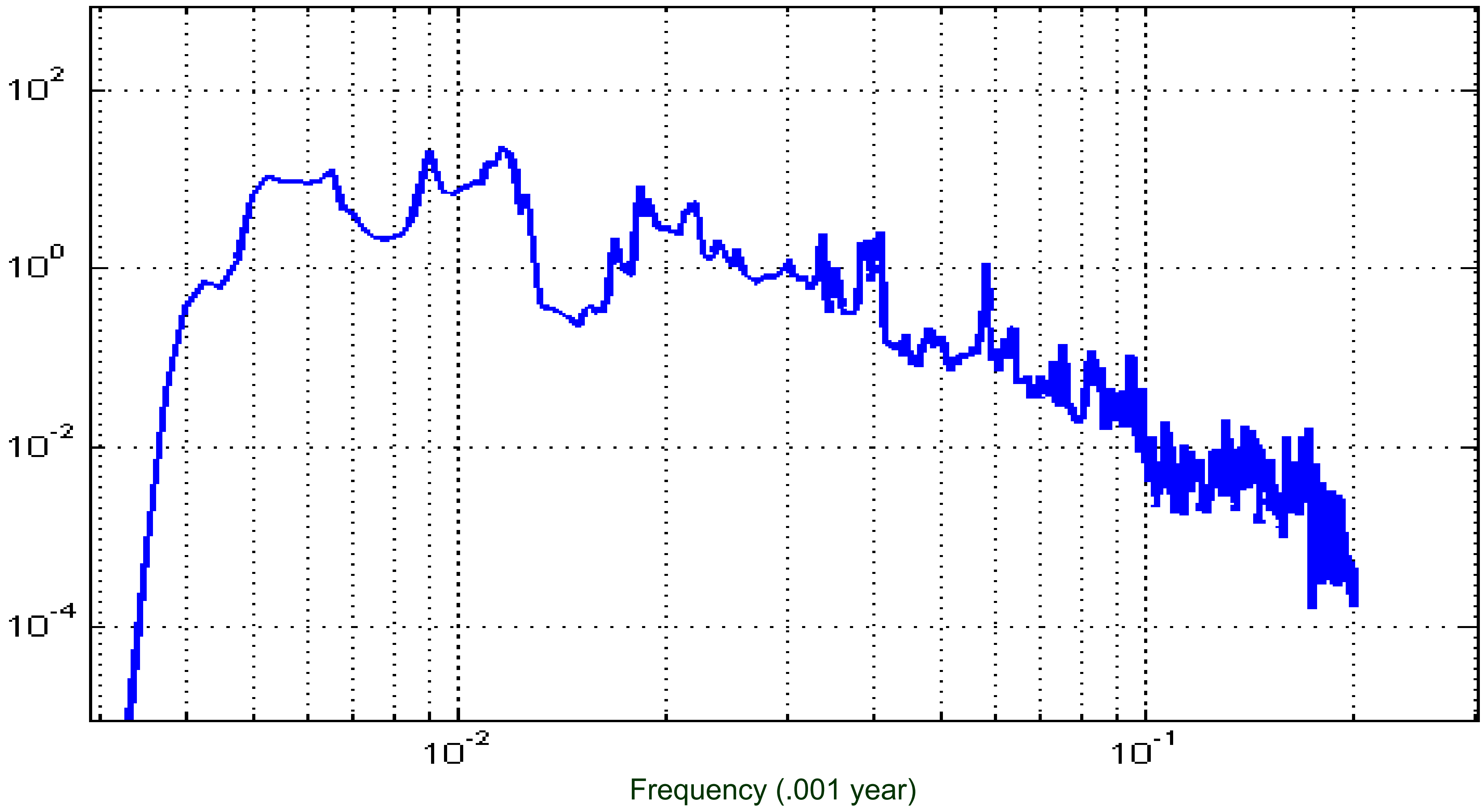

Findings

Zoom of Marginal Spectrum

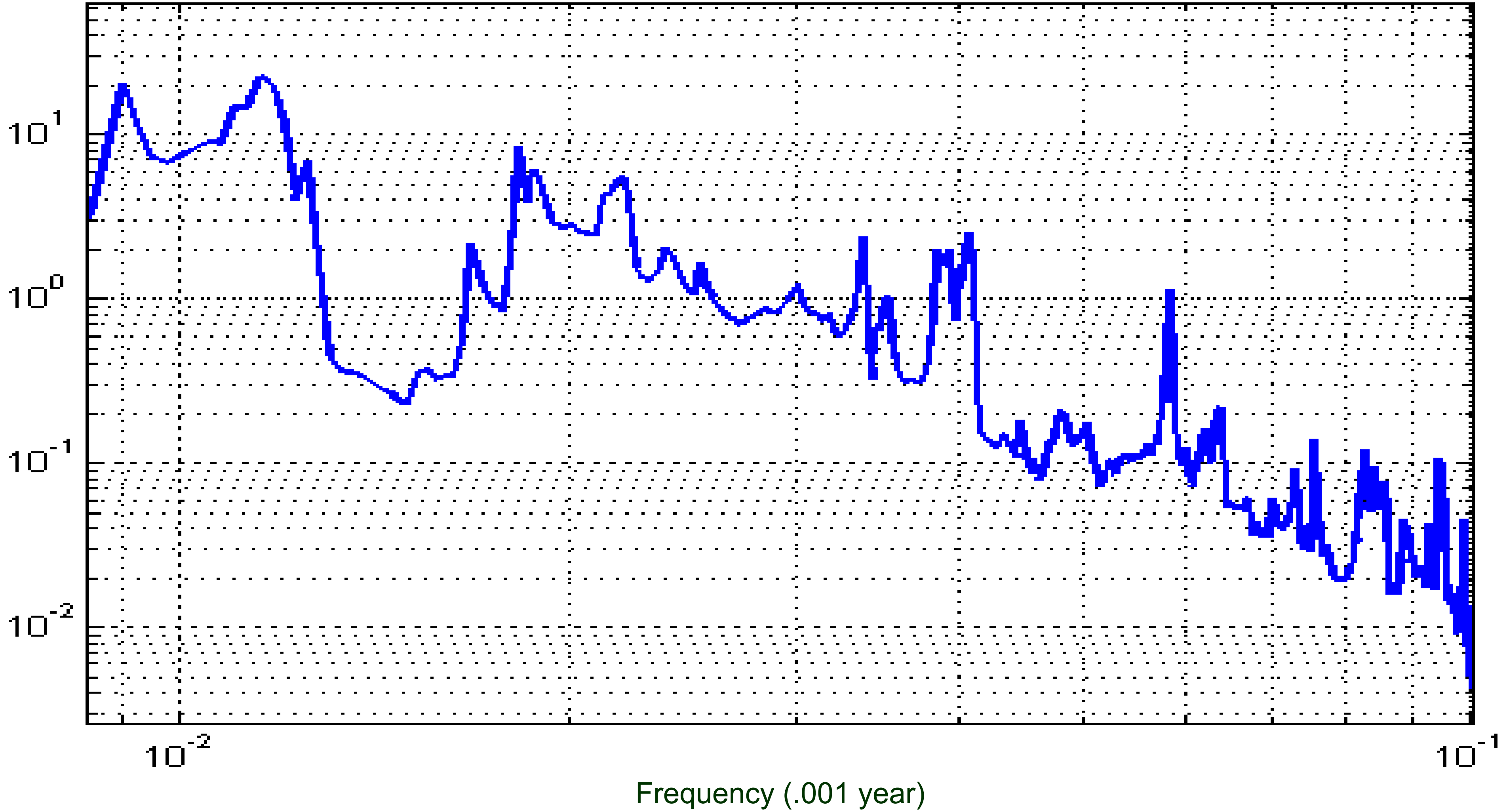

Findings

Fourier Power Spectral Density (PSD)

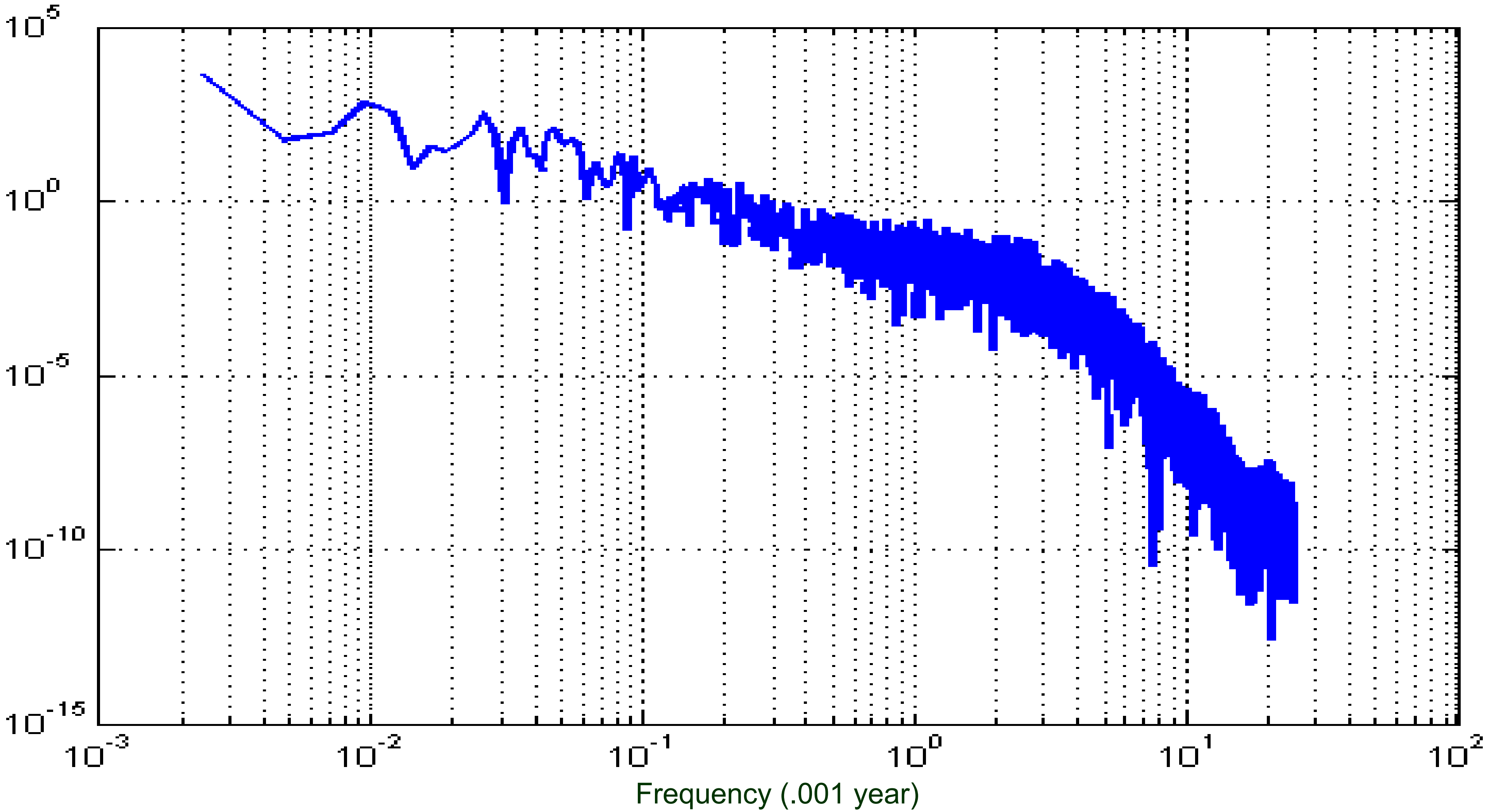

Findings

Zoom of Fourier PSD

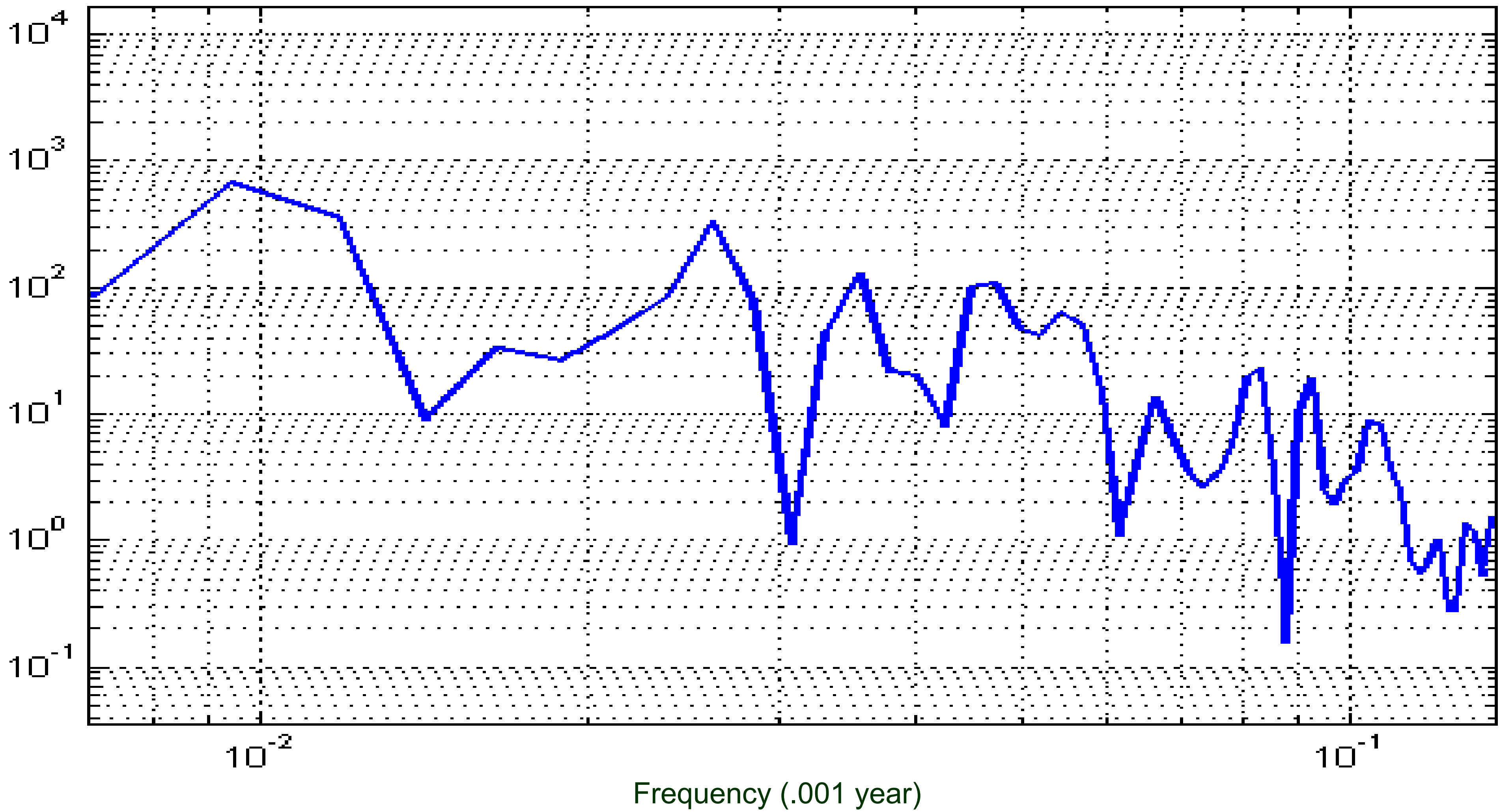

Findings
Comparison of HHT Marginal and Fourier PSD

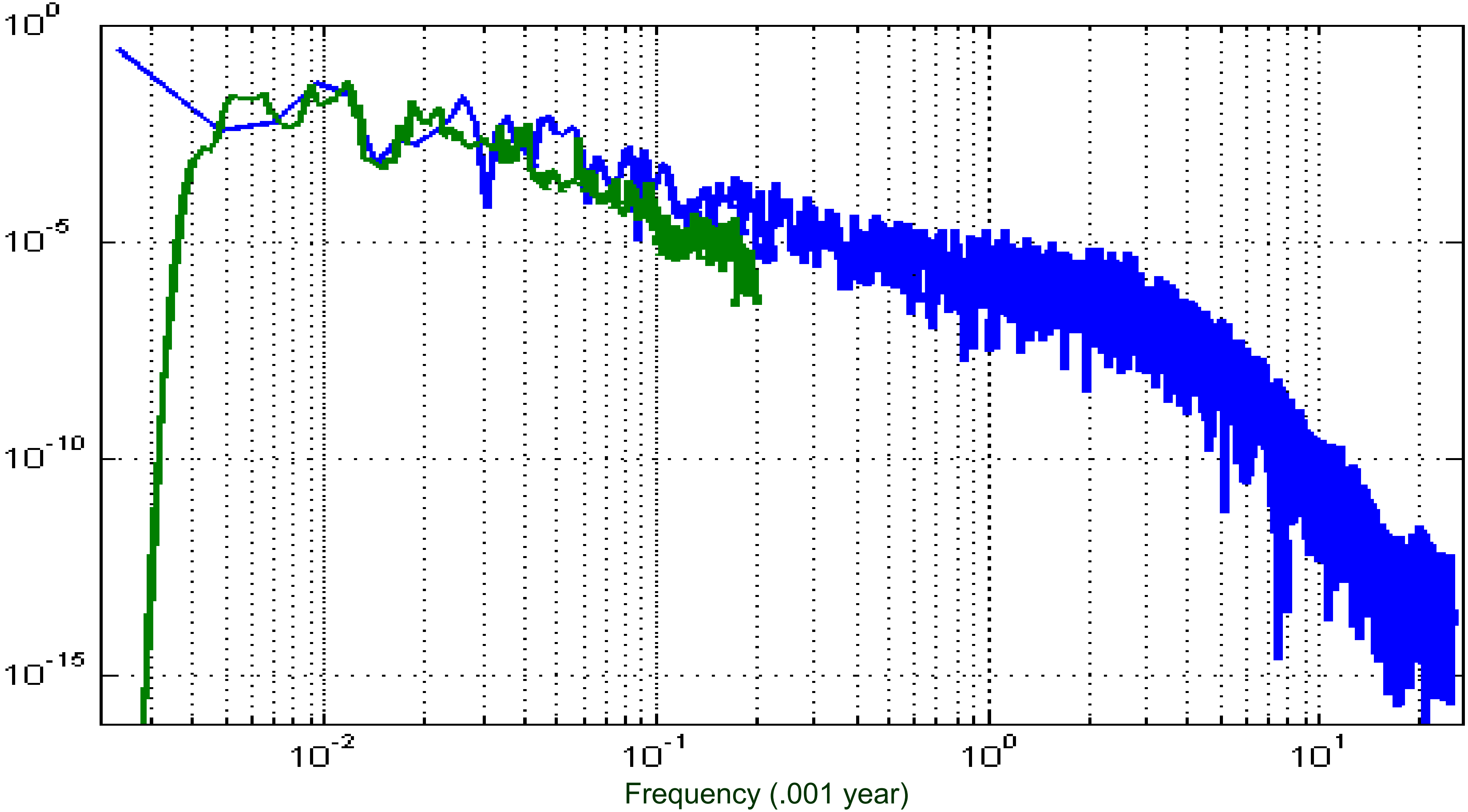

Findings

Zoom of the Comparison

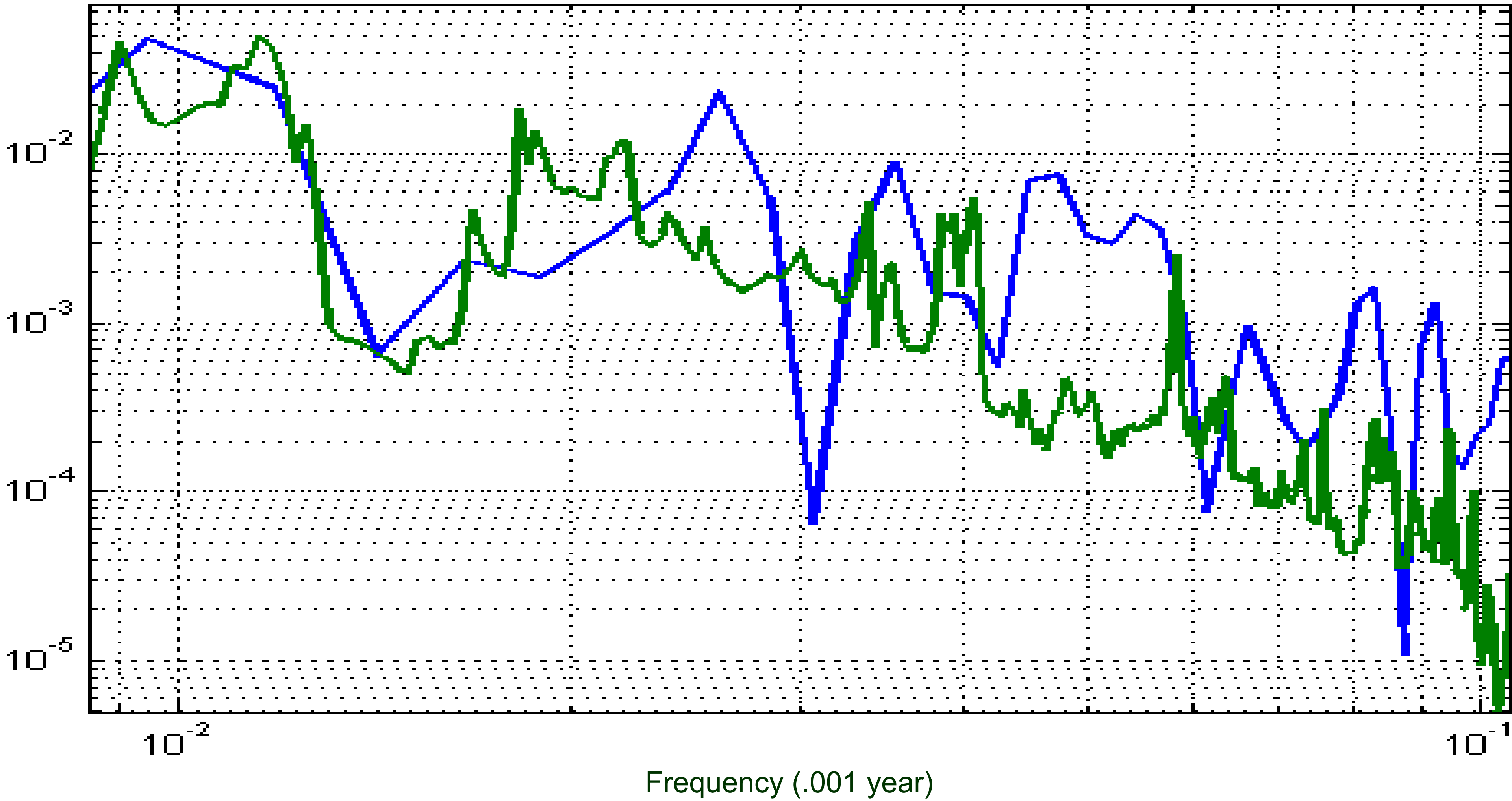

Findings
Original Data and Residual Added

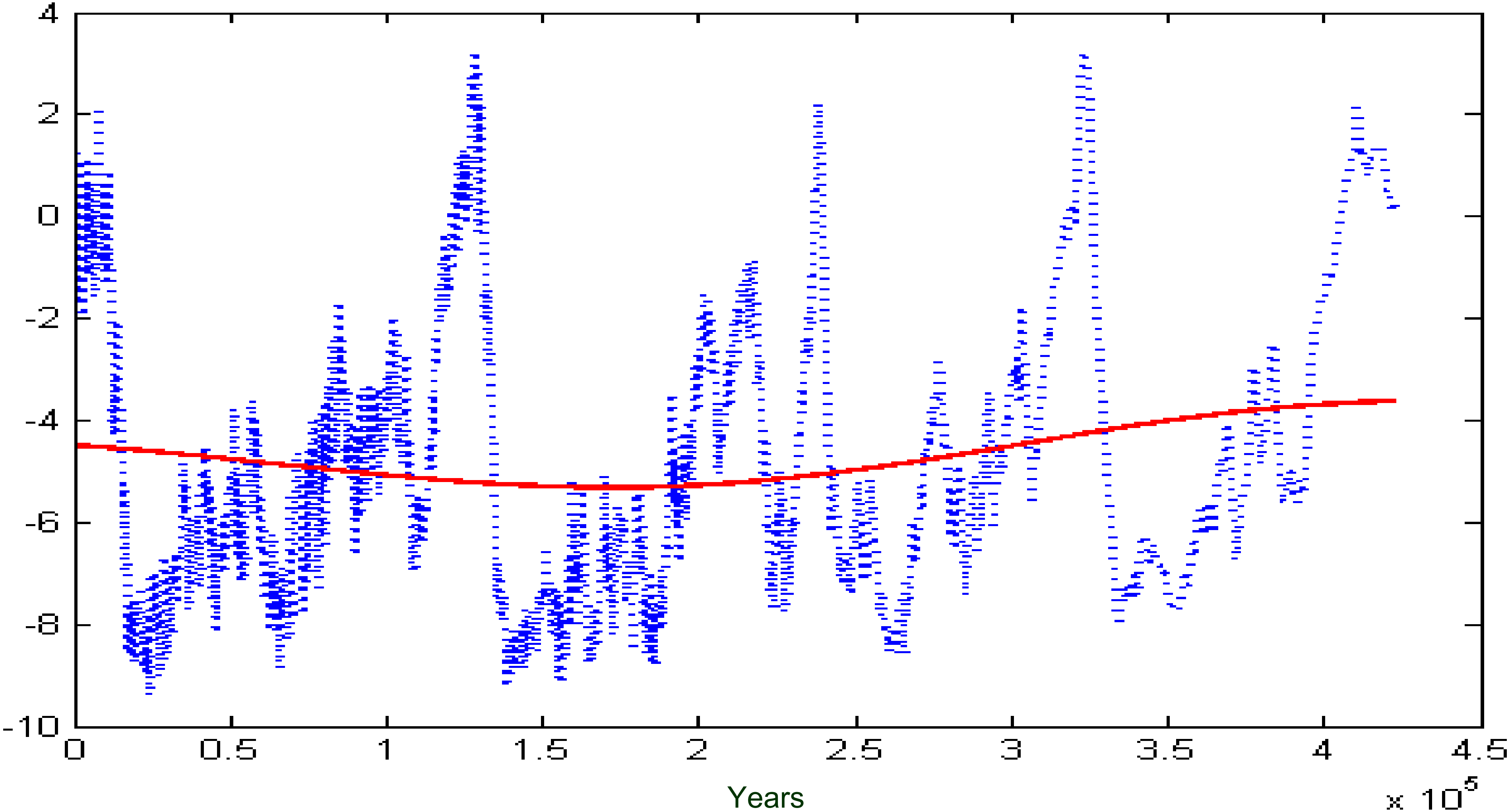

Findings
Residual + 1 Component

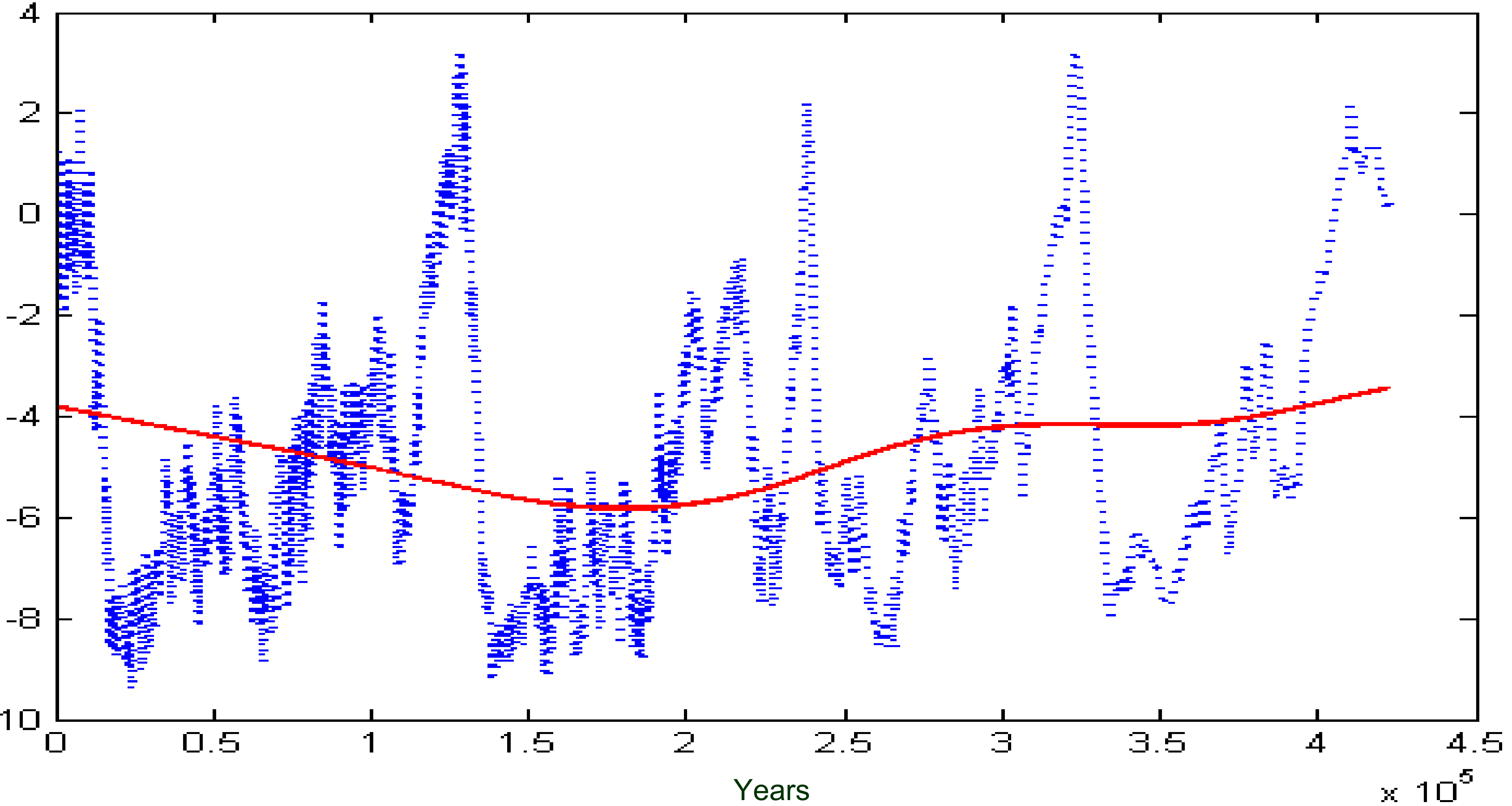

Findings
Residual + 2 Components

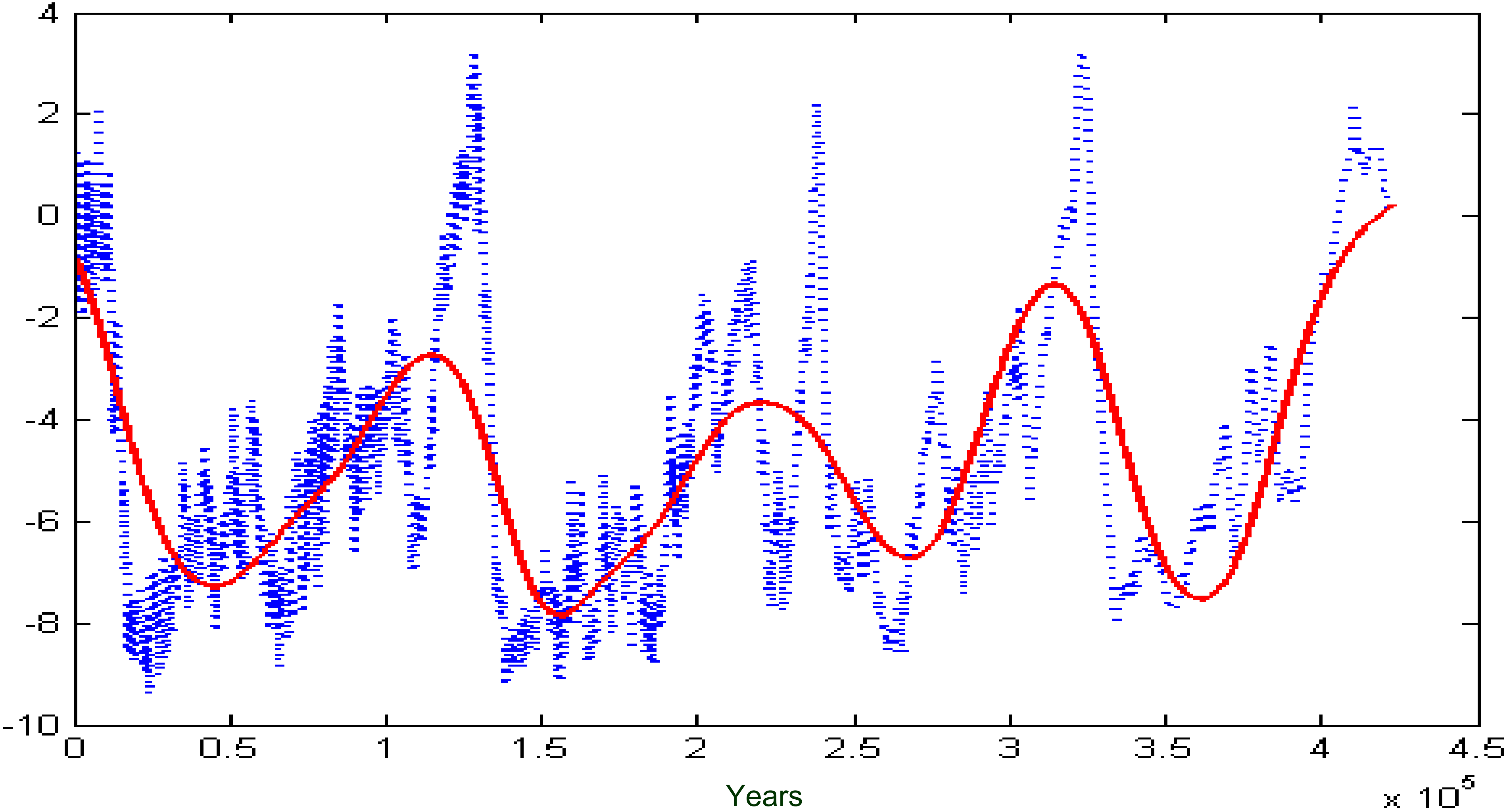

Findings

Residual + 3 Components

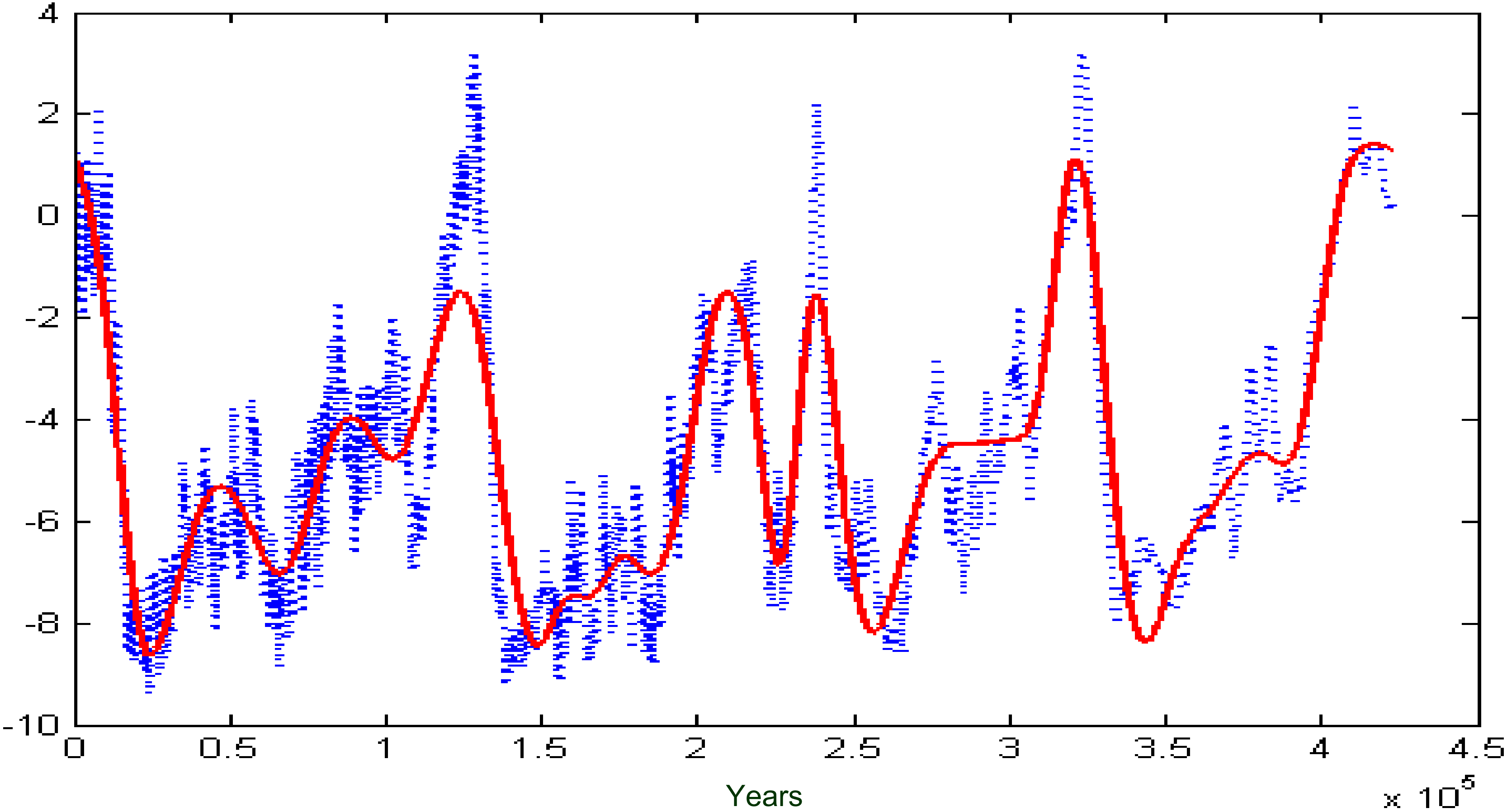

Findings

Residual + 4 Components

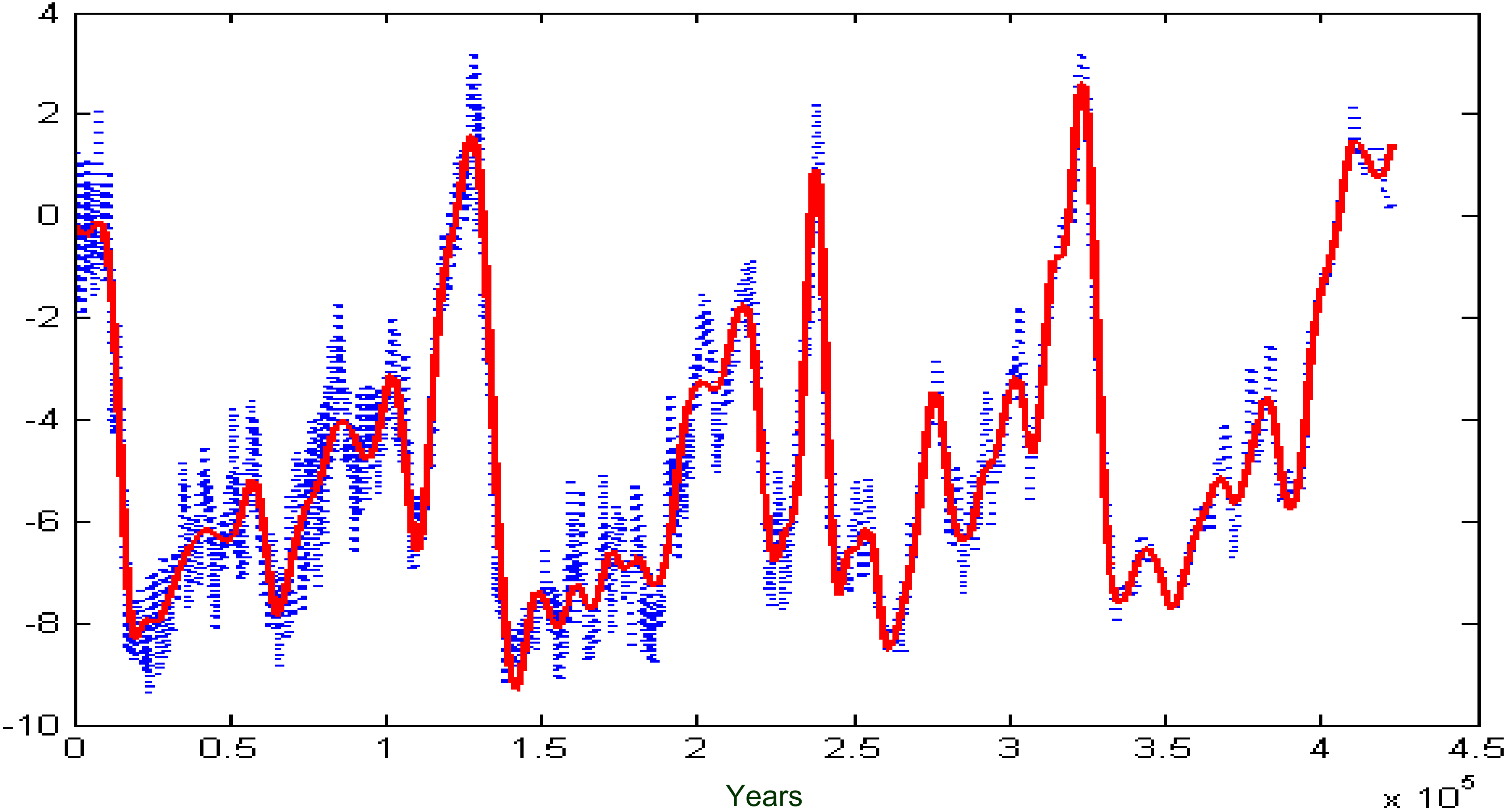

Findings
Residual + 5 Components

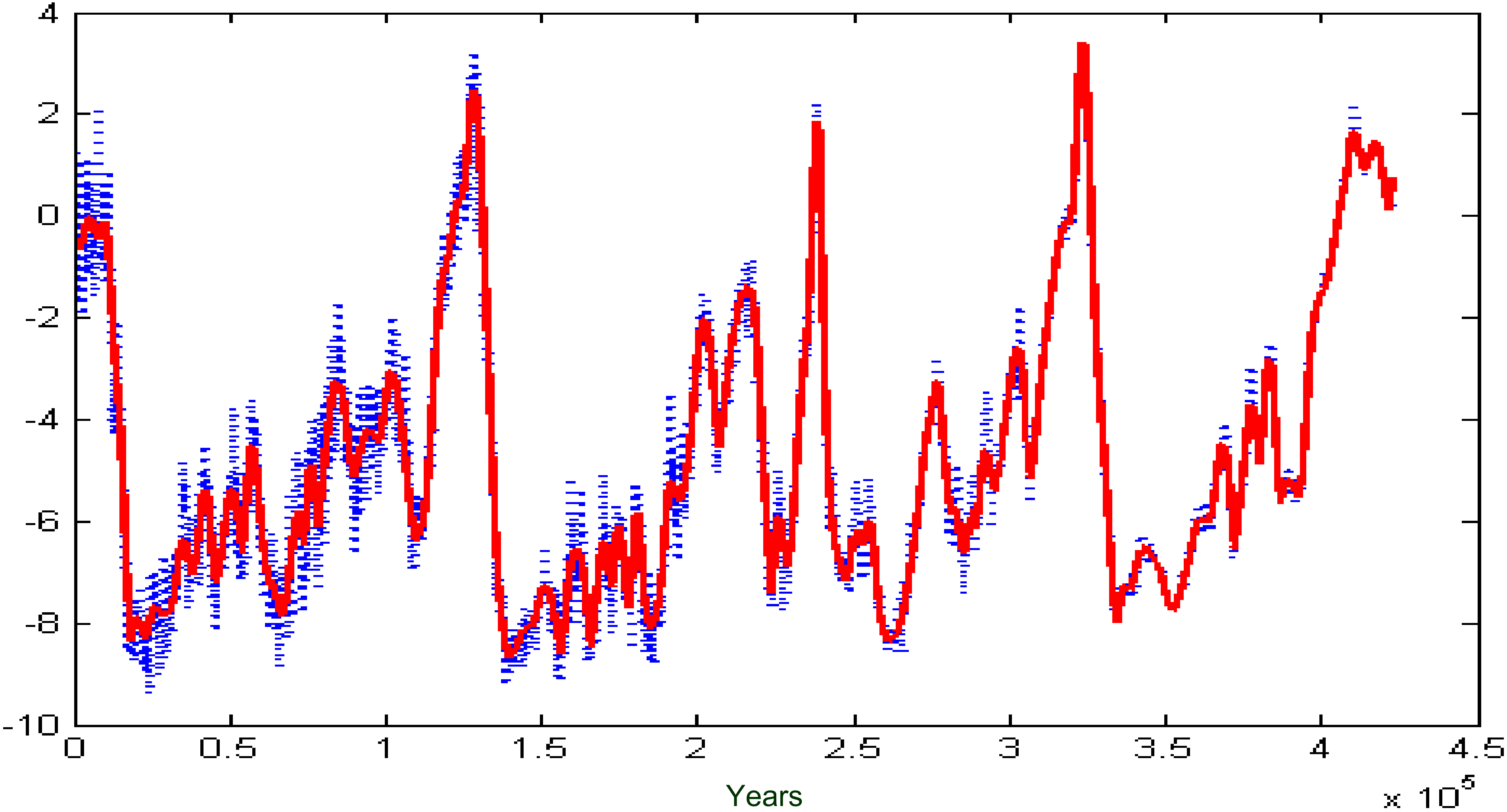

Findings

Lower Components + All Other Components

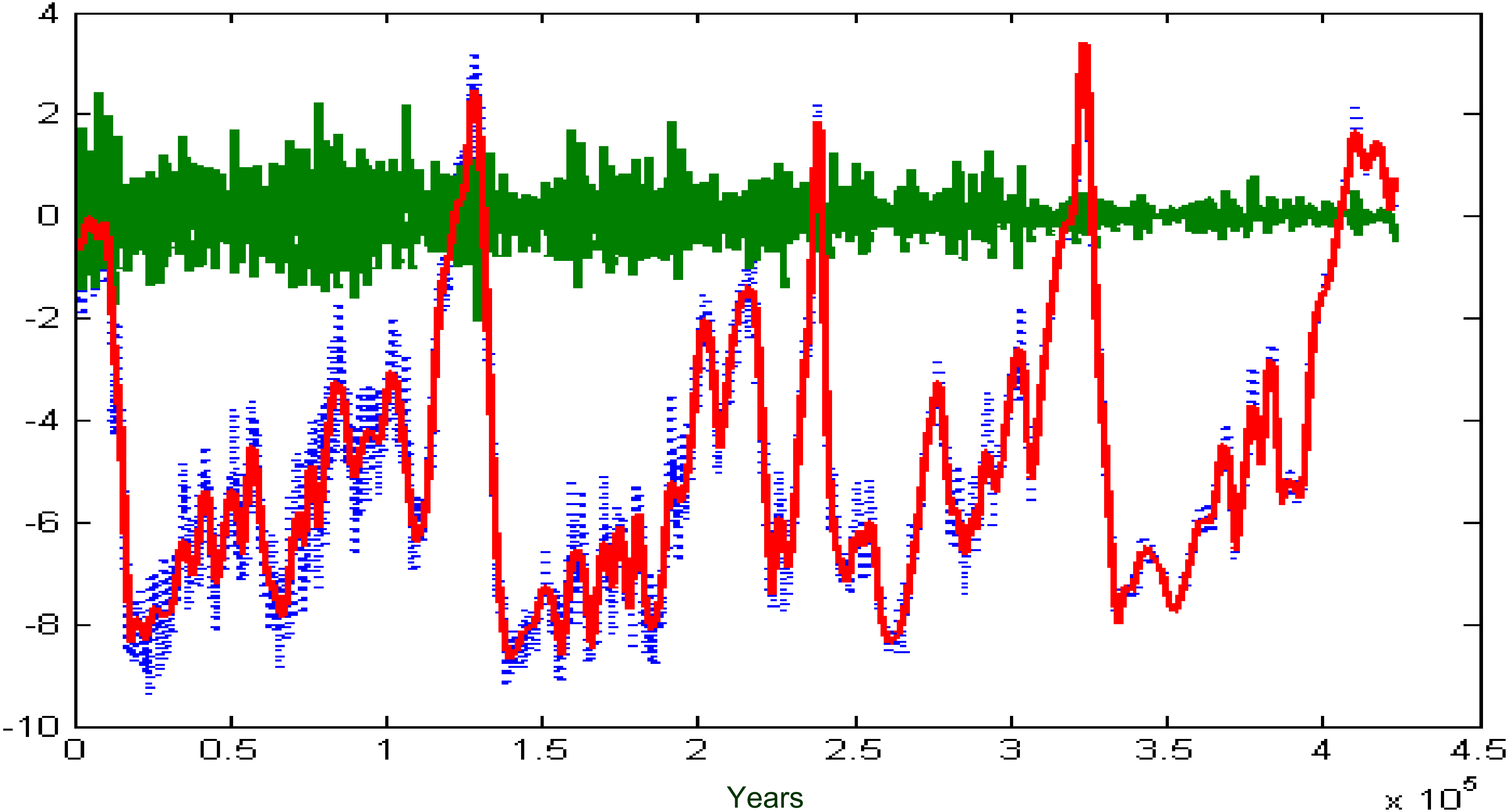

Conclusion

- Precession, Obliquity, and Eccentricity can be found in the Vostok Ice Core data
  – Play a major role in climate
- HHT method of data analysis is more capable than methods such as Fourier.
  – Displays the frequency ranges, not bands

References

- Bradley, R. S. (1999), *Paleoclimatology. Reconstructing Climates of the Quaternary, Second Edition*. Harcourt Academic Press. pp. 39, 45.
- Committee on Abrupt Climate Change. (2002), *Abrupt Climate Change: Inevitable Surprises*. National Academy Press. National Academy of Sciences. p. 25.
- Huang, N. E., Z. Shen, S. R. Long, M. C. Wu, H. H. Shih, Q. Zheng, N. Yen, C. C. Tung, and Henry H. Liu. (1998), *The Empirical Mode Decomposition and the Hilbert Spectrum for Nonlinear and Non-Stationary Time Series Analysis*. The Royal Society. pp. 903, 906.

The Melting Layer:

Erik Swenson
Mentors: Benjamin Johnson, Gail Skofronick-Jackson


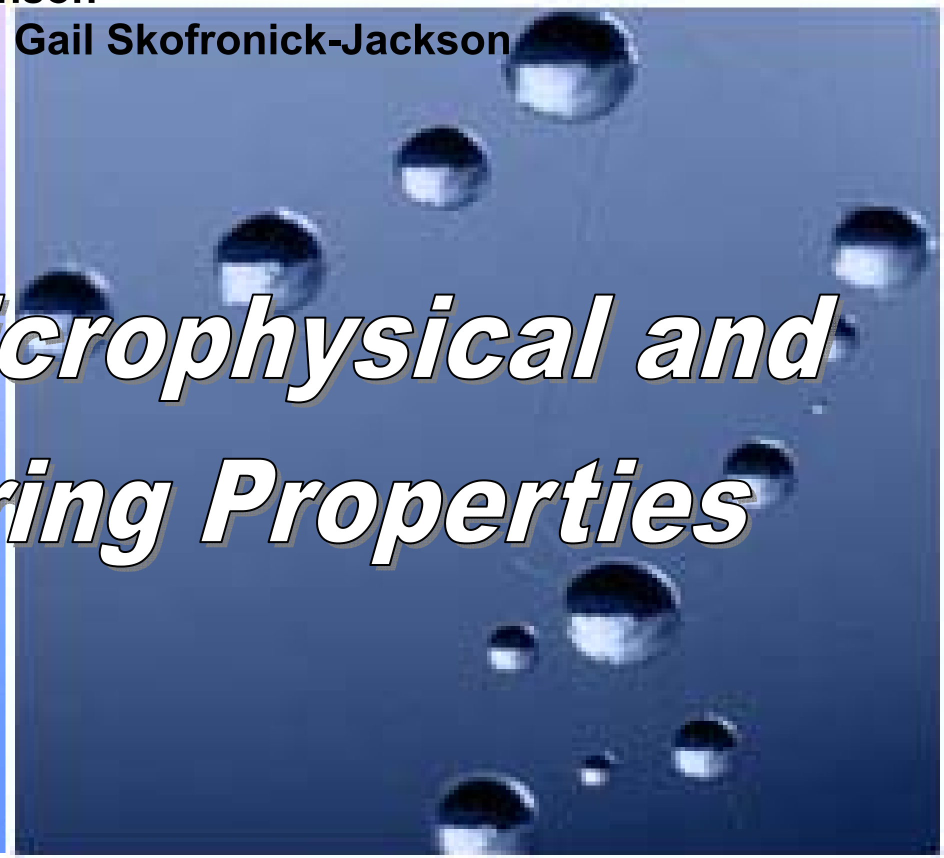

Modeling the Microphysical and Single Scattering Properties

Introduction

- Purpose:

  to better model a snowflake falling through the melting layer and learn more about its single-scattering properties

Bright Band

- A higher radar reflectivity exists at the melting layer in a precipitating cloud
- Reason:

1) dielectric constant of water 4.4 times greater than that of ice
2) a wet snowflake can produce a higher reflectivity than a spherical raindrop with the same mass
3) raindrops fall faster than snowflakes
4) increased aggregation

Single Scattering Properties

- Absorption Efficiency $Q_a = \sigma_a / A$
- Scattering Efficiency $Q_s = \sigma_s / A$
- Extinction Efficiency $Q_e = \sigma_e / A$
- Backscattering Efficiency $Q_b = \sigma_b / A$

- Single Scattering Albedo $\tilde{\omega} = Q_s / Q_e$

- Asymmetry Parameter $-1 \leq g \geq 1$

Discrete Dipole Approximation (DDA) Method

- Can calculate single scattering properties of particles with varying composition and complex shapes
- Approximates particle with an array of dipoles
- Each dipole is subject to an electric field equal to sum of the incident wave of radiation and the electric fields due to other dipoles
- Properties calculated through solution of the electric field at each dipole position

- DDSCAT 6.1 *http://arxiv.org/abs/astro-ph/0409262*

Variables in DDSCAT 6.1

- Object size
- Object composition
- Object orientation — Beta(β), Theta(θ), and Phi(Φ)
- Wavelength of radiation

Target Orientation Hypothesis

- Extinction efficiency directly proportional to the extinction cross-section exposed to radiation

Max: $\beta = 90^{\circ}$ and $\theta = 90^{\circ}$

Min: $\beta = 0^{\circ}$

The Ideal Snowflake Structure

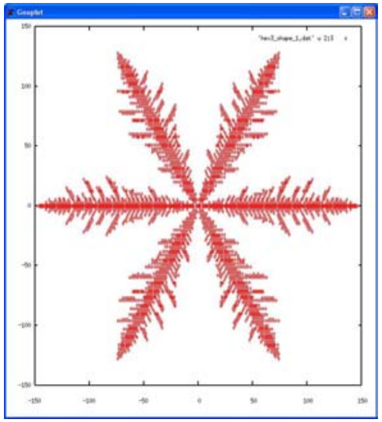

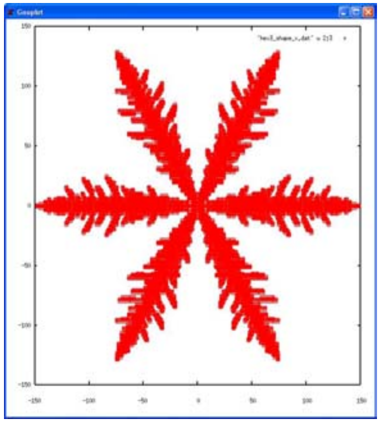

- Increased density
- Aspect Ratio:

  Snowflake's thickness divided by its maximum dimension
- **h = (9.96*10-3) d ^ 0.415**

  with thickness (h), diameter or maximum dimension (d) in cm
- Fixed d = 0.1116 cm
- Produces snowflake with a dipole thickness of 11
- Ideal snowflake ready to be melted

How To Melt a Snowflake

- 1) How are ice dipoles removed?

  - raise limit for *N*I values
- 2) How are dipoles of water added?

  - spheres of water added to each dendrite with position depending on ice thickness and length of branches
- Approximate dipole conservation

  - one dipole of ice melts into one dipole of water

  - conservation of mass

Melting Stages

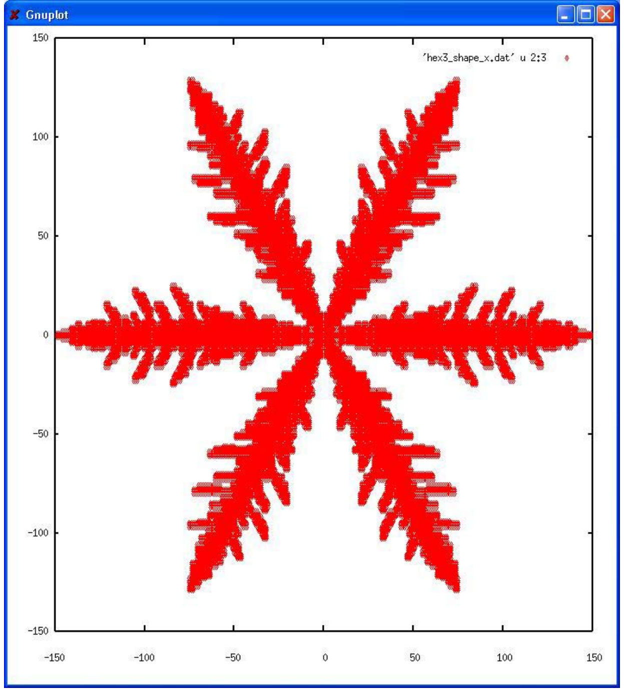

NI limit = 1.00

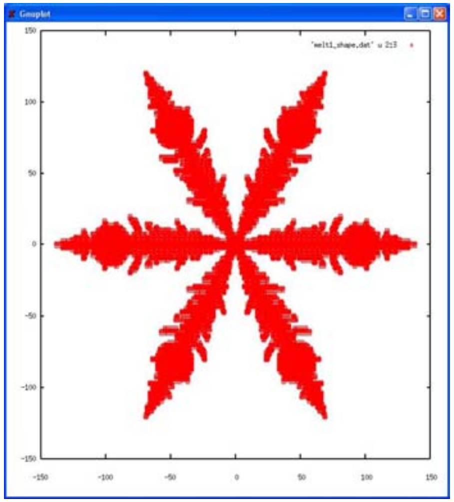

1: *NI* limit = 1.05

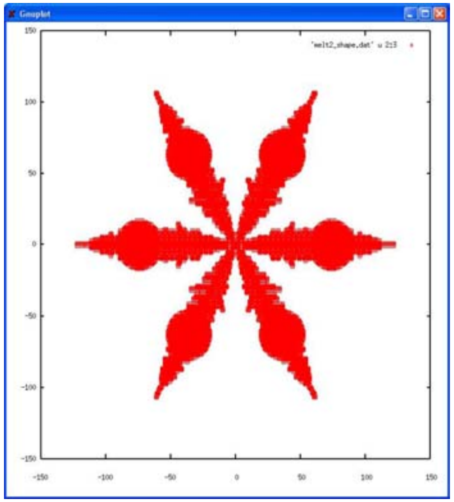

2: *NI* limit = 1.10

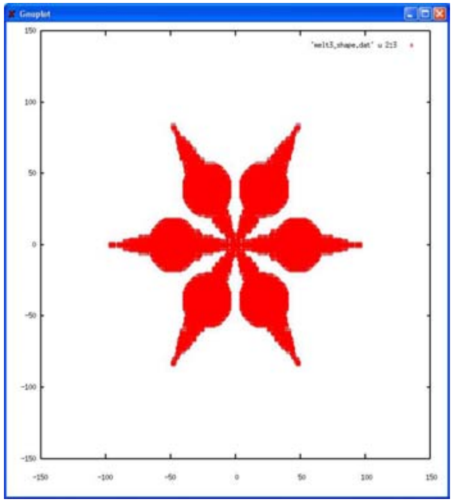

3: *NI* limit = 1.15

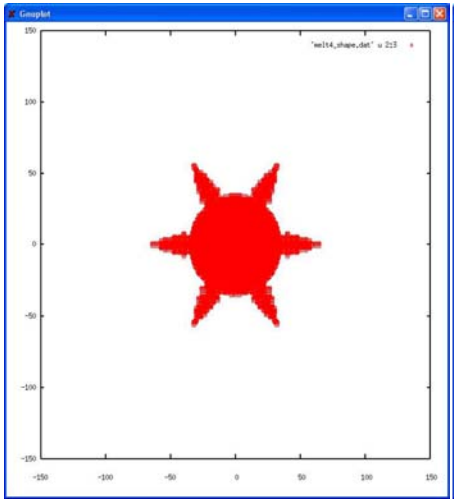

4: *NI* limit = 1.20

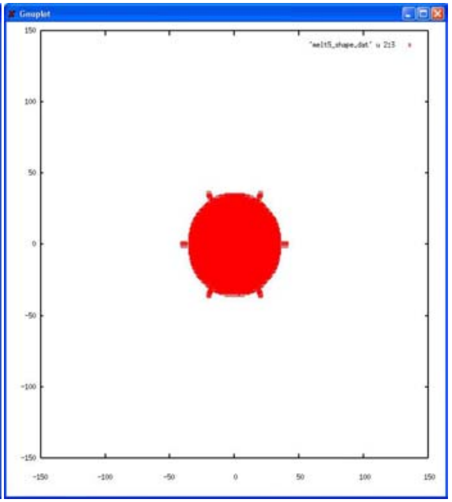

5: *NI* limit = 1.25

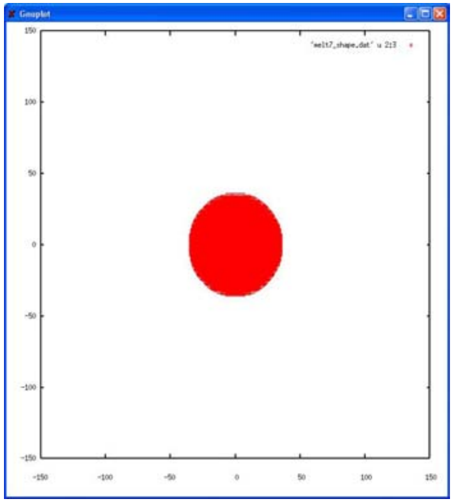

6: *NI* limit = 1.80

unmelted water fraction = 0.000

dipoles: ice: **193193** water: **0** TOTAL: **193193**

backscattering efficiency: **0.015**

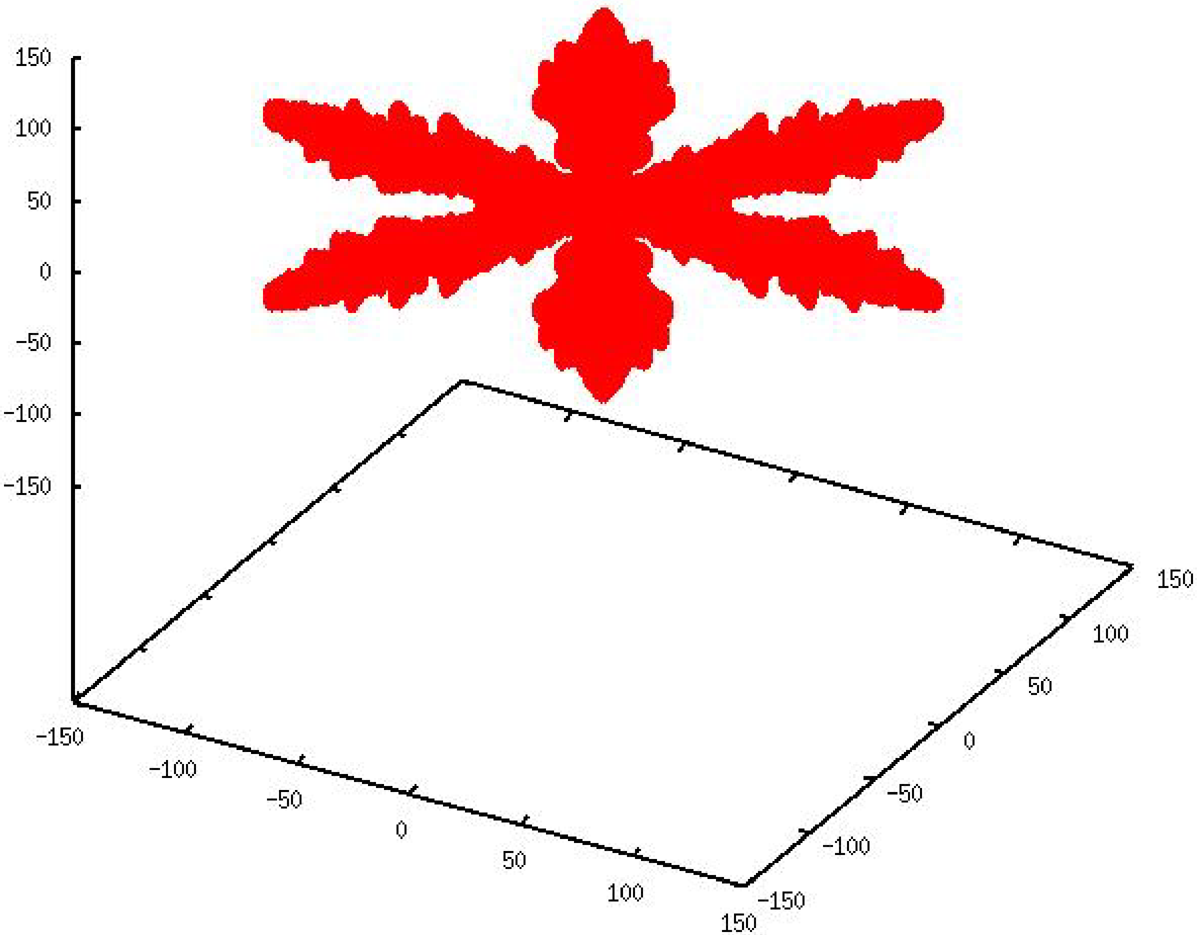

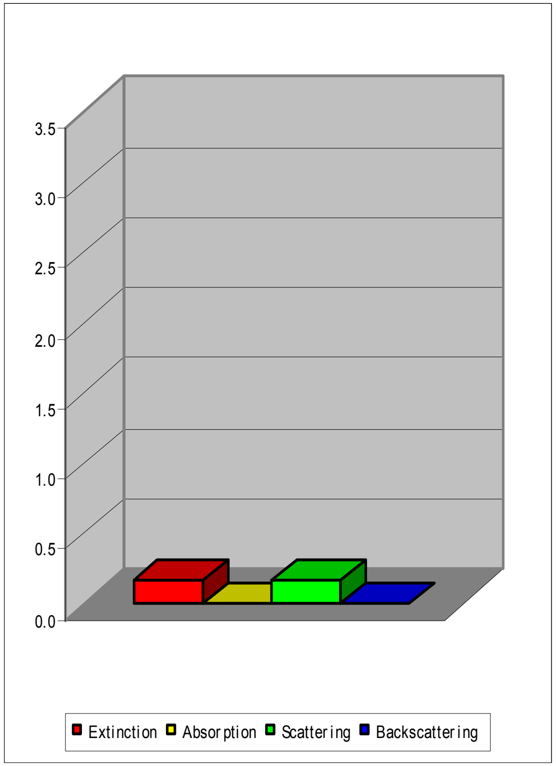

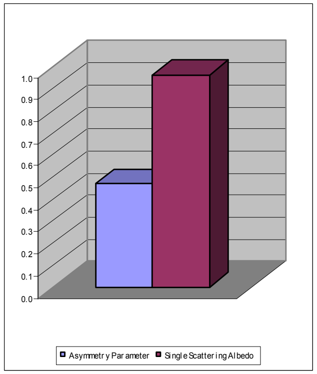

1: water fraction = 0.269

dipoles: ice: **141350** water: **51934** TOTAL: **193284**

backscattering efficiency: **0.019**

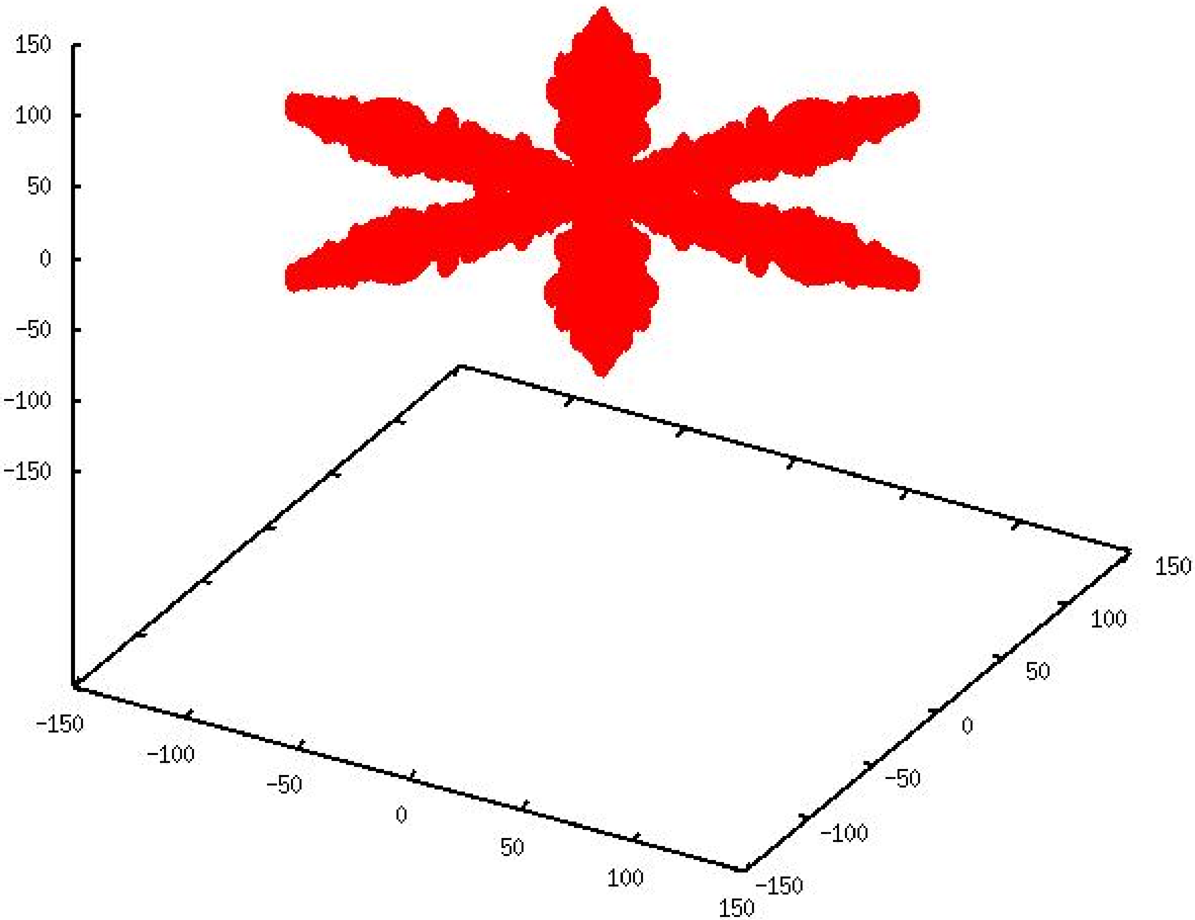

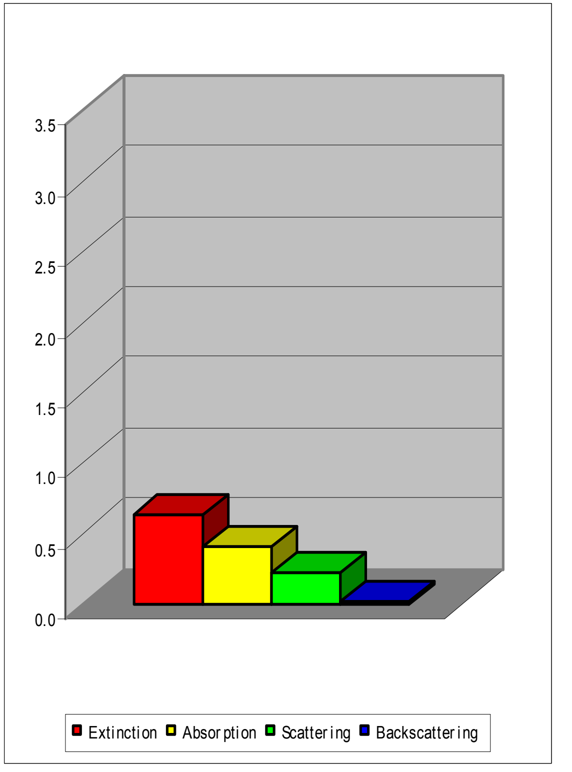

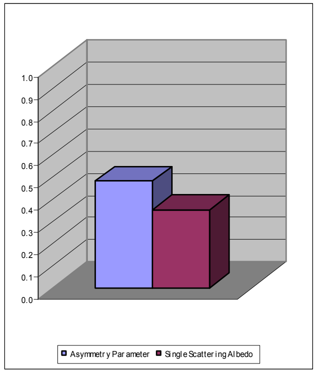

2: water fraction = 0.505

dipoles: ice: **95625** water: **97572** TOTAL: **193197**

backscattering efficiency: **0.026**

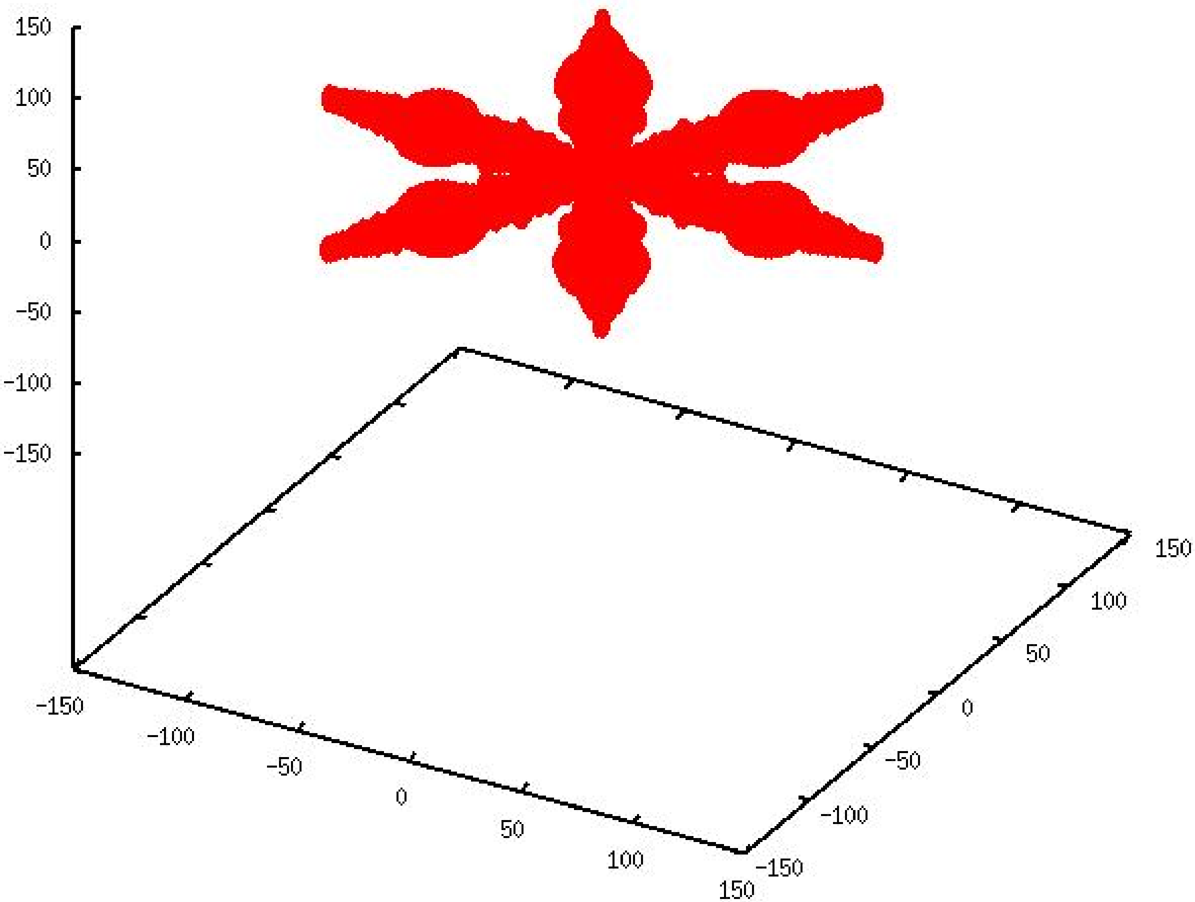

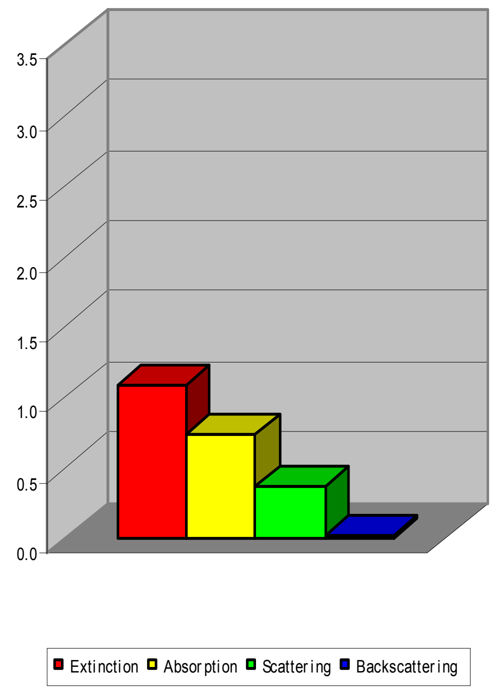

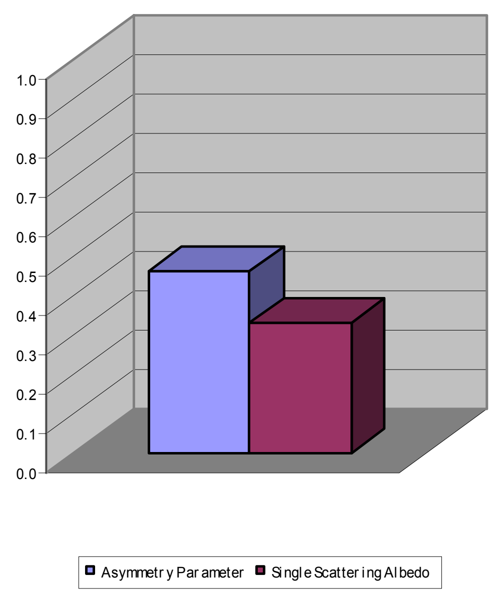

3: water fraction = 0.756

dipoles: ice: **46977** water: **145872** TOTAL: **192849**

backscattering efficiency: **0.037**

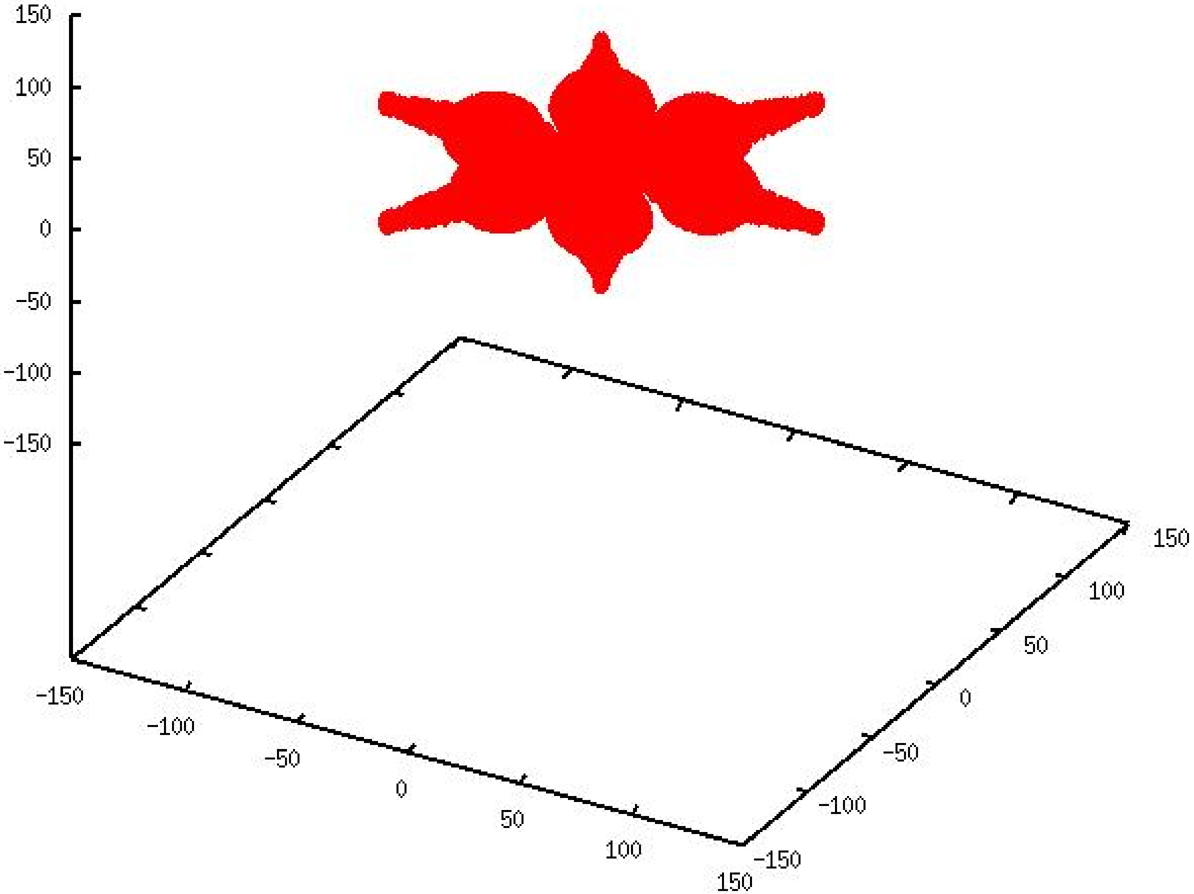

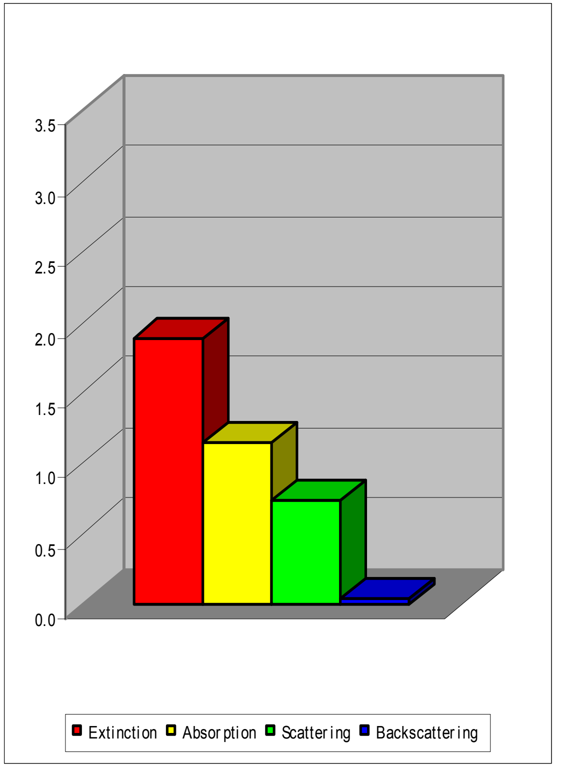

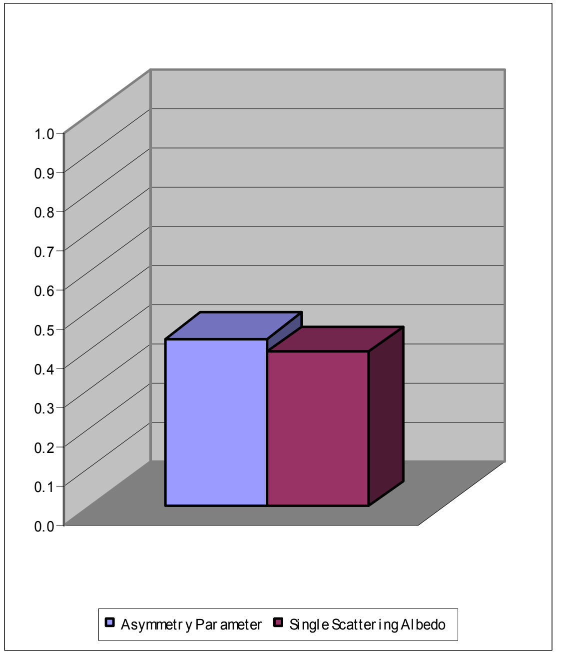

4: water fraction = 0.905

dipoles: ice: **18425** water: **174730** TOTAL: **193155**

backscattering efficiency: **0.086**

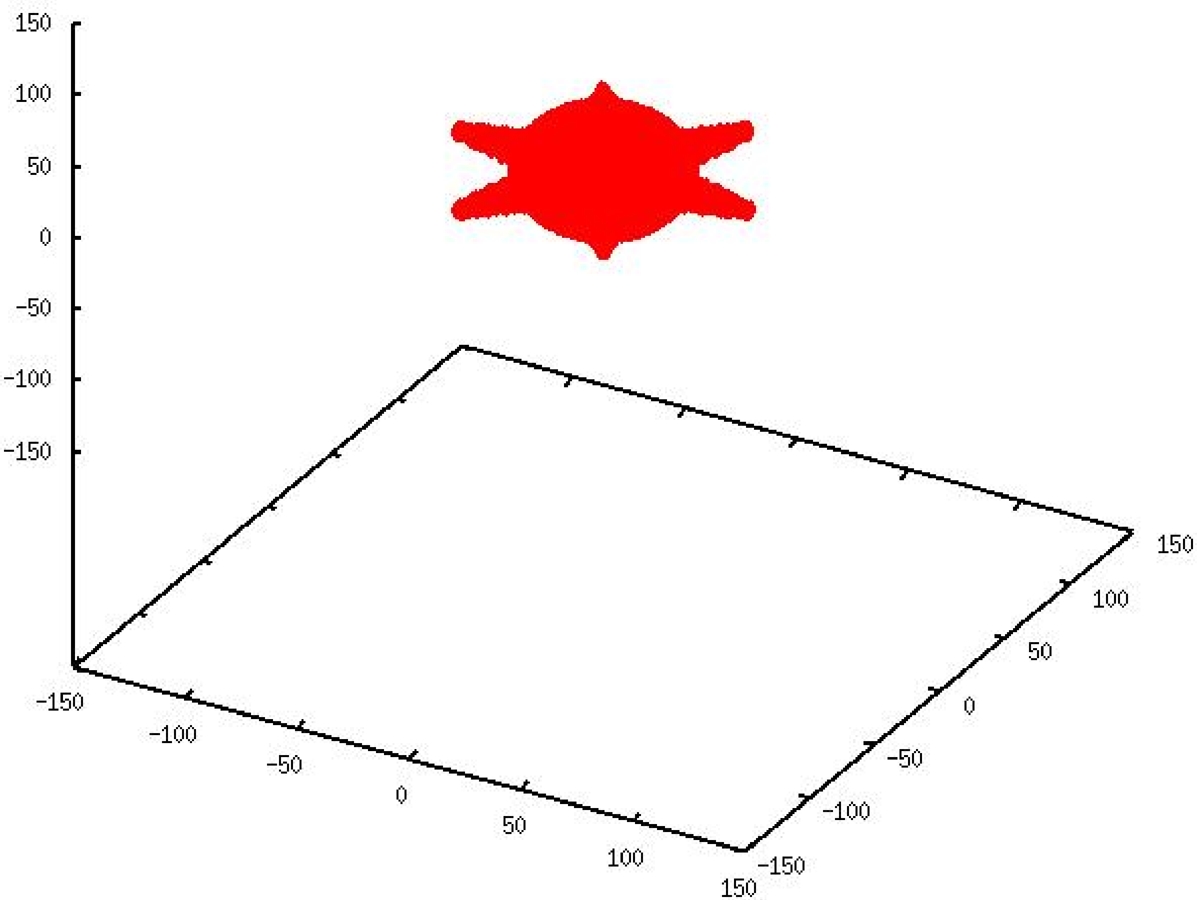

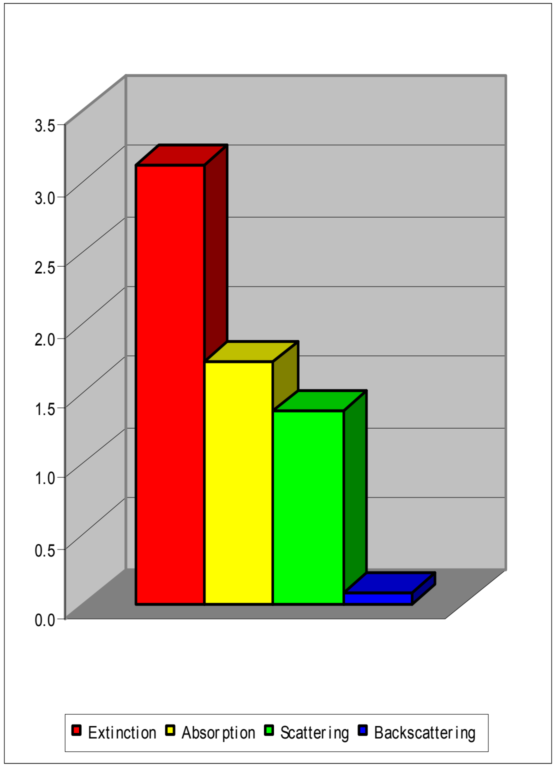

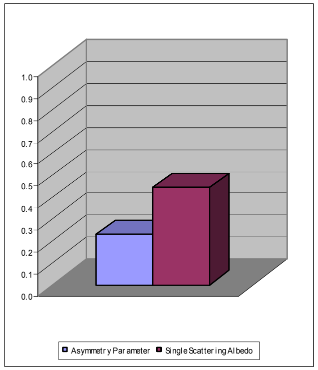

5: water fraction = 0.977

dipoles: ice: **4437** water: **188660** TOTAL: **193097**

backscattering efficiency: **0.090**

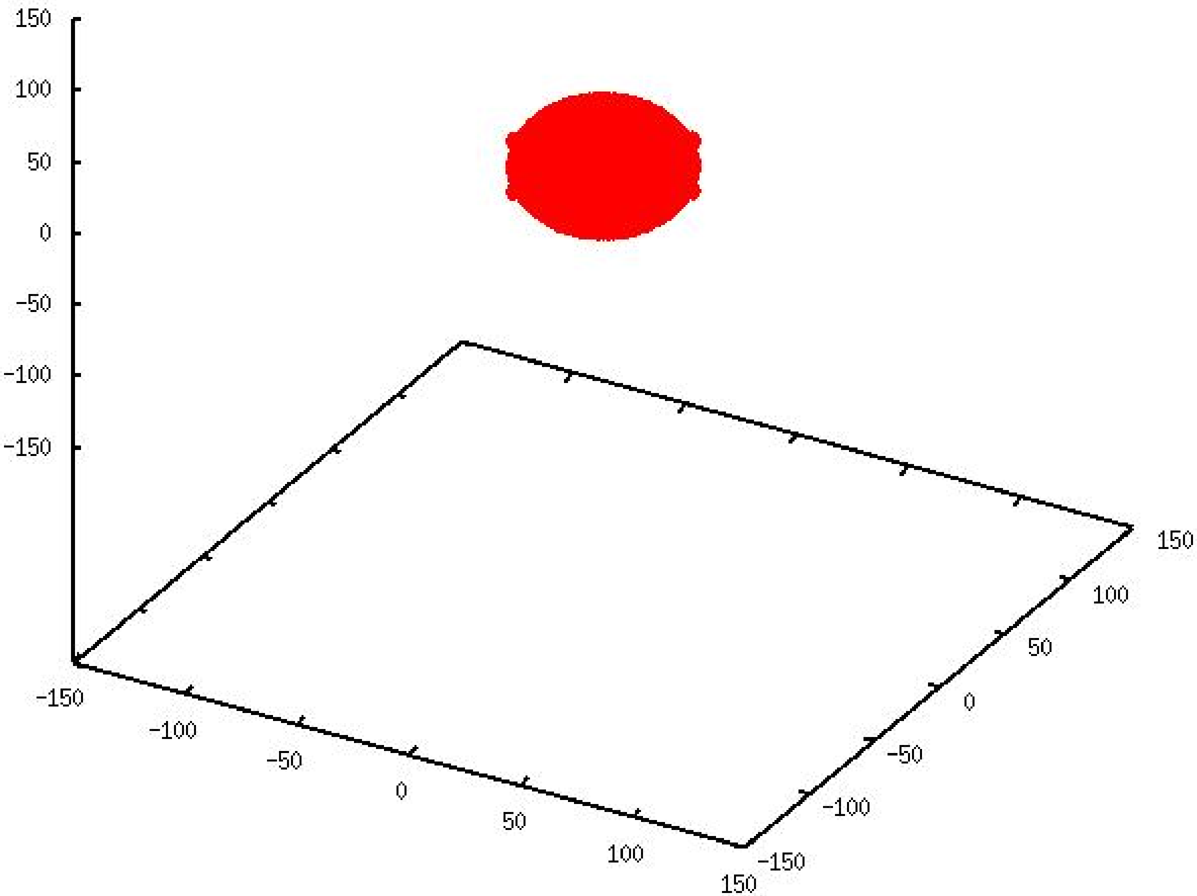

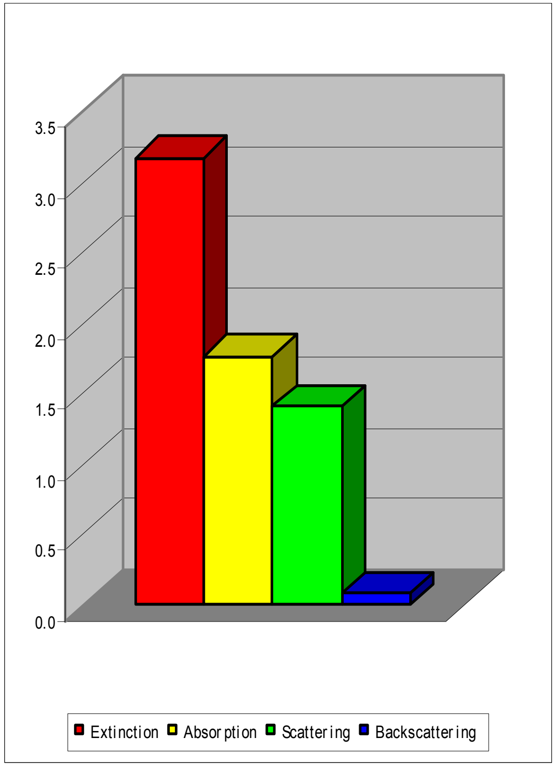

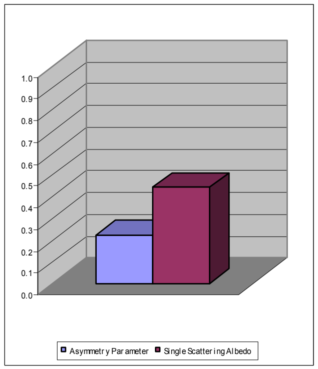

6: water fraction = 1.000

dipoles: ice: **0** water: **193511** TOTAL: **193511**

backscattering efficiency: **0.091**

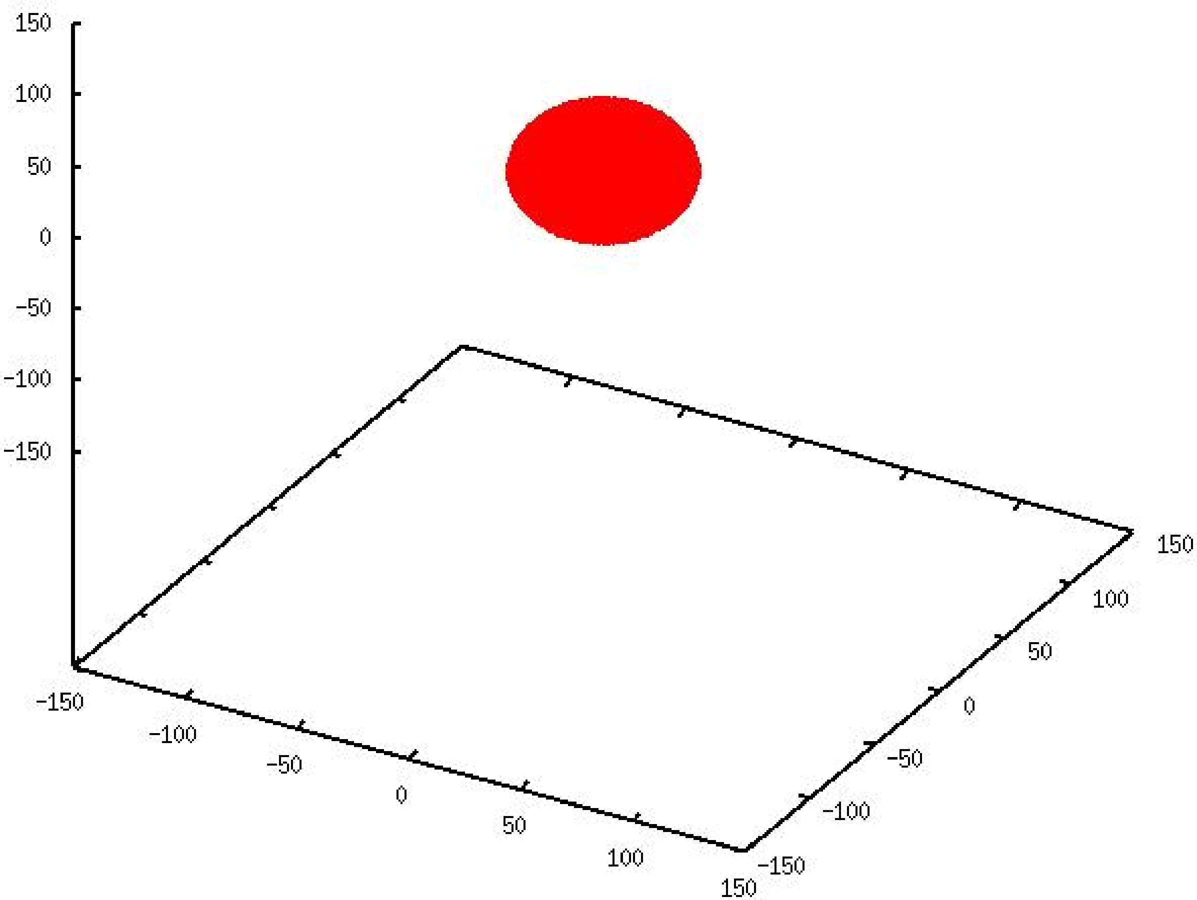

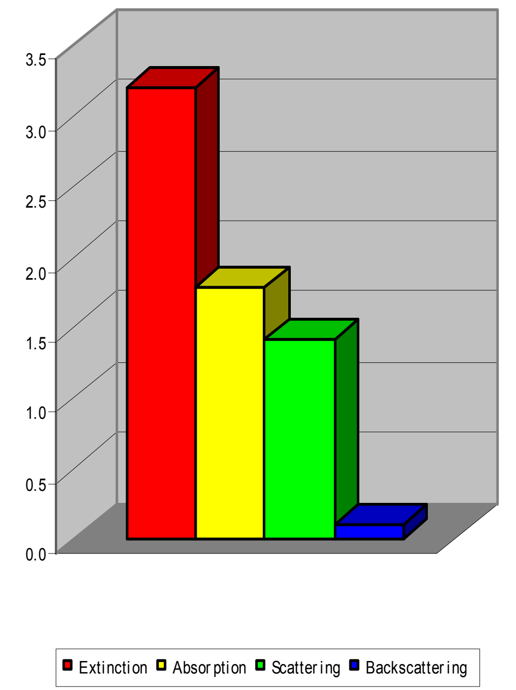

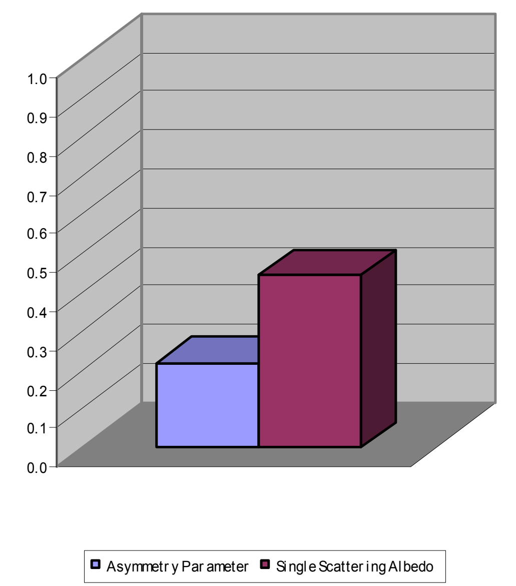

Conclusion

- Backscatter increase with melting reflects higher radar reflectivity associated with raindrops
- Snowflake switches from scattering dominant to absorption dominant early in the melting process with absorption increase related to increased emission of raindrops
- Snowflake becomes more efficient at extinguishing radiation as it melts into a raindrop especially when water spheres on dendrites coalesce into one

Future Research

- Improvements/changes
  - Develop better scientific basis for ideal snowflake shape
  - Develop better scientific basis for addition of water in melting process
  - Model multiple snowflake shapes
  - Model aggregation

- Comparison to Mie Theory using a sphere with dielectric mixing

References

- Rogers, R. R. and Yau M. K. 1989: A Short Course in Cloud Physics (third edition), Butterworth-Heinemann, pp. 200.
- Petty, G.W. 2004: A First Course in Atmospheric Radiation, Sundog, pp. 149-196.
- Kim, M.-J. and Weinman, J. A. 2004: Parameterizations of single scattering properties of frozen hydrometeors at millimeter-wave frequencies, International Geosci. And Remote Sens. Symposium (IGARSS), Anchorage, Alaska, September 20-24, 2004.
- Draine, B.T., and Flatau, P.J. 2004: User Guide for the Discrete Dipole Approximation Code DDSCAT 6.1, http://arxiv.org/abs/astro-ph/0409262.
- Kim, M.-J., Weinman, J. A., and Sun, W. 2005: Microwave scattering properties of randomly oriented ice crystals, Submitted *J. Atmos. Sci.*
- Pruppacher, H. R. and Klett, J. D. 1997: Microphysics of Clouds and Precipitation (second edition), Kluwer Academic, pp. 45,46,51.
- Oraltay, R. G. and Hallett, J. 2004: The melting layer: A laboratory investigation of ice particle melt and evaporation near 0o C, *J. Meteor*., 44.

General Purpose

- Microwave Remote Sensors produce passive microwave imagery that is most sensitive to precipitation
- Can be combined with Doppler radar
- Goal is to improve the retrieval algorithm
- Need to create a better model to simulate the radiometric response of precipitating clouds

Comparison To Mie Theory

DDA Snowflake vs. Sphere with mixed dielectric constant

Orientation:

$\beta = 90^o$ $\theta = 90^o$ $\Phi = 0^o$

Extinction Efficiency

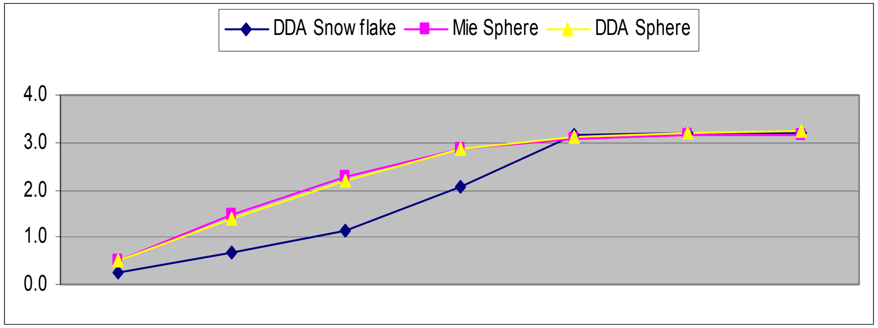

Asymmetry Parameter

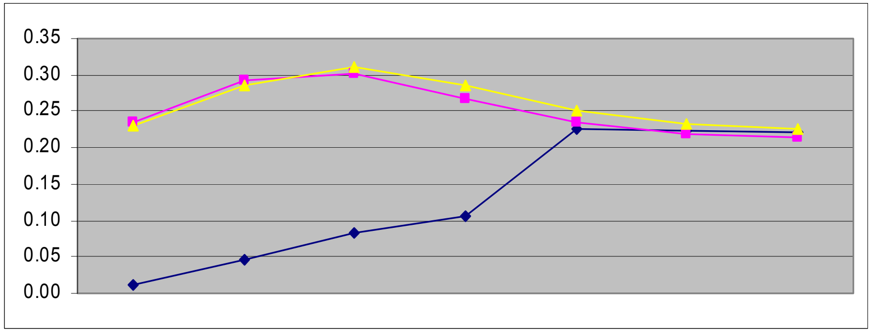

Absorption Efficiency

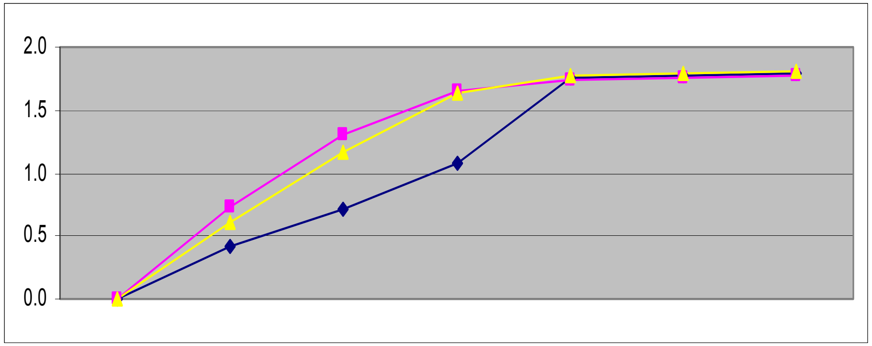

Backscattering Efficiency

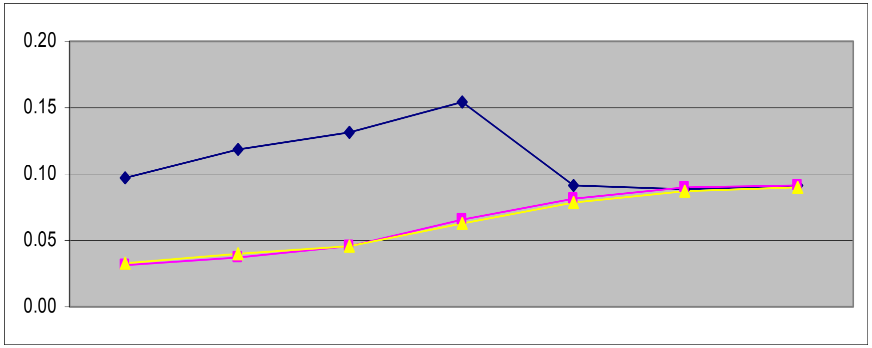

Scattering Efficiency

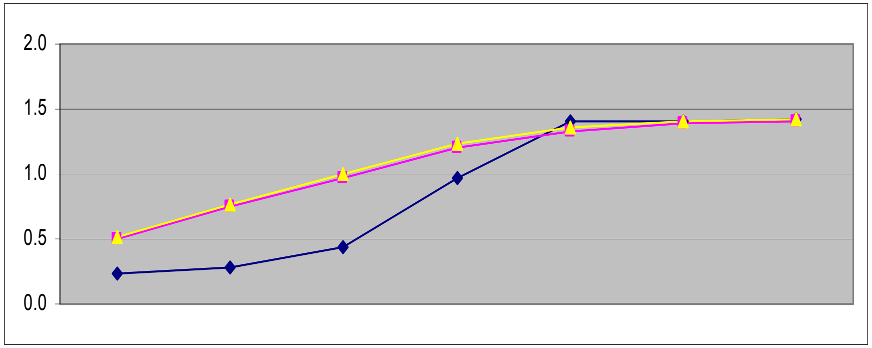

Single Scattering Albedo

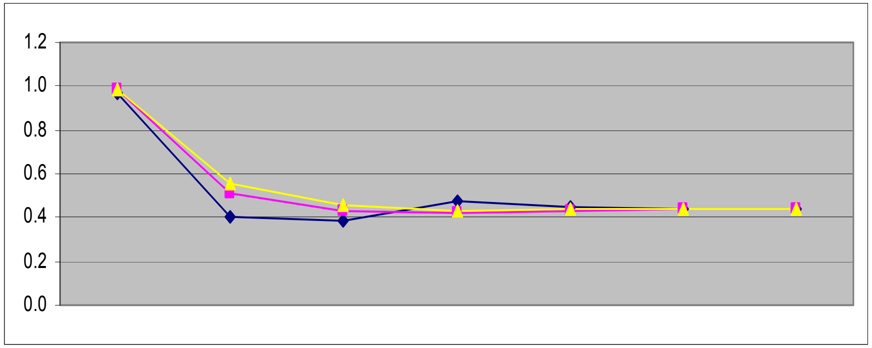

Methods For Calculating Single Scattering Properties

- Approximation with equivalent spheres
    1) equal volume
    2) equal surface area
    3) collection with same volume-to-surface area ratio
- Approximation with equivalent cylinders
- Approximation with equivalent ellipsoids

- Approximation with the dielectric mixing theory

- Discrete Dipole Approximation Method

Improving EPA's BASINS-HSPF NPS Pollution Model

Anna Nowack
Summer Institute 2005
Mentor: David Toll
Hydrological Sciences Branch

Main Topics to Discuss:

- Water Quality
- NPS (Non Point Source)/ Point Source Pollution
- Precipitation and LULC (Land Use and Land Cover)
- BASINS (Better Assessment Science Integrating Point and Nonpoint Sources)
- HSPF (Hydrological Simulations Program Fortran)

North East Branch Anacostia Study:

- How the Study Basin was Chosen
- How Rain Gage Data is assigned to a basin
- Working with the Study Basin in BASINS
- Running HSPF
- Generating Flow Charts using GenScn in HSPF
- Using Spatial Analysis to Improve Flow Rates

Water Quality

97% of the water on the earth's surface is either saltwater or undrinkable due to some form of pollution and another 2% is locked up in ice caps and glaciers. This leaves 1% of all the water on the earth available for human expenditures (USGS). According to the EPA, NPS (Nonpoint Source) pollution is the leading cause of water degradation and is the reason why some 40% of all lakes, rivers and streams are unsuitable for swimming and fishing.

In a natural landscape, about half the precipitation that falls soaks into the soil. Trees and other vegetation help decrease NPS pollution by slowing, collecting, storing and filtering precipitation before it enters surrounding waterways.

The land is more impervious in cities. Instead of soaking into the soil, most of the precipitation runs off hard surfaces into storm sewers, which empty into streams, lakes, and ponds.

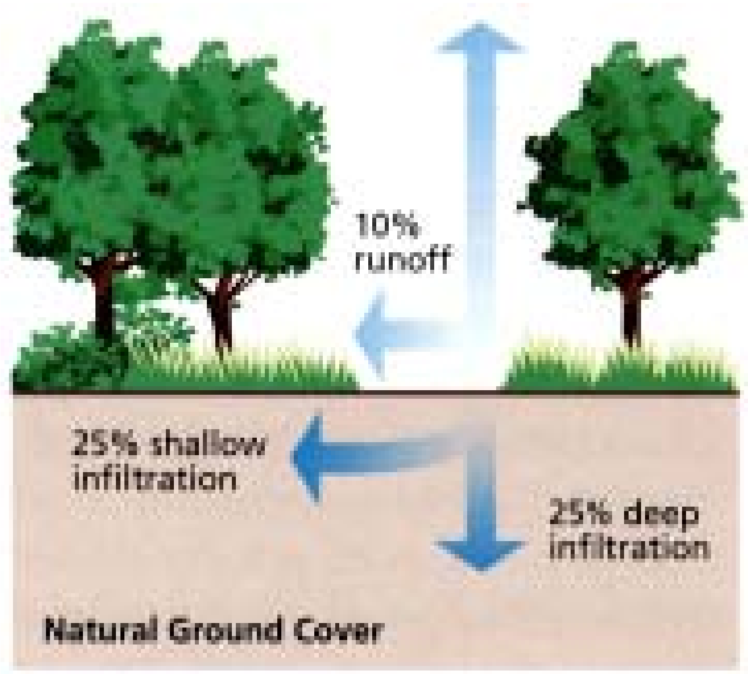

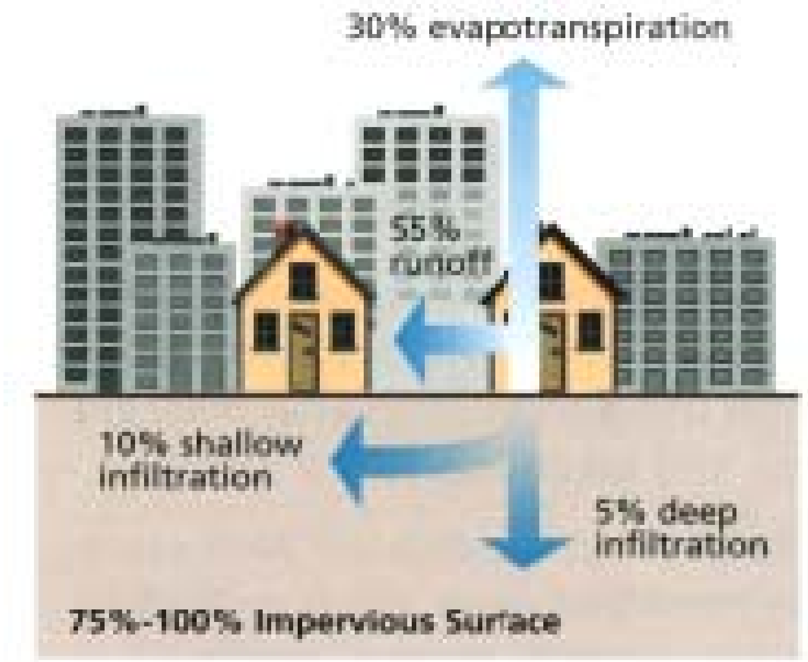

Taken from EPA's NPS pollution web site.

Precipitation

- Rain fall amounts, duration, and intensities vary spatially within the area of the storm
- Large precipitation events are more uniform with longer durations
- Small precipitation events have shorter durations with larger amounts of rainfall at the center of the storm and less towards the edges making them less uniform.
- Summer storms are convective and thus are less uniform

BASINS and HSPF

BASINS:
- Work in a GIS Interface
- Linked to Several Models Including HSPF
- Download datasets to help interpret flow

HSPF:
- Local and Spatial Meteorological Datasets
- Various LULS (Land Use/Land Cover)
- Set the perviousness/imperviousness for different land types
- Estimate Stream Flow and TMDLs (Total Maximum Daily Loads) via hydrographs

6 basins chosen for the study

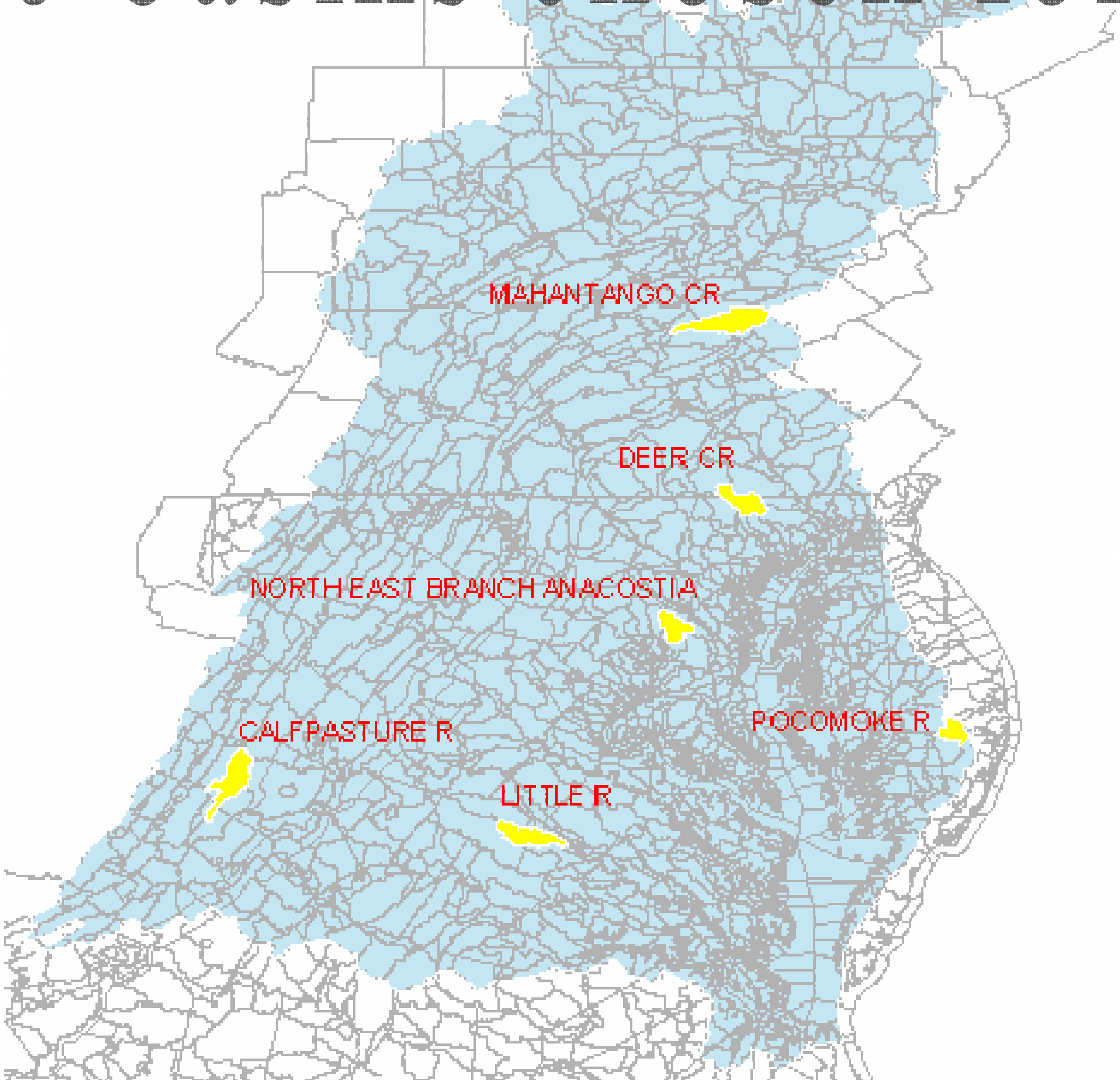

Requirements:

- Area of 50-200 square miles
- No upstream reservoir
- Within the Chesapeake Bay Watershed Boundary
- Already have water quality data
- Contain varying land cover and elevation
- USGS stream flow record

Assigning Stations to a Basin

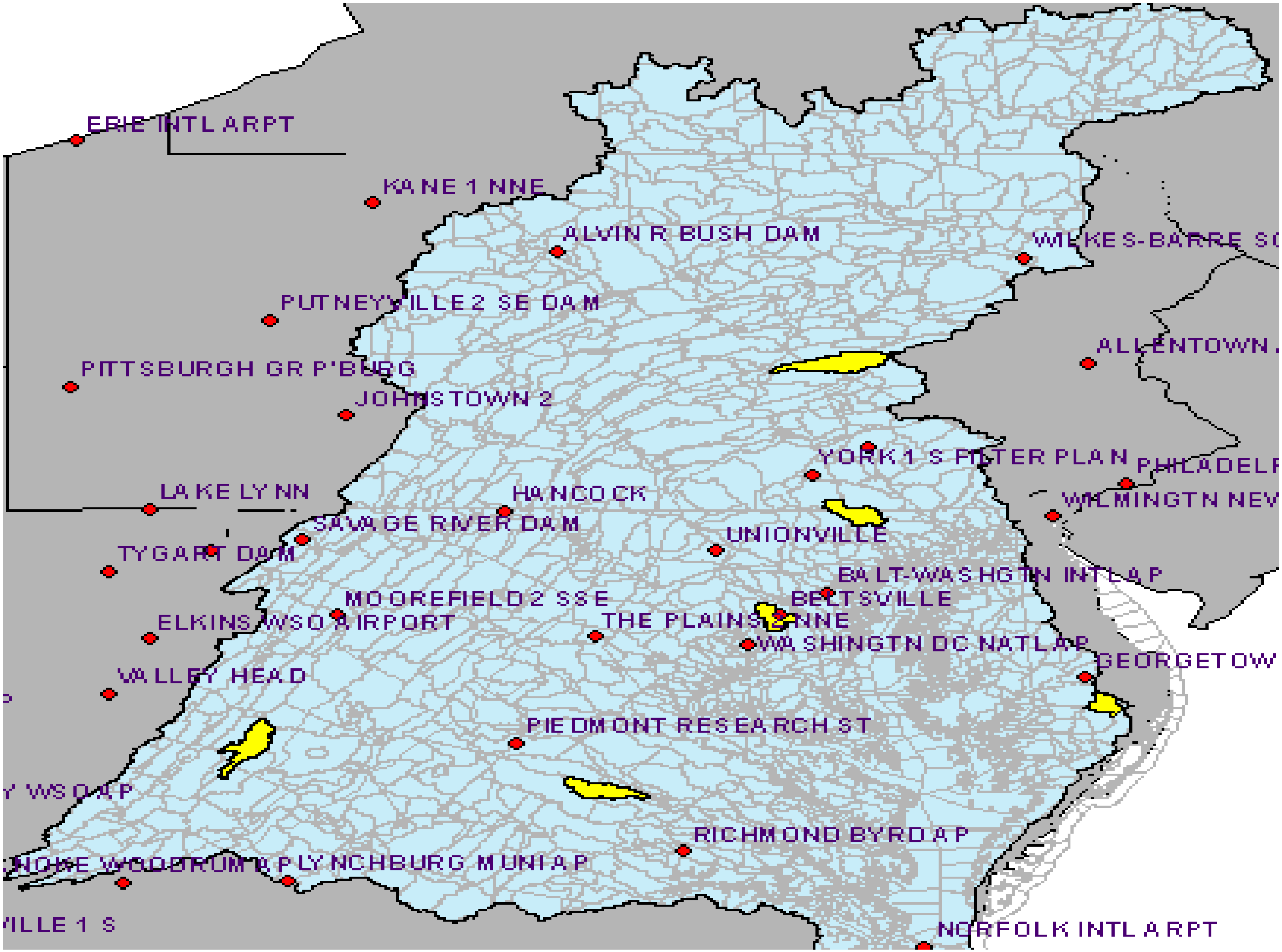

Approach:

- The EPA assigns stations to a basin using the nearest neighbor technique
- If a station is missing data the next closest station is used instead

Problems with this approach:

- Stations tend to be very far away from the basin they are assigned to
- Data is for one point in the entire basin

North East Anacostia

Rain gage stations: Beltsville, DCA and BWI

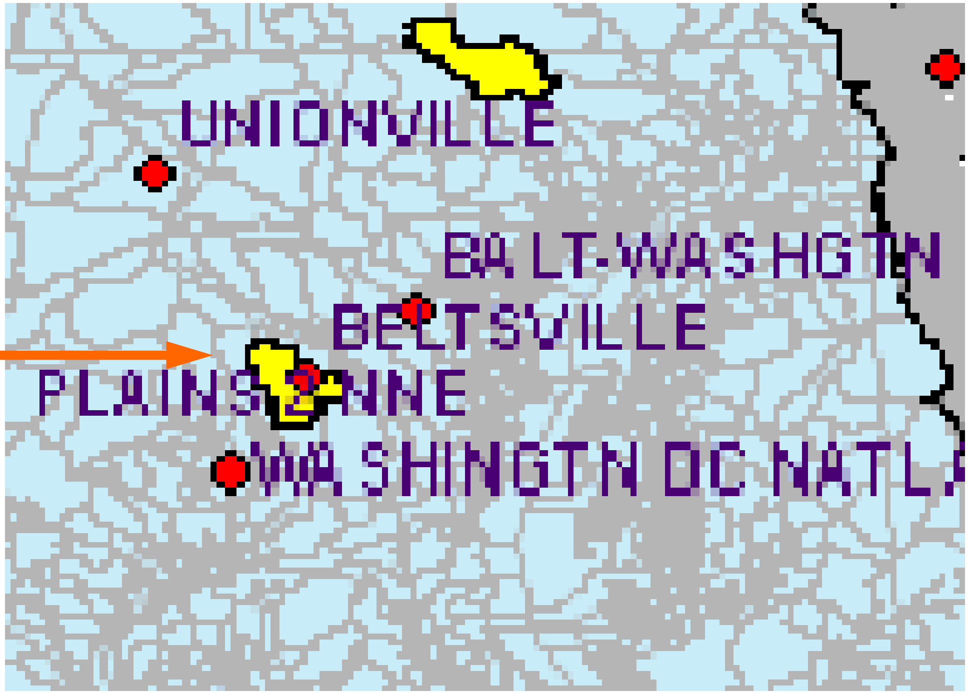

Rain Gage Correlations

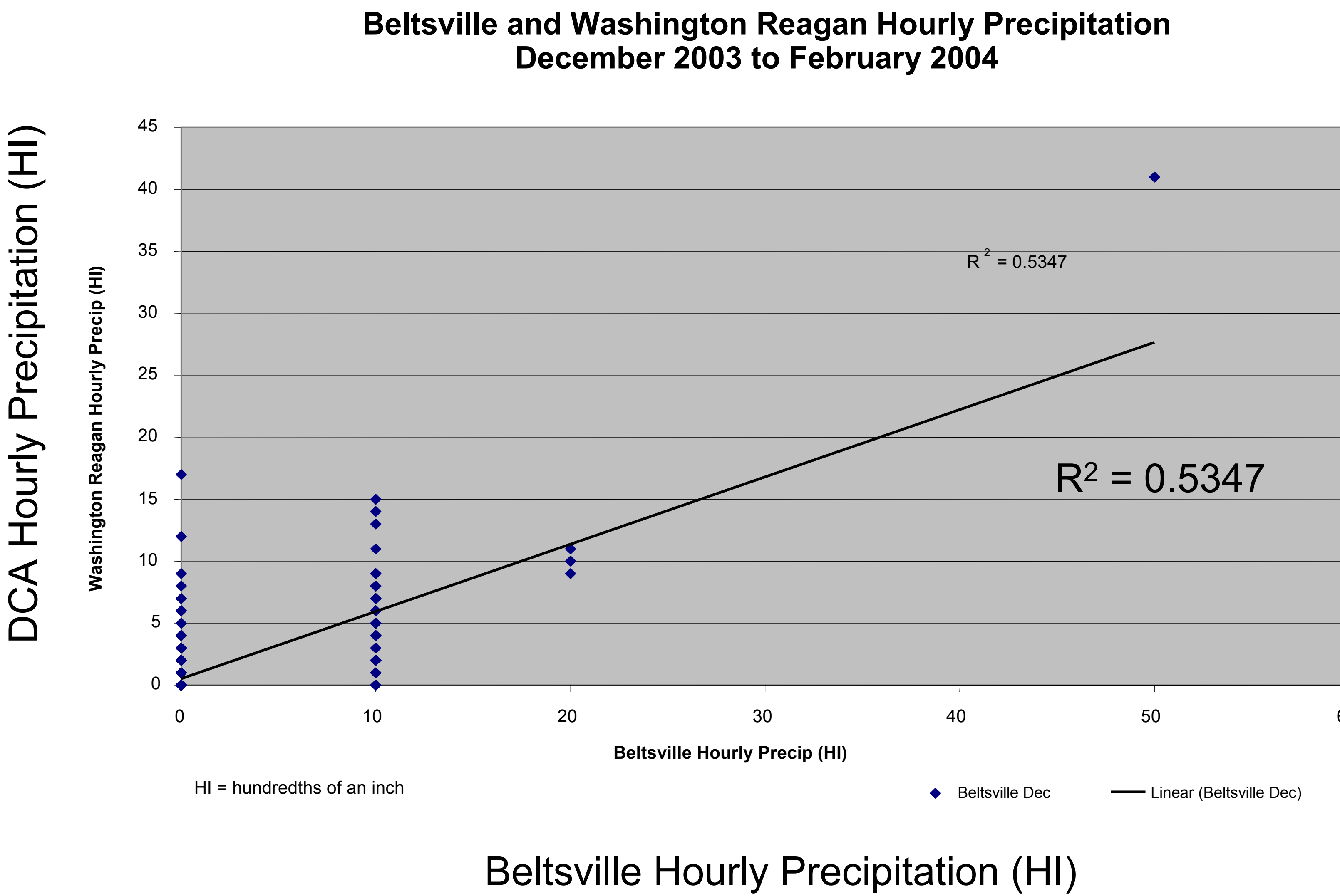

Rain Gage Correlations

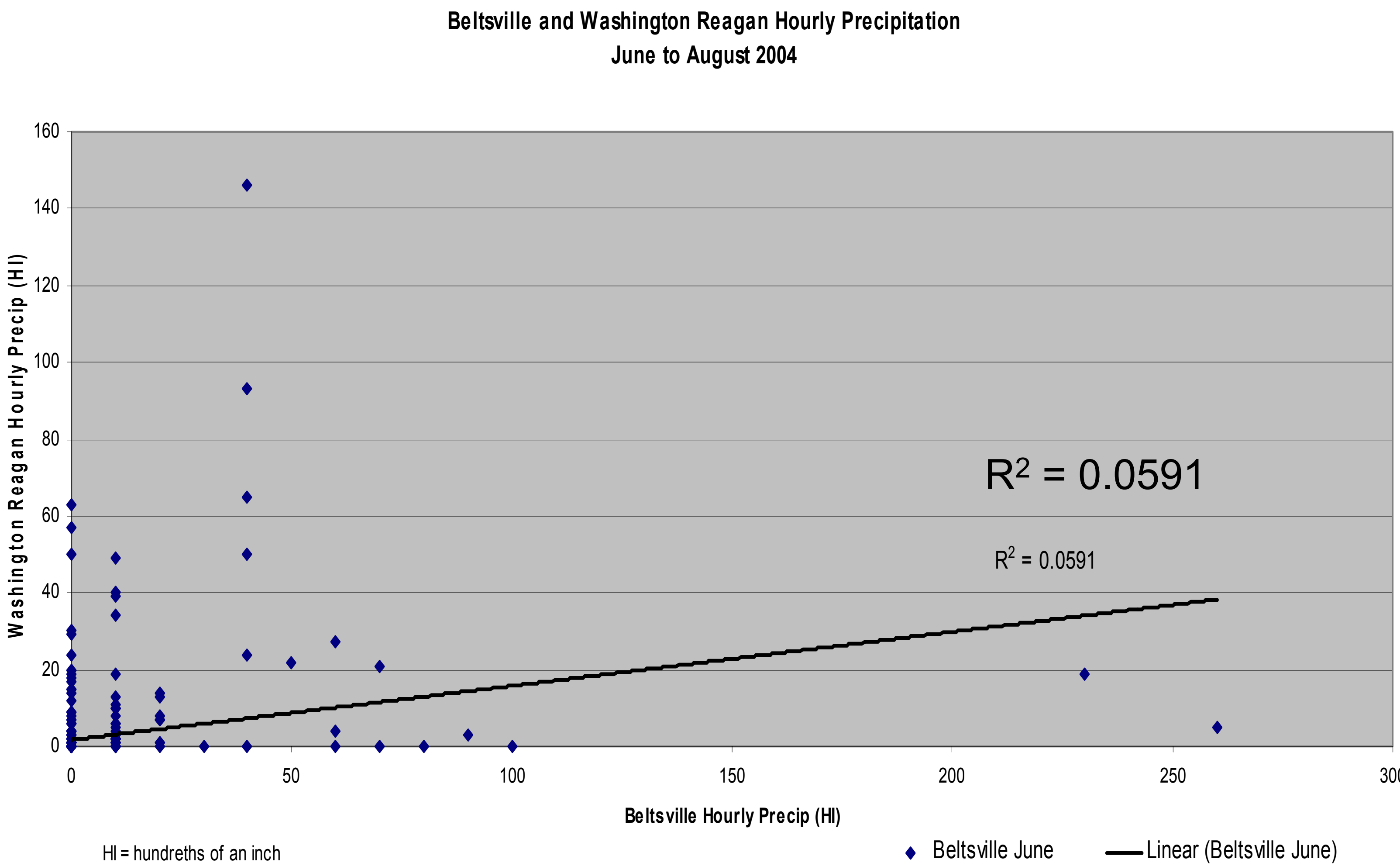

DCA Hourly Precipitation (HI)

Beltsville Hourly Precipitation (HI)

Using Spatial data to Improve Rain Gage Data

- When missing rain gage data, spatial data can be used to fill in the gaps or estimate new data
- When a storm isn't in the area of the rain gage station the precipitation is likely to be picked up by the radar or satellite
- Forcing of spatial data can improve accuracy of rain gage data

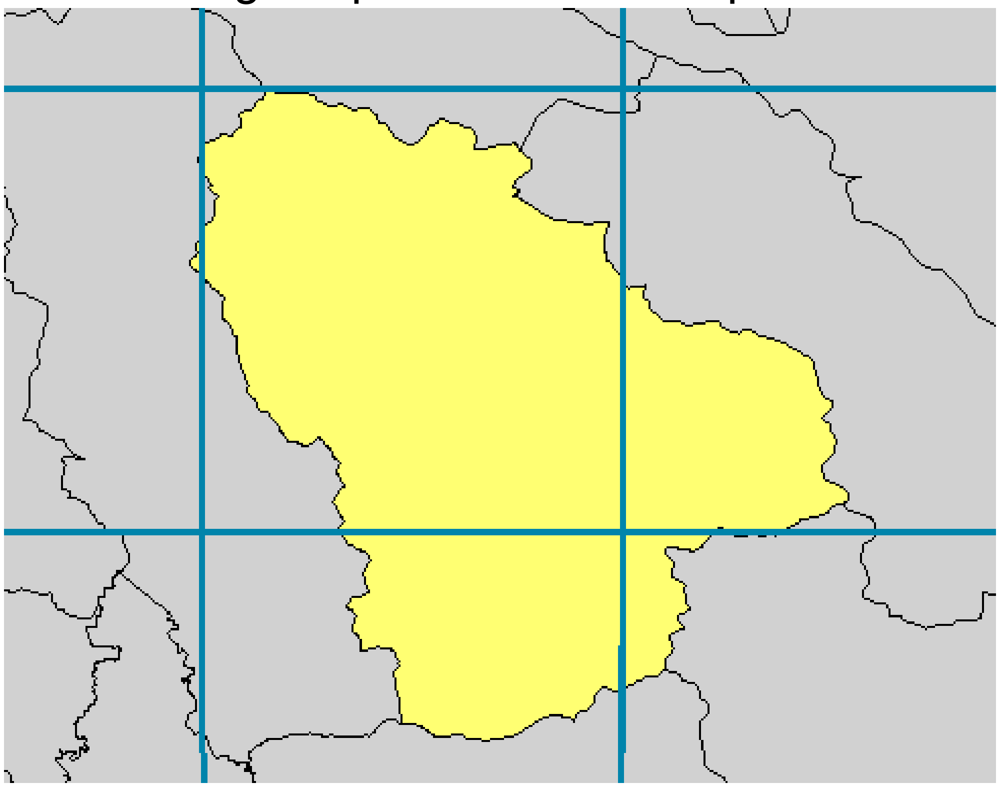

= 1/8th° NLDAS Grid Cell

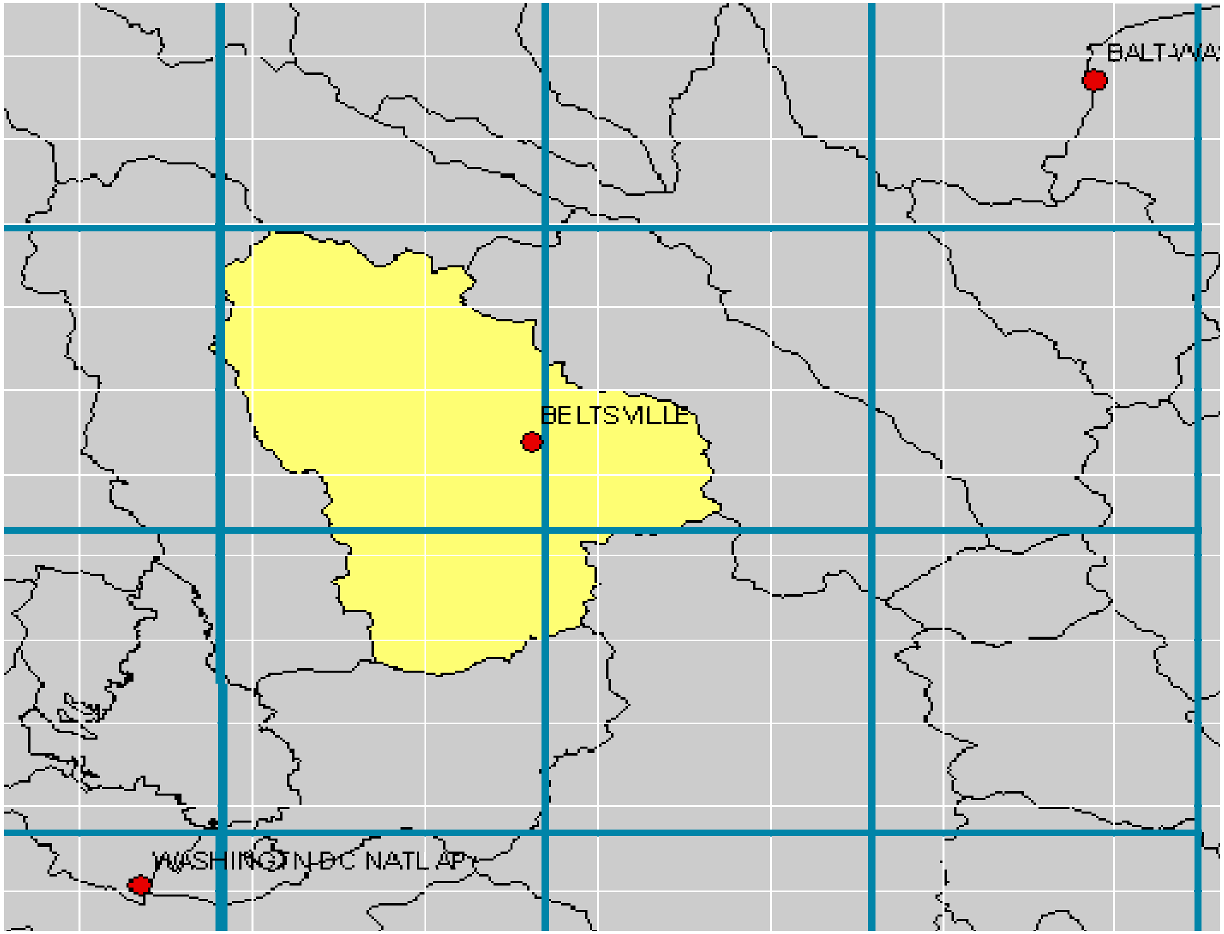

= 1/8th° NLDAS Grid Cell

= Beltsville weather station

Spatial Correlation

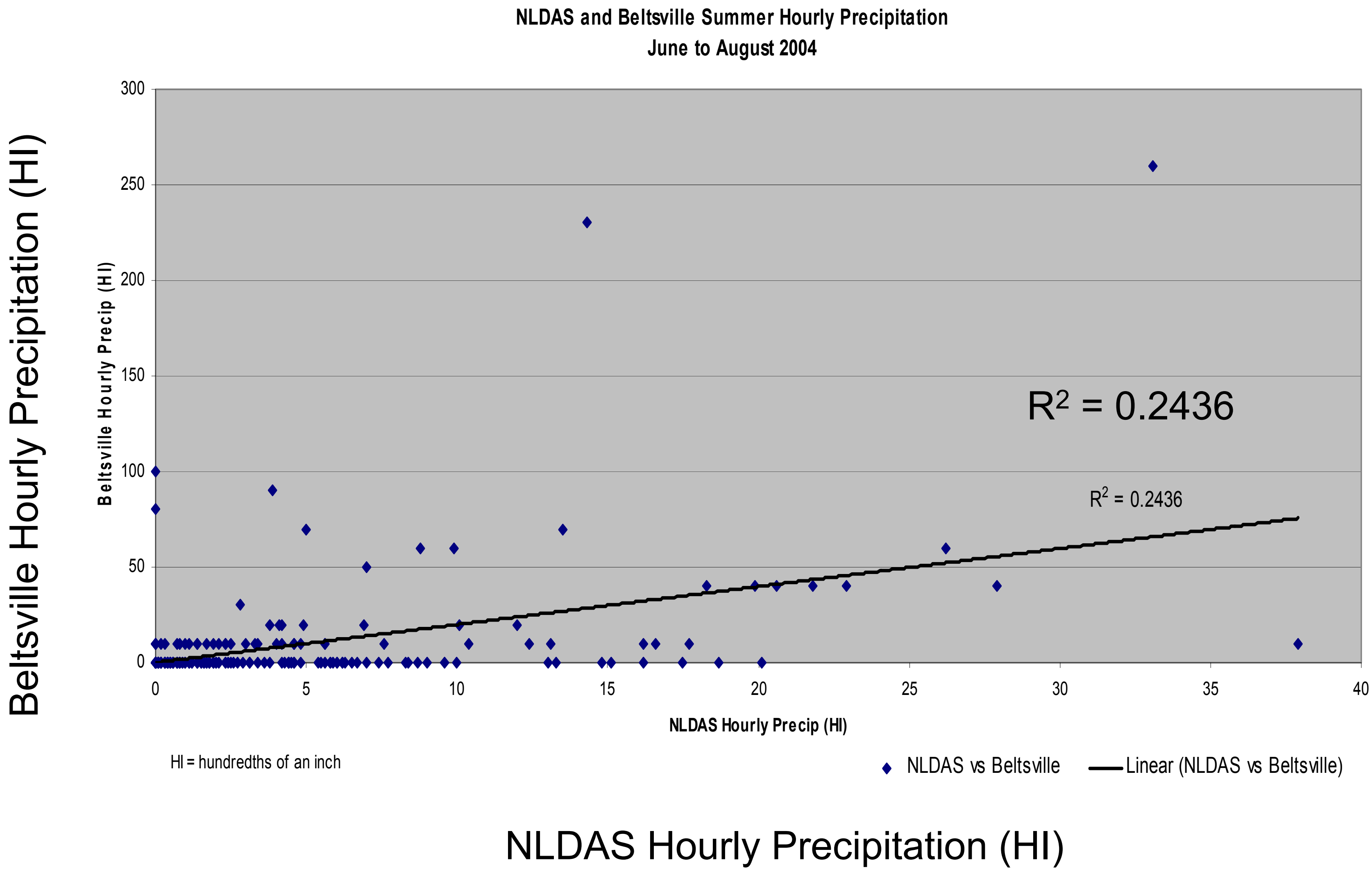

North East Branch Anacostia

North East Branch Anacostia is a subbasin in the Middle Potomac-Anacostia basin

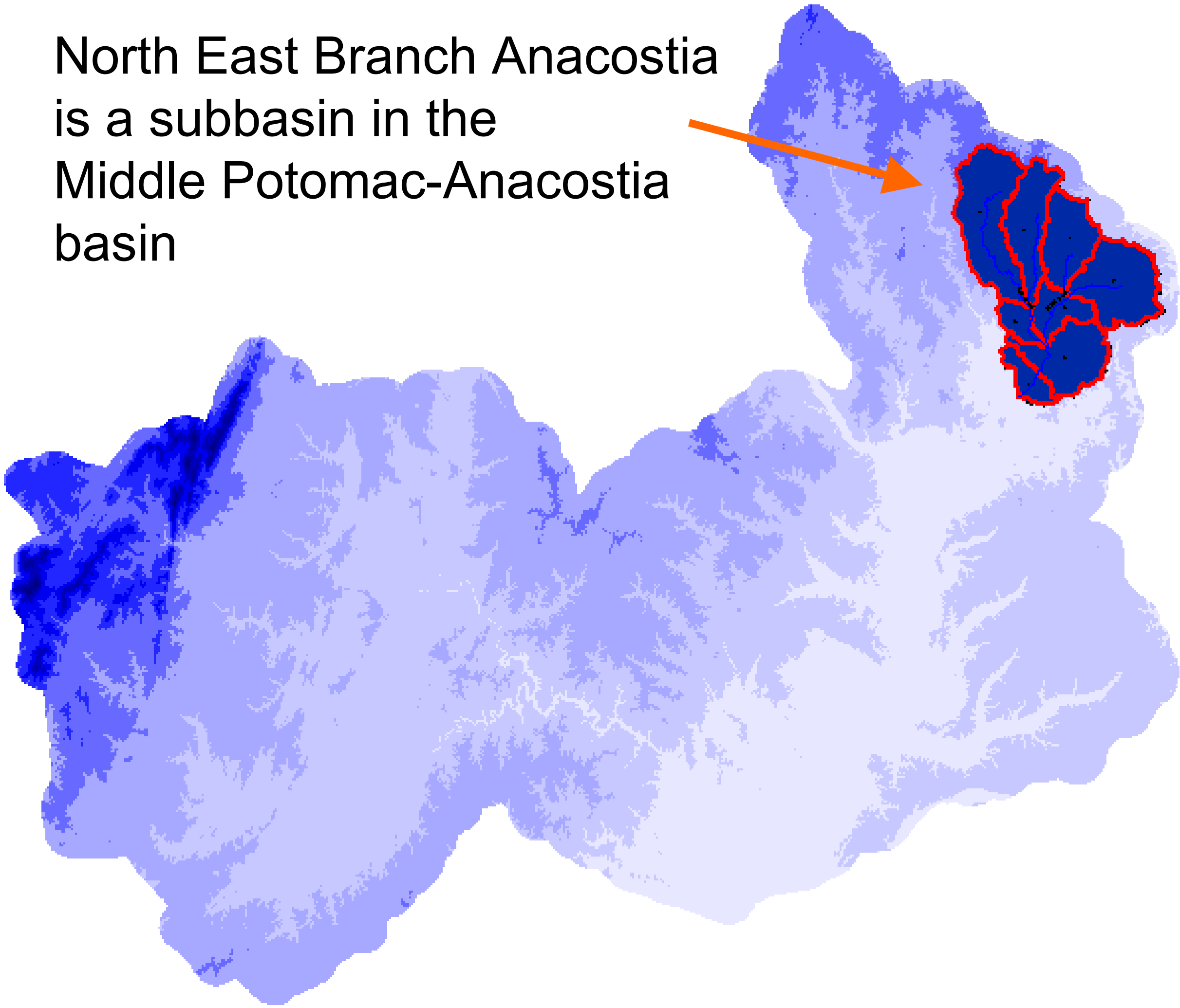

Setup in Basins:

- Delineated with NED (National Elevation Dataset) within BASINS instead of DEM (Digital Elevation Model) to create subbasins

- Used NLCD 2001 (National Land Cover Dataset) within BASINS to classify land use and cover

LULC

<u>Impervious values:</u>

- (11, Orange) Developed Open Space = 90%
- (21, Teal) Developed, Low Intensity = 65%
- (22, Dark Green) Developed, Medium Intensity = 35%
- There is no Developed, High Intensity within this basin

<u>LULC used:</u>
NLCD 2001

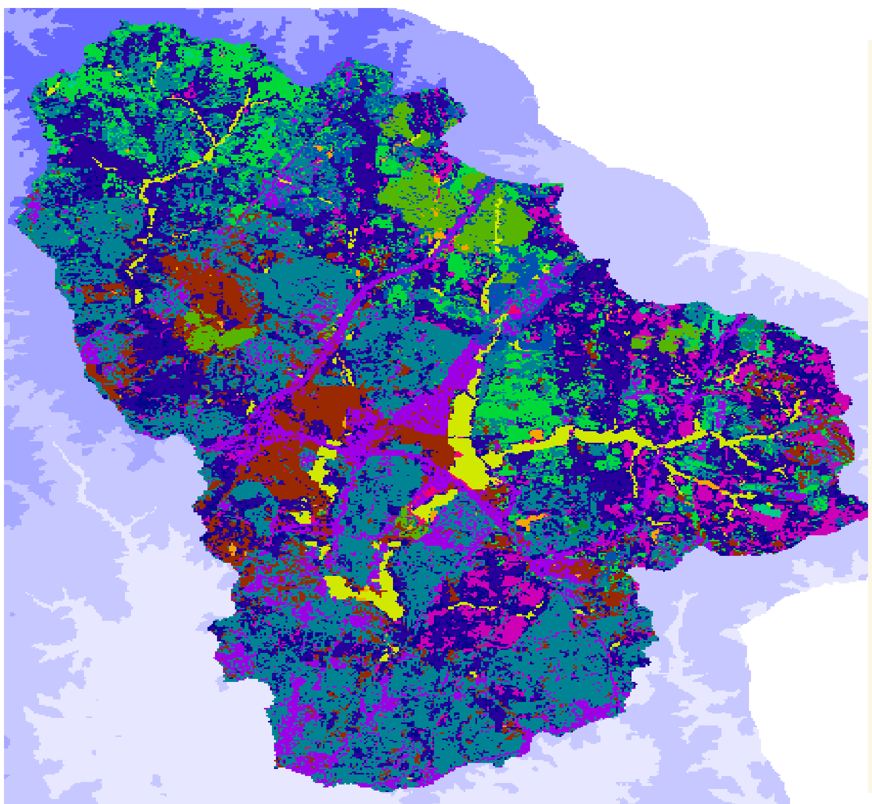

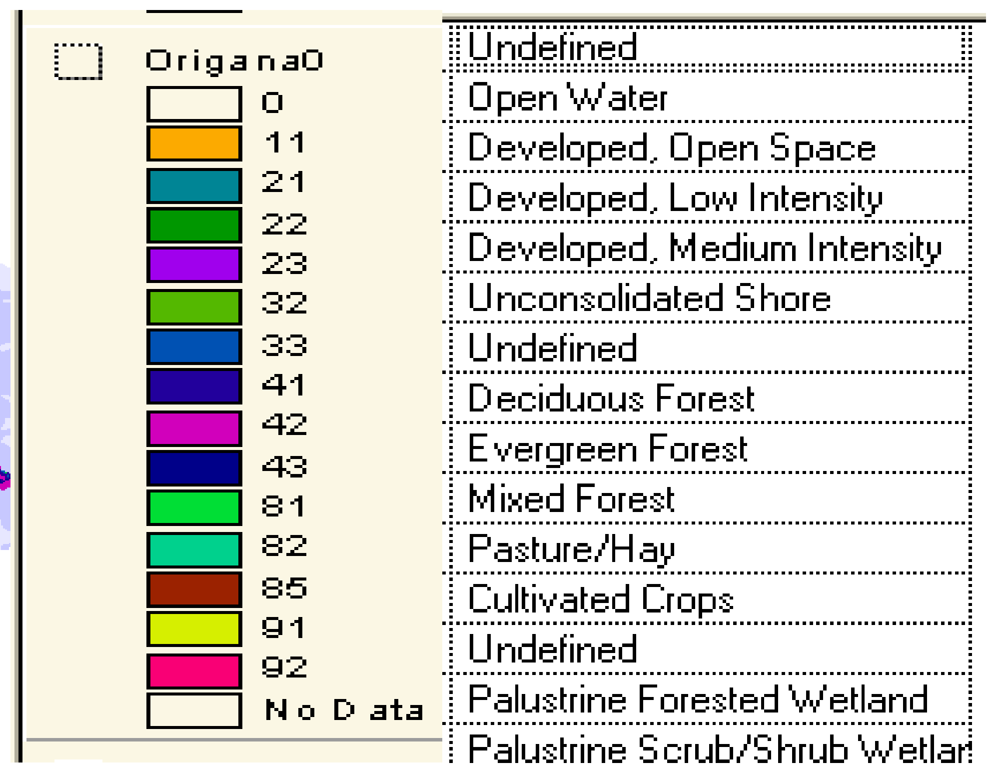

HSPF

When running HSPF the EPA uses 12 months of data for spin up time. The time frame for this study was from January 1, 2002 to September 9, 2003. The analysis was over an 8 month span due to time constrictions. The cloud data only went back to January 2002 and the flow data from BASINS only went up to September 2003.

Hydrographs

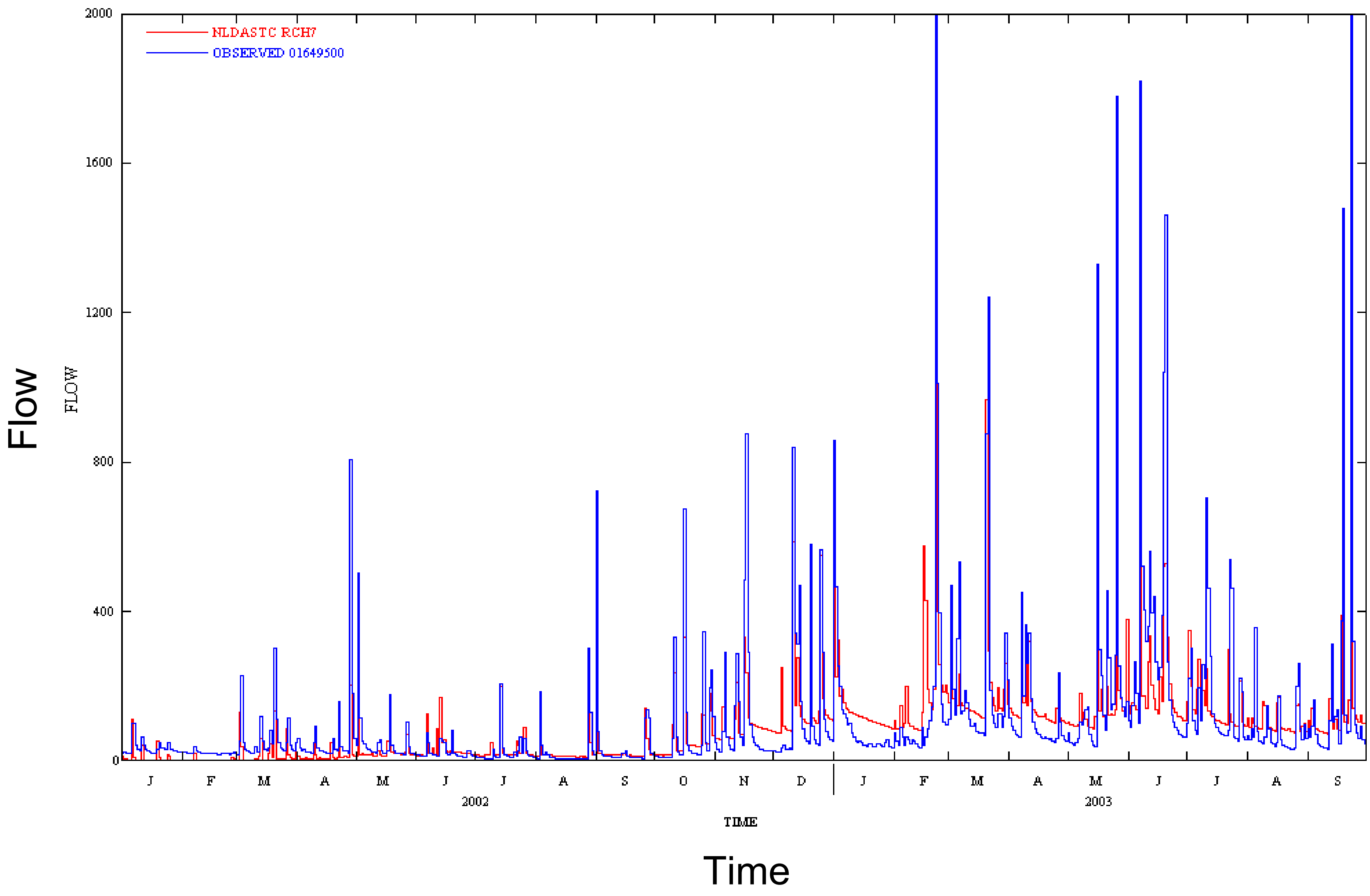

Hydrograph of NLDAS for an 8 Month Span

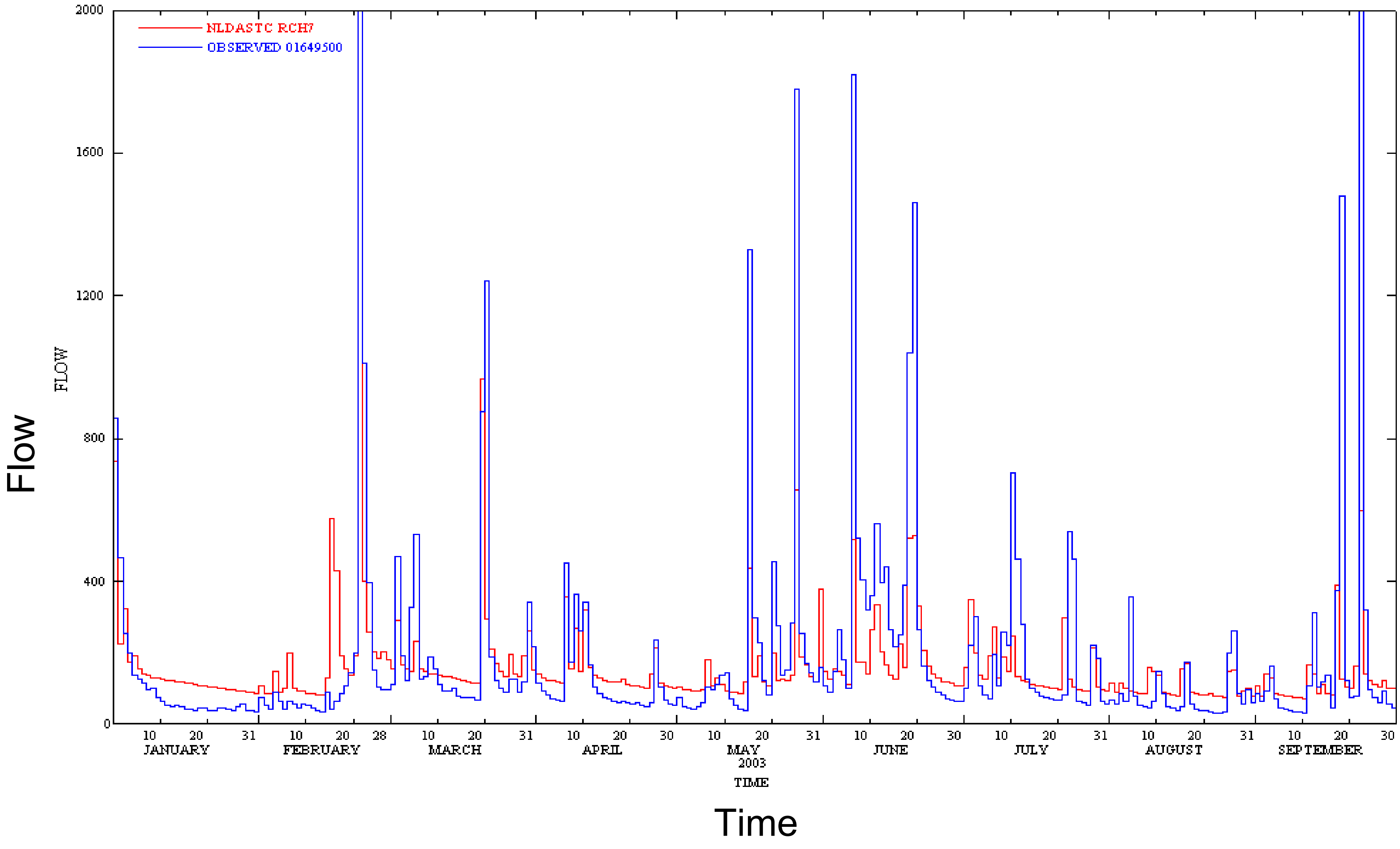

Hydrograph of DCA for an 8 Month Span

Flow

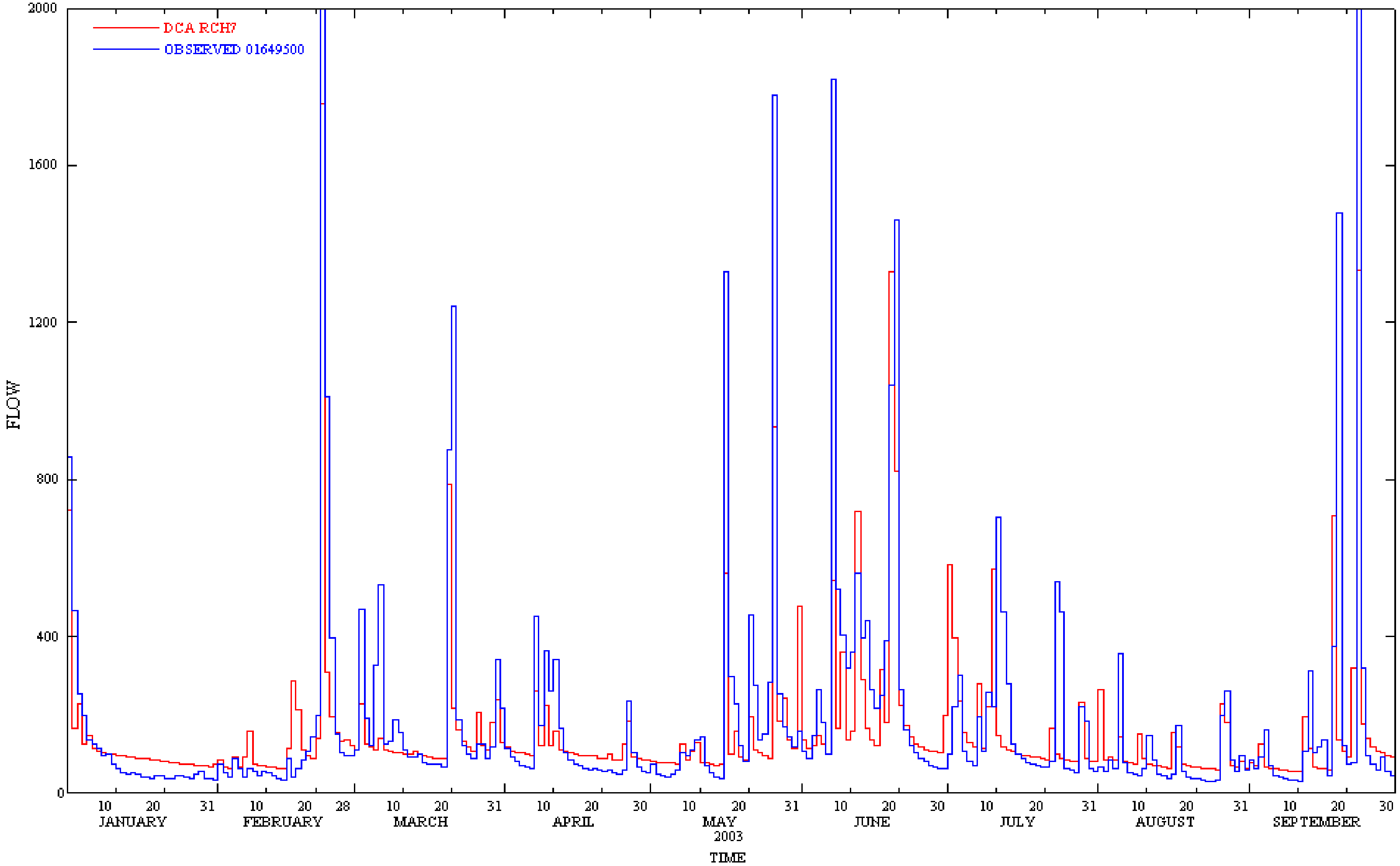

Time

Hydrograph of Beltsville for an 8 Month Span

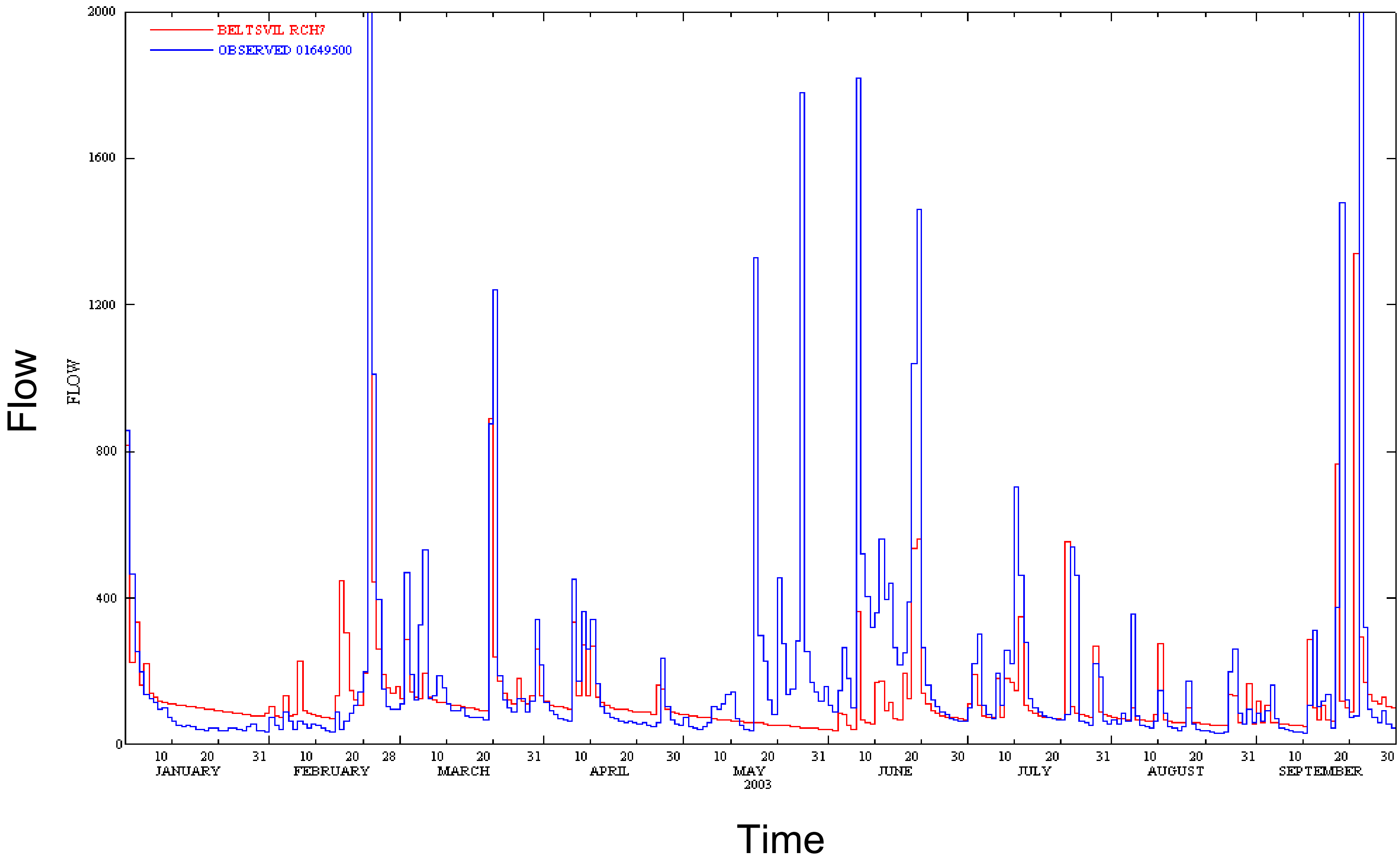

Hydrograph of NLDAS for the Month of June

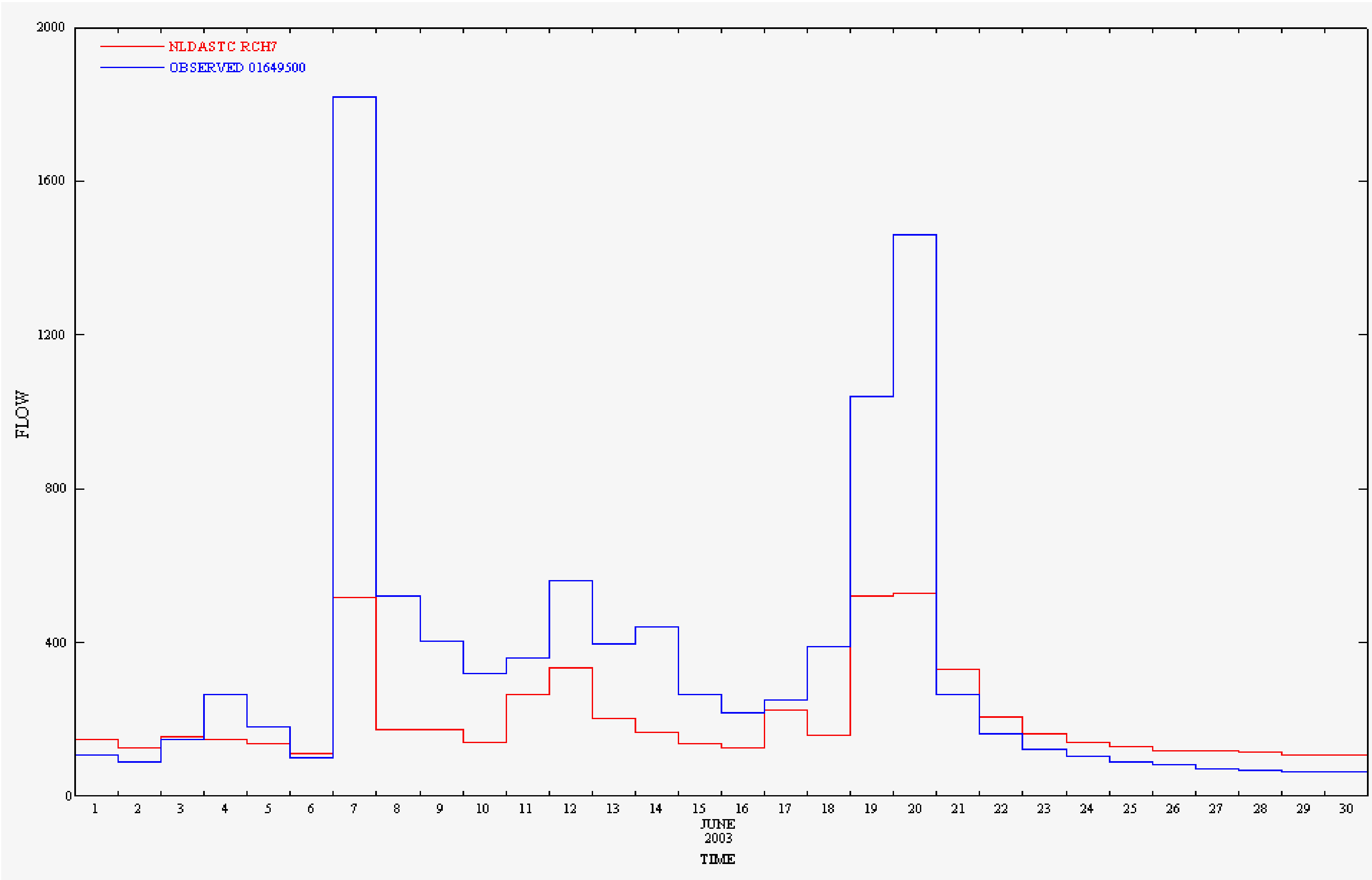

Flow

Time

Hydrograph of DCA for the Month of June

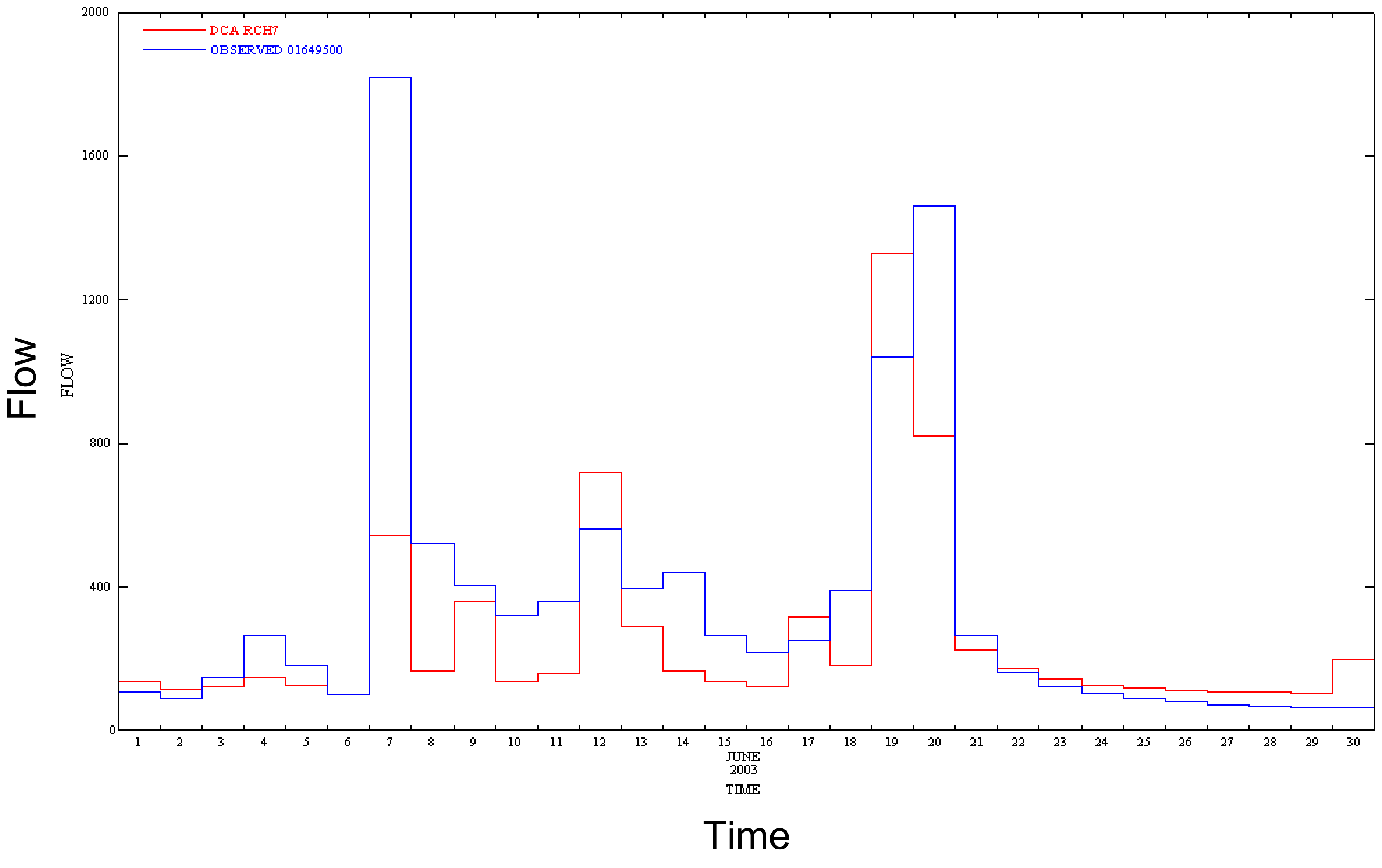

Hydrograph of Beltsville for the Month of June

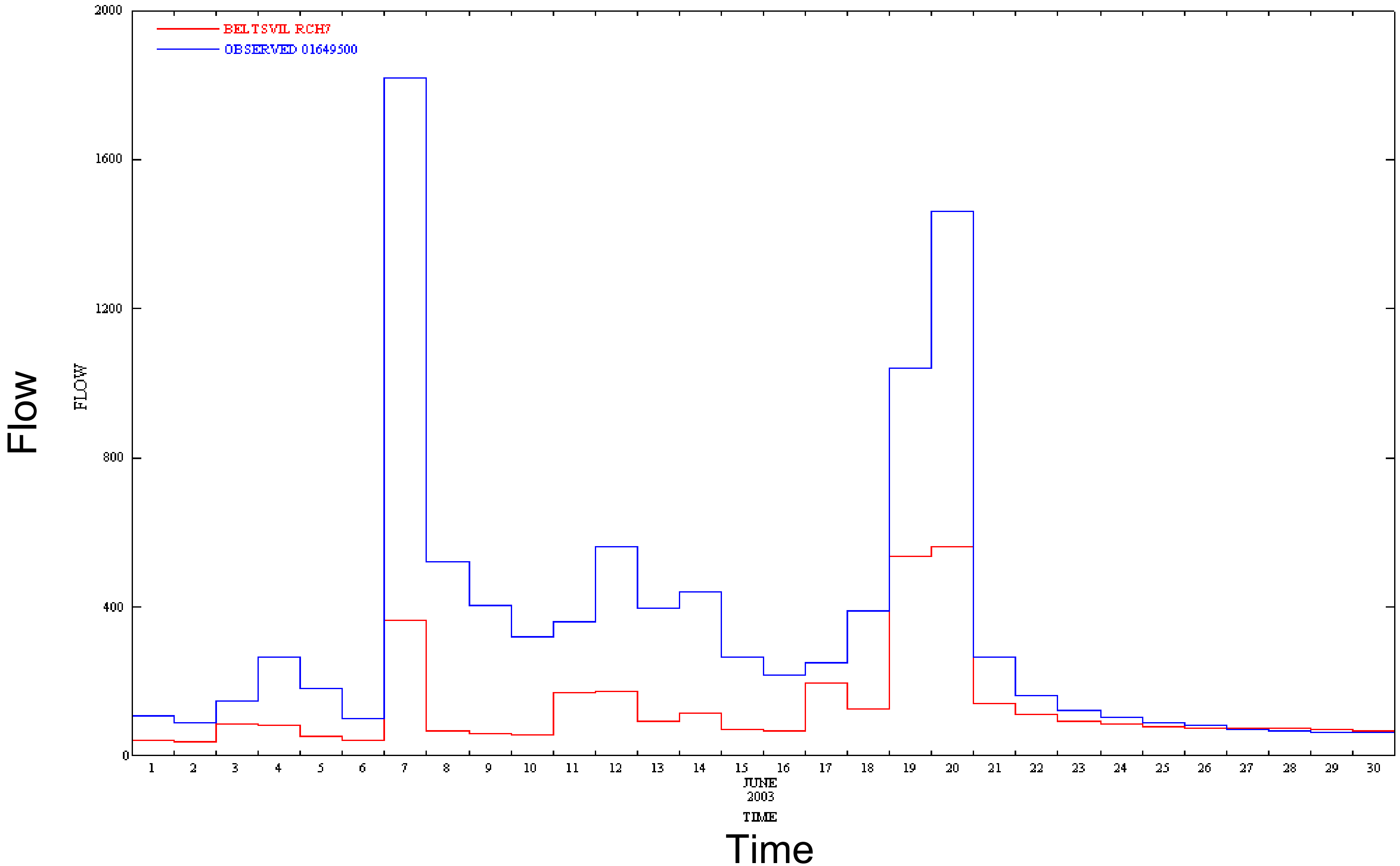

Flow Rate Statistics

Statistics for 8 Month Span

Statistics	NLDAS	Beltsville	DCA
Model Efficiency (NS)	0.6	0.27	0.64
RMS Error	219.95	308.28	208.65
% Mean Absolute Error	59.83	87.04	57.99
Mean Absolute Error	106.355	115.967	93.05
% Mean Error	-16.06	-46.1	-28.59
Mean Error	-28.56	-61.41	-45.87
Coefficient of Determination	0.71	0.3	0.74
Correlation Coefficient	0.84	0.55	0.86

Statistics for the Month of June

Statistics	NLDAS	Beltsville	DCA
Model Efficiency (NS)	0.32	0.14	0.48
RMS Error	333.61	373.56	291.74
% Mean Absolute Error	91.54	172.83	61.73
Mean Absolute Error	182.769	220.247	155.915
% Mean Error	-73.57	-171.9	-37.2
Mean Error	-146.9	219.1	-93.97
Coefficient of Determination	0.8	0.72	0.54
Correlation Coefficient	0.9	0.85	0.73

Conclusion

- EPA uses only surface gauge data for flow
- Flow is very important for concentrations and pollutant loading
- Very low correlations between station precipitation data, especially for summer convective (not uniform) rainfall
- Doppler radar and satellite provides spatially contiguous data but also may have errors.
- Most optimal approach is likely the merger of spatial Doppler/satellite with gauge data.

The Search for Global Teleconnections

A Hydroclimatic Analysis of 25 Years of Modeled Water Cycle Data

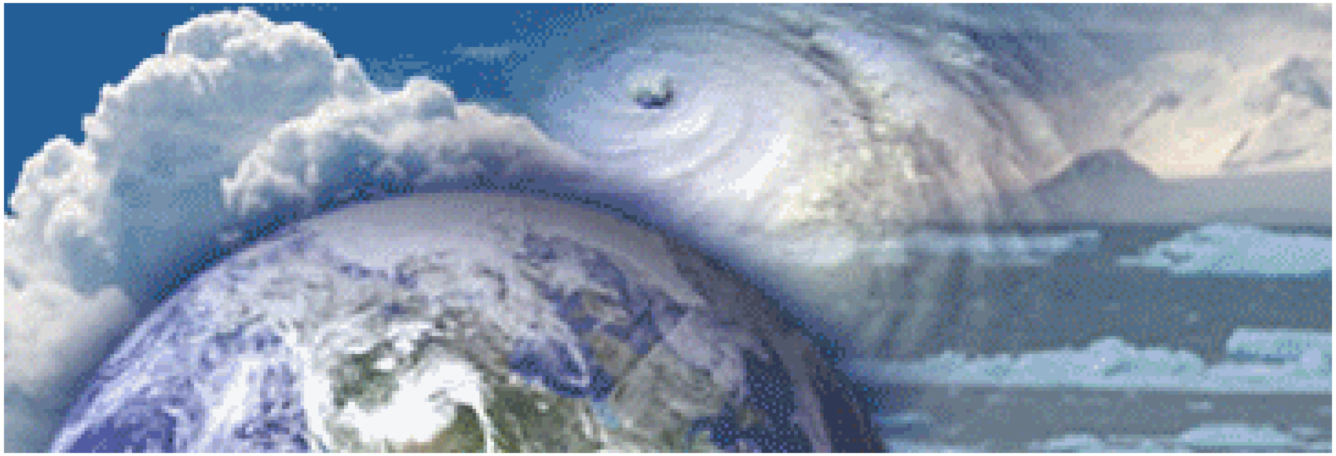

Matthew Stepp
Matt Rodell, Ph.D.
Summer Institute Symposium
August 12rd, 2005
Hydrological Sciences Branch
NASA Goddard Space Flight Center

Background

- The Global Water Cycle is essential to all life on Earth.
- Flooding, droughts, food shortages, drinking water, etc.
- In the past climate water storage variables were deficient across the globe, causing inaccurate climate predictions.
- Now, due to…
  - New observing satellites like TRMM and TERRA
  - Global Land Data Assimilation System (GLDAS)
- In particular, this research will focus on the movements of droughts and pluvials (periods of wetness) in regard to atmospheric circulation.

Research Objectives

- To search for Global Teleconnections.
- Visualize 25 years of Land Surface Model Output.
- Conduct statistics of Water Storage Anomalies between various regions.
- Correlate these Anomalies with Precipitation to identify trends.
- Identify time step of any correlations to be used in possibly predicting water cycle variables (e.g. precipitation) between particular regions.

Research Information

- Analyzed 25 years of GLDAS/NOAH 2.7.1 output data

- Manipulated data to compute a Global Water Storage and Precipitation Anomaly field.
  - Canopy + 4 Layer Soil Moisture + Snow – Monthly Climatology
  - Snow Fall + Rain Fall – Monthly Climatology

- Conducted two studies
  - Case 1: Gulf of Mexico – Plains Region (used as benchmark)
  - Case 2: Europe – Asia - Africa

The Movie

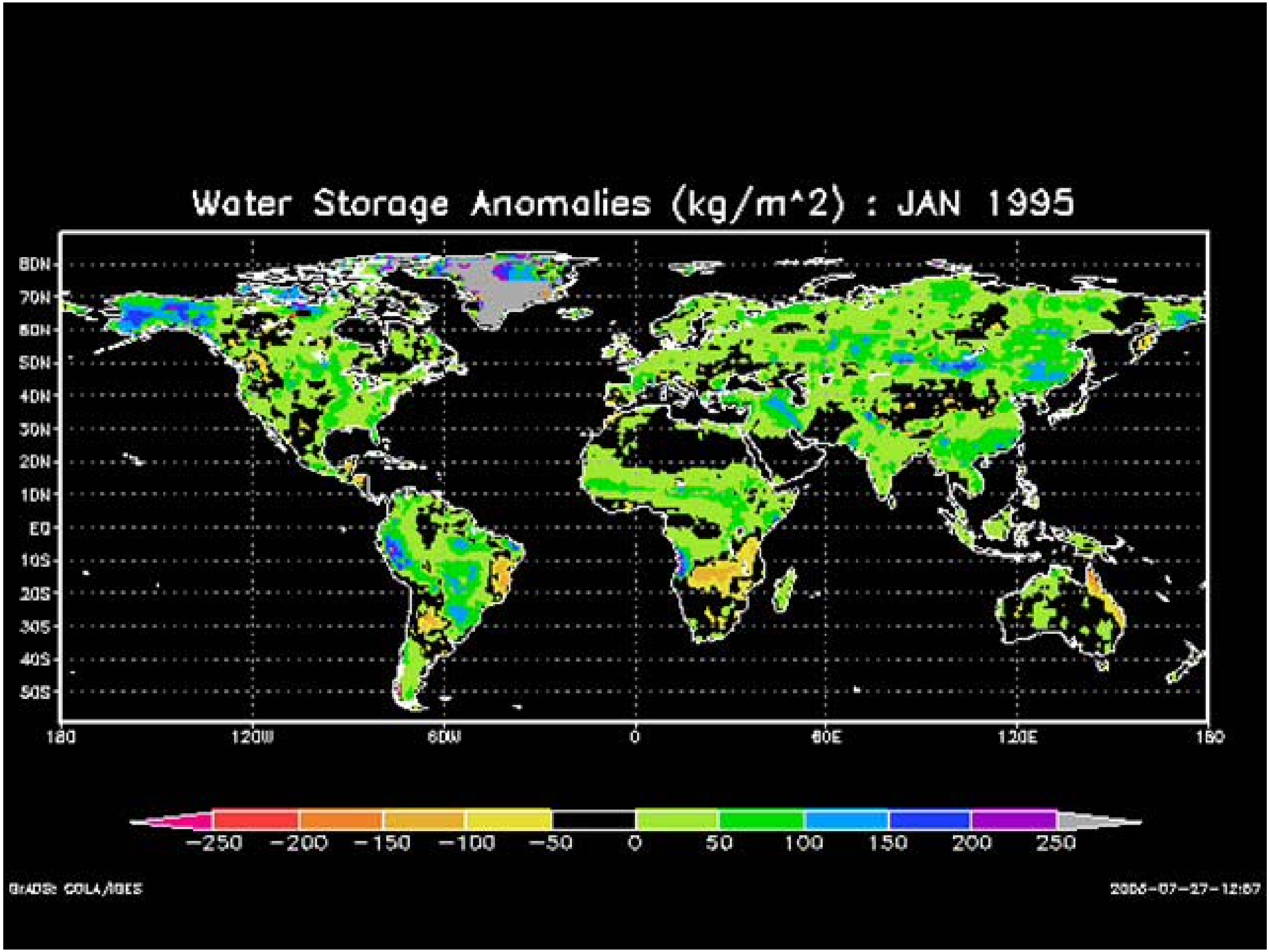

Water Storage Anomalies (kg/m^2) : JAN 1995
80N
70N
60N
50N
40N
30N
20N
10N
EQ
10S
20S
30S
40S
50S
180
120W
60W
0
60E
120E
180
-250
-200
-150
-100
-50
0
50
100
150
200
250

Case 1: Gulf of Mexico - Plains

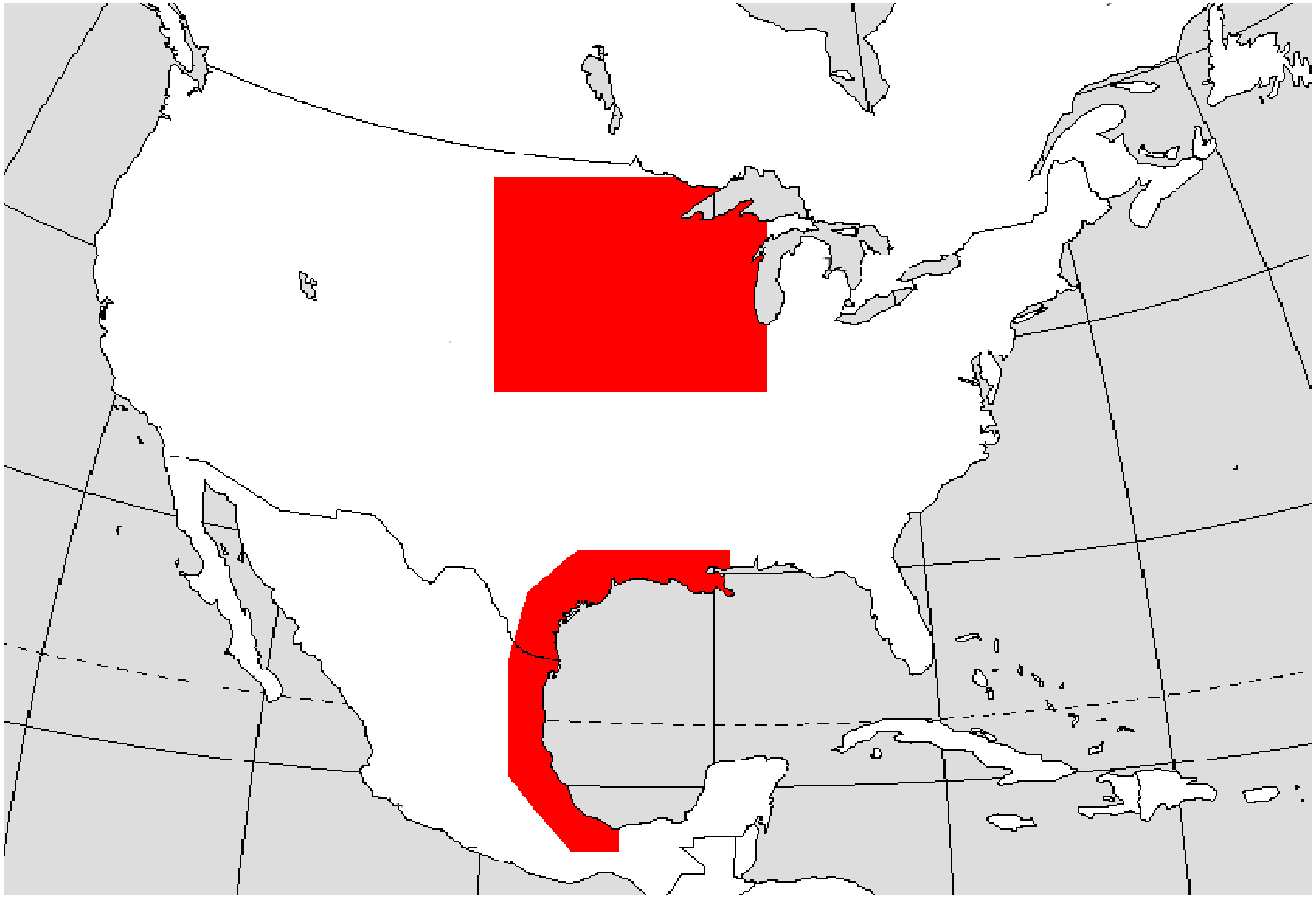

- Gulf Coast Coordinates: Lon. 100W – 89W Lat. 17N – 31N
- Plains Coordinates: Lon. 100W – 85W Lat. 37N – 48N

Case 1: Correlations

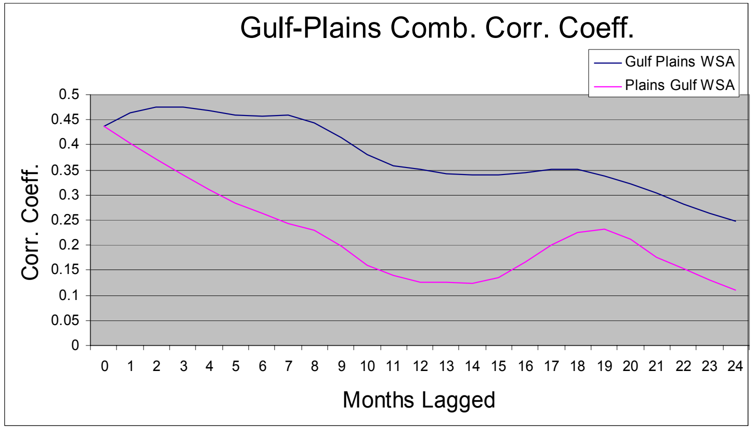

Case 1: Normalized Correlation

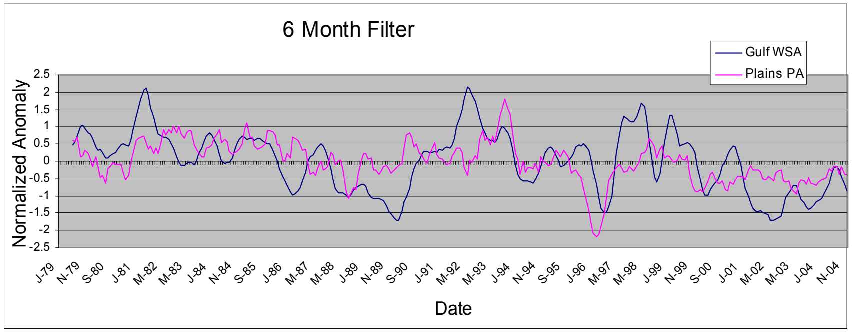

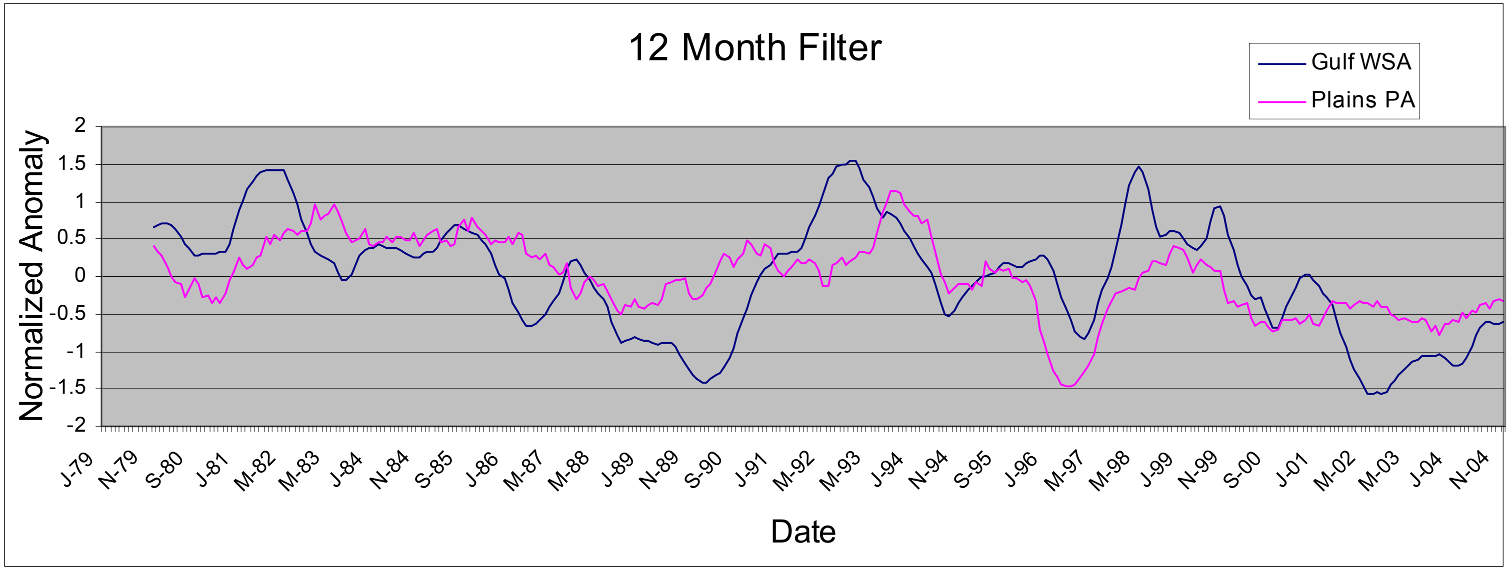

Case 2: Europe and Asia

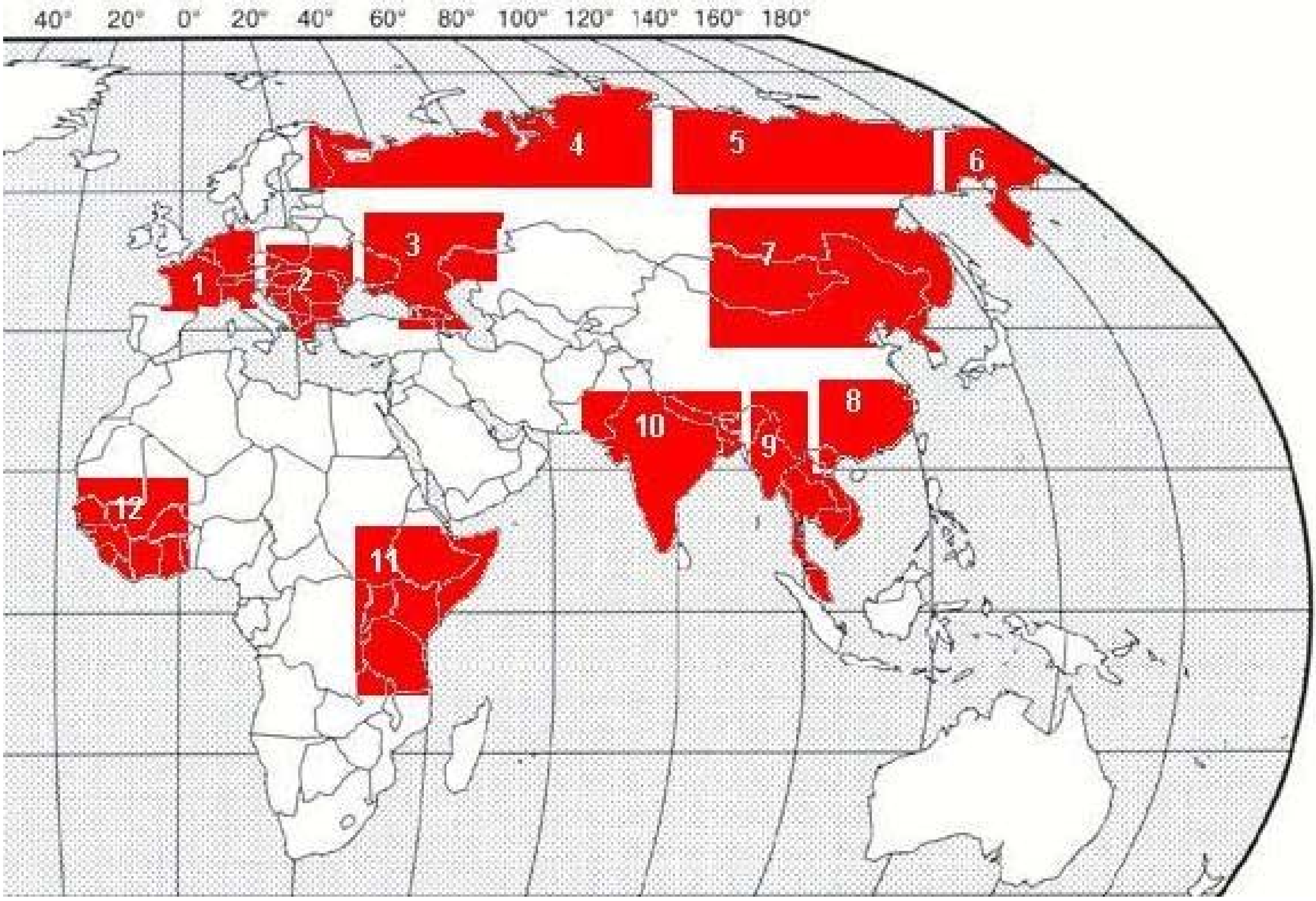

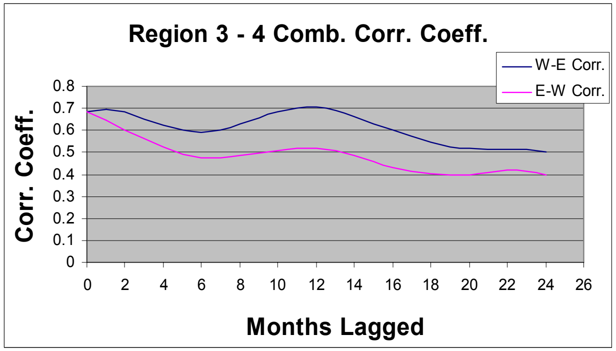
Region 3 - 4 Comb. Corr. Coeff.
W-E Corr.
E-W Corr.
Corr. Coeff.
Months Lagged

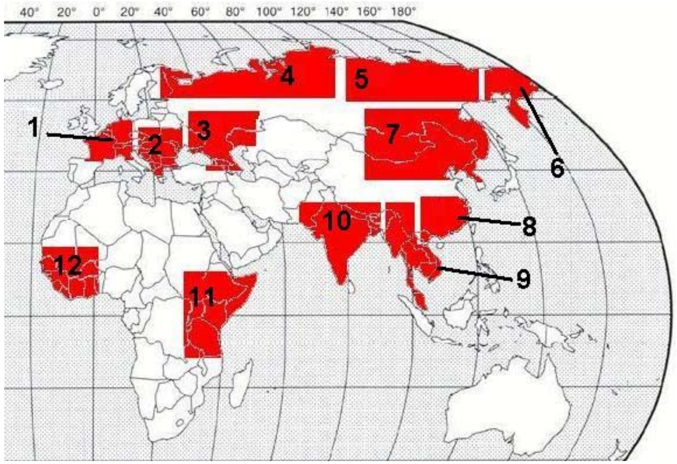
1
2
3
4
5
6
7
8
9
10
11
12

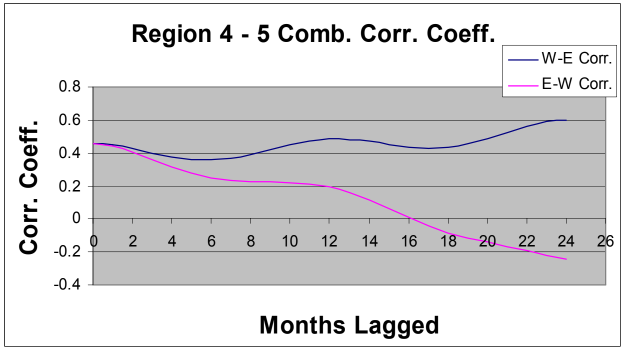
Region 4 - 5 Comb. Corr. Coeff.
W-E Corr.
E-W Corr.
Corr. Coeff.
Months Lagged

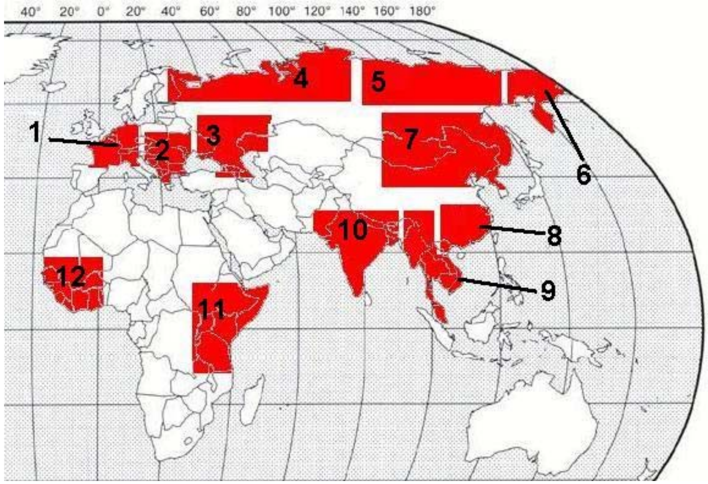
40° 20° 0° 20° 40° 60° 80° 100° 120° 140° 160° 180°
1
2
3
4
5
6
7
8
9
10
11
12

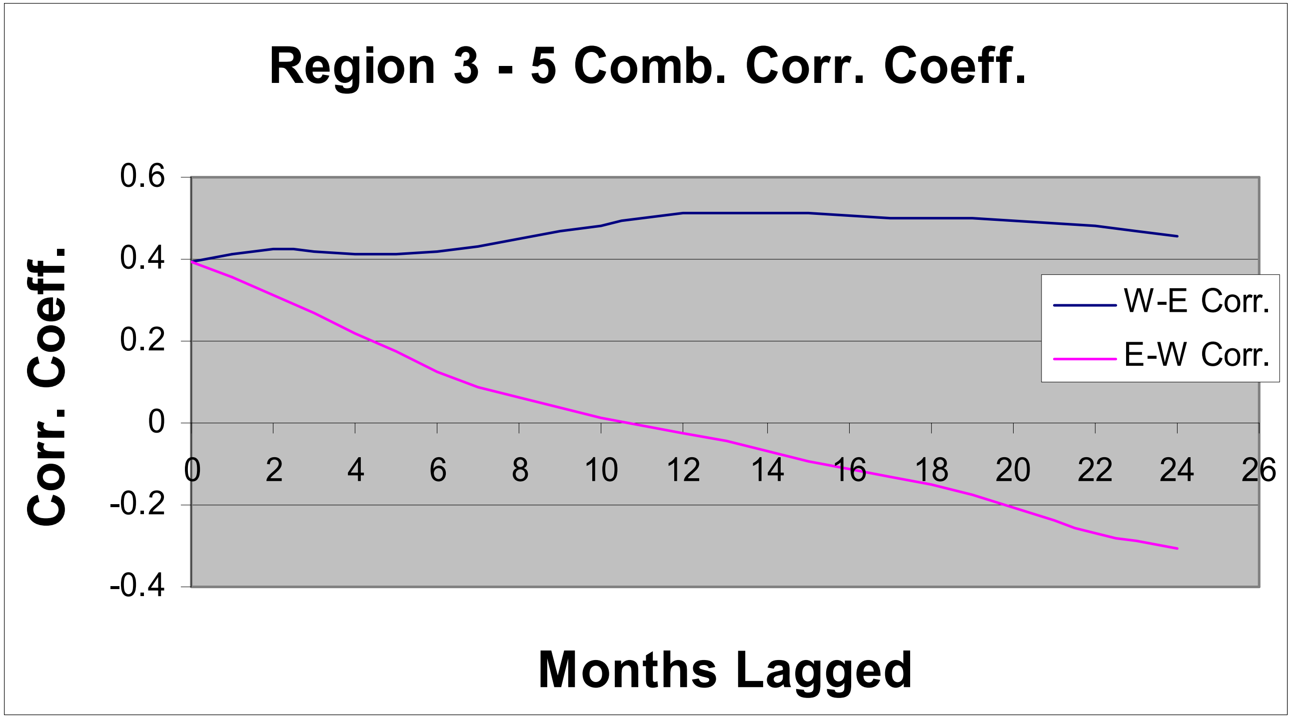
Region 3 - 5 Comb. Corr. Coeff.
Corr. Coeff.
0.6
0.4
0.2
0
-0.2
-0.4
0
2
4
6
8
10
12
14
16
18
20
22
24
26
W-E Corr.
E-W Corr.
Months Lagged

Region 3 - 4

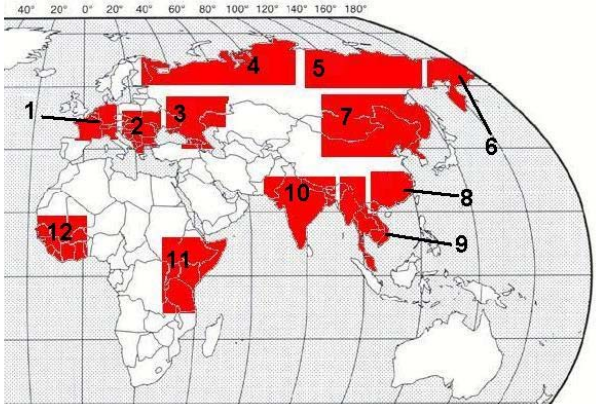
40° 20° 0° 20° 40° 60° 80° 100° 120° 140° 160° 180°
1
2
3
4
5
6
7
8
9
10
11
12

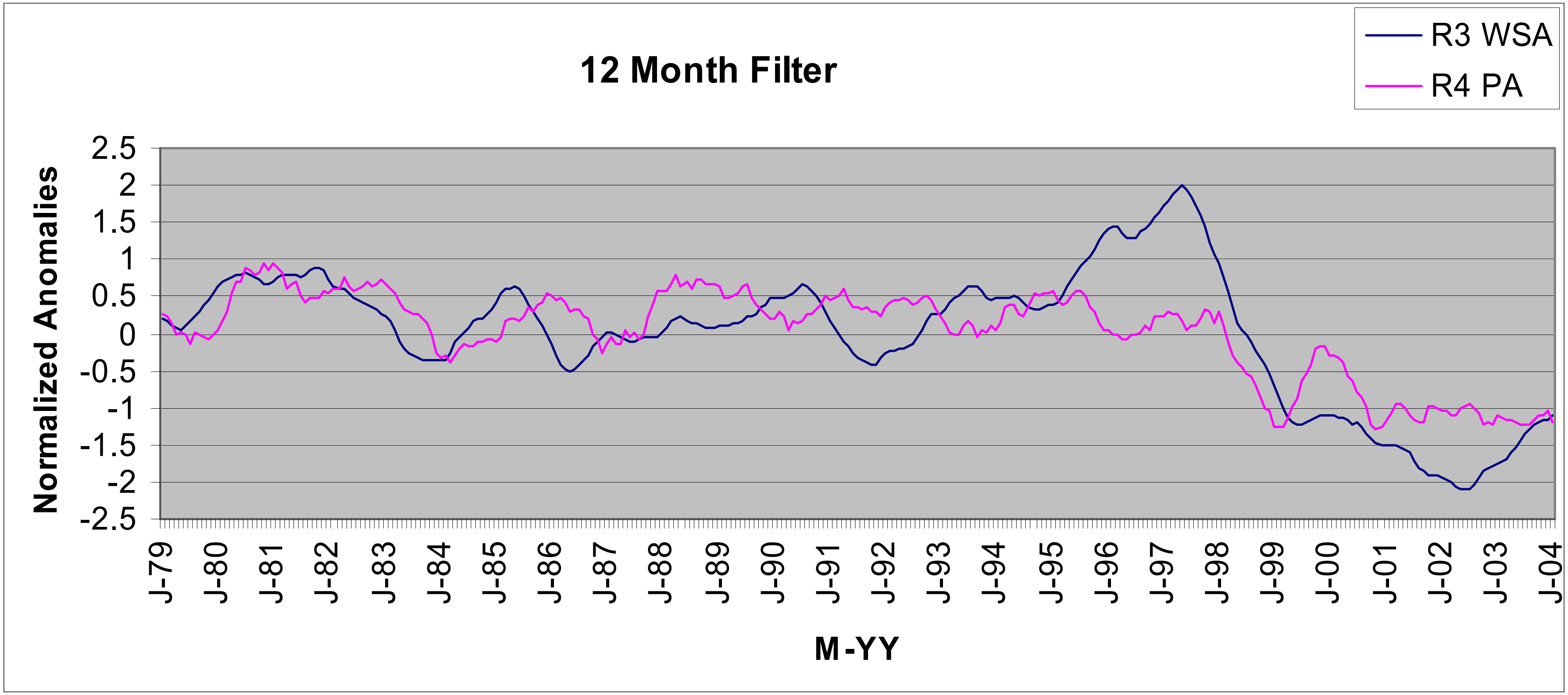
12 Month Filter
R3 WSA
R4 PA
Normalized Anomalies
2.5
2
1.5
1
0.5
0
-0.5
-1
-1.5
-2
-2.5
J-79
J-80
J-81
J-82
J-83
J-84
J-85
J-86
J-87
J-88
J-89
J-90
J-91
J-92
J-93
J-94
J-95
J-96
J-97
J-98
J-99
J-00
J-01
J-02
J-03
J-04
M-YY

Region 4 - 5

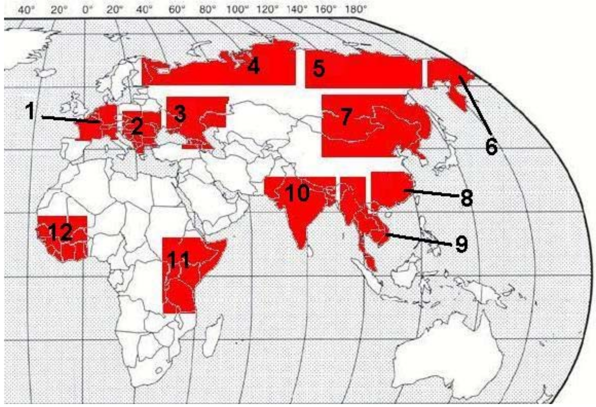

1
2
3
4
5
6
7
8
9
10
11
12

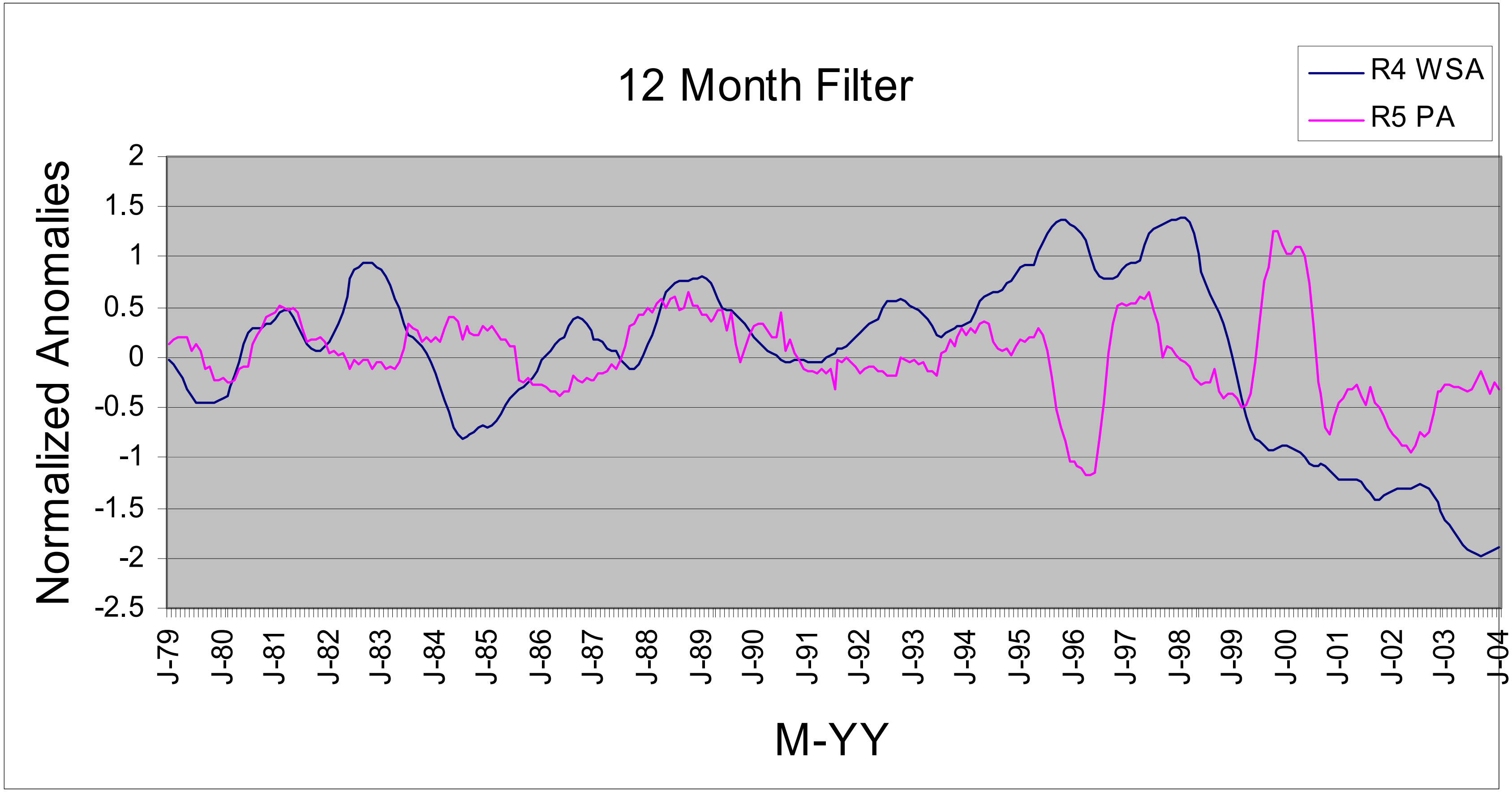

12 Month Filter
R4 WSA
R5 PA
Normalized Anomalies
2
1.5
1
0.5
0
-0.5
-1
-1.5
-2
-2.5
J-79
J-80
J-81
J-82
J-83
J-84
J-85
J-86
J-87
J-88
J-89
J-90
J-91
J-92
J-93
J-94
J-95
J-96
J-97
J-98
J-99
J-00
J-01
J-02
J-03
J-04
M-YY

Region 3 - 5

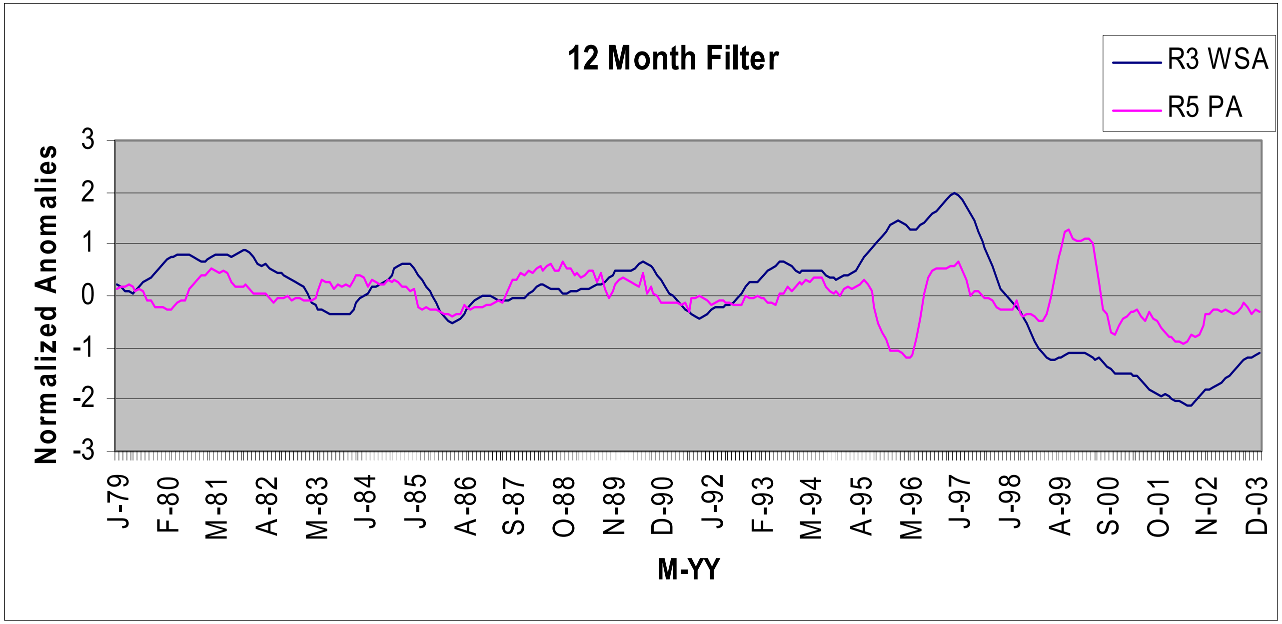

12 Month Filter
R3 WSA
R5 PA
Normalized Anomalies
3
2
1
0
-1
-2
-3
J-79
F-80
M-81
A-82
M-83
J-84
J-85
A-86
S-87
O-88
N-89
D-90
J-92
F-93
M-94
A-95
M-96
J-97
J-98
A-99
S-00
O-01
N-02
D-03
M-YY

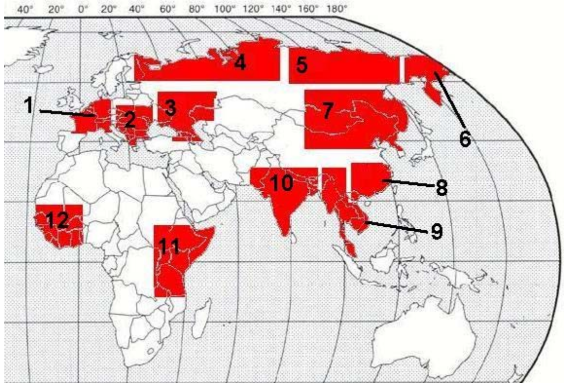

1
2
3
4
5
6
7
8
9
10
11
12

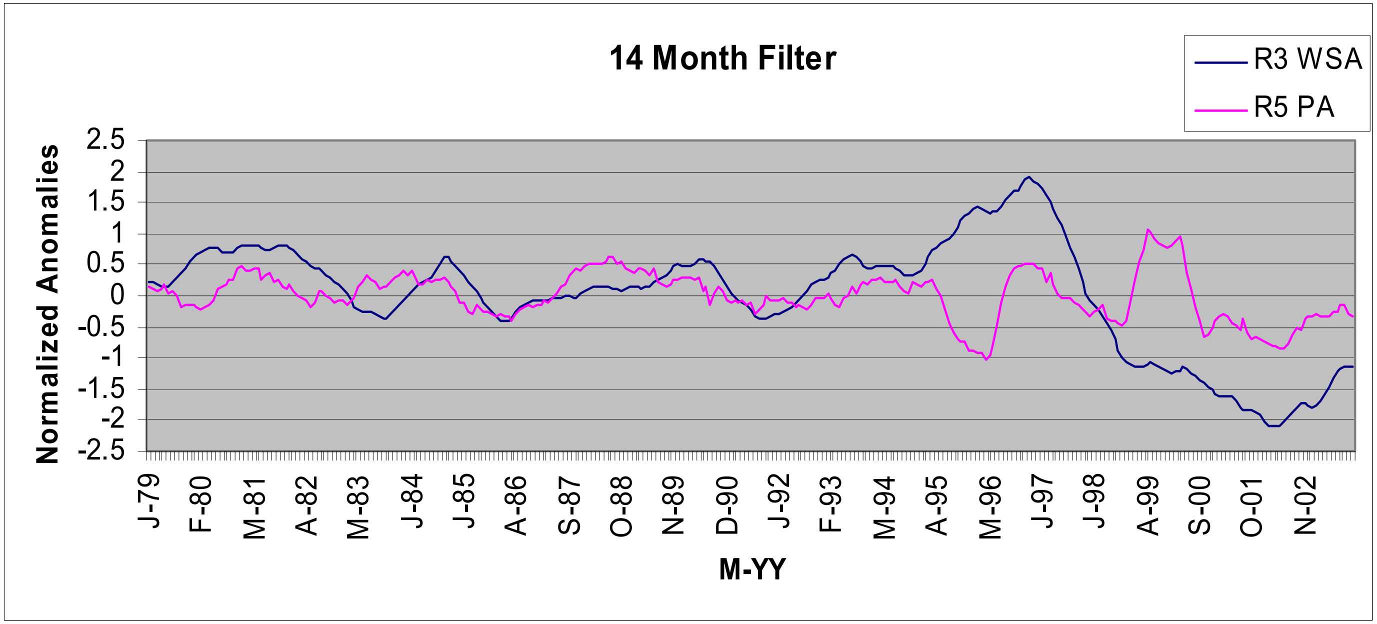

14 Month Filter
R3 WSA
R5 PA
Normalized Anomalies
2.5
2
1.5
1
0.5
0
-0.5
-1
-1.5
-2
-2.5
J-79
F-80
M-81
A-82
M-83
J-84
J-85
A-86
S-87
O-88
N-89
D-90
J-92
F-93
M-94
A-95
M-96
J-97
J-98
A-99
S-00
O-01
N-02
M-YY

Summary

Preliminarily,

- There is a clear connection between the water storage of the Coast of Gulf of Mexico and the Precipitation of the Plains of the United States, with a 6 and 12 month lag.

- At this point, there seems to be a correlation between Central and Eastern regions of Europe and the Northern and Western sections of Asia. Though the correlations and filters were not as strong as Case One, further refinement of the regions may yield better correlations. The lag from Region 3 to 5 is roughly a year for each region.

- There is an apparent correlation, both visually and through the combined plots, in South Eastern Asia and India. Due to the change in the dominant upper atmospheric flow in connection with the seasons, this run of analysis wasn't very strong.

- This same problem goes for the two African regions.

Further Work…

- A refinement to the regions to better catch "hot-spots" seen from the animation that may lead to better correlations.

- The addition of regions, smaller in size, could better catch the path of pluvial and droughts.

- A dissection of the South Eastern Asia/ India and African regions, by way of seasons, could yield a clear cut correlation.

- Further research into even more global teleconnections.

- Work into the use of the apparent lag times between these regions as a climate prediction method.

References

- Causes of Long-Term Drought in the U.S. Great Plains. Siegfried D. Schubert, Max J. Suarez, Philip J. Pegion, Randal D. Koster, Julio T. Bacmeister, pages 485-503. J. Climate Volume 17 No. 3 1 February 2004
- Koster, R. D., and M. J. Suarez, 2003: Impact of Land Surface Initialization on Seasonal Precipitation and Temperature Prediction, Journal of Hydrometeorology: Vol. 4, No. 2, pp. 408-423.
- Koster, R. D., M. J. Suarez, R. W. Higgins, H. M. van den Dool, 2003. Observational Evidence that Soil Moisture Variations Affect Precipitation. Geophysical Research Letters, 30, 45/1 - 45/4. DOI: 10.1029/2002GL016571.
- Koster, R. D., M. J. Suarez, 2004. Suggestions in the Observational Record of Land-Atmosphere Feedback Operating at Seasonal Timescales. Journal of Hydrometeorology, 5, 567-572.
- Koster, R. D., and M. J. Suarez, 2003: Impact of land surface initialization on seasonal precipitation and temperature prediction. J. Hydrometeorology, 4, 408-423.
- Beljaars, A. C. M., P. Viterbo, M. Miller, and A. K. Betts, 1996: The anomalous rainfall over the USA during July 1993: Sensitivity to land surface parameterization and soil moisture anomalies. Monthly Weather Review, 124, 362-383.

Tracking Icebergs in the Ross Sea

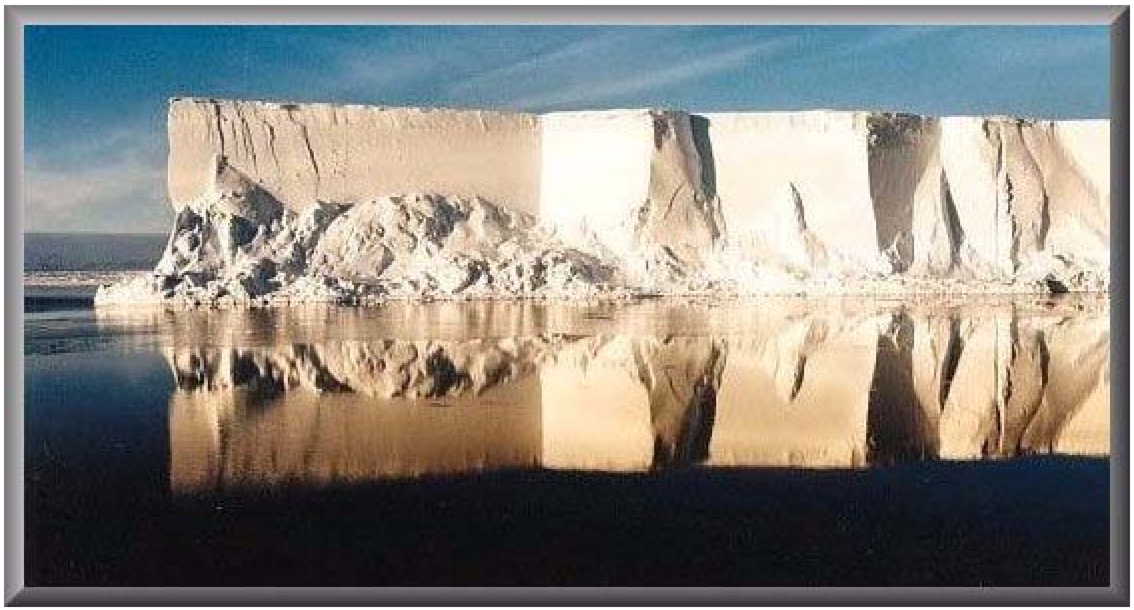

Tami McDunn
NASA GSFC
August 12, 2005

Overview

- Objective
- Background
- Method
- Analysis
- Conclusions of this study
- Opportunities for further study
- Sources

Objective

- Use polarization ratio from AMSR-E data to identify and track B15a and C19 in the Ross Sea region.
- Analyze the motion of these icebergs to determine the forcings behind their dynamics
  - Wind fields
  - Ocean depth (via bathymetry)

Iceb

- Freshwater
- Very thick, up to hundreds of meters deep
- Motion leads to areas of open water within sea ice

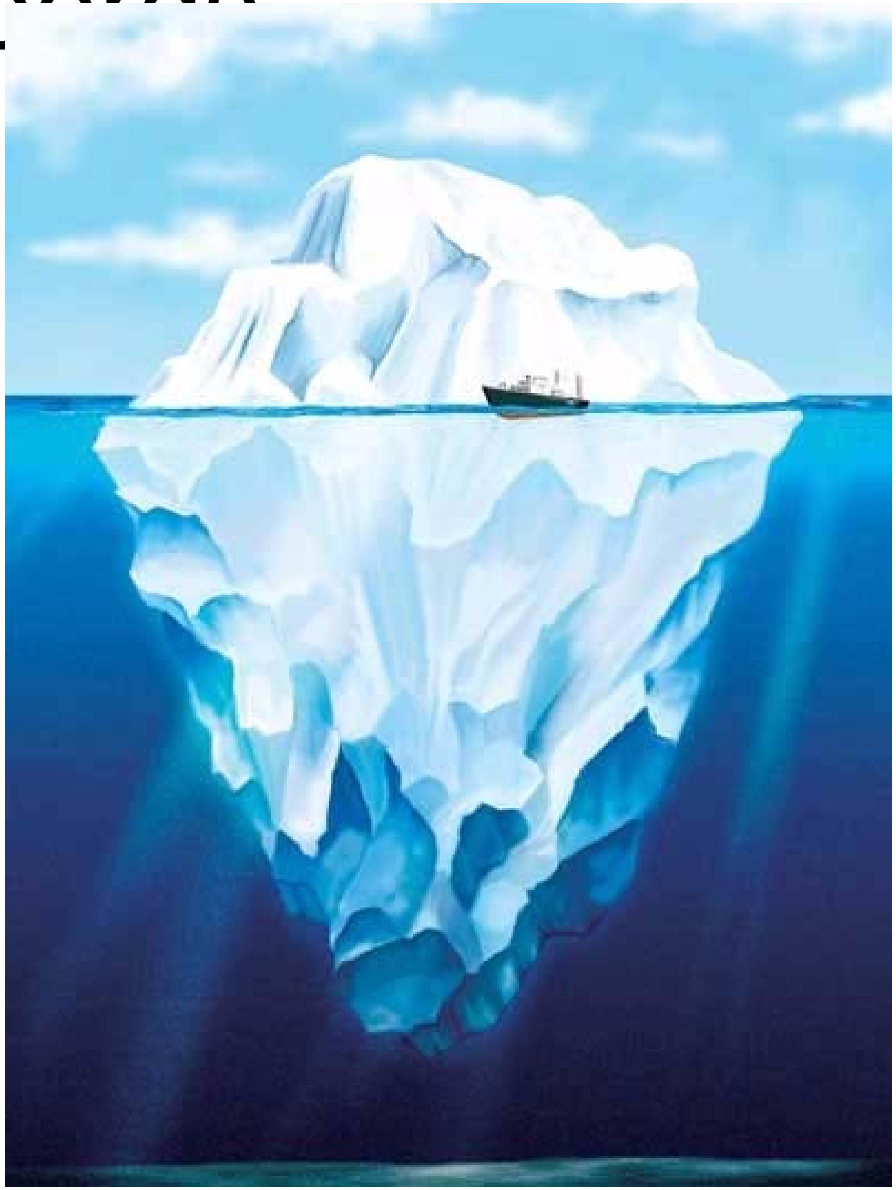

Ross Sea Region

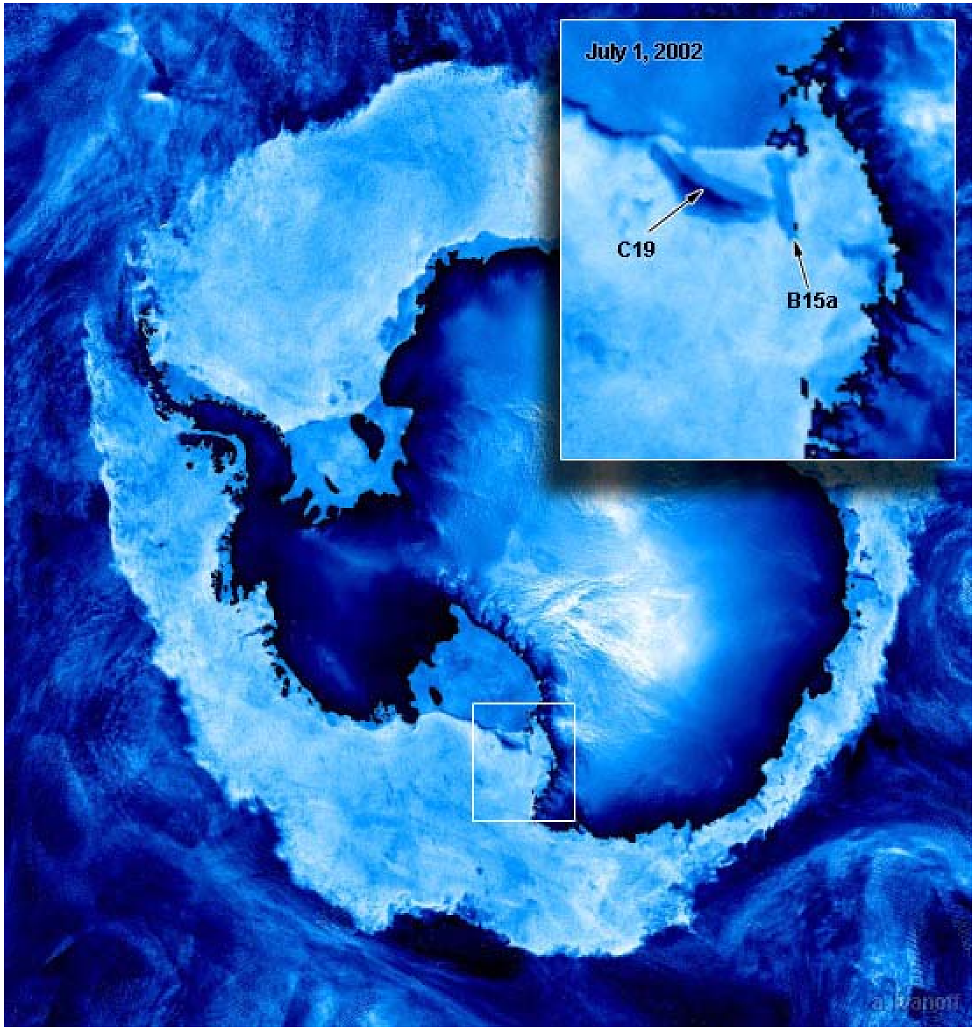

Satellite Data

- AMSR-E satellite data → Polarization Ratio:

$$PR_\lambda = (T_B(\lambda V) - T_B(\lambda H))/(T_B(\lambda v) + T_B(\lambda H))$$

where T_B = brightness temperature
λ = signal wavelength (89 GHz)

$PR_{seaice} \sim 0.0$

$PR_{water} \sim 0.1$

$PR_{icebergs} \sim 0.02\text{-}0.09$

Tracking Method

- IDL
  - Identified initial threshold range for PR values of iceberg
  - Used a dynamic threshold range for each iceberg
    - Manually determined threshold ranges for summer months
    - Used this to identify clusters that were candidates
  - Checked for spatial continuity of iceberg midpoint

Movie 1: Initial Data

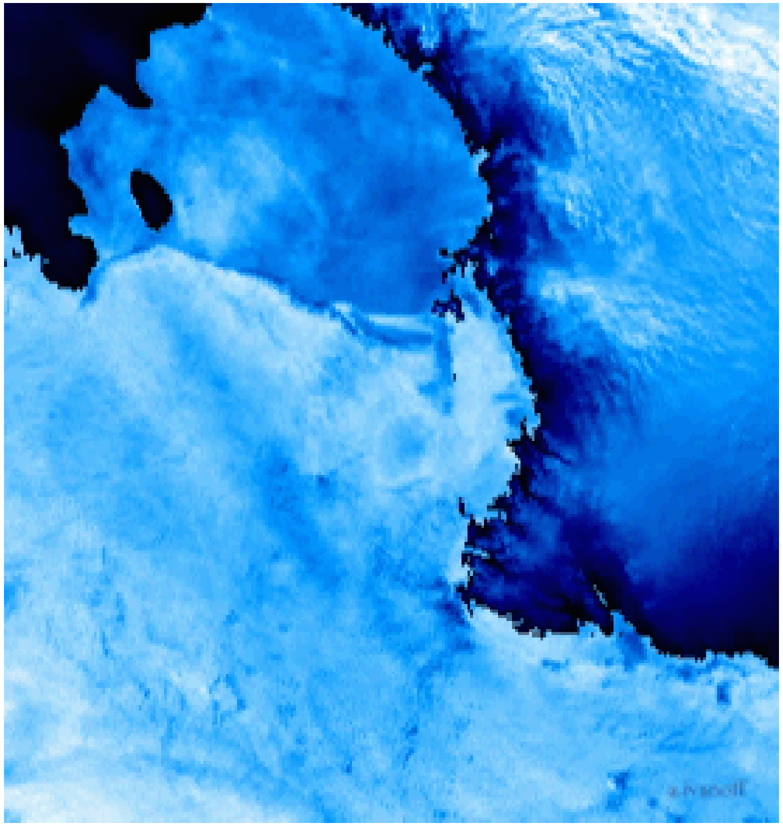

Movie 2 : Result Images

Iceberg Trajectories: B15a

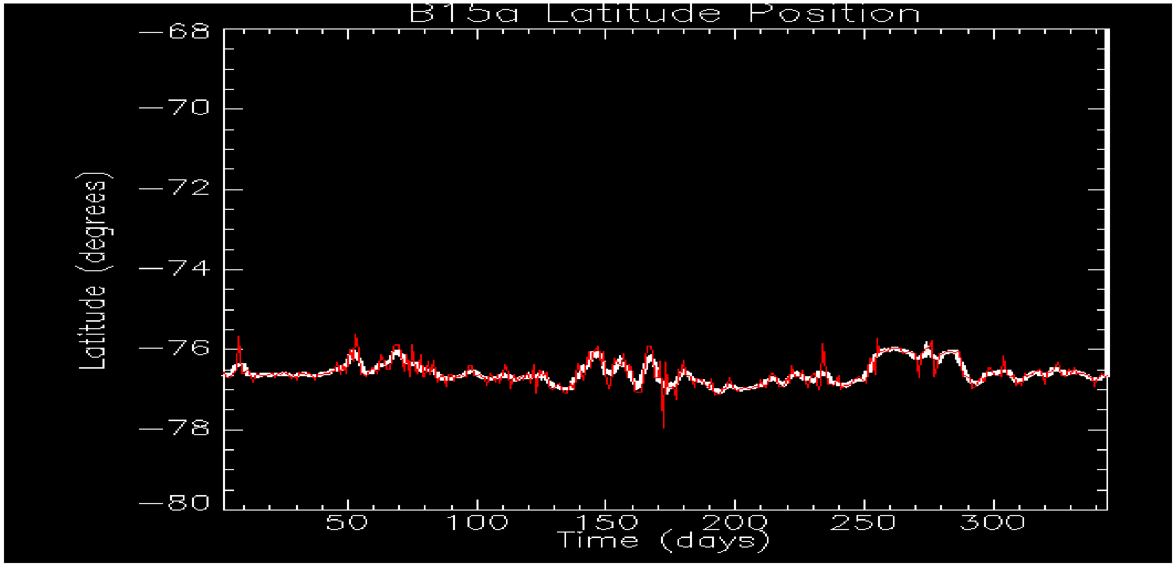

Total distance = 30.32 km

Average speed = 0.087 km/day

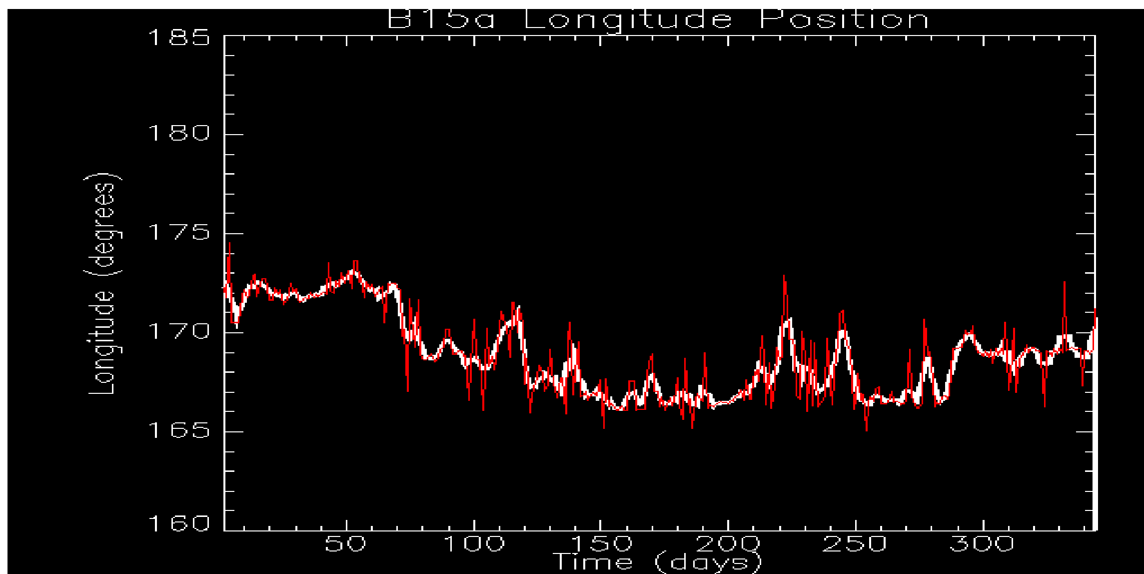

Iceberg Trajectories: C19

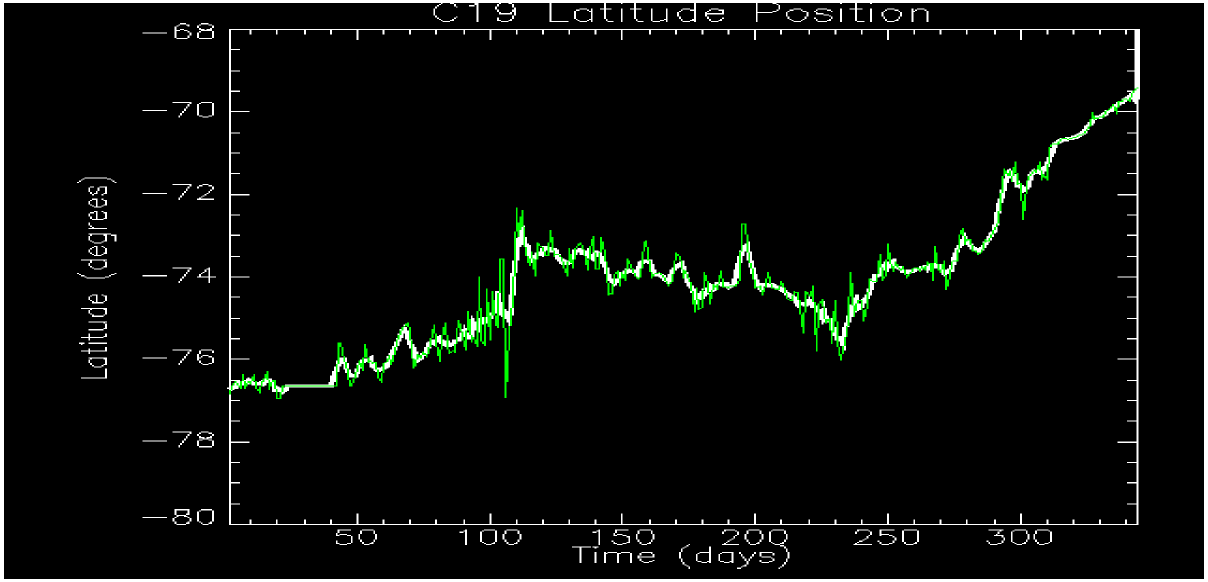

Total distance = 872.41 km

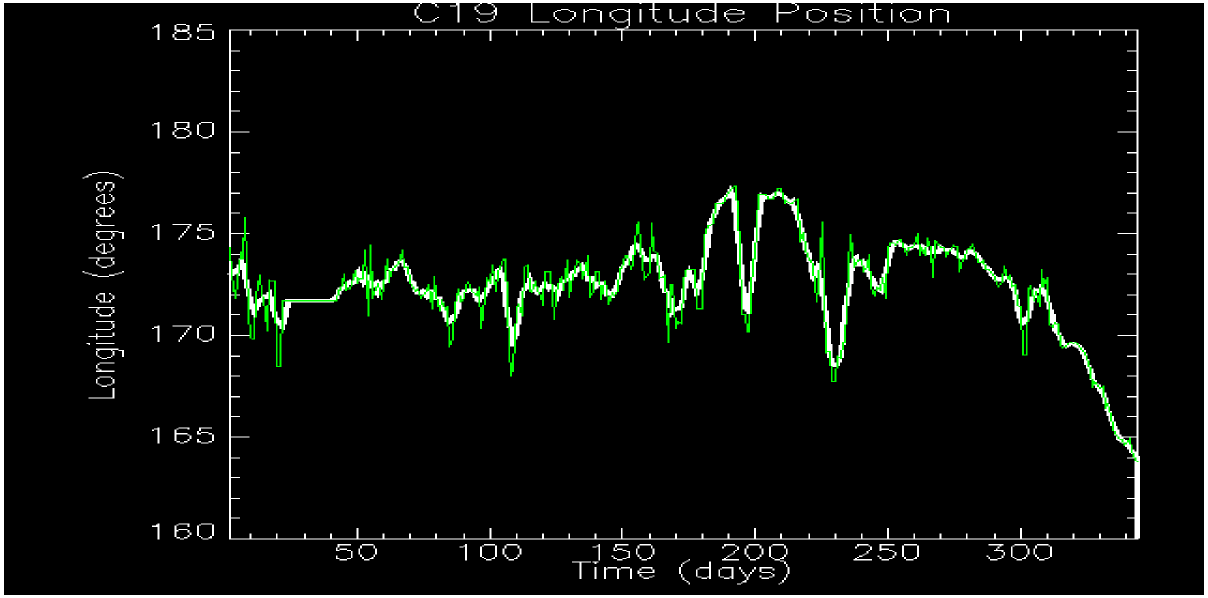

Average speed = 2.51 km/day

Wind Field Analysis with B15a

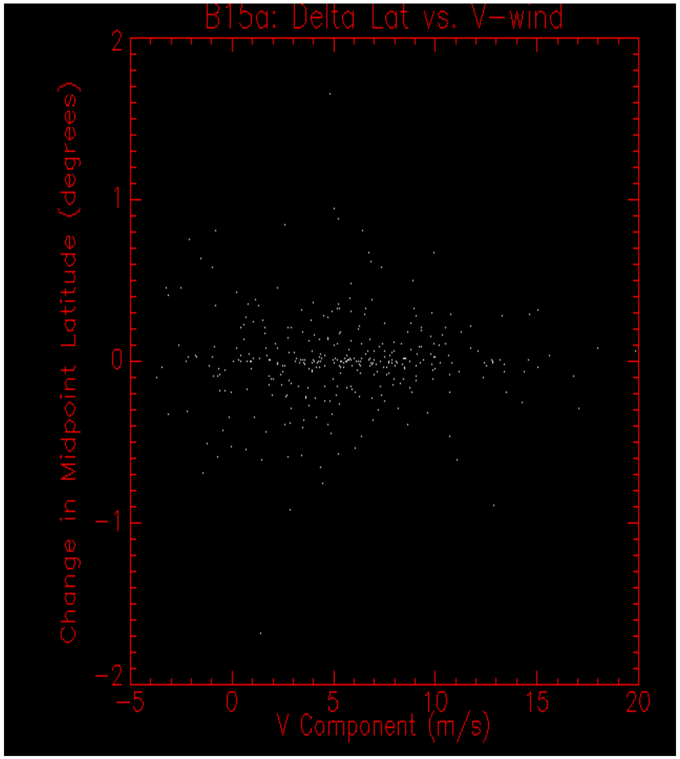

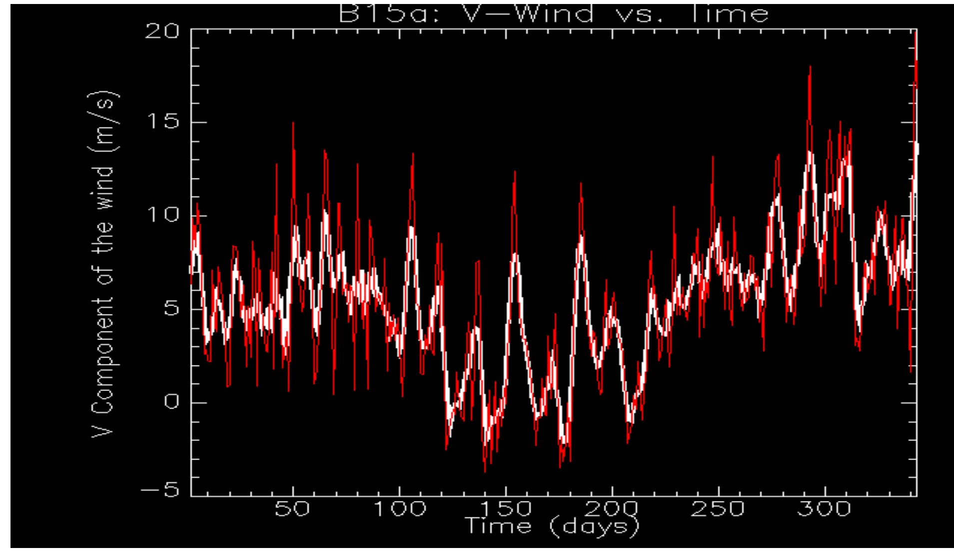

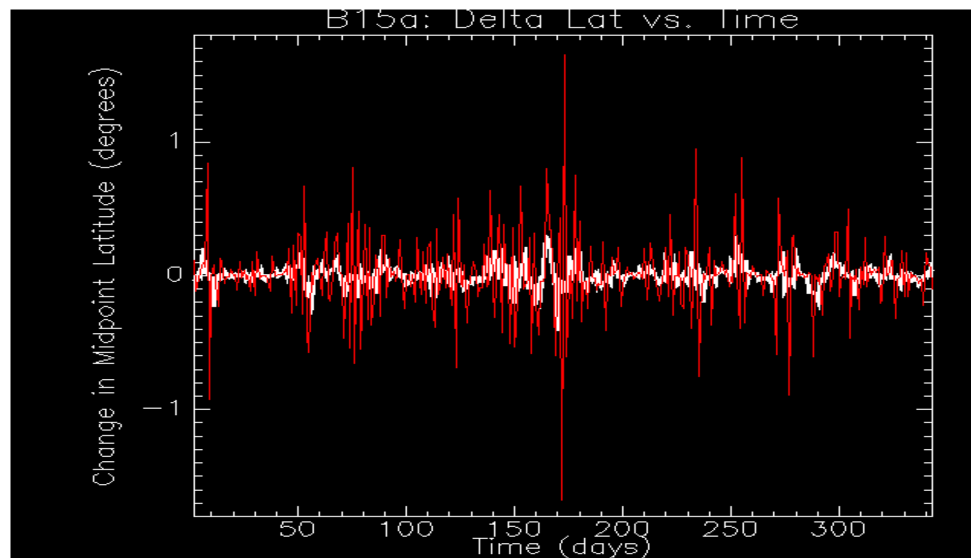

Correlation Coefficient
= -0.0463

Wind Field Analysis, cont'd

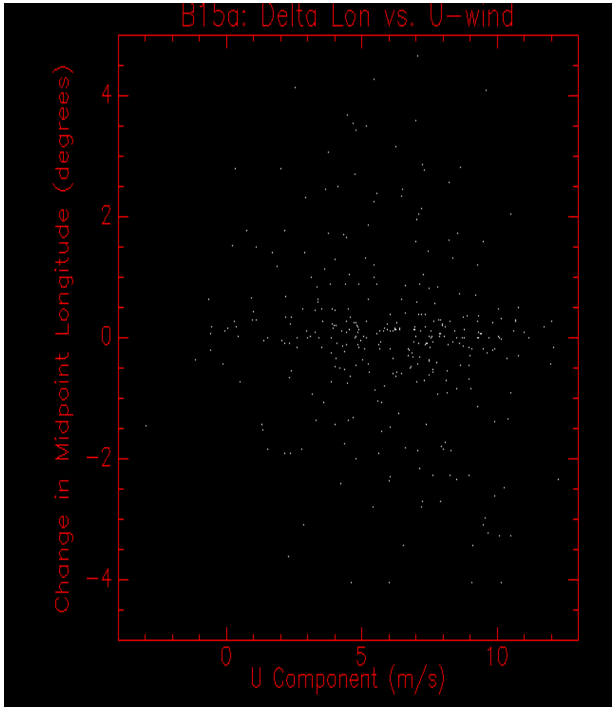

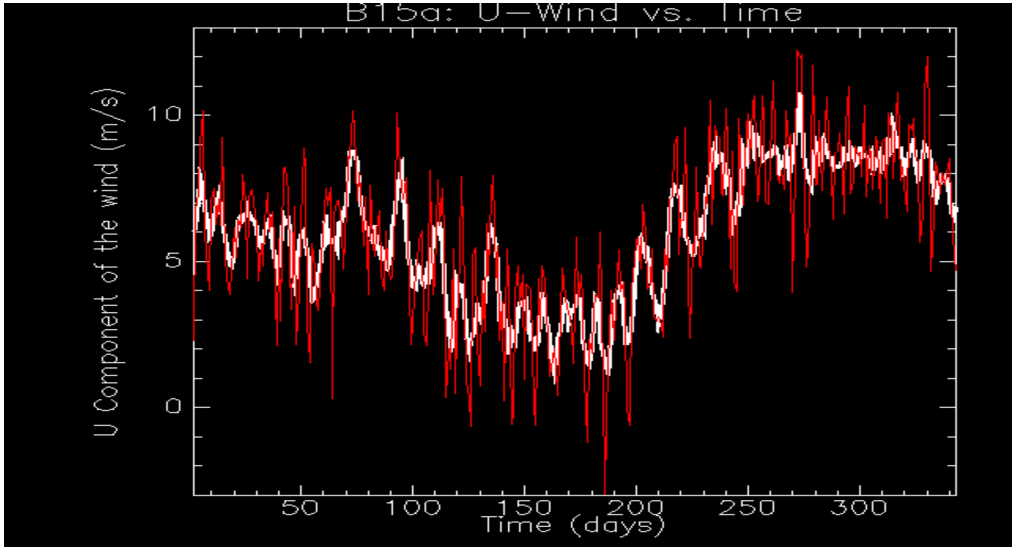

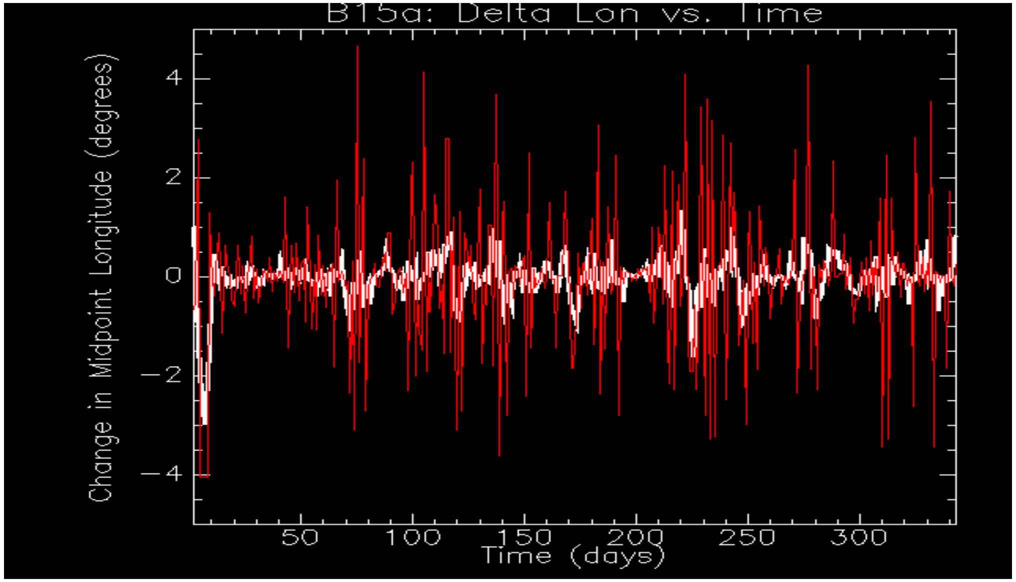

Correlation Coefficient
= -0.0463

Wind Field Analysis with C19

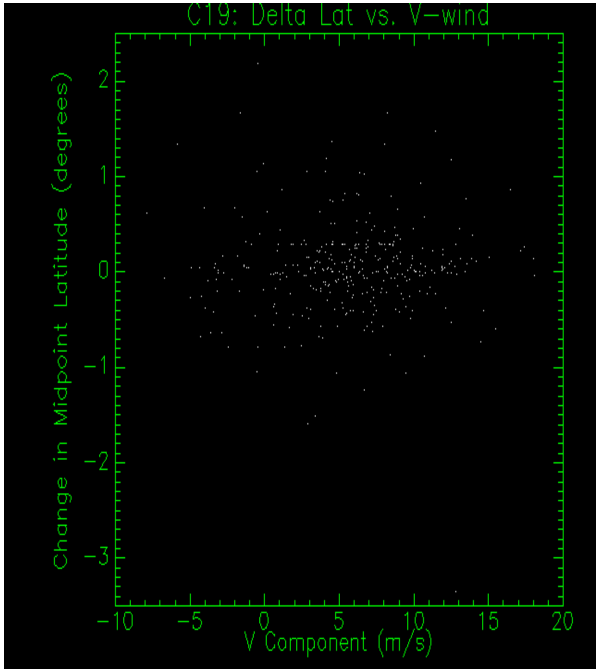

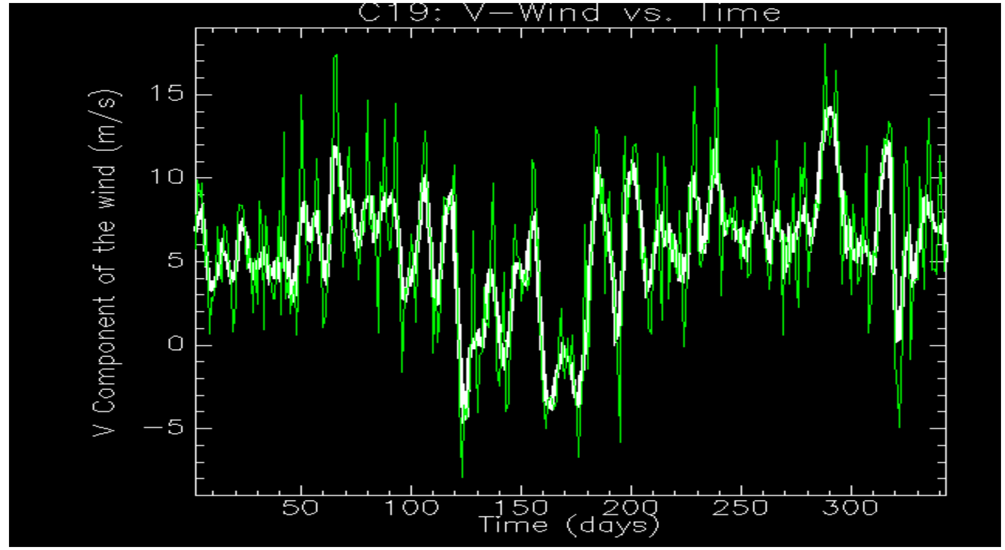

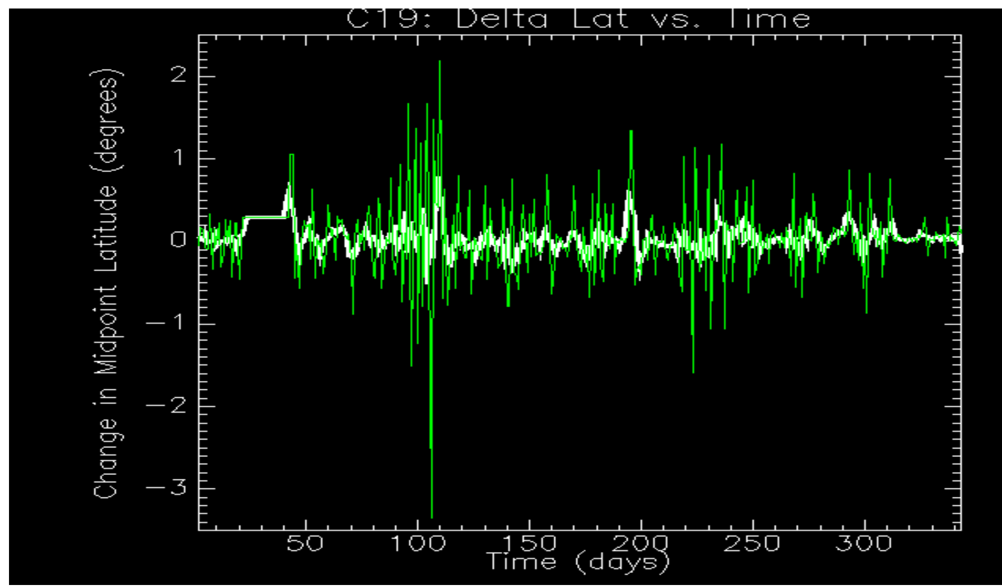

Correlation Coefficient
= +0.1251

Wind Field Analysis, cont'd

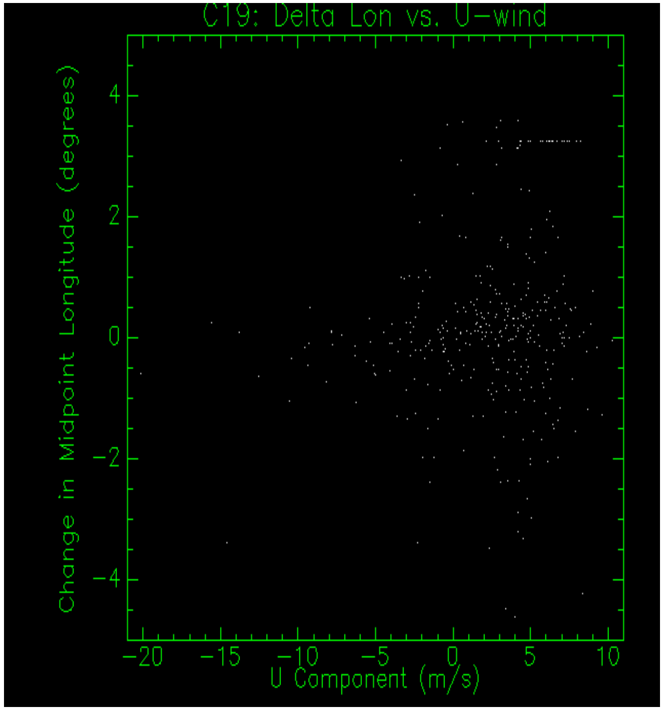

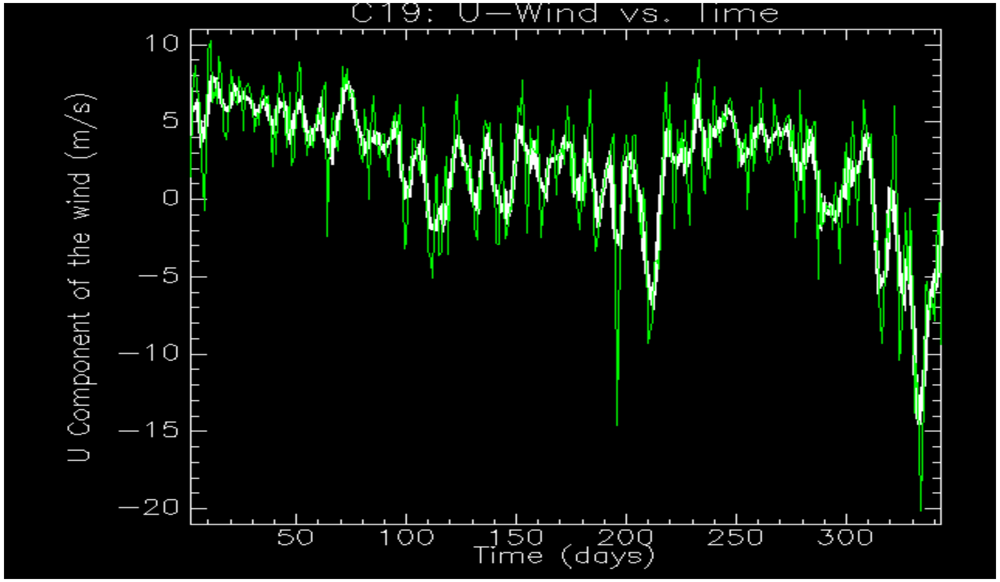

Correlation Coefficient
= +0.2913

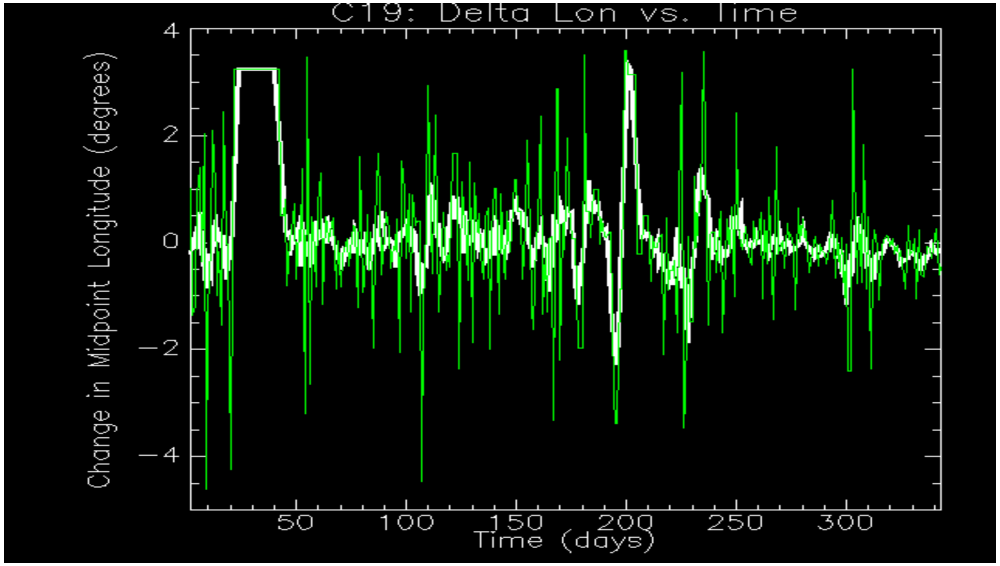

A Possible Explanation… Ocean Depth

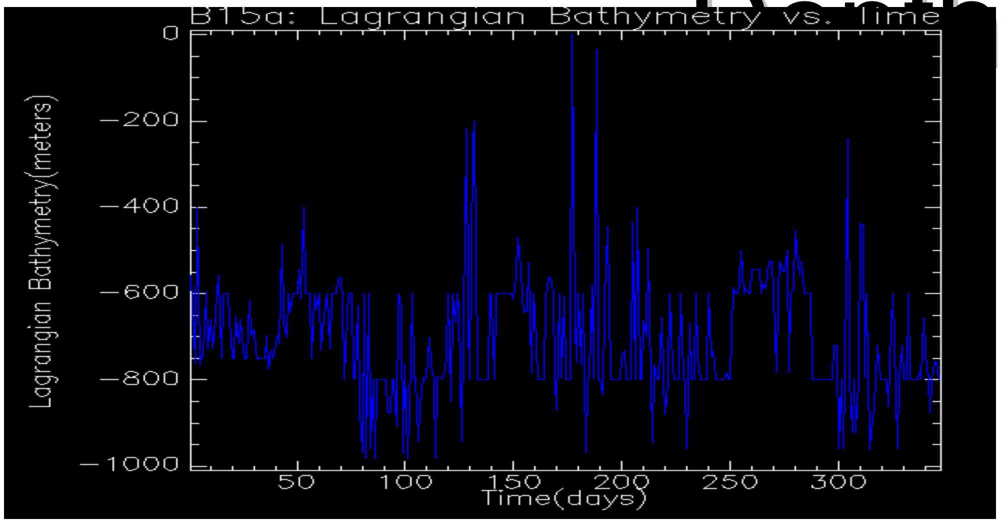

Previous studies have determined that B15a is approximately 500m thick, while C19 is roughly 200m thick…

Improves correlation between wind fields and iceberg motion, however these correlations remain unimpressive

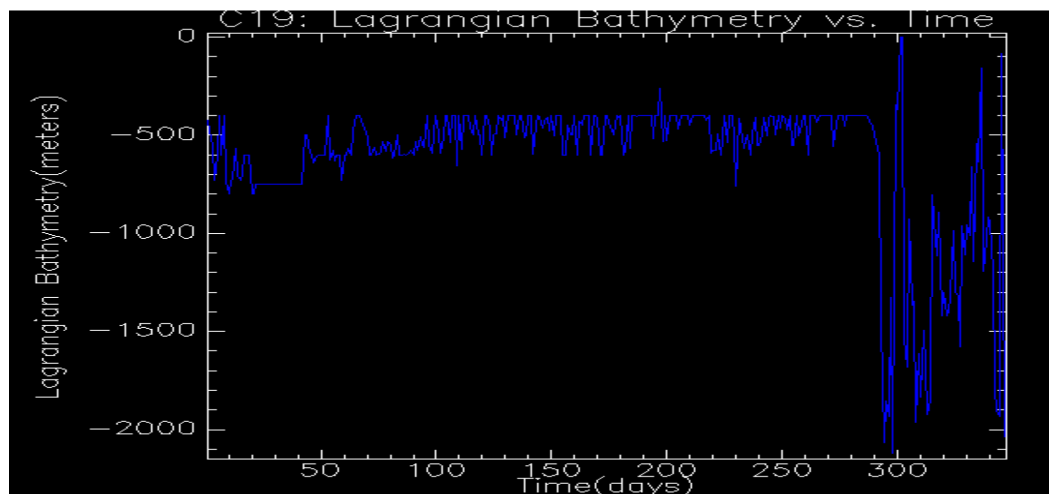

Another Possibility…Season and Sea Ice Concentration

During Antarctic summer, melting increases and sea ice breaks apart, making iceberg flow more likely

→Taking season into account significantly improves correlation between wind field and iceberg drift

Conclusions from Study

- Iceberg drift initially appears to have little correlation with wind field
  - Correlation improves when iceberg thickness and ocean depth are considered.
  - Correlation improves more when seasonal variations of sea ice concentrations are considered.

Further Study

- Develop method to eliminate noise from iceberg tracks during summer months
- Analysis with respect to:
  – Sea ice concentration data
  – Ocean currents
- Fast Fourier Transform analysis to search for patterns within the iceberg motion time-series
- Longer data series

Sources

- Acknowledgements:
  - Thorsten Markus, NASA GSFC → my mentor
  - Alvaro Ivanoff, NASA GSFC → preprocessed raw satellite data to develop polarization ratio data array, developed border search technique
- Data:
  - NASA GSFC: AMSR-E data
  - NCEP/NCAR Reanalysis: wind field data http://www.cdc.noaa.gov/cdc/data.ncdp.reanalysis.derived.html
  - Texas A&M University: bathymetry data http://woceatlas.tamu.edu/Sites/html/atlas/SOA_MAPS_INFO.html
- Background:

Gloersen, Per; William Campbell, Donald Cavalieri. *Arctic and Antarctic Sea Ice, 1978-1987: Satellite Passive-Microwave Observations and Analysis.* Library of Congress Cataloging, 1992.

Gurney, R.J., Foster, J.L., Parkinson, C.L. *Atlas of Satellite Observations related to Global Change.* Cambridge University Press: New York, 1993.

Parkinson, Claire L. (1997). *Earth From Above: Using Color-Coded Satellite Images to Examine the Global Environment.* University Science Books: Sausalito, CA. 1997.

MAC UAV

Mars Astronaut Companion Unmanned Aerial Vehicle

Prototype and Profile

Brian Smith, Code 698

Mentor: Mark Bulmer, NASA JCET Program, UMBC

Current Mars Status To Date:

- Orbiters: 5 (Mars Global Surveyor, Mars Odyssey, Mars Express, Viking 1/2)
- Rovers: 3 (Pathfinder, Mars Exploration Rovers Spirit and Opportunity)
- Landers: 2 (Viking 1 & 2)
- MOC resolution: max 1.5 meters/pixel
- HRSC DEM 10-2 m resolution

- Plans for Mars Plane
- First Sample Return Mission in 2014

Goals and Background

- Test MAC UAV Prototype for mission science and operational support roles, e.g. resource location, scouting, atmospheric testing, and search and rescue
- Identify landing sites and develop mission profiles for potential MAC missions.
- Manned Mission: crew of 6, 2 on rovers
- Mars Reference Mission specifies 10 day scientific mission windows operating within 500 km range of base
- Develop a system promoting astronaut autonomy

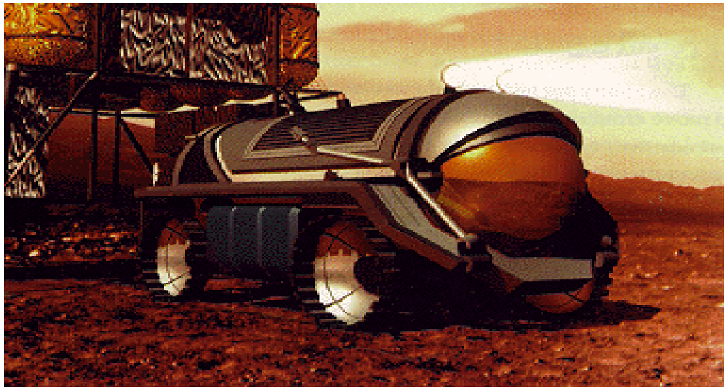

UAV Prototype

- Hanger 9 Trainer RC Aircraft
- Uses MP2000 autopilot

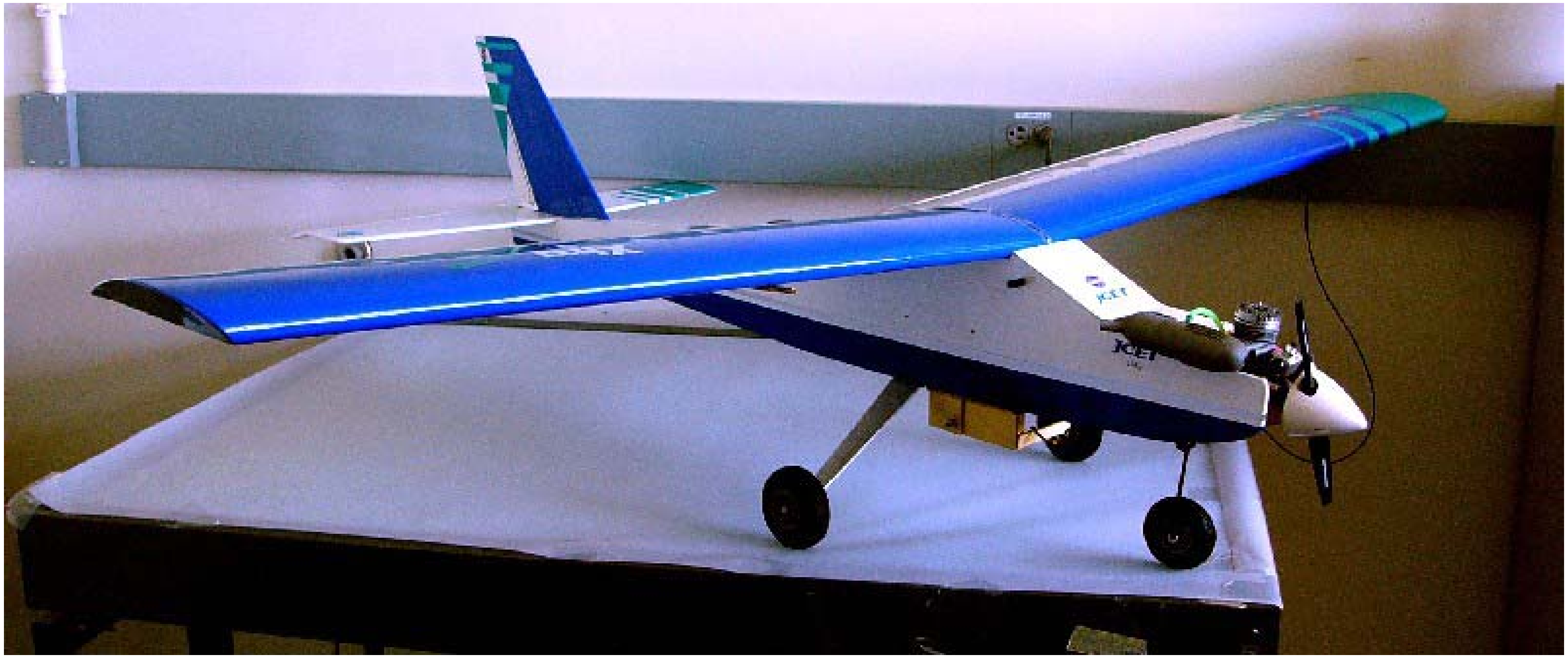

UAV Prototype Components

- MP2000 Autopilot

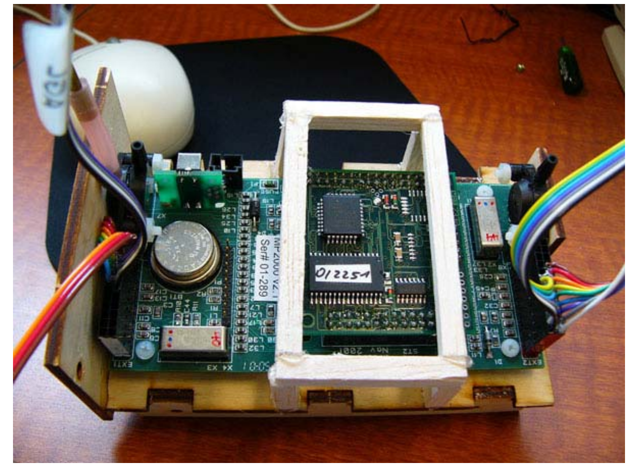

- AGL (Ultrasonic Altimeter) Board

Components Cont.

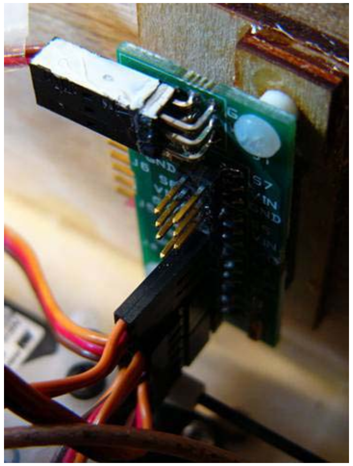

GPS Receiver

Servo Board

Wing-Mounted
AGL

Test Instrumentation

- Sony Cyber-shot 3.2 MP Camera
- 3x Optical Zoom,
- f-stop 1:2.8-5.3
- Nadir mounted
- Single axis
- Servo activated
- Coded operation
- On-instrument storeage

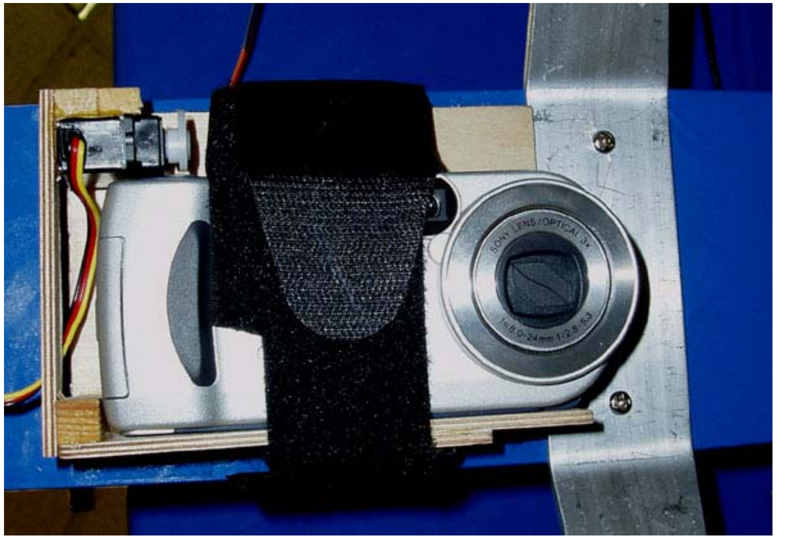

Camera Tests.

- Camera: Calibration – 3x @ 500 ft

- Potential for
  - more sophisticated payloads
  - modular payloads

Optimum Flight Parameters

- 150-200ft runway
- Cruise speed: 47mph
- ~ 2 mi between necessary payload use
- Optimal altitude: ~500 feet for maximum focus and target visibility
- Approx. 15 mile range
- Flight planning software with graphical interface

Resolved Issues

- Fuel Tank Failure
  - Need for access
- Lack of Documentation
  - Computer interface
  - Trimming of aircraft
- Lack of AGL Altimeter
  - Restricted autonomous operation
- MP2000 Board Failure
  - Need to improved error checking
- Payload Limitations
  - Need to attachment options
- Absence of Geospatial Input for Ground Control Software
  - Need to work with designers
- Flight test damage

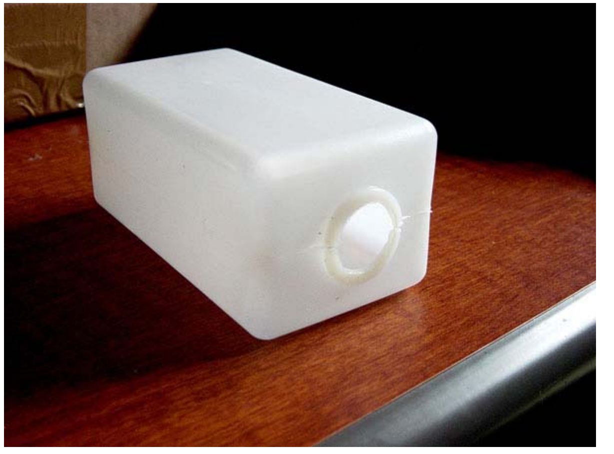

Mars Profiling

- Landing sites chosen for topographic variety, accessibility, mission range, resource availability
- Science desire matched to engineering constraints
- All sites must be trafficable
- Sites chosen:
  - Gusev Crater
  - Perepelkin Crater/Tempe-Mareotis Fossae
  - Stokes Crater/Phlegra Montes Range

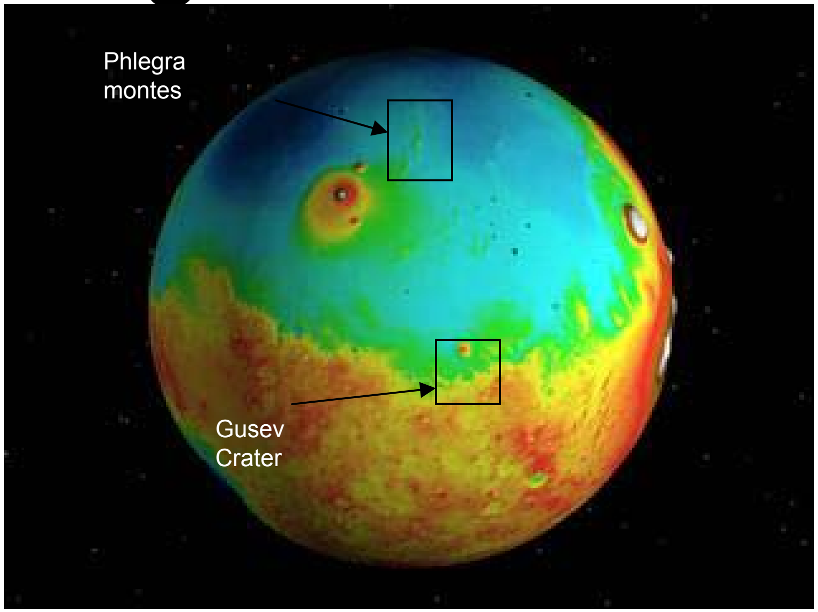

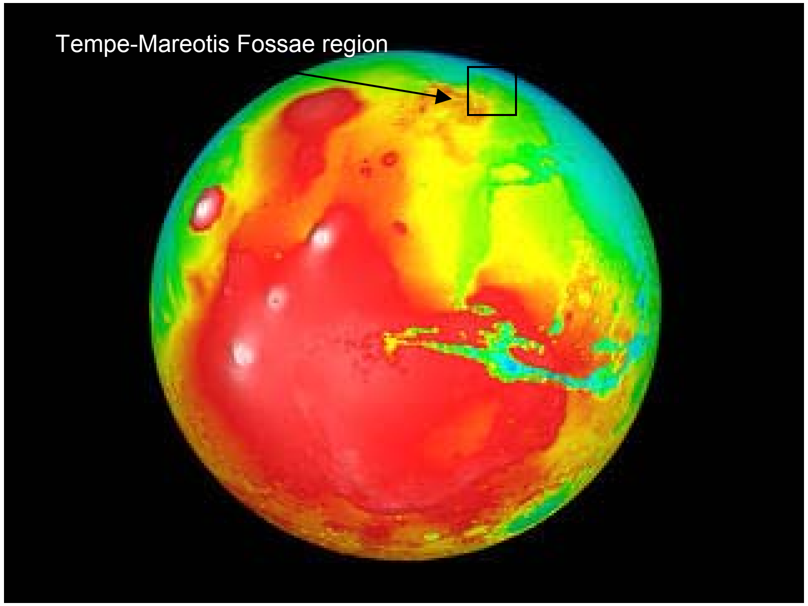

Gusev Crater

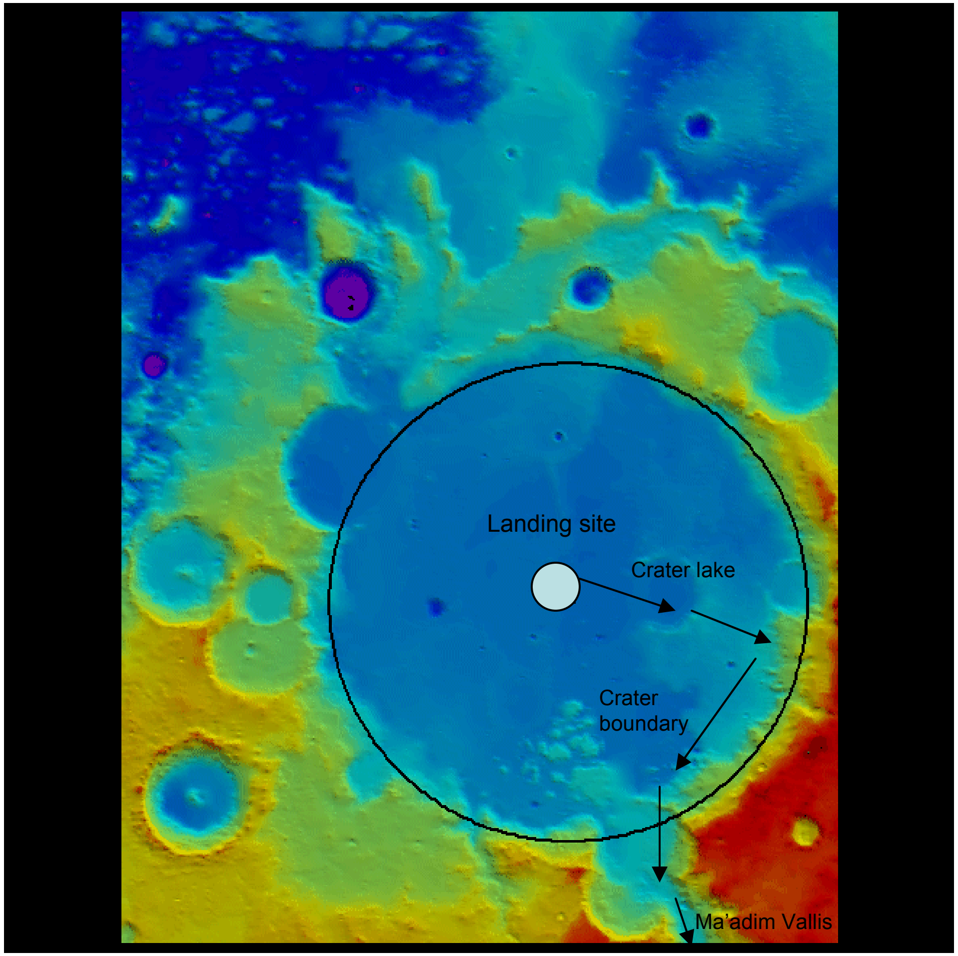

14.48˚ S, 175.27˚ E

- Priority landing site
- Expansive Noachian crater (older than 3.6-4.3 bn. years), 150 km diameter
- Rover requirement: Spirit has already traversed part of the site
- Only takes 2-3 MAC missions to traverse a diameter
- Known wind patterns, potential “dust-devil” hazard

MAC Goals

- Science
  - Examine/search areas inaccessible to rover, such as steeper southern crater boundary
  - Potential study site evaluation
  - Crater lake: study of “shoreline”
  - Ma’adim Vallis to south (potential water evidence)
  - Study flooding from Vallis, possibly a lake/system of lakes

- Operational Support
  - Route planning
  - Communication relay
  - Search and rescue

Perepelkin / Tempe-Mareotis Fossae

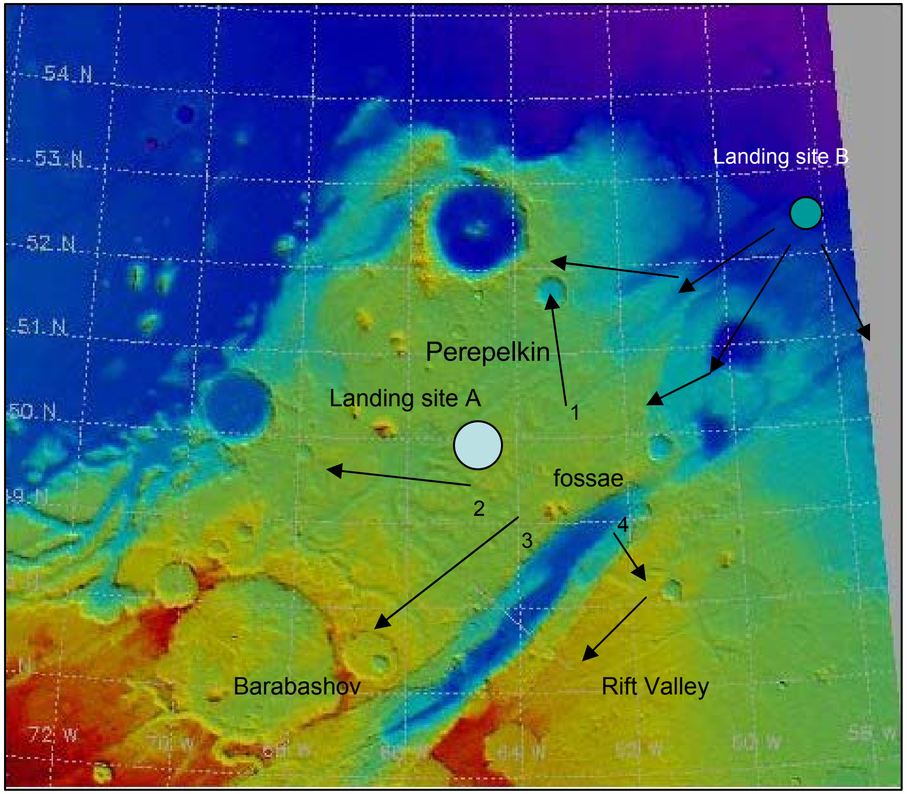

46-54˚N, 288-302˚E

- Multiple surrounding craters, including Barabashov (similar to Gusev in size / depth)
- Includes features of Noachian/Hesperian ages (1.8-4.3+ bn. years)
- Several faults/troughs and one major rift valley to the southeast
- Two landing sites: A has greatest potential for scientific discovery, B is safer

MAC Goals

- Science
  - Initial area scouting
  - Examine Perepelkin - crater inaccessible on foot, steep edges, 2km deep
  - Study the central peak in crater up close
  - Study of local crustal deformation in the fossae area
  - Look for evidence of erosion in Barabashov
- Operational Support
  - Use as navigational tool: locate accessible routes
  - Communication relay
  - Search and rescue

Stokes Crater / Phlegra Montes

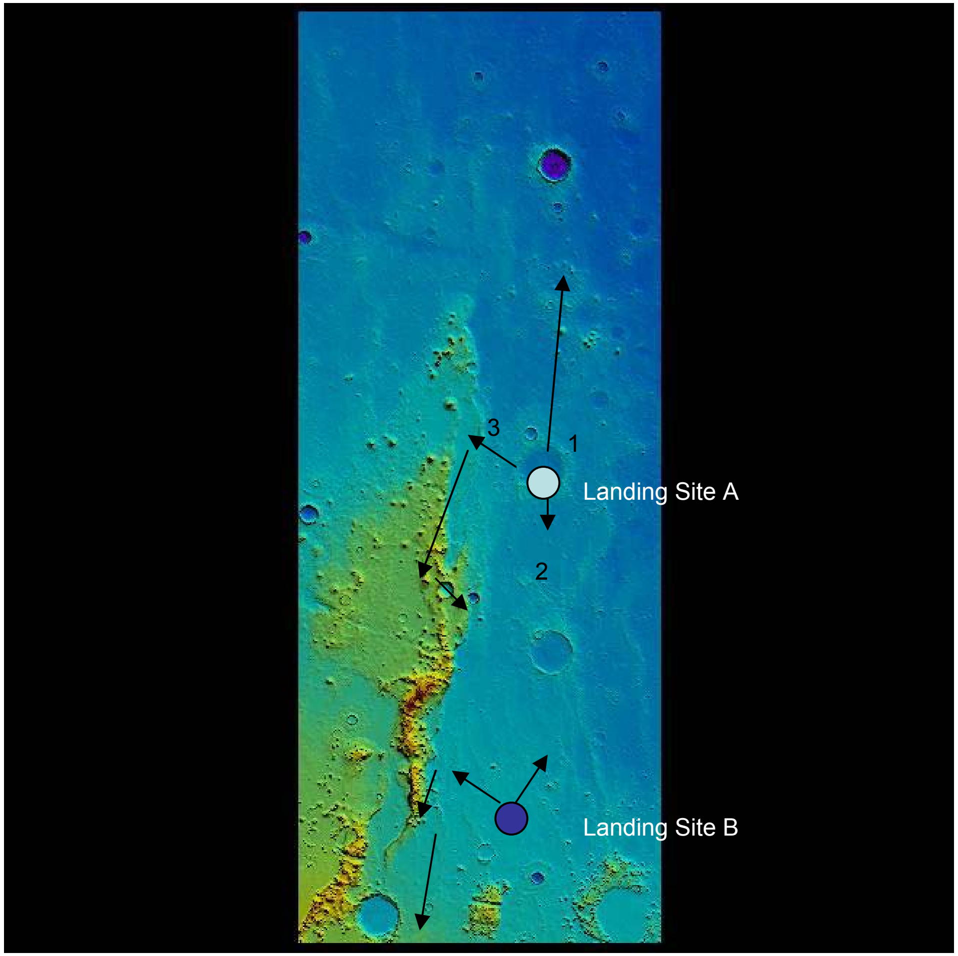

32.5-56.5˚N, 162-172˚E

- Stokes Crater to north
- Shallower, broad craters to south
- Phlegra Montes: mountain range to the southeast. Structural, not volcanic
- Plains so access is simplified
- Landing site A would give access to greatest variety of features to study, while site B allows study of higher southern mountains

MAC Goals

- Science
- Stokes: study central peak, ejecta material surrounding crater border
- Phlegra Montes: take data in areas unreachable via rover
- Measure meteorological events in mountain setting
- Operational Support
- Use as a navigational aid in the mountains
- Potential search aid for resources

Mars Atmosphere

- Lift
  - atmospheric density (based on temperature / pressure)
- Wind Considerations
  - Seasonal wind increase in Fall
- Extreme atmospheric temperatures
- Thermal tides
  - Pressure Cycle

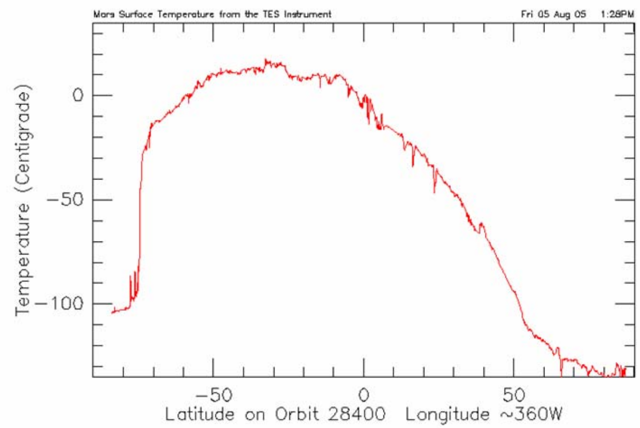

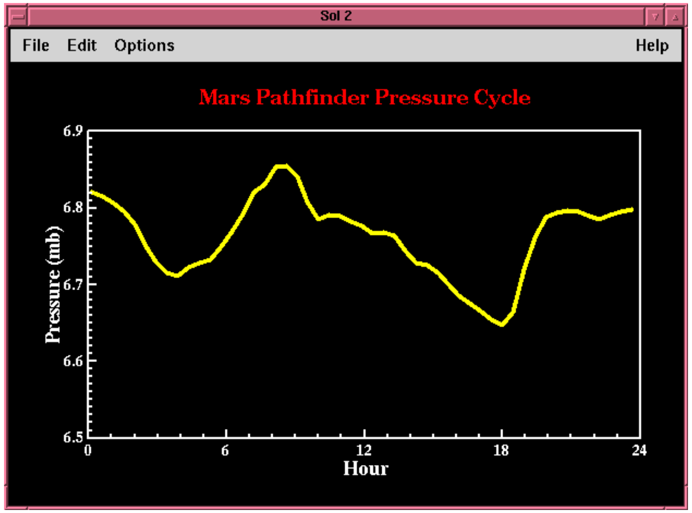

Mars Weather

- Dust Devils
  - Electric in nature
  - Fare poorly in rocky terrain
- Planet-wide dust storms
  - Also believed to have electric causes: dust suspended electrostatically
  - Impedes visibility
  - Electronic interference
  - Extreme winds (~40 knots)

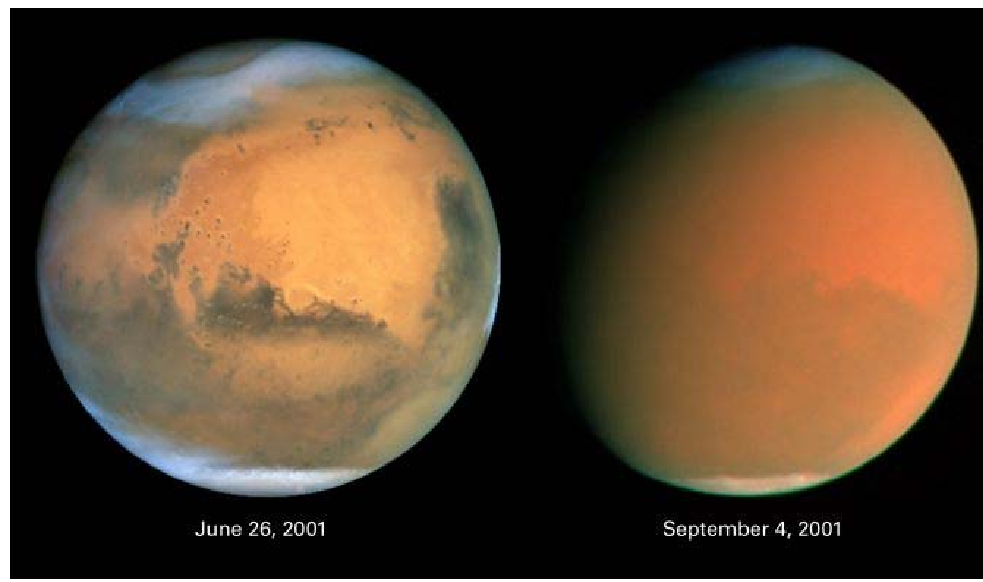

UAV Design Considerations

- Development of electrical shielding
- Interchangeable replacement parts
- Payload damage reduction design
- Rechargeable electric power supply
- Lightweight solar power supplement
- Payloads: IR, Visible, Radar, Video Feed, micro LIDAR, atmospheric sensors